Harmonic Analysis in Power Network with Renewable Power Generator

A thesis submitted for the degree of

Doctor of Philosophy

At the University of Strathclyde

By

Xinyi Gu

Supervisor: Professor K. L. Lo

Power Systems Research Group

Department of Electronic and Electrical Engineering

University of Strathclyde

2017

Declaration of Author's Right

This thesis is the result of the author's original research. It has been composed by the author and has not been previously submitted for examination which has led to the award of a degree.

Acknowledgements

First of all, I would like to express my sincere appreciation to my supervisor, Professor K. L. Lo, Associate Dean (International), for his supervision and support throughout my research work. The completion of this thesis would not be possible without his constant encouragement and patient guidance.

I also wish to extend my gratitude to my colleagues at Power System Research Group for providing me with a stimulating and fun environment. My colleagues and many friends outside work that I would like to thank are too many to be squeezed into one page. In addition, I would like to thank Dr. Zhemin Lin and Dr. Jiangfeng Lv, for enjoyable collaboration during projects.

Most importantly, I wish to express my sincere gratitude to my parents for their financial supports, love and inspiration during my research. Very special thanks to my beloved Husband, Dr. Ke He, for his understanding, support and endless love during my PhD period. Last but not least, I would like to thank my lovely daughter who was born during my writing-up period. Although her birth changed my life a lot, I could not have finished my thesis without her.

Contents

List of Figures

List of Tables

List of Symbols

a	Phase Angle
$a(h)$	Phase Angle of the h^{th} Harmonic Voltage
$\beta(h)$	h^{th} Harmonic Current Phase Angle
θ_n	Phase of the n th Harmonic Component
a_o,	Constant Fourier Coefficients
a_n	Fourier Coefficients
$a_j(n)$	Approximation Coefficients
b_n	Fourier Coefficients
c_0	Magnitude of the DC Component
c_n	Magnitude of the n th Harmonic Component
$d_j(n)$	Detail Coefficients.
E_{ao}	Energy of the Approximated Version
E_{dj}	Disturbance Energy at the Detail Version
f	Fundamental Frequency
f_n	Signal Frequency.
f_p	Resonant Frequency
f_s	Series Resonant Frequency
h^{th}	Harmonic Order
I_{equ}	RMS Value of Line Current
$I_{equ\ max}$	Maximum of the RMS Value of Current
$I^{(h)}$	h^{th} Maximum Magnitude of Harmonic Current
I_L	Maximum Demand Load Current,
$I_2, I_3, \ldots I_n$	Higher Frequency of Harmonic Currents
s_1	Load Rating.
s_{equ}	Rated Apparent Power
s_c	Capacitor Rating
s_s	Short Circuit Rating
s_{sc}	Short-circuit Power

s_t	Transformer Rating
T	Period of the Waveform
U_i	Interphase Rated Voltage
U_p	Single-phase Rated Voltage
V_1	Fundamental Voltage,
w_o	Fundamental Angular Frequency
z_t	Transformer per unit Impedance

Glossary of Terms

CWT	Continuous Wavelet Transform
DFIG	Double Fed Induction Generator
DFT	Discrete Fourier Transform
DWPT	Discrete Wavelet Packet Transform
DWT	Discrete Wavelet Transform
EMC	Electro-Magnetic Compatibility
ER	Engineering Recommendation
FFT	Fast Fourier Transform
FHM	Fast Hybrid Method
FIS	Fuzzy Logic Toolbox
FS	Fourier Series
FT	Fourier Transform
GIC	Geomagnetically Induced Currents
HMM	Hidden Markov Model
HP	High-pass
IEC	International Electro-technical Commission
IEEE	Institute of Electrical and Electronics Engineer
LP	Low-pass
MRA	Multi-resolution Analysis
PCC	Point of Common Coupling
PMSG	Permanent Magnetic Synchronous Generator
PQ	Power Quality
PWHD	Partial Weighted Harmonic Distortion
RMS	Root Mean Square
SLG	Single Line-to-ground
STFT	Short-time Fourier transform
TDD	Total Demand Distorted
THD	Total Harmonic Distortion
THDv	Total Harmonic Voltage Distortion
WRIG	Wound Rotor Induction Generator

WRSG	Wound Rotor Synchronous Generator
WT	Wavelet Transform
WTG	Wind Turbine Generator

Abstract

Considering the rapidly rising cost of primary fuel for electricity generation and the extensive concern of the international community for global warning, electricity generation with renewable sources has been actively developed all over the world. A large number of renewable energy generators, more highly sensitive electronic equipment and more electronics or microprocessor controllers are used in the power system. It has brought new challenges to supply quality, and thus the study of Power Quality (PQ) has become obviously important. Harmonic analysis plays an important role in PQ study because harmonic has great influence on the power system equipment as well as on their operation. Harmonics can lead to operation failure of electrical and electronic components, overheating of neutral wires and transformer, failure of power factor correction capacitors, loss in power generation and transmission, and interference with protection, control and communication networks as well as customer loads. Therefore, developing an advanced PQ disturbances classification system and a more accurate harmonic analysis method is the key of this thesis.

It is necessary to determine the sources and causes of such disturbances to solve PQ problems. When the type of disturbance has been classified accurately, PQ engineers can define the major effects at the load and analyse the source of the disturbances. Many approaches based on Fourier Transform (FT) and neural network for the classification of PQ disturbance have been developed in the last few years. The key factor of these methods is that the correct rate for the actual event is not high enough and thus there is still space to improve accuracy. In this thesis, a fuzzy-expert system based on Wavelet Transforms (WT) to classify power supply waveforms into different groups or categories for PQ classification is proposed with the aim which is to classify the disturbance type with higher accuracy.

A new approach for the evaluation of harmonic contents of power system waveforms is also proposed in thesis. The conventional harmonic analysis method is Fourier analysis. However, Fourier analysis provides signals which are mainly localised in the frequency domain and it gives limited information of the signals in the time domain.

Furthermore, the FT cannot obtain accurate values of amplitude and phases from harmonics with frequencies different from that of the window function frequency.In order to overcome the limitations of Fourier analysis and obtain better results, wavelet analysis has been proposed. A novel harmonic analysis method using Discrete Wavelet Packet Transform (DWPT) filter bank decomposition and Continuous Wavelet Transform (CWT) identification has been proposed. In order to evaluate the performance and result of the proposed analysis method, another two conventional methods, i.e. Fast Fourier Transform (FFT) and the combination method of Discrete Wavelet Transform (DWT) filter bank and CWT calculation, are compared through a large number of identical applications.

Based on the harmonic analysis, the harmonic penetration is considered and its effects to power networks with increasing of renewable power generations are investigated. With increasing of renewable generators in power networks, it creates PQ problems caused by harmonic injections with a large frequency range, such as integer-harmonics, inter-harmonics and sub-harmonics. Therefore, the steady state harmonic power flow in power system with discrete frequencies is calculated with Root Mean Square (RMS) values of bus current and voltage magnitudes and Total Harmonic Voltage Distortion (THDv) values. Variable of tests are designed to investigate the effects to the harmonic penetration with multiple types of harmonic sources in power networks.

Chapter 1 Introduction

1.1 Overview

1.1.1 Power Quality Issues

In recent years, Power Quality (PQ) study has become an important subject in power systems, with direct impacts on efficiency, security and reliability. It covers all aspects of transmission and distribution level analysis and customer satisfaction. Nowadays, electricity customers are satisfied with not only the quantity of power supply but also a high level of quality of power supply. Hence, more and more researchers and industries pay attention on PQ [1] [2].

Until now there is no fully accepted definition about what exactly PQ is, but the quality should involve the waveforms of voltage and current in an AC system, the presence of harmonic signals in bus voltages and load current, the presence of spikes and momentary low voltages, and other issues of distortion. The IEEE (Institute of Electrical and Electronic Engineers) standard dictionary defines PQ as “the concept of powering and grounding sensitive electronic equipment in a manner that is suitable to the operation of that equipment.” [3]

According to some references [1][4] [5], the origins of PQ problems are unpredictable events; and problem for electric utilities, customers and manufactures. Power supply with poor quality is normally caused by power-line disturbances, such as voltage sag/swell, harmonic distortion, flicker, momentary interruptions, impulses. The poor PQ can have a large detrimental effect on both the industrial process and commercial users. The effect due to PQ disturbances can be performed from the perspective of either electricity customers or power grid owners depending on the consequences considered by either side. Examples of economic losses due to PQ issues for power grid owners may include compensations and losses of customer royalties. While for electricity

customers, the examples of losses may come from damaged products, disrupted industrial process and losses of revenues [1].

According to specific properties of PQ problems, they are categorized into several different classifications. Due to different factors, different categories of PQ disturbances such as IEC (International Electro-technical Committee)-61000 [6] and IEEE-1159[3] are introduced in **Chapter 2**. To solve PQ problems, it is necessary to determine the sources and causes of such disturbances. When the type of disturbance has been classified accurately, the PQ engineer can define the major effects at the load and analyse the source of the disturbances. Since the traditional methods to analyse and identify power disturbances are mainly based on visual inspection of the disturbance waveforms, the PQ engineers' knowledge plays a serious position, and the PQ engineers cannot always handle huge amount of data to inspect. Therefore, many new and powerful automatic tools [7]-[17] for the analysis and classification of PQ disturbance have been developed in the last few years which will be introduced in **Chapter 4**. However, the correct classification rate for the actual event is not high enough; there is still space for improving accuracy [1]. Thus it is desirable to develop the method for detecting, identifying and analysing all kinds of disturbances.

1.1.2 New Harmonic Sources and Penetration

Nowadays, new sources of harmonics have become increasingly important aspect of PQ because use of renewable sources for electricity generation has been actively developed all over the world, considering the rapidly rising cost of primary fuel for electricity generation and the extensive concern of the international community for global warning. Electricity generation with renewable sources requires a large number of renewable energy generators, more highly sensitive electronic equipment and more electronics or microprocessor controllers are used in power systems, resulting in more harmonics injection in power system. As a result, the actual voltages and current waveforms in the power system are distorted and are a combination of many sin waves with different frequencies, which are integer or non-integer multiples of the fundament frequency (50 Hz or 60 Hz). These periodical waveforms are regarded as harmonics.

According to the report [19], 24.5 GW of new power generating capacity has been installed in the EU during 2016. Of the 24.5 GW installed, wind and solar photovoltaic, described as two of primary renewable sources, occupied the first and second largest parts, accounting for 51% (12.49 GW) and 27.4% (6.7 GW) respectively, as shown in Figure 1-1.

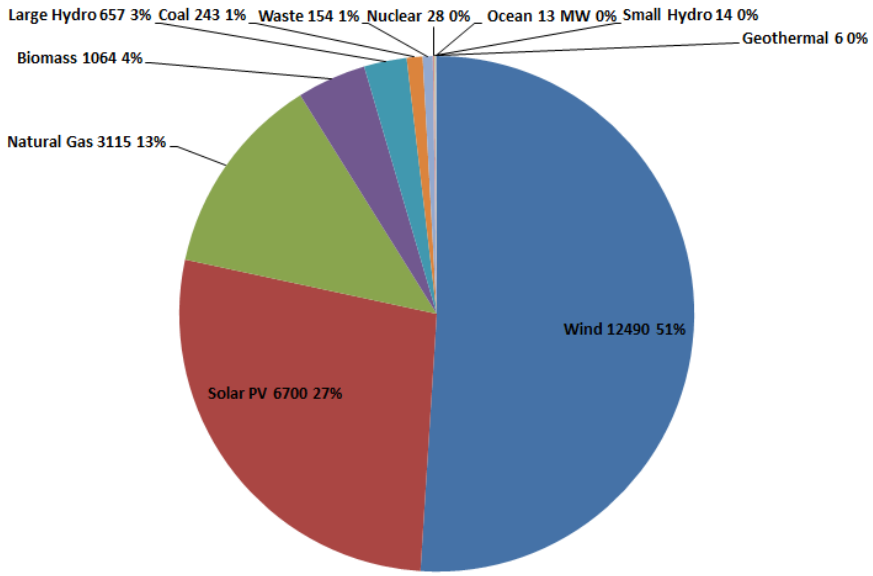

Figure 1-1 EU Countries for New Capacity Installation in 2016 [18]

According to the Figure 1-1, it is clear that wind energy plays an important role in generating electricity and consequently has been widely developed in the EU. Of the capacity installed in the EU, 10,923 MW was onshore and 1,567 MW offshore. Germany represents 43.6 % with 5443 MW and is the largest market in EU. The next is France, reaching 1560 MW and occupies 12.5%, an increase of 45% on 2015. The Netherlands came third with record installations of 887 MW and 7.1%. UK comes in fourth with 736 MW and 5.9%, as illustrated in Figure 1-2. The UK has a tremendous potential for wind power because it has one of the windiest places in Europe, especially the west of Scotland which is one of the richest wind sources in the world.

In the future, the EU has already made an aim that 20% and 33% of entire energy will be generated by renewable source in 2020 and in 2030 respectively [20]. In order to

achieve that goal, European countries need to increase wind farms installation to 230GW by 2020 and 400GW by 2030 **Error! Reference source not found.**.

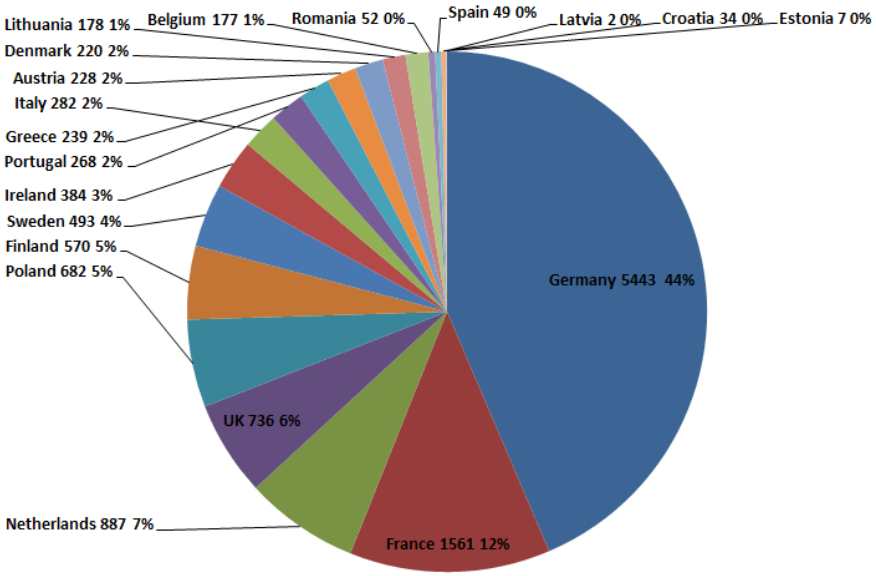

Figure 1-2 EU Countries for New Capacity Installation in 2016 [18]

Annual wind power installations in the EU have increased steadily over the past 16 years from 2.3 GW in 2000 to 12.5 GW in 2016, with a maximum level in 2015 of 12.8 GW. Offshore wind represented 13% of the annual EU wind energy market with 1,567 MW of new gross capacity connected to the grid in 2016. This is a 48.4% decrease compared with 2015, which was an exceptional year in grid-connections due to grid-connection delays in Germany being resolved [18].

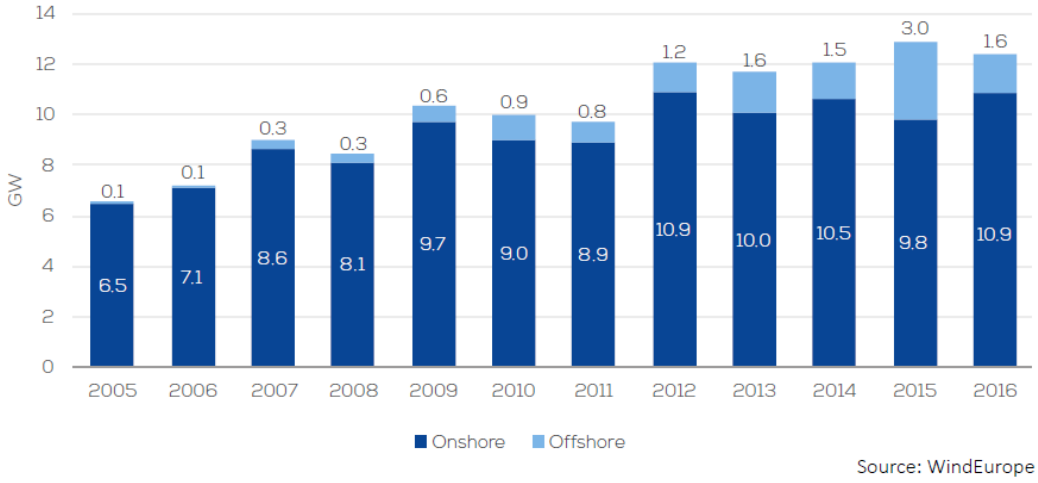

Figure 3 Annual onshore and offshore wind installation in the EU [18]

Unlike conventional generation, the output of wind power is intermittent and depends heavily on wind speed. In order to fully utilise the benefit of wind power, new management techniques need to be investigated. Traditional power system is designed with a 'top-down' power flow structure. Electrical power is immediately step-up by power transformers to much higher voltages after generated, and then is transmitted to customer concentration areas where it is step-down to distribution voltages. Renewable generations can be much smaller in capacity compared to conventional generations, therefore many of them are connected directly to distribution networks. This enables distribution networks to become 'active', while the conventional distribution looks like 'passive' and contains no generation sources. As a result, the addition of renewable such as wind power introduces more harmonic.

Nowadays, power electronic devices can produce not only integer but also sub-integer and non-integer harmonics in power system waveforms. The harmonics can have significant impact on power system equipment and its operation. There are several types of problems due to harmonics, such as failures of electrical and electronic components, power factor correction capacitors, loss in power generation and transmission, and interferences with protection, control and communication networks and customer loads. Harmonic distortion with high levels can cause heating problems of transformer, capacitor, motor and generator. As a result, the level of harmonics has been strictly limited in many public standards in power systems, such as IEC 61000 series standard, IEEE 519 standard and Engineering Recommendation G5/4. It is necessary to determine and reduce harmonic contends to obtain the electricity supply with high PQ.

The conventional signal processing method for harmonic analysis is referred to as the Fourier analysis [21] [22]. The resulting series can be obtained by the Fourier Series (FS) which represents the special case of the Fourier Transform (FT) applied to a periodic signal. However, the outputs of the FS often contain spurious components and spectral leakage [23] [24] [25].For digital signal processing, the Discrete Fourier Transform (DFT) has been considered as the most important method for Fourier analysis. DFT uses window functions to mitigate the spectral leakage effect. Because of huge computation required by DFT, the Fast Fourier Transform (FFT) has been widely applied in many practical applications. With finite samples for input data, the

DFT/FFT cannot obtain accurate values of amplitude and phases from harmonics with frequencies different from that of the window function frequency. These characteristics present one of the most important limitation of the FT, which is that harmonics must be integer multiples of the supply frequency. Furthermore, the FT provides signals which are mainly localised in the frequency domain and it gives limited information of the signals in the time domain. Therefore, a harmonic analysis method which can overcome these limitations is required.

Based on the harmonic analysis, the harmonic penetration is also considered and its effects to power networks are investigated. In this thesis, the process of evaluating the steady state network current at harmonic frequencies is defined as harmonic power flow evaluation as well as harmonic penetration evaluation [26]. The steady state harmonic power flow in power system with discrete frequencies is calculated to investigate the effects to the harmonic penetration with increasing of renewable power generations in power networks.

1.2 Objectives

Taking into account all of considerations mentioned in Section 1.1, the overall aims of this thesis are proposed: classifying PQ disturbances, analysing harmonic contents and evaluating harmonic penetration in renewable energy generators. The objective of this thesis includes:

- **Developing a fuzzy-expert system based on wavelet transform (WT) to classify power supply waveforms into different groups or categories for PQ classification.** To solve PQ problems, it is necessary to know the sources and causes of such disturbances. Although many new and powerful tools for classification of PQ disturbance have been developed in the last few years, the correct classification rate for the actual event is not high enough; there is still space for improving accuracy. Therefore, the aim of this new approach is to classify the disturbance type with higher accuracy.

- **Developing a WT approach for the evaluation of harmonic contents of power system waveforms.** To overcome the limitations of Fourier analysis, which is that harmonics must be integer multiples of the supply frequency, WT is applied for harmonic analysis.

- **Evaluating the harmonic penetration to investigate the effects to power networks with increasing of renewable power generations.** With increasing of renewable generators in power networks, it creates PQ problems caused by harmonic injections. Therefore, the purpose of this objective is essentially to calculate the harmonic penetration and investigate the effects to power networks with increasing of renewable power generations.

The objectives of this thesis can be implemented by the following steps:

1. Review the existing PQ classification method and explore their advantages and disadvantages in detail.

2. Develop a wavelet-based fuzzy-expert system for PQ disturbance classification. Then apply the proposed method to classify different disturbances including voltage sag/swell, interruption, harmonic, and flickers.

3. Review the traditional harmonic analysis method of FT. Then introduce the proposed method WT in detail. Compare these two methods to investigate the limitation of FT and the advantages of WT.

4. Apply the proposed method which is the combination of the Discrete Wavelet Packet Transform (DWPT) filter bank and Continuous Wavelet Transform (CWT) to analyse synthesised signals including time-invariant waveforms and non-stationary waveforms, and field-test waveforms. All of these results are compared with the results of the FFT and the results of the combination of the Discrete Wavelet Transform (DWT) filter bank and CWT to explore whether the proposed method has better accuracy.

5. Evaluate the harmonic penetration in a 118 bus power system and explore the effects of changing renewable generators' harmonic capacities to the harmonic penetration, harmonic capacity increased from 20% to 40% by changing capacity of WTG and changing numbers of Wind Turbine Generator (WTG). The results and discussions are presented in Root Mean Square (RMS) values of bus current and voltage magnitudes and Total Harmonic Voltage Distortion (THDv) values.

1.3 The Original Contributions

According to the mentioned objectives, this research has achieved the following contributions:

- A detailed introduction of the concept and characteristics of the PQ and harmonics. The existing PQ disturbance classification methods have been reviewed, and the advantages and disadvantages of each existing models are summarised. The FT which is the traditional harmonic analysis approach has been reviewed as well, and the characteristics and limitations are given in detail. These have provided the basic information for further PQ researches.

- A detailed review of the concept and characteristics of the WT, especially the WT filter bank. Two kinds of WT filter bank have been introduced, including DWT filter bank and DWPT filter bank.

- Based on the existing PQ disturbance classification methods, a fuzzy-expert system based on WT has been proposed to improve the accuracy. The WT decomposition based on DWT filter bank is employed to decompose the disturbance waveform. According to the Parseval's theorem, the energy distribution of wavelet at each decomposition level is calculated to extract features in PQ disturbance. Then, a fuzzy-expert system is employed to classify disturbance according to the wavelet decomposition level and the numerical values of the energy distribution.

- To overcome the limitations of FT, that harmonics must be integer multiples of the supply frequency, the WT approach, which is the combination of the DWPT filter bank and CWT is proposed. Based on the decomposition by using DWPT filter bank, the CWT is employed to identify the harmonic contents of power system waveforms. The results of the FFT and the results of the combination of the DWT filter bank and CWT are used as reference values for the purpose of comparison.

- In order to investigate the effects to the harmonic penetration with increasing renewable generators' capacities to power networks, the harmonic penetration is

evaluated in two tests: Test 1 is designed to replace larger capacity's WTGs with fixed location and number of WTGs; Test 2 is employed to increase of the number and location of WTGs with fixed power capacity of each WTG. In both of these two tests, the total renewable power generations raise from 20% to 40%. A 100MV，33KV，118 bus power system is employed to do the simulation. A method named Fast Hybrid Method (FHM) is used to calculate the harmonic power flow. The WTG, arc-furnace and convertors are connected to the power system as harmonic sources. A large number of results and discussions for these two tests are presented through RMS values of bus current and voltage magnitudes and THDv.

1.4 Thesis Structure

In addressing the scope, this thesis is composed of seven chapters whose contents are summarised as in the following:

Chapter 1: provides an introduction to the whole thesis. The motivation of this research is introduced, and then the research objectives and scopes are discussed. Furthermore, the original contributions of this thesis are presented.

Chapter 2: presents an overview of the power system waveform distortion. It provides the component of PQ and the classification of PQ disturbances. Then, harmonic basic theory is introduced, such as the definitions of harmonics, sequence of harmonics, source of harmonics, general harmonic indices, effects of harmonics, harmonics distortion limited standards and harmonics filters.

Chapter 3: provides a detailed introduction of FT and WT. The brief summaries and applications of the FS, FT, DFT, and FFT are presented. And then, to overcome the limitations of the FT, the WT including development and definition of the WT, wavelet basic and examples of wavelet function are introduced. Moreover, for practical implementation of the WT, the WT filter banks implementing DWT and DWPT are discussed.

Chapter 4: proposes a new approach based on WT and fuzzy logic for PQ classification. After giving an overview of the existing methods for PQ classification, the WT decomposition based on DWT filter bank and the Parseval's theorem are introduced. To extract features in PQ disturbance, the energy distribution of wavelet at each decomposition level is calculated. Then, a fuzzy-expert system is employed to classify disturbance according to the wavelet decomposition level and the numerical value of the energy distribution. The types of disturbances concerned are related to voltage sag/swell, interruption, harmonic, and flickers.

Chapter 5: proposes a WT based approach which is the combination of the DWPT filter bank and CWT to harmonic analysis. After the brief summaries of existing methods for harmonic analysis, the DWPT filter bank is used to decompose and reconstruct the signal for the uniform frequency sub-band, and then the CWT is presented to calculate the harmonic components which contain frequencies, amplitudes and phases. The proposed method is tested with the synthesised signal including time-invariant waveforms and non-stationary waveforms, and field-test waveform. All of these results are compared with the results of the FFT and the results of the combination of the DWT filter bank and CWT.

Chapter 6: evaluate the harmonic penetration and explore the effects to the harmonic penetration with increasing renewable power generations in power networks. After the brief introduction of test power system, evaluation method and the harmonic sources, the summaries of two tests are presented. Though these two tests, the effect of increasing renewable power generations to the harmonic power flow is investigated.

Chapter 7: detail the conclusion of the thesis and suggestion for future work.

1.5 Associated Publications

According to the research work that has been done in this thesis, the following publications have been published or submitted for review:

Xinyi Gu and K L Lo: "*Wavelet transform based fuzzy logic for power quality classification*", this paper appears in: 45th International Universities Power Engineering Conference (UPEC), Cardiff, UK, September 2010.

Xinyi Gu, Gengyin Li, Ming Zhou and K L Lo: "*Wavelet transform based approach to harmonic analysis*", this paper appears in: 11th International Conference on Electrical Power Quality and Utilisation (EPQU), Lisbon, Portugal, October 2011.

Xinyi Gu and Professor K L Lo, "*Harmonic penetration effects of increasing renewable power generations in power networks*", under preparation.

Chapter 2 Power System Waveform Distortion

2.1 Introduction

There are no general agreements on what Power Quality (PQ) is. However, any literatures concerned with PQ do agree that PQ is an important factor in power system. Utilities would like to deliver products to meet the quality refererences in the standards, while all customers want to obtain electricity supply with high PQ. The understandings of PQ may vary from different kinds of views. Power utilities may consider that PQ is the reliability of systems. As for equipment manufacturers, the PQ may be treated as the levels of power supply that enable the proper operations of equipment. Meanwhile, from the customers' view, the PQ could be considered as ensuring the continuous power supply to maintain normal life [27].

According to some references [4], the origins of PQ problems are caused by unpredictable events, the electric utility, the customer and the manufacture. Power supply with poor quality is normally caused by power-line disturbances, such as voltage sag/swell, harmonic distortion, flicker, momentary interruptions, impulses and so on. The poor PQ can have a large detrimental effect on both the industrial process and commercial users.

Harmonic analysis plays an important role in PQ study because harmonic have great influence on the power system equipment as well as on their operation. Electricity generation with renewable sources requires a large number of renewable energy generators, more highly sensitive electronic equipment and more electronics or microprocessor controllers are used in the power system, resulting in more harmonics injection in power system.

In this chapter, a detailed survey on PQ issues especially on harmonics is presented. Then, the next section starts by introducing a brief summary of PQ including PQ disturbance. The PQ classification and main components in PQ problems are discussed in **Section 2.3** in order to solve PQ problems. The definitions, standards and relative information are presented in **Section 2.4** and **Section 2.5** respectively. Following this, an overview of harmonic filer is presented in order eliminate harmonic effects in **Section 2.6**. Finally, a brief conclusion is given in **Section 2.7**.

2.2 Introduction to Power Quality

2.2.1 Definition of Power Quality

Back in the 1970s [28], the term of PQ was first mentioned by electrical power utilities, including the limits on voltage and frequency fluctuations, voltage unbalance, transient voltage, voltage harmonics and interruptions. The purposes of introducing the terms of PQ were increasing the reliability of power supply system and reducing the cost of equipment failures.

In 1983, Meynaud [29] declared that the quality of the electricity could be described by two factors: the continuity of power supply and the quality of the voltage. In his publication, he introduced the sources and effects of voltage distortion, and then presented the characters of rapid voltage variation, asymmetry, transient overvoltage, and harmonics in terms of parameters and consequences.

Until now, there is no fully accepted definition about what exactly is PQ. In fact, PQ is a term which can have different meanings for different people. For utilities' sides, PQ means reliability of the system. In equipment manufactures' and customers' opinions, PQ is compatibility, i.e. they care whether the power supply characteristics are compatible with their load or not, and whether the characteristics of power supply system enable the equipment to work properly. However, almost everyone accepts that electric PQ is a very important aspect of power systems and electric machinery with direct impacts on efficiency, security and reliability. And surely the response involves the waveforms of voltage and current in an AC system, the presence of harmonic signals in bus voltages and load current, the presence of spokes and momentary low voltages, and other issues of distortion [30].

In electricity industry, engineers and researchers have tried different terminologies to describe the PQ such as "supply reliability," "service quality," "voltage quality," "current quality," "quality of supply," and "quality of consumption" [31]. In the IEC standards, the term of Electro-Magnetic Compatibility (EMC) is proposed.

EMC: is the ability of a device, equipment or system to function satisfactorily in its electromagnetic environment without introducing intolerable electromagnetic disturbances to anything in that environment [6]. It covered two aspects: a device, equipment or system should have the ability to perform normally in its environment; it should not produce too much pollution to its environment. The first aspect could stand for the voltage quality that concerned with power 'delivering end', while the second one stands for the current quality that concerned with power 'receiving end'[32].

The most common concept of PQ is defined by IEEE standard dictionary [3]:
PQ: the concept of powering and grounding sensitive electronic equipment in a manner that is suitable to the operation of that equipment.

In general, PQ is employed to express the quality of voltage and quality of current, including all momentary and steady-state phenomena. Therefore, it is considered as the measurement, analysis and improvement of the voltage or current to maintain a sinusoidal waveform at rated voltage and frequency.

2.2.2 Definition of Power Quality Disturbance

As mentioned in **Section 2.2.1**, PQ is more concerned with the deviations of voltage or current from the ideal waveform, magnitude or frequency. Such deviations are called "power quality disturbance" (PQ disturbance) [27]. In practice, it is almost impossible to keep exactly the same values as ideal voltage or current. There are always deviations in system. According to different characters of deviations, PQ disturbance could be further divided into two groups which need to be treated in different ways.

Voltage and current variation: are the small deviations from their ideal value. Actually, voltage and current magnitude are never exactly equal to their ideal values. Taking frequency as an example, it is very difficult to have the frequency operating exactly on 50 Hz or 60 Hz. Because of these considerations, the monitoring of variations needs to take place continuously. An overview of voltage and current variation is listed below [27]:

- Voltage magnitude variation
- Voltage frequency variation
- Current magnitude variation
- Current phase variation
- Voltage and current unbalance
- Voltage fluctuation
- Harmonic voltage distortion
- Harmonic current distortion
- Interharmonic voltage and current components
- Periodic voltage notching
- Mains signaling voltage
- High-frequency voltage noise

Events: are sudden and dramatic deviations from ideal values which appear to voltage (or current). For example, the magnitude of voltage suddenly drops to zero caused by the operation of a circuit breaker, which is a voltage event; a rapid overcurrent due to lighting stroke on transmission lines., which is a current event. In general, events can be monitored by triggering mechanism where starting from the moment exceeding the pre-defined threshold. An event can be classified in two often-used characteristics.

- Magnitude: the magnitude is the maximum voltage (or current) or the maximum voltage (or current) deviation from the ideal sine wave.
- Duration: the time period in which the voltage (or current) is deviated from the normal sine wave.

2.2.3 Origins of Power Quality Disturbances

According to some references [1], the origins of the PQ problems can be examined from the perspective of either customers or utility. It can be seen clearly from Figure 2-1 that in both perspective of customers and utility, most of the disturbances are caused by unpredictable events.

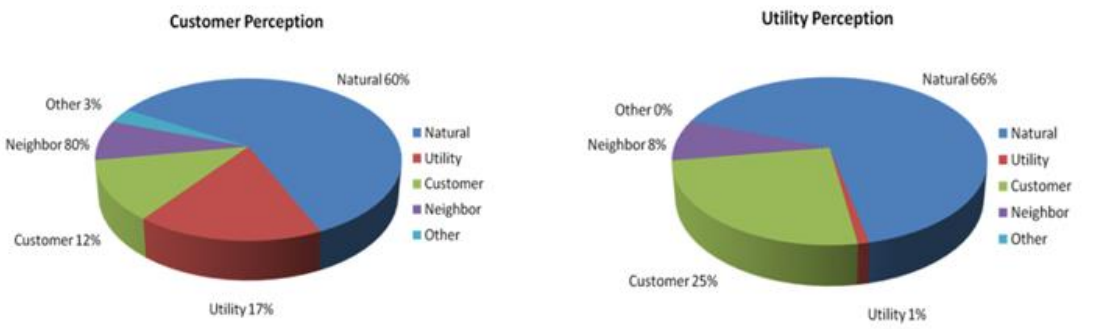

Figure 2-1 Cause of Disturbance in Power System [1]

Unpredictable Events: Basically, more than 60% of PQ problems are generated by unpredictable reasons [4], such as, storm and environment-related damage, faults, lightning surge propagation, resonance, ferroresonance, and Geomagnetically Induced Currents (GIC) due to solar flares [5].

Electric Utilities: There are three main sources of poor PQ related to utilities, including, the point of supply generation, the transmission system and the distribution system. The PQ problems caused by generating plants are mainly due to maintenance activity,, capacity and expansion constraints, load transferring from one substation to another and events leading to forces outages [1]. There are some typical PQ problems originating in the transmission system and distribution system, such as, interruptions, voltage dips, transient overvoltage, slow voltage variations, improper operation of voltage regulation devices and so on.

Customers: Customer loads may generate some PQ problems, such as, harmonic (generated by nonlinear loads), frequency variation, flicker and other relevant standard.

Manufactures: There are two aspects of causing PQ problem related to manufacturing regulations which are standards and equipment sensitivity.

2.3 Classification of Power Quality Disturbances

2.3.1 General Classes of Power Quality Disturbances

To solve PQ problems, it is necessary to fully understand the PQ classification. There are a number of methods for classifying PQ disturbances. Some of them concede that the most important factor of the classification is the duration of event and the main classification of PQ problems is steady state and transient. The table below contains a list of commonly encountered PQ problems [30].

Table 2-1 Selected Characteristics of AC Wave Distortion

Type of Distortion	Duration	Frequency Characteristics	Occurrence	Causes
Momentary low voltages (sags)	Transient	Low frequency components	In networked systems, or in radial systems fed by networked systems	Remote faults
High voltage "spikes"	Transient	High frequency components	Due to lightning, inductive circuit switching	Lightning, switching, Improper grounds
Harmonics	Steady state	Generally confined to odd integer multiples of the power frequency, usually third, fifth, seventh, eleventh, thirteenth harmonics	In load currents for solid state switched loads(e.g., adjustable speed drives, compact fluorescent lamps)	Solid state switched loads
Ringing waves (decaying oscillatory)	Transient	A transient high frequency (e.g., 17^{th} harmonic)	Capacitor switching, transformer energization	Inrush current, shunt capacitors

Three phase unbalance/neutral currents	Steady state	Power frequency	Three-phase systems	Unbalanced load, improper ground, unbalanced voltage supply
Noise	Transient/ steady state	High frequencies present	In many ac systems	Improper ground
Notches in sinusoidal wave	Steady state	High frequencies	Due to switching of inductive circuits using solid state switches	Adjustable speed drives

Some standards, e.g., IEC use the frequency range of the event for the classification. For example, IEC 61000-2-5 uses the frequency range and divides the problems into three types: low frequency (<9 kHz), high frequency (>9 kHz), and electrostatic discharge phenomena [6] and [1]. The principal phenomena causing electromagnetic disturbances according to IEC classification are shown in Table 2-2.

Table 2-2 Main Phenomena Causing Electromagnetic and Power Quality Disturbance

Conducted low-frequency phenomena	Harmonics, inter-harmonics Signaling voltage Voltage fluctuations Voltage dips Voltage imbalance Power frequency variations Induced low-frequency voltages DC components in AC networks
Radiated low-frequency phenomena	Magnetic fields Electric fields
Conducted high-frequency phenomena	Induced continuous wave (CW) voltages or currents Unidirectional transients Oscillatory transients
Radiated high-frequency phenomena	Magnetic fields Electric fields Electromagnetic field Steady-state waves Transients
Electrostatic discharge phenomena (ESD)	
Nuclear electromagnetic pulse (NEMP)	

The PQ disturbances listed in Table 2-2 can be further described with appropriate attributes [6]:

For steady-state phenomena, the required attributes are introduced as follows:

- Amplitude
- Frequency
- Spectrum
- Modulation
- Source Impedance
- Notch Depth
- Notch Area

For non-steady-state phenomena, the following attributes can be used:

- Rate of Rise
- Amplitude
- Duration
- Spectrum
- Frequency

- Rate of Occurrence
- Energy Potential
- Source Impedance

Other guidelines (e.g., IEEE-519) also classify events by using the wave shape in terms of duration and magnitude [1], as shown in Figure 2-2.

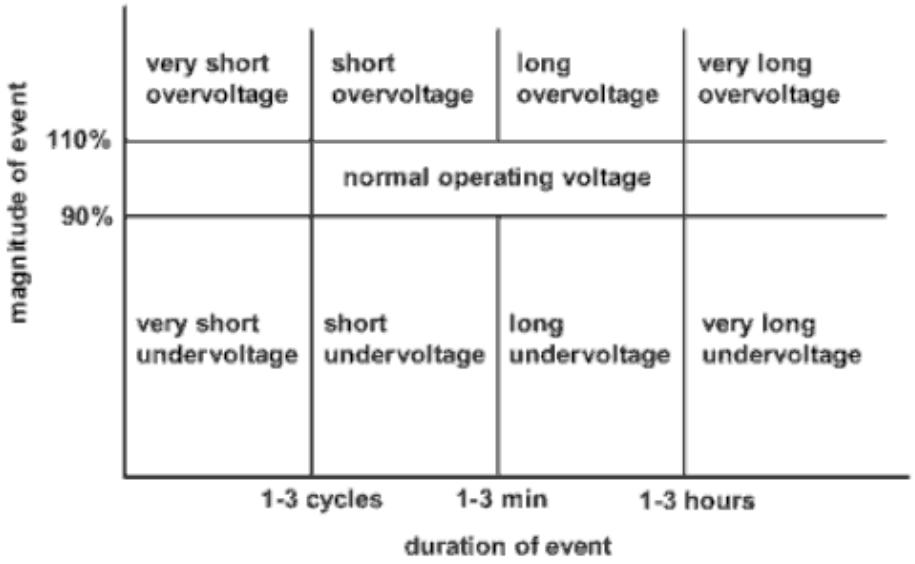

Figure 2-2 Magnitude-duration Plot for Classification of Power Quality Events [1]

According to the Figure 2-2, the duration of event is divided into four regions: very short, short, long and very long respectively, while the voltage magnitude is divided into three categories: interruption, undervoltage and overvoltage respectively.

- Interruption: voltage magnitude is zero
- Undervoltage: voltage magnitude is below the idealvalue
- Overvoltage: voltage magnitude is above the ideal value

The border of the Figure 2-2 can be set differently according to the standard defined by users.

IEEE standard adds several terms based on IEC terminology to classify PQ issues. For example, they use the “short-duration variation” instead of “voltage sags” and “interruption”, and add a new term “voltage swells”. Table 2-3 provides information

about categories and characteristics of electromagnetic phenomena defined by IEEE-1159 [3] and [4].

Table 2-3 Categories and Characteristics of Electromagnetic Phenomena in Power System as Defined by IEEE-1159

Categories	Typical spectral content	Typical duration	Typical voltage magnitude
1.0 Transients			
1.1 Impulsive			
1.1.1 Nanosecond	5-ns rise	<50 ns	
1.1.2 Microsecond	1-μs rise	50 ns–1 ms	
1.1.3 Millisecond	0.1-ms rise	>1 ms	
1.2 Oscillatory			
1.2.1 Low frequency	<5 kHz	0.3–50 ms	0–4 pu
1.2.2 Medium frequency	5–500 kHz	20 μs	0–8 pu
1.2.3 High frequency	0.5–5 MHz	5 μs	0–4 pu
2.0 Short-duration variations			
2.1 Instantaneous			
2.1.1 Interruption		0.5–30 cycles	<0.1 pu
2.1.2 Sag (dip)		0.5–30 cycles	0.1–0.9 pu
2.1.3 Swell		0.5–30 cycles	1.1–1.8 pu
2.2 Momentary			
2.2.1 Interruption		30 cycles–3 s	<0.1 pu
2.2.2 Sag (dip)		30 cycles–3 s	0.1–0.9 pu
2.2.3 Swell		30 cycles–3 s	1.1–1.4 pu
2.3 Temporary			
2.3.1 Interruption		3 s–1 min	<0.1 pu
2.3.2 Sag (dip)		3 s–1 min	0.1–0.9 pu
2.3.3 Swell		3 s–1 min	1.1–1.2 pu
3.0 Long-duration variations			
3.1 Interruption, sustained		>1 min	0.0 pu
3.2 Undervoltages		>1 min	0.8–0.9 pu
3.3 Overvoltages		>1 min	1.1–1.2 pu
4.0 Voltage unbalance		Steady state	0.5–2%
5.0 Waveform distortion			
5.1 DC offset		Steady state	0–0.1%
5.2 Harmonics	0–100th harmonic	Steady state	0–20%
5.3 Interharmonics	0–6 kHz	Steady state	0–2%
5.4 Notching		Steady state	
5.5 Noise	Broadband	Steady state	0–1%
6.0 Voltage fluctuations	<25 Hz	Intermittent	0.1–7% 0.2–2 Pst
7.0 Power frequency variations		<10 s	

NOTE: s = second, ns = nanosecond, μs = microsecond, ms = millisecond, kHz = kilohertz, MHz = megahertz, min = minute, pu = per unit.

2.3.2 Transients

The term ‘transient’ has been used in the analysis of PQ variations to indicate that an event is undesirable and momentary in nature. The common definition is broad in scope

and simply states that 'transient' is "that part of the change in a variable that disappears during transition from on steady state operating condition to another" [33]. However, this definition is used to describe just about anything unusual that happens on the power system. "Transient" is more referred to as the temporary state between two steady states. The "transient" is also considered as "surge".

According to IEEE-1159 [3], normally, the waveform variation of a transient could be unidirectional impulse or damped oscillatory. Based on their different wave shapes, transient could be divided into two groups, impulsive and oscillatory.

2.3.2.1 Impulsive Transient

An impulsive transient is a sudden, non-power frequency change in the steady-state condition of voltage, current, or both, and the polarity is unidirectional (primarily either positive or negative) [4]. In general, an impulsive transient is characterised by its rise and decay time. For example, a 1.2/50us 2000V impulsive transient is a transient whose voltage rises from zero to its peak value of 2000 V within 1.2 us and then decays to half its peak value in the next 50us [3]. A lightning current surge is the most common origin of impulsive transients. Figure 2-3 shows a typical current impulsive transient caused by lightning strike. The shape of impulsive transient will change quickly by circuit components due to the high frequency involved. In the first few microseconds, the current raises extremely fast in negative direction, then decays slowly with a few variations.

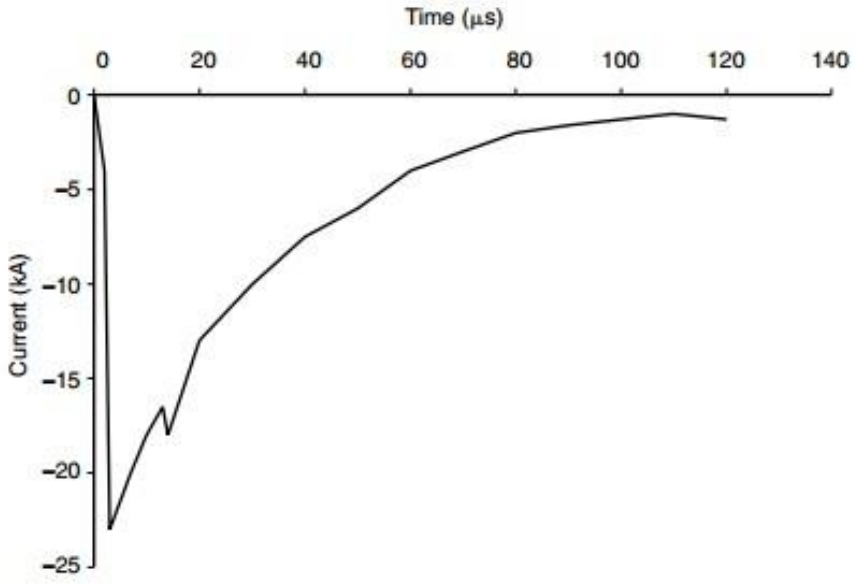

Figure 2-3 Lightning Stroke Current Impulsive Transient [4]

The shape of impulsive transients will change quickly by circuit components, because of the high frequency involved. And it shows different characteristics when viewed from different parts of the power system.

2.3.2.2 Oscillatory Transient

An oscillatory transient is a sudden, non- power frequency change in the steady-state condition of voltage, current, or both. It occurs in both positive and negative polarity. An oscillatory transient contains a voltage of current whose instantaneous value changes rapidly in polarities [4]. It is described by its predominate frequency, duration, and magnitude. The origins of the oscillatory transients are appliance switching, capacitor bank switching, fast-acting overcurrent protective, and ferroresonance. Switching actions are the main reasons for oscillatory transient. An oscillatory current transient caused by capacitor switching is illustrated in Figure 2-4 [3]. The value of current is changing rapidly in polarities, while the magnitude is reducing.

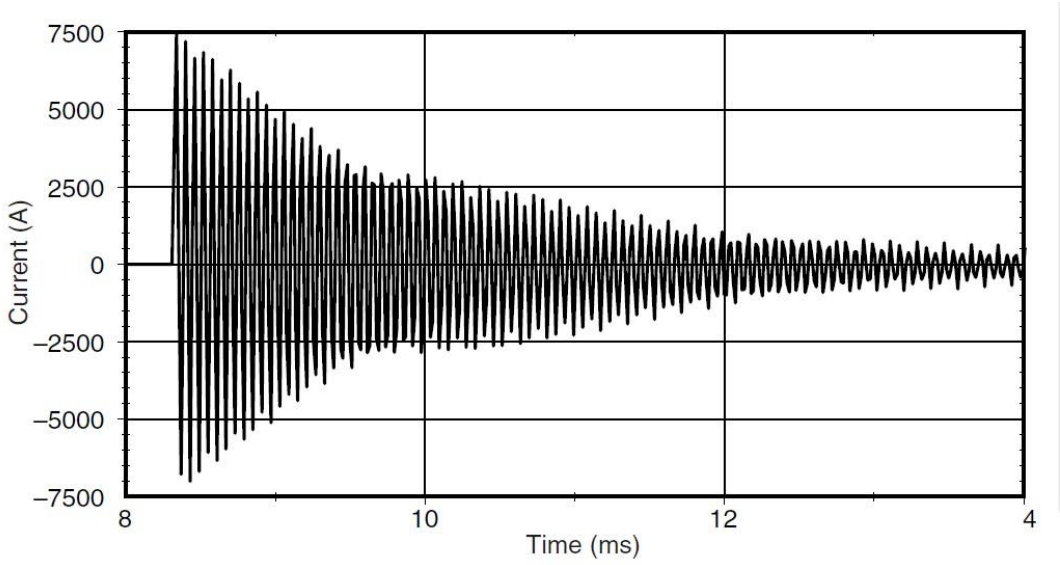

Figure 2-4 Lightning Stroke Current Impulsive Transient [3]

2.3.3 Short-duration Voltage Variations

It can be seen from Table 2-3 obviously that there are three different types of short-duration voltage variation events, depending on its duration. They are instantaneous, momentary and temporary events, and each type contains interruption, sag and swell, respectively.

The origins of short-duration voltage variations are large load energisation intermittent loose connections in power wiring and so on. Those faults can cause voltage sag, voltage swell or interruption, depending on the fault location and the system conditions.

2.3.3.1 Interruption

As depicted in European standard EN 50160 [34], a short interruption can be defined as “lower than 5% of the declared voltage”. In IEEE standard 1159 [35], a short interruption is defined as “lower than 10% of the declared voltage”. Similarly, the duration of short interruption also has different definitions. IEC defines the “short” as events up to 3 minutes, while IEEE considers the “short” as no longer than 1 min. The IEEE standards define the short interruption as “the complete loss of voltage or current (less than 0.1 pu) on one or more phase for a period of time greater than 0.5 cycles but

not longer than 1 minute" [3]. In general, a short interruption occurs when the supply voltage or load current decreases to less than 0.1 pu for a period of time less than 1 minute.

The origins of short interruptions are caused by power system faults, equipment failures, and control malfunctions. The short interruptions can further distinct into instantaneous, momentary and temporary interruptions based on their durations.

- Instantaneous interruption: is an interruption caused by non-permanent fault of less than 30 cycles.
- Momentary interruption: is an interruption lasting from 30 cycles to 3 s.
- Temporary interruption: is an interruption lasting between 3s to 1min.

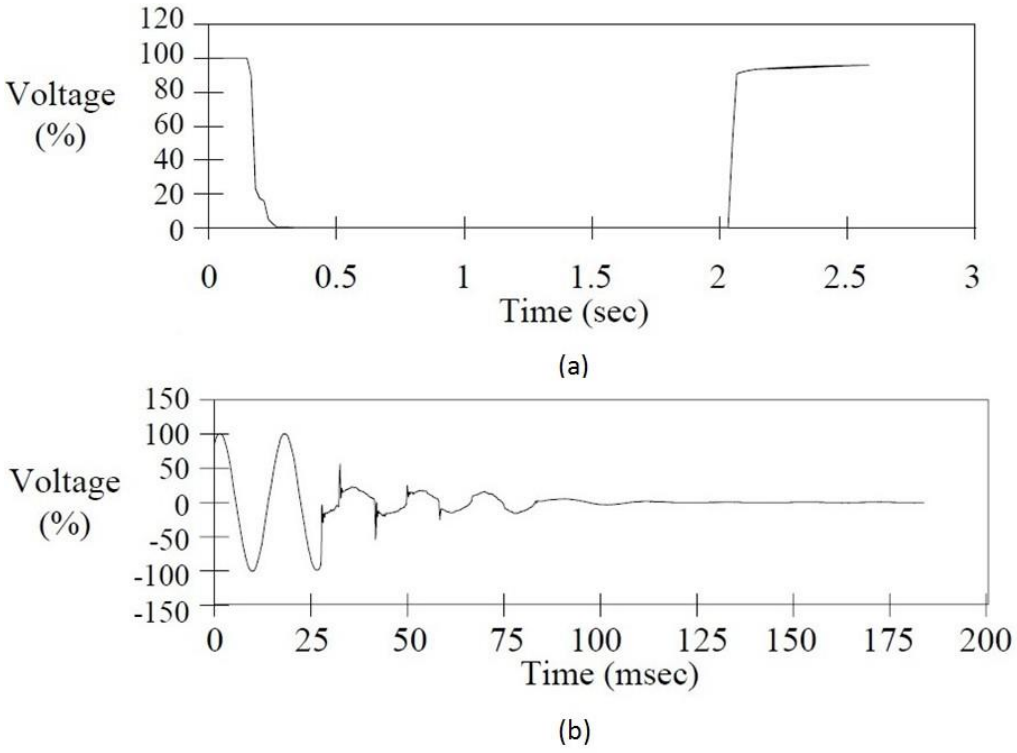

Figure 2-5 Momentary Interruption due to a Fault and Subsequent Recloser Operation [3]

Figure 2-5 is a typical momentary interruption due to a fault and subsequent recloser operation [3]. Figure 2-5 (a) is RMS value of voltage waveform for a momentary interruption event, and Figure 2-5 (b) is momentary interruption waveform. It can be

seen clearly from Figure 2-5, a momentary interruption during which voltage drops to zero for about 2.3 s. The upper plot depicts the rms variation of the entire event over a range of approximately 3 s, whereas the lower trace depicts the instantaneous voltage during the initiation of the event only. The instantaneous voltage could not completely drop to zero immediately and it takes around 0.1 second to become complete loss of voltage. In this case, the rest of voltage is due to the back-electromotive-force effect of induction motors on the interrupted circuit. Furthermore, the magnitude of voltage cannot reach the normal value as soon as fault has been cleared.

2.3.3.2 Voltage Sag

According to IEEE standards, the voltage sag is a sudden decrease to the value between 0.1 and 0.9 pu in terms of RMS values of voltage or current at the power frequency for durations from 0.5 cycle to 1 minute [3]. The definition for this phenomenon by IEC is considered as voltage dip. The concept of voltage dip is a "sudden reduction of the supply voltage recovery after a short period of time" [34]. The "short period of time" is between 10 millisecond and 1minute. Both the terms of "interruption" and "voltage sag" are used to illustrate the event of voltage magnitude decreased. The period of duration of the voltage sag is the same as short interruption.

Normally, it is hard to define the duration of voltage sag. Voltage sags have been defined from 2ms to several minutes in a variety of publications. However, the duration of sags is usually from 0.5 cycles to 1 minute. The voltage sag which is less than one-half cycle is considered as transient, while the voltage sag with the duration of longer than 1 minute is regarded as long-duration variations.

Like interruptions, sags are subdivided here into three categories depending on their durations. They are instantaneous, momentary, and temporary [4].

Voltage sags can be the results of switching operations associated with a temporary disconnection of supply, the flow of heavy current associated with the start of large motor loads, and the flow of fault current produced by customers' systems or the public supply network. Figure 2-6 illustrates a typical voltage sage caused by a Single Line-to-ground (SLG) fault on another feeder from the same substation [3].

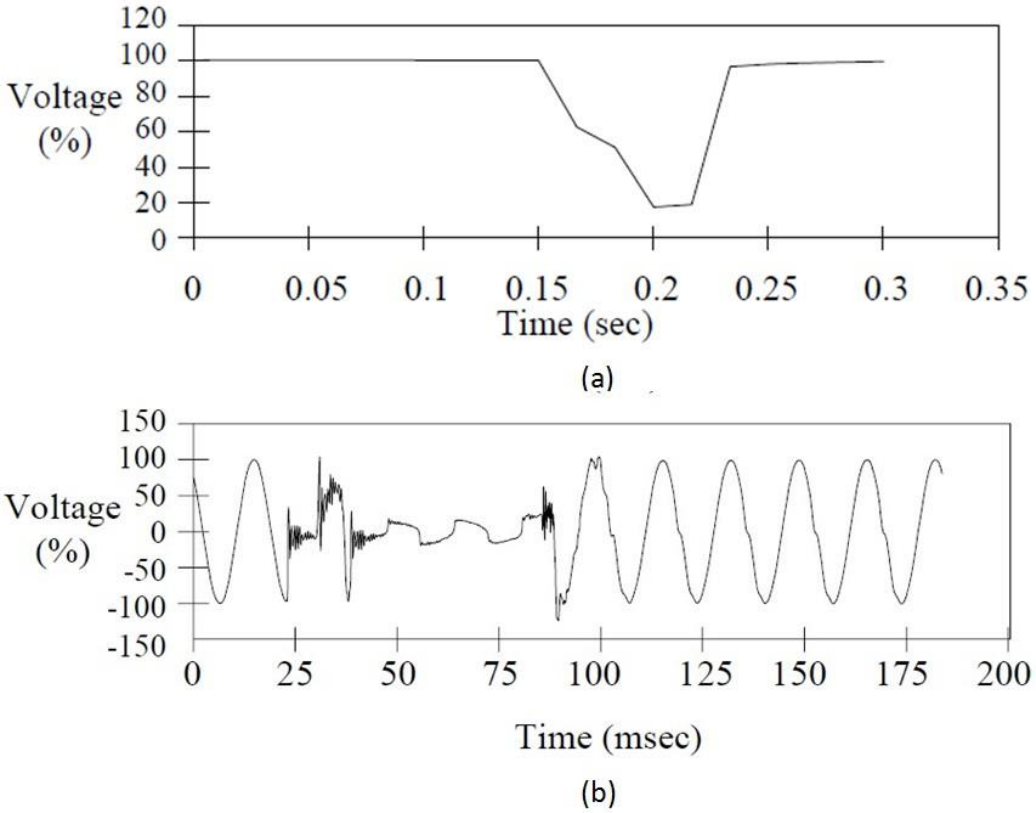

Figure 2-6 Voltage Sag Caused by SLG Fault [3]

Figure 2-6 (a) depicts RMS waveform for a voltage sag event, and Figure 2-6 (b) illustrates voltage sag waveform. A sag to 20% exists for about 0.1s. Note that there are different time scales for the upper and lower plots, and note that the initiation and end times of the RMS plot and instantaneous plots do not correspond precisely. In general, the typical fault clearing times range from 3 cycles to 30 cycles due to the fault current magnitude and the type of protection equipment.

2.3.3.3 Voltage Swell

The definition of swell is a sudden increase magnitude above 1.1 pu in terms of RMS voltage or current at the power frequency for durations from 0.5 cycle to 1 minute. The term momentary overvoltage is normally used as a synonym for the term swell. Typical value of magnitude is between 1.1 pu and 1.2 pu [3]. The swell magnitude is also referred to as its remaining voltage, and thus it will always be larger than 1.0 pu.

Voltage swells are characterised by their magnitudes and durations, and swell durations can be further divided into three categories: instantaneous, momentary, and temporary, which is consistent with interruptions and sags [4].

There are three main causes for voltage: swells, switching off a large load, energising a capacitor bank, and voltage increase of the unfaulted phase during a SLG fault. Like sags, swells are usually associated with system fault conditions, but they are much less common than voltage sag. Figure 2-7 shows a voltage swell that can be associated with a SLG fault.

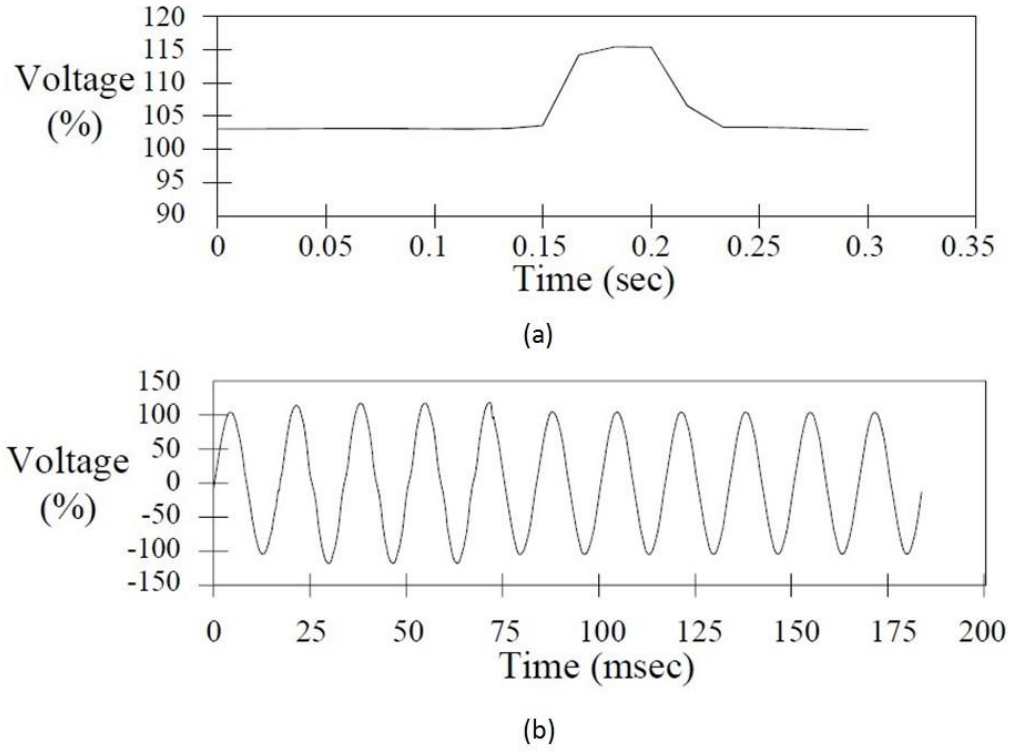

Figure 2-7 Voltage Swell Caused by SLG Fault [3]

The Figure 2-7 (a) shows the RMS value of the instantaneous voltage, and the voltage swell waveform is depicted in Figure 2-7 (b). Note that there are different time scales for the upper and lower plots, and note that the initiation and end times of the RMS plot and instantaneous plots do not correspond precisely.

2.3.4 Long-duration Voltage Variations

According to the standards such as IEEE-1159 [3] and ANSIC84.1 [36], the definition of long-duration voltage variation is that the RMS value of voltage deviates from the nominal value for longer than 1 minute. This type of event can be further divided into three categories: sustained interruption, undervoltage, and overvoltage respectively, depending on the cause of the variation.

2.3.4.1 Sustained Interruption

The sustained interruption also named long interruption is introduced as any interruptions last longer than short interruption. In the IEC definition, the duration of long interruption is more than 3 minutes [34]. In IEEE standards [3], the decrease of the supply voltage less than 10% of nominal for a period of time in excess of 1 minute is considered as a sustained interruption. Normally, the sustained interruption is defined as interruption longer that 1 minute.

The origins of sustained interruption are due to fault occurrence in a part of power systems without redundancy or with the redundant part out of operation, an incorrect intervention of a protective relay leading to a component outage, and scheduled interruption in a low-voltage network without redundancy.

2.3.4.2 Undervoltage

An undervoltage is a decrease in the RMS voltage magnitude less than 0.9 pu at the power frequency for a duration longer than 1 minute. Typical values are between 0.8 pu and 0.9 pu [3].

Undervoltages are generated by switching events which are the opposite of the overvoltages caused event. A load on switching or a capacitor bank switching off can result in undervoltage until voltage regulation equipment on the system can bring the voltage back to tolerances. Undervoltages can also be caused by overloaded circuits.

2.3.4.3 Overvoltage

The definition of overvoltage is an increase in the RMS voltage greater than 1.1 pu at the power frequency for a duration longer than 1 minute. Typical values are from 1.1 pu to 1.2 pu [3].

The causes of overvoltage can be concluded into four aspects. The first one is load switching; the second one is variations in the reactive compensation; the thirds one is poor system voltage regulation capabilities or controls; and the last one is incorrect tap setting on transformers.

2.3.5 Voltage Unbalance

When the rms values of voltage (or current) or the phase angles are not equal in a three phase system, this phenomenon is referred as unbalance. The maximum deviation from the average of the three-phase voltages or currents, divided by the average of the three-phase voltages or currents is expressed as a percentage [4]. Normally, the voltage unbalance of a three-phase service is less than 3%, while the current unbalance may be higher, especially when single-phase loads are present [3].

Voltage unbalances (< 2%) usually come from unbalanced single-phase loads on a three-phase circuit. The other sources of voltage unbalance are blown fuse on one phase of a three-phase bank, single-phase line regulators, etc. Voltage unbalances (>5%) normally caused by single-phasing conditions.

2.3.6 Waveform Distortion

Waveform distortion is considered as a steady-state deviation from an ideal sine wave of power frequency principally characterised by the spectral content of the deviation. There are primary types of waveform distortion.

- DC offset
- Harmonics
- Inter-harmonics

- Notching
- Noise

The three types of waveform distortion, including DC offset, notching and noise will be introduced as follows. The harmonics will be discussed in detail in **Section 2.4**.

2.3.6.1 DC Offset

The presence of a DC voltage or current in an AC power system is defined as DC offset. The main origins of DC offset are geomagnetic disturbance, and asymmetry of electronic power converters. DC in AC networks can cause the increase in transformer saturation, additional heating and loss of transformer life. The other effects of DC are the electrolytic erosion of grounding electrodes, additional stressing to insulation, and other connectors [4].

2.3.6.2 Notching

A periodic voltage disturbance caused by the normal operation of power electronic devices when current is commutated from one phase to another is called notching. Since notching is in steady-state, it can be characterised through the harmonic spectrum of the affected voltage. However, the frequency components associated with notching can be quite high and may not be readily characterised with typically harmonic measurement equipment [4].

Figure 2-8 is a voltage notching caused by three-phase convertors. The voltage notching occurs when the current commutates from one phase to another. At the same time, there is a momentary short circuit between two phases. The notches at any points in the system are decided by the source inductance and the isolating inductance between the convertor, the magnitude of the current, and the monitored point [3].

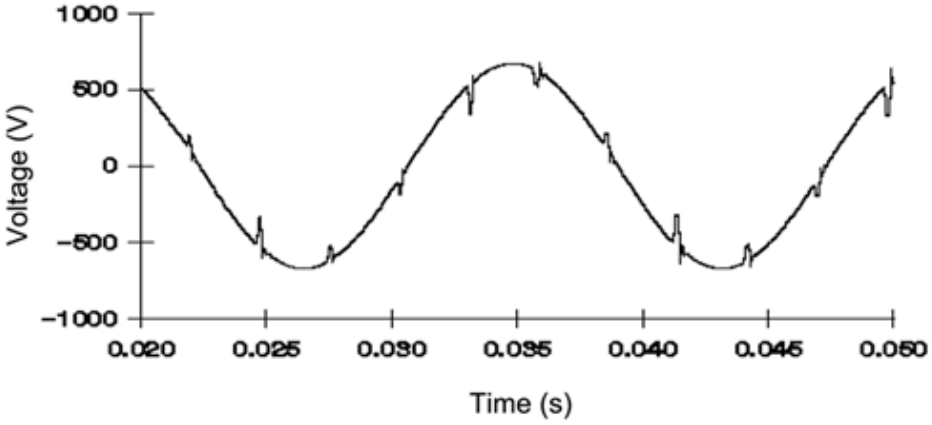

Figure 2-8 Voltage Notching Caused by Convertor Operation [3]

2.3.6.3 Noise

The definition of noise is unwanted electrical signals with broadband spectral content typically lower than 200 kHz superimposed upon the power system voltage or current in the phase conductors, or found on neutral conductors or signal lines [1].

The origins of electric noise are due to fault isolation in transmission or distribution systems, arc furnaces, electrical furnaces, power electronic devices, switching power supplied, loads with solid-state rectifiers and control circuits. Noise problems are usually exacerbated by improper grounding. The major effect of noise is disturbing electronic devices such as microcomputers and programmable controllers. Basically, problems caused by noise can be mitigated by using filters, isolation transformers, and line conditioners.

2.3.7 Flicker

Flicker is referred to as voltage variation which is caused by continuous and rapid variations in the load current magnitude [37]. The term of flicker is derived from the impact of the voltage fluctuation on lighting intensity so that they are perceived by the human eye.

The major cause of flicker is arc furnaces, which is one of the most common causes of flickers in utility transmission and distribution system. Figure 2-9 shows a voltage waveform that produces lamp flicker due to an arc furnace operation [3].

Flickers are generally defined by the RMS magnitude of the modulation signal expressed as a percent of the fundamental frequency. This can be obtained by demodulating the waveform to remove the fundamental frequency and then measuring the magnitude of the modulation components. Typically, magnitudes as low as 0.25 percent can result in perceptible lamp flicker if the frequencies are in the range of 6 to 8 Hz. Flickers mainly impact on people rather than equipment, and may bring inconvenience and disturbance to low voltage level customers.

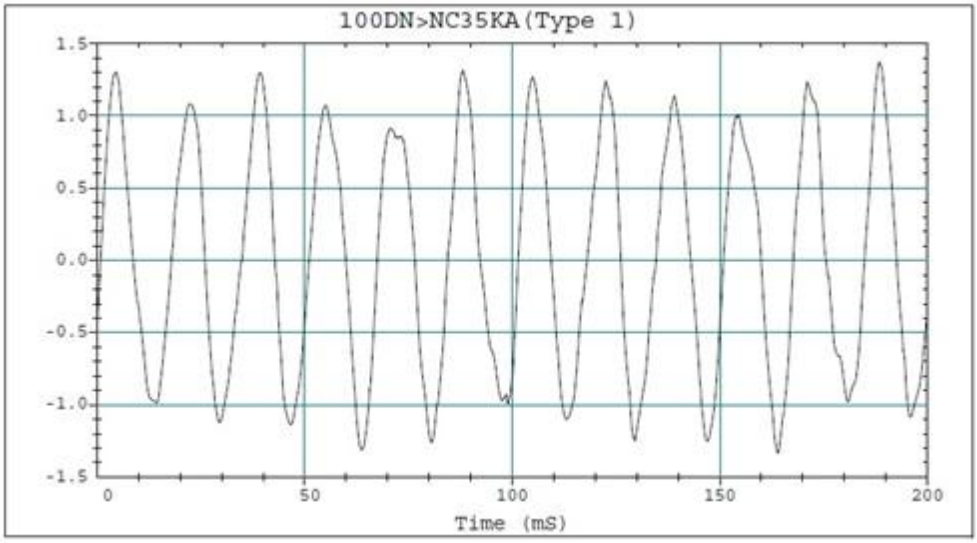

Figure 2-9 Flickers Caused by Arc Furnace Operation [3]

2.4 Power Quality- Harmonic

2.4.1 Definition of Harmonic

The electricity supply is represented in the form of voltage and current with a RMS value. The voltage has a sinusoidal wave-shape with a fixed frequency 50Hz or 60Hz depending on countries. The voltage is supplied with a linear load, and thus the current flowing for that load is also a sinusoidal wave of the same frequency for that voltage. However, if the load is non-linear, then the current is not proportional to the applied voltage and thus the distortion is generated.

2.4.1.1 Integer Harmonic

Any periodic distorted waveform can be expressed as a sum of sinusoids. These individual sinusoids are called harmonics. Both the IEEE and IEC organisations have defined harmonics in the same way based on UIE-DWG-3-92-G [38]. The definition is "harmonics are sinusoidal voltages or currents having frequencies that are integer multiples of the frequency at which the supply system is designed to operate." The fundamental frequency is 50 Hz or 60 Hz depending on the countries.

$$\boldsymbol{f^{(h)}(t) = A^{(h)} \times \sin\left(2\pi hft + \alpha^{(h)}\right)} \quad \textbf{(2.1)}$$

where f is the fundamental frequency and h^{th} is the harmonic order. A means the amplitude and the a is the phase angle. The characteristic currents that are determined by the pulse number, the Figure 2-10 shows the typical 6-pulse rectifier generated fifth and seventh integer harmonic waveforms.

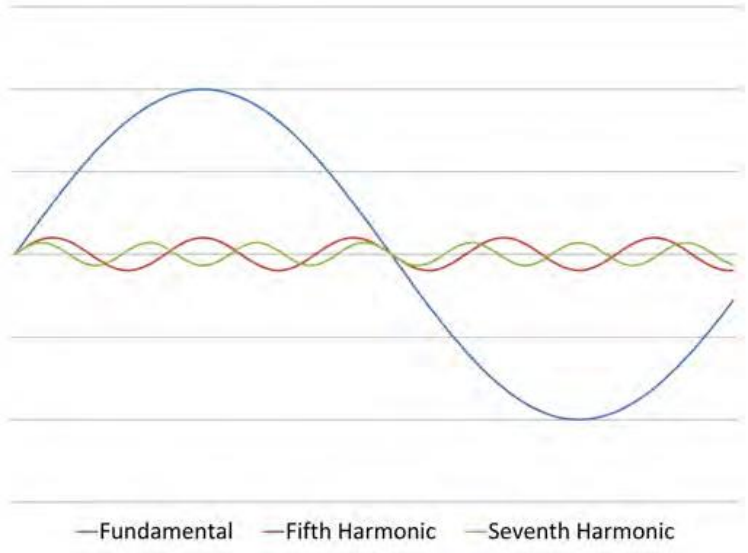

Figure 2-10 First, Fifth and Seventh Harmonic Waveforms [22]

However, with the development of electronic technology, situations become more complicated. The waveform can also be distorted by non-linear equipment, and thus it contains harmonic components with non-integer multiples of the fundamental frequency. Therefore, the concept of the harmonic can be extended that any components in the signal with different frequencies from the fundamental frequency can be referred to the harmonic. Any frequencies involves integer, non-integer or sub integer multiples of the fundamental frequency [22].

2.4.1.2 Inter Harmonic

The non-integer of the harmonic is also referred to as the term inter harmonic. Based on Equation 2.1, *h* is a fraction with the value larger than one, e.g. 2.5, 3.6 …

2.4.1.3 Sub Harmonic

There is still a part of components between zero and one for the analysed harmonic, which can be named as sub harmonic. Similarly, *h* is a fraction between zero and one, e.g. 0.5, 0.8 etc. based on Equation 2.1.

2.4.2 Expression of Harmonics

As defined by the IEEE and IEC organisations, the distorted or non-sinusoidal waveforms with periodic characteristic can be composed of the sum of various sinusoids, and each sinusoid component can be considered as harmonics, compared to the original waveform. Fourier series (FS) is involved to reformulate this kind of non-sinusoidal waveform for convenient and better analysis. Any continuous signals with a repetitive interval T can be represented by the sum of an infinite series of sinusoidal or cosinusoid components, which is referred to as FS proposed by J.B.J. Fourier in 1822 [21]. The analysis of harmonics with FS is a conventional method. The concept and expression of FS will be considered in detail in Chapter 3 in the thesis.

2.4.3 Odd and Even Harmonics

Based on the order of the harmonic, two groups can be divided. There are odd and even harmonics. The differences between them are list below [39].

Odd harmonic: When the response function is odd $f(x) = -f(-x)$, the resulting signal consists of only odd harmonics of the input sine wave;

- Odd harmonics (1^{st}, 3^{rd}, 5^{th},…) are the characteristic harmonic components in modern power systems due to the three-phase symmetry of the present infrastructure.
- The output signal is symmetric. Symmetry is very important in a power system waveform.
- A simple example is clipping in a symmetric push-pull amplifier.

Even harmonic: When the response function is even $f(x) = f(-x)$, the resulting signal consists of only even harmonics of the input sine wave;

- The even harmonics (2^{nd}, 4^{th}, 6^{th}, …) are not symmetric.
- The fundamental is also an odd harmonic, and thus is not presented.
- A simple example is a full-wave rectifier.

The comparison: Figure 2-11 shows the difference between odd and even harmonic distortion waveforms. The y-axis is the magnitude of current, while the x-axis is the phase degree.

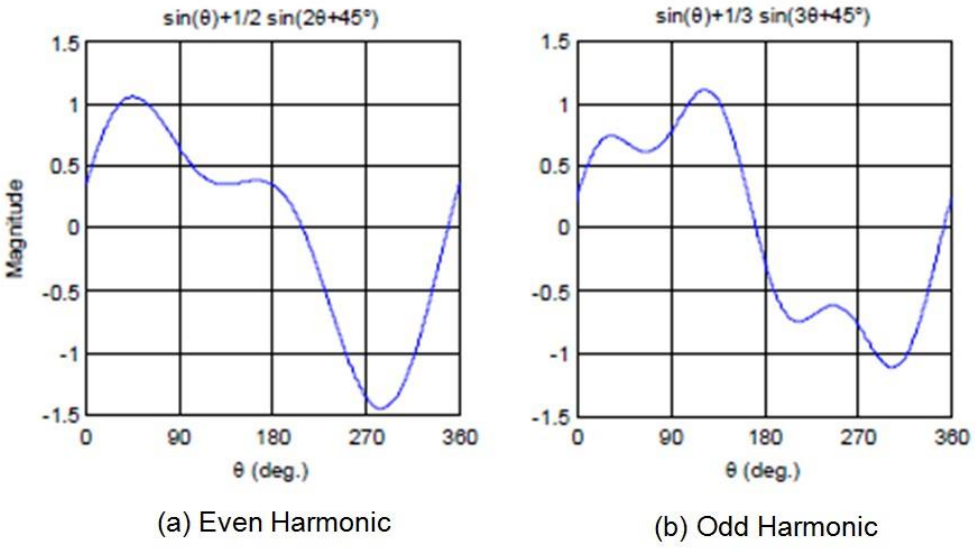

Figure 2-11 Comparison of Even and Odd Harmonic Current Waveforms [39]

- The waveform containing the even harmonic is an asymmetrical one, which has unequal positive and negative peaks, as shown in Figure 2-11 (a). The waveform containing the odd harmonic remains symmetric despite its distortion as shown in Figure 2-11 (b).
- Symmetrical waveforms contain only odd harmonics but asymmetrical waveforms may contain both even and odd harmonics.
- Symmetry is essential to the performance of AC system, while asymmetry can cause a number of problems to system operation, and result in a DC offset. Direct current in AC system will bring additional stresses on insulation and other adverse impact. Therefore, even harmonic in the power network can have a more harmful impact than odd harmonic.
- Most power system elements are symmetrical. They produce only odd harmonics and have no DC offset.

2.4.4 Sequence of Harmonics

An important concept in harmonics is called “sequence”. There are three types of sequences: [40]

Zero sequence: consisting of three phasors with equal magnitudes and with zero phase displacement, as shown in Figure 2-12.

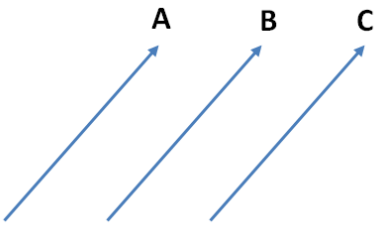

Figure 2-12 Zero Sequence

Positive sequence: consisting of three phasors with equal magnitudes, + -120 phase displacement, and positive sequence, as shown in Figure 2-13.

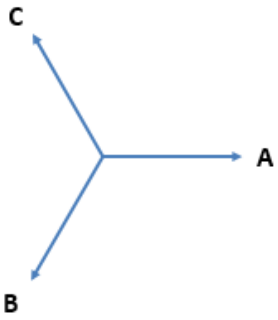

Figure 2-13 Positive Sequence

Negative sequence: consisting of three phasors with equal magnitudes, + - 120 phase displacement, and negative sequence, as shown in Figure 2-14.

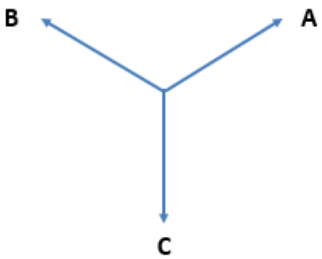

Figure 2-14 Negative Sequence

As illustrated in Table 2-4, in AC system, the fundamental three phase voltage or current have equal magnitude and 120^o phases-shifted, which A-B-C is placed in order when it takes phasor A as reference.

Table 2-4 Sequence of Harmonic

Fundamental	A 0°	B 120°	C 240°	C-B-A
3rd harmonics	A' 3 X 0° (0°)	B' 3 X 120° (360°=0°)	C' 3 X 240° (720°=0°)	No rotation
5th harmonics	A" 5 X 0° (0°)	B" 5 X 120 （600°=360°+240°） （240°）	C" 5 X 240° （1200°=1080°+120°） （120°）	A-B-C
7th harmonics	A'" 7 X 0° (0°)	B'" 7 X 120° （840°=720°+120°） （120°）	C'" 7X 240° （1680°=1440°+240°） （240°）	C-B-A
9th harmonics	A'''' 9 X 0° (0°)	B'''' 59X 120° （1080°= 0°）	C'''' 9 X 240° （2160°= 0°）	No rotation

- Harmonics such as 3rd, 9th become 0^o phase-shifted to each other, which does not "rotate" at all because they are equal in phase with each other, are called zero sequence.
- Harmonic such as 5th is 120^o phase-shifted to each other, which "rotate" in opposite sequence as the fundamental, are called negative sequence.
- Harmonic such as 7th is 120^o phase shifted to each other, which "rotate" with the same sequence as the fundamental, are called positive sequence.

Table 2-5 continues to categorize other odd-numbered harmonics, lending itself to expression in a table shown as below. '+', '-' and '0' represent positive, negative and zero sequence respectively. Sequence especially matters when it comes to dealing with AC motors, since the mechanical rotation of the rotor depends on the torque produced by the sequential "rotation" of the applied 3-phase power. Positive sequence frequencies work to push the rotor in the proper direction, whereas negative sequence frequencies actually work against the direction of the rotor's rotation. Zero-sequence frequencies neither contribute to nor detract from the rotor's torque

Table 2-5 Rotation Sequences According to Harmonic Number

Harmonic Order	Harmonic Sequence	Harmonic Order	Harmonic Sequence	Harmonic Order	Harmonic Sequence
1	+	14	-	27	0
2	-	15	0	28	+
3	0	16	+	29	-
4	+	17	-	30	0
5	-	18	0	31	+
6	0	19	+	32	-
7	+	20	-	33	0
8	-	21	0	34	+
9	0	22	+	35	-
10	+	23	-	36	0
11	-	24	0	37	+
12	0	25	+	38	-
13	+	26	-	39	0

2.4.5 Source of Harmonics

According to references [41] and [42], the origins of electrical power system harmonic problems are mainly due to the substantial increase of power electronic equipment and the electronics or microprocessor controllers in modern industry. There are many reasons for harmonics generated in power systems, such as industrial nonlinear loads, residential loads with switch-mode power supplies. The most common sources are non-linear loads, which are including electric arc furnaces, static VAR compensators, inverters, DC converters, switch-mode power supplies, and AC or DC motor drives [43]. These sources can be divided into three groups of equipment.

- Magnetic core equipment, like transformers, electric motors, generators, etc.
- Arc furnaces, arc welders, high-pressure discharge lamps, etc.
- Electronic and power electronic equipment.

Among these sources, the major sources of harmonics are power electronic converters and arcing devices. Converters are used to convert AC to DC and vice versa. The cyclo-converter which is the AC to AC converter is the main source of inter-harmonics. Other non-linear equipment, such as adjustable-speed motor drives, dc motor drives, electronic power suppliers, battery chargers and electronic ballasts can also produce the

harmonics. Arcing devices include arc furnaces, arc welders, and discharge-type lighting with magnetic ballasts.

In recent years, the use of wind power for electricity generation is actively developed all over the world. In the case of wind power generation, the designs of the systems involve some power electronic devices to act as reactive power compensators, variable-speed controllers or power converters. All of these would introduce harmonics, therefore, wind power generator become another important source of harmonics in power system.

Wind power generators are classified into two types according to the wind turbine speed control topologies. One is fixed speed turbines; the other is variable speed turbines. In the early 1990s, the fixed speed wind turbines with induction generators were commonly used. The advantages of fixed speed wind turbines are simple, robust, cheap, and reliable, while the disadvantages are uncontrollable wind speed, uncontrollable reactive power consumption, and limited PQ control. Hence, this type of wind turbines cannot utilize the wind power efficiently. Variable speed wind turbines overcome the disadvantages of fixed speed wind turbines, and have now become the dominant wind turbines. It improves the PQ and reduces mechanical stress. However, it increases the cost of equipment for more complicated electrical and control systems. More harmonics and losses are generated by the power converters connected between the machines and the power network [44].

According to reference [44][45][46], four different types of Wind Turbine Generator (WTG) including fixed speed and variable speed wind turbines are shown in Figure 2-15. In Figure 2-15(a), a fixed speed wind turbine that an induction generator is connected to WTG step-up transformer directly through a soft starter. Figure 2-15(b) indicates a wound rotor induction generator (WRIG) is connected to WTG step-up transformer directly similar to type A. Figure 2-15(a) and Figure 2-15(b) are fixed speed wind turbines, while Figure 2-15(c) and Figure 2-15(d) are variable speed wind turbines. In Figure 2-15(c), the generator speed is controllable by a variable rotor resistance. The stator of a doubly fed induction generator (DFIG) is connected to the WTG step-up transformer directly, while the rotor is connected to the transformer through a power

converter. Figure 2-15(d) illustrates a variable speed wind turbine that permanent magnetic synchronous generator (PMSG) or wound rotor synchronous generator (WRSG) or WRIG is connected to the step-up transformer through a full scale power converter as well

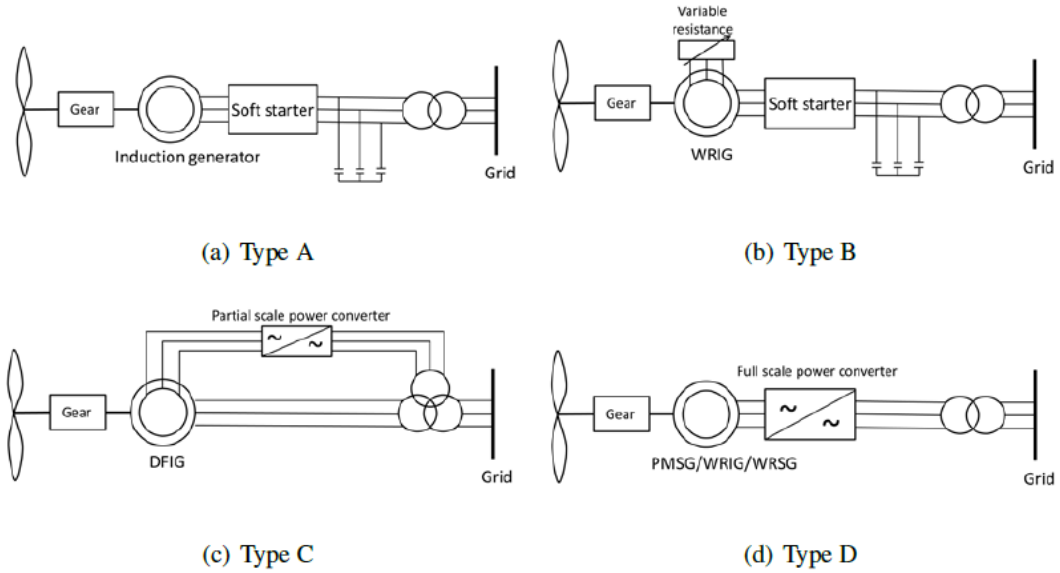

Figure 2-15 Four Types of Wind Turbine Generators [44]

The harmonic emissions of WTG are considered as the following three aspects: [44] [46] [48] [49] [50]

- Grid-side power electrical converters.
- Significant amount of capacitance in wind power plant.
- A long high voltage transmission cable in a typical wind farm.

And the power electrical converters are regarded as the main source for harmonic emissions of wind turbines.

2.4.6 Current and Voltage Harmonic Distortion

2.4.6.1 Current Harmonic Distortion

Harmonic distortion can be represented in terms of current and voltage waveforms in the power system. The major source of current distortion is still non-linear loads. These

non-linear loads might be single phase loads, such as point-of-sale terminals, or three-phase in variable speed drives.

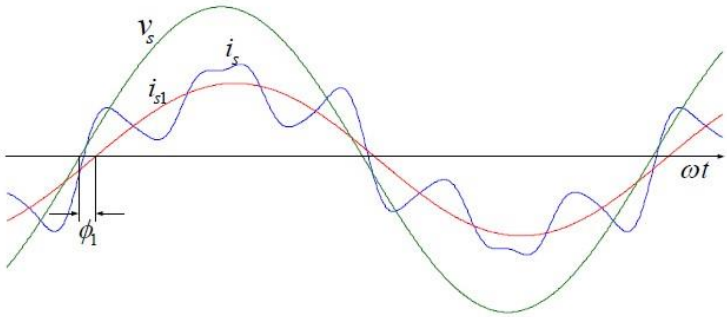

Figure 2-16 Distorted Line Current Waveform [51]

Figure 2-16 presents a distorted line current waveform and identifies key parameters used in analysis [51]. Figure 2-17 illustrates the measurement of current drawn by a non-linear load. The RMS of the current contains both the fundamental and harmonics [52].

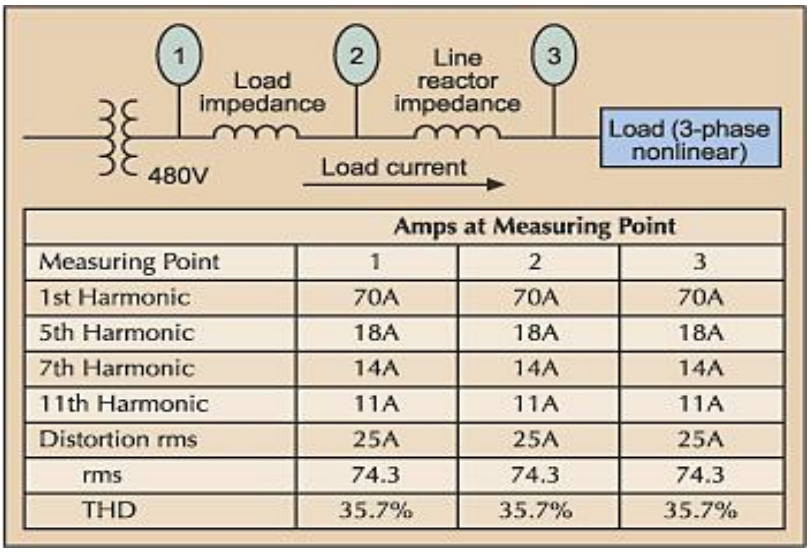

	Amps at Measuring Point		
Measuring Point	1	2	3
1st Harmonic	70A	70A	70A
5th Harmonic	18A	18A	18A
7th Harmonic	14A	14A	14A
11th Harmonic	11A	11A	11A
Distortion rms	25A	25A	25A
rms	74.3	74.3	74.3
THD	35.7%	35.7%	35.7%

Figure 2-17 Measurement of Current Drawn by a Non-linear Load [52]

It can be seen from Figure 2-17 that the value of current and the RMS value of the current are the same at each measuring point for each harmonic. It can be considered as a system only containing fundamental current. The term “distortion RMS” is used to denote the RMS value of harmonic current with the fundamental left out of the summation. The RMS current is basically equal to the total effective load current. Total

Harmonic Distortion (THD) can be calculated by using the value of distortion RMS current.

Since operation of non-linear loads generates the current distortion waveform, which is path dependent, the effect of current distortion on loads within a facility is minimal. Therefore, current harmonic distortion cannot flow into equipment other than the non-linear loads that cause them. However, the effect of current distortion on distribution systems can be serious, primarily because of the increased current flowing in the system. Current harmonic distortion can cause the destruction of loads or loss of production directly or indirectly. Harmonic current also may increase heat losses in transformers.

2.4.6.2 Voltage Harmonic Distortion

As the current distortion is conducted through the normal system wiring, it creates voltage distortion. Voltage distortion is generated when harmonic currents flow across circuit reactance and resistances, producing voltage drops at the harmonic frequencies. While current distortion travels only along the power path of the non-linear load, voltage distortion impacts all loads connected to the particular bus or phase.

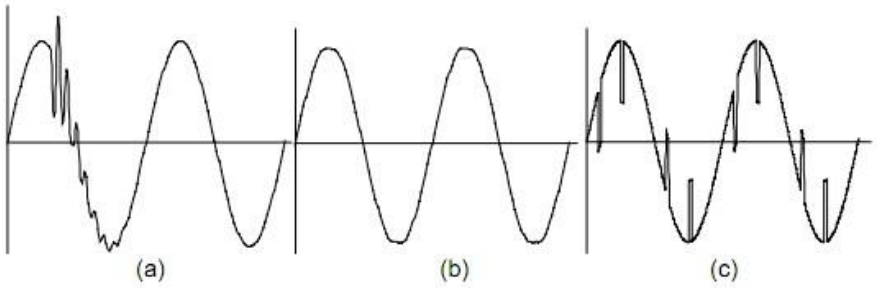

Figure 2-18 Distorted Voltage Waveform [51]

Figure 2-18 (a) illustrates a distortion appeared on one cycle occasionally. It is not a harmonic distortion. This distortion is caused by switching of power factor correction capacitors on the power system Figure 2-18 (b) and (c) show voltage harmonic distortions due to flat-topped and notching effect respectively [51].

Figure 2-19 presents the measurement of voltage in a system powering a nonlinear load. As seen in this figure the values of harmonic voltage and the RMS value of the voltage are not the same at each measuring point in each harmonic [52]. It can be considered as this system containing both the fundamental and harmonics voltage. The term "distortion RMS" is used to indicate the RMS value of harmonic voltage with the fundamental left out of the summation. The RMS voltage is basically equal to the total effective load voltage. THD can be calculated by using the value of distortion RMS voltage.

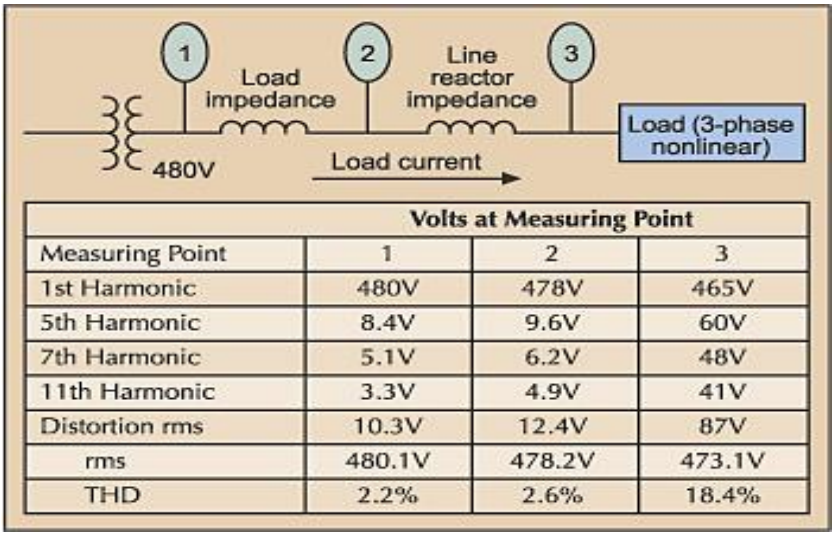

	Volts at Measuring Point		
Measuring Point	1	2	3
1st Harmonic	480V	478V	465V
5th Harmonic	8.4V	9.6V	60V
7th Harmonic	5.1V	6.2V	48V
11th Harmonic	3.3V	4.9V	41V
Distortion rms	10.3V	12.4V	87V
rms	480.1V	478.2V	473.1V
THD	2.2%	2.6%	18.4%

Figure 2-19 Measurement of Voltage Drawn by a Non-linear Load [52]

High-voltage distortion with a non-linear load at the terminals is not proportional to the high distortion which will be present throughout the system. In fact, the lower voltage distortion, the closer a bus is located to the service transformer. However, if excessive voltage distortion does exist at the transformer, it can pass through the unit and appear in facilities distant from the origin.

Distorted voltage can cause overheat and vibrate excessively of motors. It can also cause damage to the motor shaft. Voltage distortion appears to have slight effect on operation of nonlinear loads connected either phase-to-phase or phase-to-neutral. Unlike current distortion, it is not path dependent, harmonic voltages generated in one part of a facility will appear on common buses within that facility. The effect of voltage

distortion on loads within a facility is high. However, voltage distortion has minimal effect on a distribution system.

2.4.7 General Harmonic Indices and Measures

In this section, concepts and expressions of formulations are introduced in detail, which are often used to analyse harmonic characteristics directly or perform calculation and describe features of harmonics.

2.4.7.1 Harmonic Voltage and Current

Referred to as FS, the voltage and current of harmonic can be described as follows:

$$\boldsymbol{v(t) = V_{DC} + \sum_{h=1}^{n} V^{(h)} \cos\left(h\omega_0 t + \alpha^{(h)}\right)} \quad \textbf{(2.2)}$$

$$\boldsymbol{i(t) = I_{DC} + \sum_{h=1}^{n} I^{(h)} \cos(h\omega_0 t + \beta^{(h)})} \quad \textbf{(2.3)}$$

V_{DC} - DC component voltage

I_{DC} - DC component current

h - Harmonic order

$V^{(h)}$ - h^{th} maximum magnitude of harmonic voltage

$I^{(h)}$ - h^{th} maximum magnitude of harmonic current

w_o - fundamental angular frequency

$\alpha^{(h)}$ - phase angle of the h^{th} harmonic voltage

$\beta^{(h)}$ - h^{th} harmonic current phase angle

2.4.7.2 Root Mean Square Value of Voltage and Current

Similarly, the RMS value of voltage and current can be represented as below according to the concept of RMS

$$V_{rms} = \sqrt{(V_{DC})^2 + \sum_{h=1}^{n} (v_{rms}^{(h)})^2}$$

$$= \sqrt{(\boldsymbol{V_{DC}})^2 + (\boldsymbol{V_{rms}^{(1)}})^2 + (\boldsymbol{V_{rms}^{(2)}})^2 + \cdots + \left(\boldsymbol{V_{rms}^{(n)}}\right)^2} \quad \textbf{(2.4)}$$

$$I_{rms} = \sqrt{(I_{DC})^2 + \sum_{h=1}^{n} (i_{rms}^{(h)})^2}$$

$$= \sqrt{(\boldsymbol{I_{DC}})^2 + (\boldsymbol{I_{rms}^{(1)}})^2 + (\boldsymbol{I_{rms}^{(2)}})^2 + \cdots + \left(\boldsymbol{I_{rms}^{(n)}}\right)^2} \quad \textbf{(2.5)}$$

where *h* means the h^{th} order of the harmonic components for voltage and current. V_{DC} and I_{DC} might be equal to zero if there is no DC components for voltage and current.

2.4.7.3 Active Power and Reactive Power

Based on the concept of RMS, the active power and reactive power can be expressed in equations as below:

$$\boldsymbol{P = V_{DC} I_{DC} + \sum_{h=1}^{n} v_{rms}^{(h)} i_{rms}^{(h)} \cos\left(\alpha^{(h)} - \beta^{(h)}\right)} \quad \textbf{(2.6)}$$

$$\boldsymbol{Q = \sum_{h=1}^{n} v_{rms}^{(h)} i_{rms}^{(h)} \sin\left(\alpha^{(h)} - \beta^{(h)}\right)} \quad \textbf{(2.7)}$$

2.4.7.4 Total Harmonic Distortion

Usually, the harmonic distortion levels are measured by Total Harmonic Distortion (THD).

THD: a measurement of harmonic distortion based on fundamental frequency, is defined as the sum of all harmonic components of the voltage or current waveform compared to the fundamental components of the voltage or current wave [53].

$$THD = \frac{\sqrt{V_2^2 + V_3^2 + V_4^2 + \ldots + V_n}}{V_1} \quad \textbf{(2.8)}$$

where, V_1 is the fundamental voltage, and V_2, V_3,…V_n are referred to as the higher frequency of harmonic voltages.

2.4.7.5 Total Demand Distortion

For harmonic current characteristics, according to IEEE standards [54], the Total Demand Distorted (TDD) can be used instead of THD.

TDD: This term is defined that the distortion is expressed as a percent of current, such as the peak demand, rather than as a percent of the rms fundamental current magnitude.

$$TDD = \frac{\sqrt{I_2^2 + I_3^2 + I_4^2 + ... + I_n^2}}{I_L} \quad \textbf{(2.9)}$$

where, I_L represent the maximum demand load current, and I_2, I_3,…I_n are the higher frequency of harmonic currents.

TDD has the same meaning as the THD, and the only difference is to use maximum demand load current instead of fundamental current.

2.4.7.6 Point of Common Coupling

PCC: point of common coupling (PCC) is generally defined as the electrical connecting point or interface between the utility distribution system and customer's electrical distribution system. The PCC can be located at either the primary side or the secondary side of the service transformer depending on whether multiple customers are supplied from the transformer or not. Figure **2-20** proves these two conditions [4].

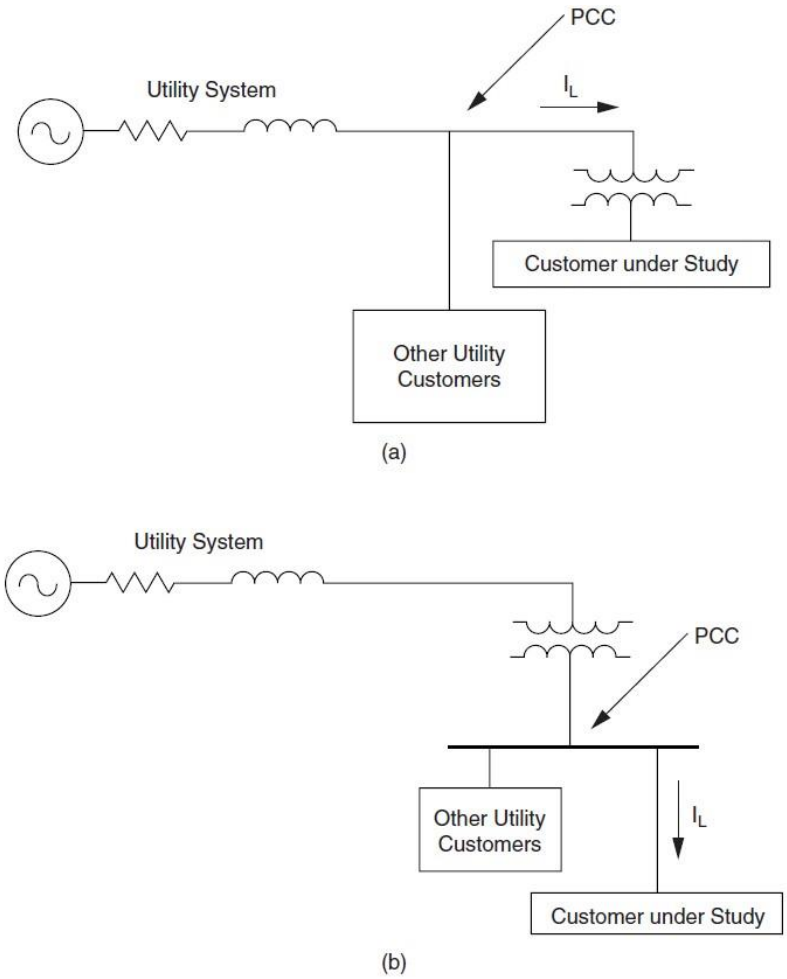

Figure 2-20 **PCC Selection Depends on Where Multiple Customers are Served: (a) PCC at the Transformer Primary Where Multiple Customers are Served; (b) PCC at the Transformer Secondary Where Multiple Customers are Served [4]**

2.4.8 Resonance

The presence of capacitors such as those used for power factor correction can result in local system resonances which lead in turn to excessive currents with subsequent damage to such capacitors [55].

2.4.8.1 Parallel Resonance

Parallel resonance results in a high impedance being presented to the harmonic source at the resonant frequency. Because the major sources of harmonic can be considered as

current sources, this results in increased harmonic voltages and high harmonic currents in each leg of the parallel impedance.

Parallel resonance can occur through different ways. The most common one is caused between the system impedance and the capacitor which is connected to the same busbar as the harmonic source. Assuming that the source is entirely inductive, the resonant frequency is

$$f_p = f\sqrt{(\frac{s_s}{s_c})} \tag{2.10}$$

where, f is the fundamental frequency, f_p is used to denote the resonant frequency, s_s is the short circuit rating (VAr) and s_c is the capacitor rating(VAr) [22].

Further possibilities for parallel resonance can happen with a more detailed representation of the system. An example can be illustrated in Figure 2-21. In this system, the harmonic current generated from consumer B encounters a high harmonic impedance at the busbar. This high harmonic impendence may produce by a resonance between system inductance L_s and the system capacitance C_s or load capacitance C_1 [22].

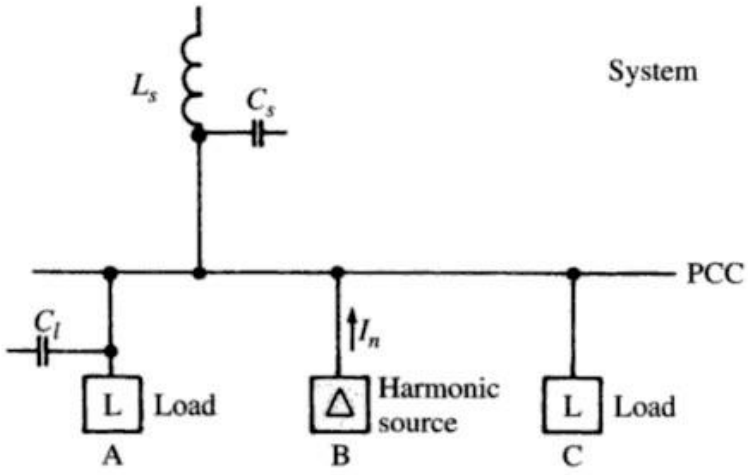

Figure 2-21 Parallel Resonance at a Point of Common Coupling [22]

To make sure which resonance condition exists, it is necessary to measure the harmonic currents in the supply, the harmonic current in each consumer loads, and harmonic voltage at the busbar. Generally, if the current flowing into the power system from the

busbar is small, while the harmonic voltage is high, the resonance occurs within the power system. If the current flowing into the consumer A's load is large and leads the harmonic voltage at the busbar, the resonance occurs between system inductance and the load capacitor.

2.4.8.2 Series Resonance

At high frequencies condition, the load can be ignored as the capacitive impedance reduces. A power system example is shown in Figure 2-22 [22].

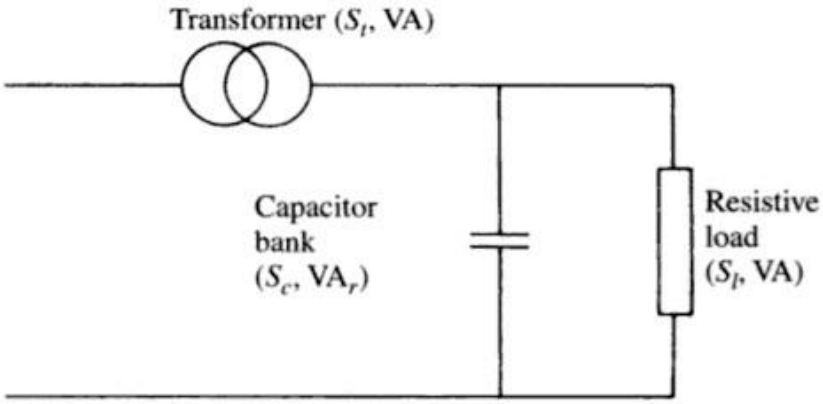

Figure 2-22 Circuit of Series Resonance [22]

Under these conditions a series resonant condition will exist when

$$f_s = f\sqrt{\left(\frac{S_t}{S_c z_t} - \frac{S_1^2}{S_c^2}\right)} \qquad \textbf{(2.11)}$$

where, f is fundamental frequency, f_s represent the series resonant frequency, s_t is the transformer rating, z_t is the transformer per unit impedance, s_c is capacitor rating and s_1 denotes load rating.

When series resonance occurred, the harmonic voltage is small, while the capacitor current is large. The actual current that will flow in power system depends on the circuit quality factor Q. This is typically of the order of 5 at 500Hz.

2.4.9 Effects of Harmonic

The existence of harmonics distortion in the power supply can seriously impact on the power system.The main effect of harmonic distortion within the power system can be concluded in several aspects [56].

- Amplification of harmonic levels
- Reduction of efficiency of power.
- Aging of the installation.
- Malfunctioning of equipment.
- Distorted voltage. Distorted current also distort the voltage which can be presented to other end users on the system.
- Overheated transformers and motor. Increased magnetization losses in steel and iron cores of transformers, motor.
- Overloading of distribution transformers and neutral conductors
- Overloading of pf correction capacitors
- Low voltage at end loads.
- High neutral to ground voltages at end loads.
- Communication problems.
- Current measurement problems because of the distorted waveform.
- Unreliable operation of electronic equipment
- Operation problems of relays and circuit breakers.
- Control of speed and voltage problems on emergency generators for supplying power.
- Capacitor bank application problems.
- Computer data errors or loss.

Most of the electrical and electronic devices have harmonic tolerance in their specification, because harmonics can cause electrical equipment overheat, malfunction, power losses etc., especially the electronic device which is more sensitive to harmonics.

Exceeding the limit can damage the equipment [57]. Therefore, in the next section the harmonic standards will be discussed.

2.5 Harmonic Standards

2.5.1 Existing Harmonic Standards

In the past, most countries have their own harmonic standards depending on local conditions. However, with the development of global equipment manufactured trade, international standards on harmonics are substantially needed.

The international standards should be built based on a globally acceptable electromagnetic environment that coordinates the setting of emission and immunity limits. To achieve this, the reference levels of electromagnetic disturbance, which is referred to as compatibility levels, can be used. The compatibility levels are considered as the levels of disturbance which can exist in the relevant environment. Thus, the equipment connected to system in that environment is required to have immunity at least at that level of disturbance. In general, a margin appropriate to the equipment concerned is calculated between the compatibility and immunity levels. The relationship between these levels is shown in Figure 2-23 [22]. In order to determine the appropriate emission limits, the concept of planning level is referred. The definition of planning level will be introduced in **Section 2.5.3.2**.

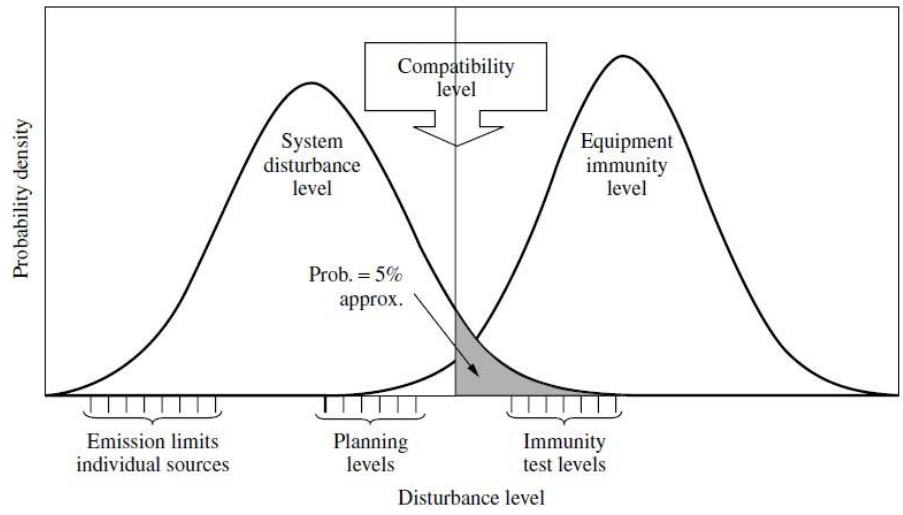

Figure 2-23 Relation between Compatibility, Immunity, Planning and Emission Levels [22]

The IEC has developed harmonic limits in IEC 61000 series document [58]. The IEEE 519-1992 document is widely used for harmonics control in electrical power system as well [54]. IEC has become the governing organisation for most European countries. At the same time, IEEE has become the prominent governing organisation for all electrical-related things in the US. A brief overview of each is provided below.

IEEE standard 519-1992 provides separate harmonic voltage and current limits. This standard focuses on the PPC with the consumer-utility interface. The main point of this standard is that the limitation on customers regarding maximum amount of harmonic currents at the connection point with the power utility do not pose a threat for excessive voltage distortion. IEEE 519 also published recommended THD levers for current and voltage and created the concept of TDD. The harmonic distortion levels were concerned for customers on current and for utilities on voltage signals at the PCC.

Similar to IEEE 519, IEC 61000 developed limits at the utility customer interface. Based on these, IEC 61000 also set limits for customer equipment, in a clear reference to residential installations. In IEC 61000-3-2 [59], the each individual harmonic current limit is listed as four different classes of equipment with an input current up to 16A per phase. IEC 61000-3-4 [60] extends the field of application of IEC 61000-3-2 for equipment with an input current over 16A per phase. The harmonic voltage limitation is given in IEC 61000-3-6 [61]for evaluating harmonic voltage emissions from faculties that are connected to MV, HV and EHV system.

Unlike IEEE 519, IEC 61000 considers the harmonic distortion assessment to cover short and long term effect. Compared with IEEE 519, the IEC 61000 has developed harmonic limits with more direct focus on harmonic voltage distortion. The inter-harmonic voltage compatibility limits related to flicker in lighting devices are sets in IEC 61000. However, IEEE 519 does not provide limits for inter-harmonic.

While the international standards are used, individual countries make their own standards depends on various national priorities. In the UK, unlike other countries, a highly interconnected power system with distributed generation serves a large number of loads which are closed to the points of generation. In 2001, Engineering

Recommendation (ER) G5/4 instead of ER 5/3 came into force in UK for considering harmonic distortion limits [62]. In this revised standard planning levels for individual harmonics and for THD are listed for all system voltages from 400v to 400kV.

2.5.2 IEEE 519-1992

IEEE 519-1992: IEEE Recommended Practices and Requirements for Harmonic Control in Electric Power System [54].

2.5.2.1 Current Harmonic Distortion Limits

According to IEEE 519, the current harmonic limits vary based on the short circuit strength of the system which they are injected into. The harmonic voltage distortion on the system will be a function of the total injected harmonic current and the system impedance at each of the harmonic frequencies. The total injected harmonic current depends on the number and size of individual customers injecting harmonic currents. In general, the system has more ability to handle harmonic currents, the more customers are allowed to inject. Table 2-6 provides the harmonic current limits [54].

In this table, the harmonic current limits identify the maximum amount of harmonic current that customers can inject into the utility system. The size of customers are indicated by the ration of the short-circuit current capacity and the customers' PCC with the utility, to the customer's maximum load current. The individual harmonic current limits are presented in percent of the maximum demand current.

Table 2-6 IEEE STD 519 Harmonic Current Limits

Maximum Harmonic Current Distortion in Percent of I_L						
Individual Harmonic Order (Odd Harmonics)						
I_{SC}/I_L	<11	11≤*h*<17	17≤*h*<23	23≤*h*<35	35≤*h*	TDD
<20*	4.0	2.0	1.5	0.6	0.3	5.0
20<50	7.0	3.5	2.5	1.0	0.5	8.0
50<100	10.0	4.5	4.0	1.5	0.7	12.0
100<1000	12.0	5.5	5.0	2.0	1.0	15.0
>1000	15.0	7.0	6.0	2.5	1.4	20.0
Even harmonics are limited to 25% of the odd harmonic limits above.						
Current distortions that result in a dc offset, e.g. half-wave converters, are not allowed.						
* All power generation equipment is limited to these values of current distortion, regardless of actual I_{sc}/I_L.						
Where I_{sc} = maximum short-circuit current at PCC. I_L = maximum demand load current (fundamental frequency component) at PCC. TDD = Total demand distortion (RSS), harmonic current distortion in % of maximum demand load current (15 or 30 min demand). PCC = Point of common coupling.						

2.5.2.2 Voltage Harmonic Distortion Limits

The voltage distortion limits in IEEE 519 define the quality of the power on the electrical distribution system. The recommended voltage distortion limits are defined with THD. Table 2-7 illustrates the voltage distortion limits for most industrial distribution system [54]. This table provides the individual and total voltage distortion limitations for different voltage levels, including 69KV and below, 69.001 to 16 kV and 161kV and higher. The limits listed in this table should be considered as the worst case of system design values for normal operation.

Table 2-7 IEEE STD 519 Harmonic Voltage Limits

Bus Voltage at PCC	Individual Voltage Distortion (%)	Total Voltage Distortion THD (%)
Below 69 kV	3.0	5.0
69 kV to 161 kV	1.5	2.5
161 kV and above	1.0	1.5
NOTE: High-voltage systems can have up to 2.0% THD where the cause is an HVDC terminal that will attenuate by the time it is tapped for a user.		

2.5.3 IEC 61000

The IEC 61000 contains six parts each with standards and technical reports [6]

- Part 1 General: Two documents discuss application and interpretation in terms of EMC.
- Part 2 Environment: Ten documents cover classification of the electromagnetic environment and compatibility levels for different environments
- Part 3 Limits: Eight documents provide emission limits for harmonics and other disturbances
- Part 4 Testing and measurement techniques: Twenty-one documents illustrate standard methods for testing equipment for emission of and immunity to the different disturbances.
- Part 5 Installation and mitigation guidelines: Six documents for this area.
- Part 6 Generic standards: Four documents describe immunity and emission standards for residential commercial, industrial and power station environments.

In these documents, the most important one is IEC 61000-4-7 [63] which provides harmonics measurement and evaluation methods for both standards. The Part 3 harmonic limits will be discussed in detail in following.

In IEC 61000-3 limits series of standards

- IEC 61000-3-2 provides the harmonic current emission limits for equipment that draws input current up to 16A per phase.
- IEC 61000-3-4 provides the harmonic current emission limits for equipment that draws input current > 16A.
- IEC 61000-3-6 provides the harmonic voltage emission limits for the connection of distorting installation to MV, HV and EHV power system.

2.5.3.1 Current Harmonic Distortion Limits

IEC 61000-3-2: is a limitation for harmonic current which is injected into public distribution networks by non-linear appliances with input current less than or equal 16A [59]. This standard classifies such appliances in four classes:

- Class A: Balanced three-phase equipment and all other equipment except those

in the following classes.

- Class B: Portable tools which are hand-help during normal operation and used for a short time only. Arc welding equipment which is not professional equipment.
- Class C: Lighting equipment including dimming devices with active input power above 25W.
- Class D: Personal computers and personal computer monitors and television receivers (Equipment must have power level 75W up to and not exceeding 600W)

According to the appliances classification, the harmonic current limits provided for different class are listed in Table 2-8 [64]. Limits are given amperes for equipment classes A and B, while given in percentage of fundamental for class C. For class D, the limits are specified in milliamperes per watt for equipment.

In this harmonic current limits:

- The THD levels are not specified.
- This limit is only for low and medium power equipment and is not suitable to high power equipment (> 1kM) for professional use.
- For order of harmonics excess 19, if the current spectrum envelope illustrates a monotonic decrease of the increasing order of harmonics, measurement can be restricted to the first 19 harmonics.
- Harmonic currents less than 0.6% of the input current measured under the test conditions, or less than 5mA are considered as disregard.

Table 2-8 IEC STD 61000-3-2 Harmonic Current Limits

Harmonics [n]	Class A [A]	Class B [A]	Class C [% of fund]	Class D [mA/W]
		Odd harmonics		
3	2.30	3.45	30 x λ	3.4
5	1.14	1.71	10	1.9
7	0.77	1.155	7	1.0
9	0.40	0.60	5	0.5
11	0.33	0.495	3	0.35
13	0.21	0.315	3	3.85/13
15 ≤n ≤39	0.15 x 15/n	0.225 X 15/n	3	3.85/n
		Even harmonics		
2	1.08	1.62	2	-
4	0.43	0.645	-	-
6	0.30	0.45	-	-
8 ≤n ≤40	0.23 x 8/n	0.345 x 8/n	-	-

IEC 61000-3-4: is a limitation for harmonic current by electrical and electronic equipment with an input current exceeding 16A per phase, and it is intended to be connected to public LV a.c. distribution systems of the types shown below: [60]

- nominal voltage up to 240 V, single-phase , two or three wires
- nominal voltage up to 600 V, three-phase ,three or four wires
- nominal frequency 50 Hz or 60Hz

For understanding IEC 61000-3-4 harmonic current limits, the following definitions apply [60].

PWHD: Partial weighted harmonic distortion (PWHD) is ratio of the RMS value of a selected group of higher order harmonics, weighted with the order of harmonic to the RMS value of the fundamental.

$$PWHD = \sqrt{\sum_{n=14}^{40} n(\frac{I_n}{I_1})^2} \quad \textbf{(2.12)}$$

Short-circuit power (S_{sc}): calculated from the nominal system voltage U_{nom} and the impedance Z at the PCC

$$S_{sc} = \frac{U_{nom}^2}{Z} \quad \textbf{(2.13)}$$

Rated apparent power (S_{equ}): calculated from the rated rms line current I_{equ} of the piece of equipment and the single-phase rated voltage U_p or interphase rated voltage U_i.

For single-phase equipment $S_{equ} = U_p I_{equ}$ **(2.14)**

For interphase equipment $S_{equ} = U_i I_{equ}$ **(2.15)**

For balanced three-phase equipment $S_{equ} = \sqrt{3} U_i I_{equ}$ **(2.16)**

For unbalanced three-phase equipment $S_{equ} = 3 U_p I_{equ\,\max}$ **(2.17)**

where $I_{equ\,max}$ is the maximum of the rms currents flowing in any one of the three phases.

Short-circuit ratio (R_{sce}):

For single-phase equipment $R_{sce} = \frac{S_{sc}}{3 S_{equ}}$ **(2.18)**

For interphase equipment $R_{sce} = \frac{S_{sc}}{2 S_{equ}}$ **(2.19)**

For all three-phase equipment $R_{sce} = \frac{S_{sc}}{S_{equ}}$ **(2.20)**

The following tables listed harmonic emission for three stages [60].

Stage 1. Simplified connection: Equipment complying with stage 1 limits can be connected at any point of the supply system provided the short-circuit ratio $R_{sce} \geqslant 33$.

Table 2-9 lists the current emission values for simplified connection of equipment ($S_{equ} \leqslant S_{sc}/33$)

Table 2-9 Current Emission Values for Stage 1

Harmonic number n	Admissible harmonic current I_n/I_1[a] %	Harmonic number n	Admissible harmonic current I_n/I_1[a] %
3	21,6	21	≤ 0,6
5	10,7	23	0,9
7	7,2	25	0,8
9	3,8	27	≤ 0,6
11	3,1	29	0,7
13	2	31	0,7
15	0,7	≥ 33	≤ 0,6
17	1,2		
19	1,1	Even	≤ 8/n or ≤ 0,6

[a] I_1 = rated fundamental current; I_n = harmonic current component.

Stage 2. Connection based on Network and Equipment Data: Equipment not complying with stage 1 limits, higher emission values may be allowed, the short-circuit ratio R_{sce} >33. Table 2-10 and Table 2-11 are shown current emission values for stage 2.

Table 2-10 Current Emission Values for Single Phase, Interphases and Unbalanced Three-phase Equipment

Minimal R_{sce}	Admissible harmonic current distortion factors %		Admissible individual harmonic current I_n/I_1[a] %					
	THD	*PWHD*	I_3	I_5	I_7	I_9	I_{11}	I_{13}
66	25	25	23	11	8	6	5	4
120	29	29	25	12	10	7	6	5
175	33	33	29	14	11	8	7	6
250	39	39	34	18	12	10	8	7
350	46	46	40	24	15	12	9	8
450	51	51	40	30	20	14	12	10
600	57	57	40	30	20	14	12	10

NOTE 1 The relative value of even harmonics shall not exceed 16/n %.

NOTE 2 Linear interpolation between successive R_{sce} values is permitted.

NOTE 3 In the case of unbalanced three-phase equipment, these values apply to each phase.

[a] I_1 = rated fundamental current; I_n = harmonic current component.

Table 2-11 Current Emission Values for Balanced Three-phase Equipment

Minimal R_{sce}	Admissible harmonic current distortion factors %		Admissible individual harmonic current I_n/I_1[a] %			
	THD	*PWHD*	I_5	I_7	I_{11}	I_{13}
66	16	25	14	11	10	8
120	18	29	16	12	11	8
175	25	33	20	14	12	8
250	35	39	30	18	13	8
350	48	46	40	25	15	10
450	58	51	50	35	20	15
600	70	57	60	40	25	18

NOTE 1 The relative value of even harmonics shall not exceed $16/n$ %.

NOTE 2 Linear interpolation between successive R_{sce} values is permitted.

[a] I_1 = rated fundamental current; I_n = harmonic current component.

Stage 3. Connection based on the consumer's agreed power: If the conditions of neither stage 1 nor stage 2 are fulfilled, or if the input current of the equipment exceeds 75A, the supply authority may accept the connection of the equipment on the basis of the agreed active power of the consumer's installation.

2.5.3.2 Voltage Harmonic Distortion Limits

Regarding voltage distortion, compatibility levels and planning levels are identified for power system to tie in with emission and immunity levels, respectively, in LV and MV installations. 61000-3-6 presents guidance for the coordination of the harmonic voltages between different voltage levels in order to meet the compatibility levels at utilization level and to avoid adverse effects on sensitive customer's equipment [61].

Compatibility Levels: These are reference values for coordinating the emission and immunity of equipment which is part of, or supplied by a supply system. Compatibility levels are normally based on the 95% probability levels of entire systems, using statistical distributions which represent both time and space variations of disturbances. For LV and MW system, compatibility levels are described in IEC 61000-2-2 [65] and IEC 61000-2-12 [66] shown in Table 2-12. This compatibility levels can be considered as references for developing equipment immunity levels by equipment supplies.

Table 2-12 Compatibility Levels for Individual Harmonic Voltages in Low and Medium Voltage Network

Odd harmonics non-multiple of 3		Odd harmonics multiple of 3		Even harmonics	
Harmonic Order h	Harmonic Voltage %	Harmonic Order h	Harmonic Voltage %	Harmonic Order h	Harmonic Voltage %
5	6	3	5	2	2
7	5	9	1.5	4	1
11	3.5	15	0.4	6	0.5
13	3	21	0.3	8	0.5
17≤ h ≤ 49	$2.27 \cdot \frac{17}{h} - 0.27$	21< h ≤ 45	0,2	10 ≤ h ≤ 50	$0.25 \cdot \frac{10}{h} + 0.25$
NOTE: The corresponding compatibility level for the total harmonic distortion is THD = 8%.					

Planning levels: The determining of emission limits depends on compatibility levels Planning levels are identified by system operator or owner for all voltage levels of the system and can be considered as internal quality objectives of the system operator. Planning levels for harmonics are equal to or lower than compatibility levels. The coordination of harmonic voltages between different voltage levels should be allowed. The indicative values for planning levels along with definition of MV, HV and EHV are provided in IEC 61000-3-6 [61]which is listed in Table 2-13.

Table 2-13 Indicative Planning Levels for Harmonic Voltage in MV, HV and EHV Power Systems

Odd harmonics non-multiple of 3			Odd harmonics multiple of 3			Even harmonics		
Harmonic Order h	Harmonic Voltage %		Harmonic Order h	Harmonic Voltage %		Harmonic Order h	Harmonic Voltage %	
	MV	HV-EHV		MV	HV-EHV		MV	HV-EHV
5	5	2	3	4	2	2	1.8	1.4
7	4	2	9	1.2	1	4	1	0.8
11	3	1.5	15	0.3	0.3	6	0.5	0.4
13	2.5	1.5	21	0.2	0.2	8	0.5	0.4
17≤ h ≤ 49	$1.9 \cdot \frac{17}{h} - 0.2$	$1.2 \cdot \frac{17}{h}$	21< h ≤ 45	0.2	0.2	10 ≤ h ≤ 50	$0.25 \cdot \frac{10}{h} + 0.22$	$0.19 \cdot \frac{10}{h} + 0.16$
NOTE: The corresponding planning levels for the total harmonic distortion are: THD_{MV} = 6.5% and $THD_{HV\text{-}EHV}$ = 3%								

The LV is 1kV or less, MW is from 1kV to 35kV, HV is between 35kV to 230 kV and EHV is over 230kV. IEC 61000-2-2 [65] also defines compatibility levels for interharmonic voltages occurring close to the fundamental frequency.

2.5.4 ER 5/4

The ER G 5/4: planning levels for harmonic voltage distortion and the connection of non-linear equipment to transmission systems and distribution networks in the UK published by Electricity Association in February, 2001

2.5.4.1 Current Harmonic Distortion Limits

The current harmonic limits provided by ER G5/4 comply with IEC 61000-3-2 for equipment rated current up to 16A per phase and comply with IEC 61000-3-4 for equipment rated current above 16A per phase [62]. The different stages' assessment.

2.5.4.2 Voltage Harmonic Distortion Limits

ER G5/4 develops the planning levels for harmonic voltage distortion to be used in the process for the connection of non-linear load. These planning levels also depend on harmonic voltage distortion compatibility levels. The planning levels listed on ER G5/4 are close to the values provided in IEC 61000-3-6. However, in ER G5/4 the planning levels above the 7^{th} order are reduced Table 2-14-Table 2-18 list the planning levels for various voltage levels.

Table 2-14 Summary of THD Planning Levels

System Voltage at the PCC	THD Limit
400V	5%
6.6, 11 and 20kV	4%
22kV to 400kV	3%

Table 2-15 Planning Levels for Harmonic Voltage in 400V Systems

Odd harmonics (Non-multiple of 3)		Odd harmonics (Multiple of 3)		Even harmonics	
Order 'h'	Harmonic voltage (%)	Order 'h'	Harmonic voltage (%)	Order 'h'	Harmonic voltage (%)
5	4.0	3	4.0	2	1.6
7	4.0	9	1.2	4	1.0
11	3.0	15	0.3	6	0.5
13	2.5	21	0.2	8	0.4
17	1.6	>21	0.2	10	0.4
19	1.2			12	0.2
23	1.2			>12	0.2
25	0.7				
>25	$0.2 + 0.5(^{25}/_{h})$				

Note: The THD level is 5%

Table 2-16 Planning Levels for Harmonic Voltage in 6.6kV, 11kV and 20kV Systems

Odd harmonics (Non-multiple of 3)		Odd harmonics (Multiple of 3)		Even harmonics	
Order 'h'	Harmonic voltage (%)	Order 'h'	Harmonic voltage (%)	Order 'h'	Harmonic voltage (%)
5	3.0	3	3.0	2	1.5
7	3.0	9	1.2	4	1.0
11	2.0	15	0.3	6	0.5
13	2.0	21	0.2	8	0.4
17	1.6	>21	0.2	10	0.4
19	1.2			12	0.2
23	1.2			>12	0.2
25	0.7				
>25	$0.2 + 0.5(^{25}/_{h})$				

Note: The THD level is 4%

Table 2-17 Planning Levels for Harmonic Voltage in System >20kV and <145kV

Odd harmonics (Non-multiple of 3)		Odd harmonics (Multiple of 3)		Even harmonics	
Order 'h'	Harmonic voltage (%)	Order 'h'	Harmonic voltage (%)	Order 'h'	Harmonic voltage (%)
5	2.0	3	2.0	2	1.0
7	2.0	9	1.0	4	0.8
11	1.5	15	0.3	6	0.5
13	1.5	21	0.2	8	0.4
17	1.0	>21	0.2	10	0.4
19	1.0			12	0.2
23	0.7			>12	0.2
25	0.7				
>25	$0.2 + 0.5\ (^{25}/_{h})$				

Note: The THD level is 3%

Table 2-18 Planning Levels for Harmonic Voltage in 275kV and 400kV System

Odd harmonics (Non-multiple of 3)		Odd harmonics (Multiple of 3)		Even harmonics	
Order 'h'	Harmonic Voltage (%)	Order 'h'	Harmonic Voltage (%)	Order 'h'	Harmonic Voltage (%)
5	2.0	3	1.5	2	1.0
7	1.5	9	0.5	4	0.8
11	1.0	15	0.3	6	0.5
13	1.0	21	0.2	8	0.4
17	0.5	>21	0.2	10	0.4
19	0.5			12	0.2
23	0.5			>12	0.2
25	0.5				
>25	$0.2 + 0.3\ (^{25}/_{h})$				

Note: The THD level is 3%

Table 2-15 and Table 2-16 are applicable to all final distribution system which is the one whose transformers have a lower voltage winding operating at lower voltage, except 33kV. Table 2-17 is applicable to the sun-transmission system and major of primary distribution which is the one whose transformers have a lower voltage winding operating at the voltage level greater than 400V. Table 2-18 is applicable to transmission system.

2.6 Harmonic Filters

A harmonic filter is used to eliminate the potentially damaging effects of harmonic distortion caused by appliances. The harmonic filter is constructed by using an array of capacitors, inductors, and resistors which can deflect harmonic currents to the ground. Each harmonic filter may contain many such elements, each of which is used to reduce the harmonics at a specific frequency.

2.6.1 Functions of Harmonic Filters

A range of functions of harmonic filter are listed as below:

- Reduces neutral currents
- Reduces transformer loading
- Protects electrical systems
- Reduces fire hazard
- Protects the neutral conductor
- Enhances system protection
- Minimizes impact on distribution transformers
- Reduces local neutral to ground voltage
- Lowers peak phase current/average phase current
- Increases system capacity
- Decreases system losses
- Improves power factor on non-linear loads
- Reduces total harmonic distortion
- Improves phase current balance
- Augments phase voltage balance

2.6.2 Types of Harmonic Filters

A harmonic filter can contain a single or a combination of several elements, and can be placed at a single node or be distributed across several nodes. In addition, it can perform actively or passively.

2.6.2.1 Passive filters

Passive filters are designed to eliminate specific harmonics rather than the full spectrum of distortion. Passive filters consist of capacitor, inductors and resistor, and typically provide an alternative impedance path for harmonics caused by the non-linear loads.

Passive filters can be classified by the ways of connection with the load.

- The series filter is a current rejecter which is placed in series with the load and its components are constructed in parallel.
- The parallel filter is a current acceptor which placed in parallel with the load and uses series components.

The passive filter can also be classified according to the functions: Band-pass and High-pass filters.

Band-pass Filter: is a common passive filter which is constructed using a capacitor connected in series with a resistor and an inductor. This type of filter is used to mitigate lowest order harmonics and can be tuned at a single frequency (single-tuned filter) or at two frequencies (double tuned filter).

High-pass Filter: has a resistor connected in parallel with an inductor. It can be used to filter high order harmonics and cover a wide range of frequencies. C-type filter is a special type of high-pass filter which is applied for complex loads, cyclo converters and electric arc furnaces. It is used to provide reactive power and avoid parallel resonances.

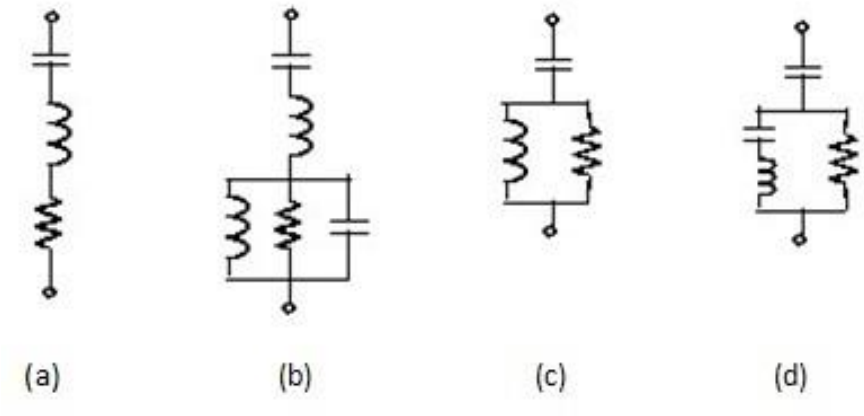

Figure 2-24 Passive Filters: (a) Single-tuned; (b) Double-tuned; (c) High-pass; (d) C-type High-pass [22]

2.6.2.2 Active filters

Active filer is designed due to the complexity and high costs of losses of the conventional passive filters. Active filters are mostly used for LV system. The principle used in active filters is the introduction of current components using power electronics to eliminate the harmonic distortions produced by the non-linear load.

Active filters can also be classified into three types based on the way they are connected to the AC distribution network shown in Figure 2-25 [22].

- The series filter is connected to AC distribution network in series. It is usually proposed to solve voltage distortion and other related issues. It is more appropriate than a shunt compensator as it is able to compensate current issues. It can be used to prevent the transfer of harmonic current.

- The parallel filter is connected to AC distribution network in parallel. Parallel filter is the earliest and most recognized active filter configuration in the technical literature and it has been utilized in practical applications. Due to the parallel connection to the load, it is also termed as shunt filter. Parallel filter is controlled as a current source and it is utilized to inject a compensating current into the system (to the load), so that its current cancels the harmonic current, the reactive power current and the unbalanced current components on the AC side of a nonlinear load.

- The hybrid filter is a combination of an active and a passive filter and could be either a series or a parallel configuration. The basic principle of hybrid filtering is to improve the filtering capacity of a passive filter and to damp series and parallel resonances with a small rated active filter.

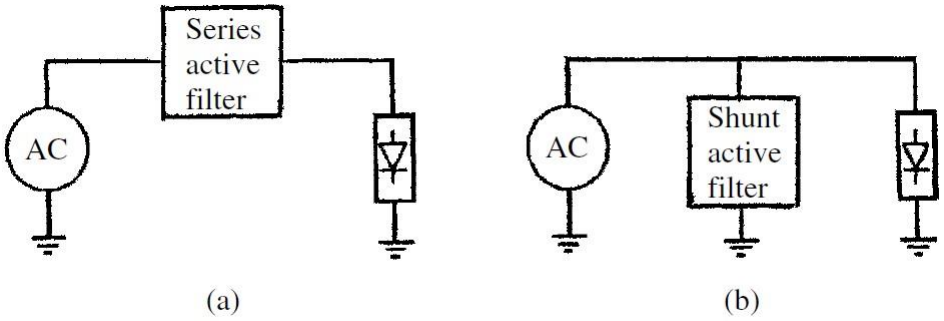

Figure 2-25 Active Filters: (a) Series; (b) Parallel [22]

Besides the above classification, active filters can be divided into 3-wire filter or 4-wire filter.

3-wire filter: is power units which is usually used in variable speed drives and other such application with a large number of non-linear loads.

4-wire filters: is used to reduce harmonics caused by switch-mode supplies and information technology equipment, typically commercial applications.

2.6.3 Filters Design Criteria

To comply with the required harmonic limitations, the key of filter design considerations include the following steps [22]:

(1) Inject the current into a circuit consisting of filters in parallel with the AC system (shown as Figure 2-26), based on the harmonic current spectrum generated by the non-linear load. And then calculate the harmonic voltage.

(2) To determine the specific parameters by using the results of (1).

(3) To calculate the filter components, include capacitors, inductors and resistors, and then compute their ratings and losses by the calculation results. The components values are determined from the filter type and the following parameters:

- Reactive power at nominal voltage
- Tuning frequencies
- Quality factor which is a measure of the sharpness of the tuning frequency. It is determined by the resistance value.

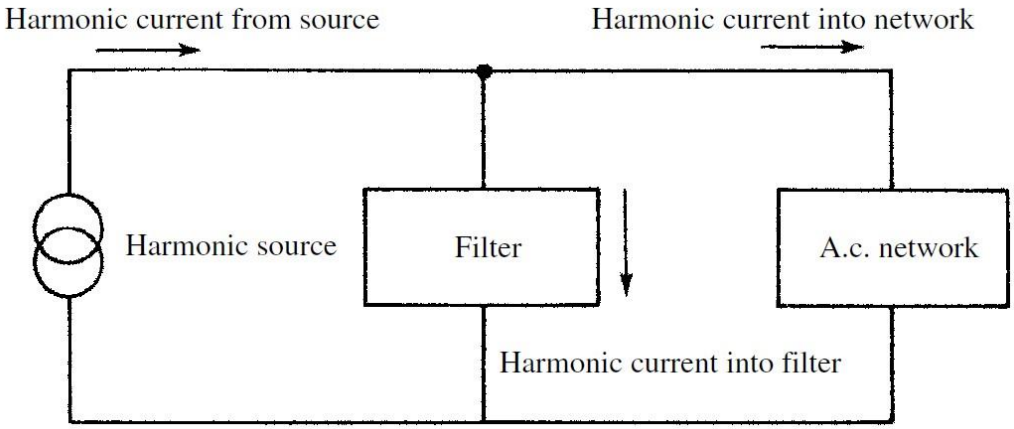

Figure 2-26 Circuit for the Computation of Voltage Harmonic Distortion [22]

2.7 Conclusion

This chapter has introduced the concept and definition of PQ and PQ disturbance. In order to analyse PQ disturbance, the classification of PQ disturbance has been required thereafter. A large number of terms, such as Transients, short-duration variations, long-duration variations etc. which are referred to throughout the rest of thesis, have been introduced in detail respectively. In addition, PQ classification with novel method proposed will be considered in **Chapter 4**

Of these points of PQ disturbance, harmonic analysis plays the most important role in this thesis, and thus the concept and analysis of harmonic have been specially represented in Section 2.4. Following this, a variety of harmonic standards in terms of current and voltage, proposed by IEEE and IEC organisations have been listed to fully support harmonic analysis proposed in this thesis. The novel approach to analysing harmonic will be proposed in **Chapter 5**.

Note that all of relevant concepts, theories, definitions and equations have been already introduced in this chapter in detail to serve the rest of the thesis. There are no particular explanations in following chapters.

Chapter 3 Wavelet Analysis: Fourier Transform and Wavelet Transform

3.1 Introduction

The conventional signal processing method used to analyse power system waveform distortion is referred to as the Fourier analysis. Any waveforms can be decomposed into a sum of sinusoid waveforms by using the Fourier Series (FS). The FS can only be applied to periodic signals. Since the most signals are aperiodic in practical, a mathematical tool known as the Fourier Transform (FT) for aperiodic signals analysis is proposed which can analyse the frequency content for aperiodic signals. The Discrete Fourier Transform (DFT) is a numerical computation of the FT. The DFT is used for dealing with the data which is often available in the form of a sampled time function. The Fast Fourier Transform (FFT) is simply an efficient method for computing the DFT. However, the FT provides signals which are mainly localised in the frequency domain and it gives limited information of the signals in the time domain. Furthermore, the FT cannot obtain accurate values of amplitude and phases from harmonics with frequencies different from that of the window function frequency. These characteristics present the most important limitations of the Fourier analysis.

To overcome the limitations of the Fourier analysis mentioned above, the Wavelet Transform (WT) is applied to the power system waveform analysis. Basic functions of the WT are small waves located in different times. The main advantages of wavelets are that they have the ability to analyse signals in both time and frequency domains, and they also have ability to be adjusted automatically for low or high frequencies because it uses short windows at high frequencies and long windows at low frequencies. As a result, the wavelets can lead to an optimal time-frequency resolution in all frequency ranges [67]. In the WT, the Discrete Wavelet Transform (DWT) is the digital representation of the Continuous Wavelet Transform (CWT). The WT provides a Multi-resolution Analysis (MRA). Based on the MRA, the WT can be implemented by using

the filter bank which can decompose and reconstruct a signal into different time and frequency resolution.

In this chapter, the information on the FT and the WT is presented in detail. The chapter is organised as follows: Firstly, the brief summaries and applications of the Fourier analysis including the FS, FT, DFT, FFT are presented in **Section 3.2**. Secondly, to overcome the limitations of the FT, the WT including development and definition of the WT, wavelet basic and examples of wavelet function are introduced in **Section 2.3**. Thirdly, for practical implementation of the WT, the WT filter banks implementing DWT or Discrete Wavelet Packet Transform (DWPT) are discussed in **Section 3.4**. Finally, a summary conclusion is given in **Section 3.5**

3.2 Fourier Transform

3.2.1 Fourier Series

In 1822 J.B.J. Fourier [21] proposed that any functions or signals repetitive with an interval *T* can be represented by the sum of an infinite series of sinusoidal or cosinusoid components, which are called 3.2.1. Fourier Series (FS). By definition, a function $f(t)$ is periodic when $f(t) = f(t+T)$, where T is the period. If the FS states in Dirichlet conditions, the periodic function $f(t)$ can be represented by a trigonometric series of elements consisting of a DC component and other elements with frequencies comprising the fundamental component and an infinite number of its integer multiples.

The Dirichlet conditions are shown below [68]

- If a discontinuous function $f(t)$ has a finite number of discontinuities over the period T.
- If $f(t)$ has a finite mean value over the period *T*.
- If $f(t)$ has a finite number of positive and negative maximum values.
- Under these conditions, any periodic $f(t)$ can be represented as the following trigonometric series

$$f(t) = a_0 + \sum_{n=1}^{\infty}[a_n \cos(\frac{2\pi nt}{T}) + b_n \sin(\frac{2\pi nt}{T})] \quad \textbf{(3.1)}$$

For a real valued periodic waveform, equation (3.1) can be simplified by sinusoidal amplitude c_n and sinusoidal phase θ_n

$$f(t) = c_0 + \sum_{n=1}^{\infty} c_n \sin(\frac{2\pi nt}{T} + \theta_n)] \quad \textbf{(3.2)}$$

Where

$$c_0 = a_0 \quad \textbf{(3.3)}$$

$$c_n = \sqrt{a_n^2 + b_n^2} \quad \textbf{(3.4)}$$

$$\theta_n = \tan^{-1}(\frac{b_n}{a_n}) \quad \textbf{(3.5)}$$

Equation (3.2) is known as the FS and it illustrates a periodic function decomposed of sinusoidal functions with different frequencies.

$\frac{2\pi n}{T}$ n th order harmonic of the periodic function

c_0 magnitude of the DC component

c_n magnitude of the n th harmonic component

θ_n phase of the n th harmonic component

When n is set to 1, the component is called the fundamental component. The FS will consist of harmonically related sine and cosine waves of the fundamental frequency and multiples. The amplitude and phase of each harmonic can be determined by the FS.

3.2.1.1 Orthogonal Functions

A set of functions θ_i, defined in $a \leqslant x \leqslant b$ is called orthogonal (or unitary , if complex) when it satisfied the condition shown as follows [69]:

$$\int_a^b \theta_i(x)\theta_j^*(x)dx = K_i\delta_{ij} \quad \textbf{(3.6)}$$

Where $\delta_{ij} = 1$ for $i = j$, and = 0 for $i \neq j$, and $*$ denote the complex conjugate.

It can also be shown that the functions:

$$\{1, \cos(\frac{2\pi t}{T}), ..., \sin(\frac{2\pi t}{T}), ..., \cos(\frac{2\pi nt}{T}), ..., \sin(\frac{2\pi nt}{T}), ...\} \quad \textbf{(3.7)}$$

for which the following conditions are valid:

$$\int_{-T/2}^{T/2} \cos kx \cos lx dx = \begin{cases} 0, k \neq l, \\ \pi, k = l, \end{cases} \quad \textbf{(3.8)}$$

$$\int_{-T/2}^{T/2} \sin kx \sin lx dx = \begin{cases} 0, k \neq l, \\ \pi, k = l, \end{cases} \quad \textbf{(3.9)}$$

$$\int_{-T/2}^{T/2} \cos kx \sin lx dx = 0 \quad (k = 1,2,3,\ldots), \quad \textbf{(3.10)}$$

$$\int_{-T/2}^{T/2} \cos kx dx = 0 \quad (k = 1,2,3,\ldots), \quad \textbf{(3.11)}$$

$$\int_{-T/2}^{T/2} \sin kx dx = 0 \quad (k = 1,2,3,\ldots), \quad \textbf{(3.12)}$$

$$\int_{-T/2}^{T/2} l dx = 2\pi \quad \textbf{(3.13)}$$

are a set of orthogonal functions . It can be seen clear from equation (3.7) to equation (3.13), the integer over the period ($-\pi \rightarrow \pi$) of the product of a sine and a cosine functions is zero.

3.2.1.2 Fourier Coefficients

According to the integrated equation (3.1) and the orthogonal function, the constant Fourier coefficients a_o, and Fourier coefficients a_n and b_n can be defined as follows [22]:

$$a_0 = \frac{1}{T}\int_{-T/2}^{T/2} f(t)dt \qquad \textbf{(3.14)}$$

Which is the area under the curve of $f(t)$ from $-T/2$ to $T/2$, divided by the period of the waveform, T

$$a_n = \frac{2}{T}\int_{-T/2}^{T/2} f(t)\cos(\frac{2\pi nt}{T})dt \qquad \textbf{(3.15)}$$

and

$$b_n = \frac{2}{T}\int_{-T/2}^{T/2} f(t)\sin(\frac{2\pi nt}{T})dt \qquad \textbf{(3.16)}$$

where $n= 1\rightarrow\infty$.

3.2.1.3 Waveform Symmetry

Odd Symmetry: If the function f (t) satisfies the following condition

$$f(-t) = -f(t) \qquad \textbf{(3.17)}$$

f (t) is called odd function. The example of even functions is shown in Figure 3-1 [68].

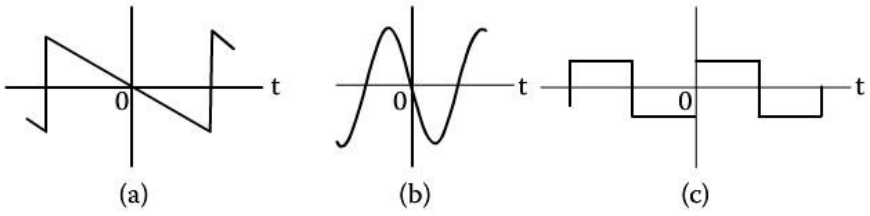

Figure 3-1 Example of Odd Functions [68]

Even Symmetry: If the function f (t) satisfies the following condition

$$f(t) = f(-t) \qquad \textbf{(3.18)}$$

f (t) is called even function. The example of odd functions is shown in Figure 3-2 [68].

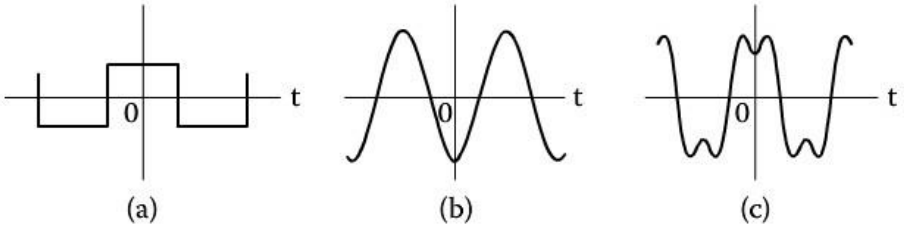

Figure 3-2 Example of Even Functions [68]

Halfwave Symmetry: If the function *f* (t) satisfies the following condition

$$f(t) = -f(t \pm T/2) \tag{3.19}$$

f (t) is called halfwave symmetry.

3.2.1.4 The Complex Fourier Series

Recalling that $e^{i\omega} = \cos\omega + j\sin\omega$, the FS can be rewritten in terms of mathematical exponentiation [22]:

$$f(t) = \sum_{n=-\infty}^{\infty} c_n e^{j\omega_0 nt} \tag{3.20}$$

$$c_n = \frac{1}{T}\int_{-T/2}^{T/2} f(t) e^{-j\omega_n nt} dt \tag{3.21}$$

where $c_n = \frac{1}{2}(a_n - jb_n)$ for $n > 0$,

and $c_n = \frac{1}{2}(a_n + jb_n)$ for $n < 0$, $\omega_0 = \frac{2\pi}{T}$

3.2.1.5 Example of Harmonic Analysis Using Fourier Series

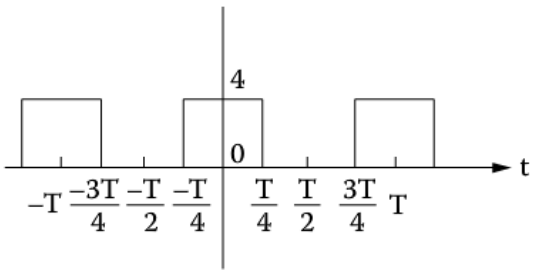

Figure 3-3 Square Wave Function

According to Figure 3-3, the periodic function can be represented as follows

$$f(t)=\begin{cases}0, -T/2<t<-T/4\\ 4, -T/4<t<T/4\\ 0, T/4<t<T/2\end{cases} \tag{3.22}$$

Then, the Fourier coefficients can be calculated by using Equation (3.14), (3.15) and (3.16)

$$\begin{aligned}a_0&=\frac{1}{T}\int_{-T/2}^{T/2}f(t)dt=\frac{1}{T}(\int_{-T/2}^{-T/4}0\cdot dt+\int_{-T/4}^{T/4}4\cdot dt+\int_{T/4}^{T/2}0\cdot dt)\\&=\frac{1}{T}[4(T/4+T/4)]=2\end{aligned} \tag{3.23}$$

$$\begin{aligned}a_1&=\frac{2}{T}\int_{-T/2}^{T/2}f(t)\cos(\frac{2\pi nt}{T})dt\\&=\frac{2}{T}(\int_{-T/2}^{-T/4}0\cdot\cos(\frac{2\pi nt}{T})dt+\int_{-T/4}^{T/4}4\cdot\cos(\frac{2\pi nt}{T})dt+\int_{T/4}^{T/2}0\cdot\cos(\frac{2\pi nt}{T})dt)\\&=\frac{4}{\pi}[\sin(\frac{\pi}{2})+\sin(\frac{\pi}{2})]=\frac{8}{\pi}\end{aligned} \tag{3.24}$$

After a_2,a_3, $a_{4,...}$and b_1,b_2, $b_{3,...}$ have been calculated, the a_n and b_n can be found equally as

$$a_n=\begin{cases}0, n=even\\ -1^{(n-1)/2}\dfrac{8}{n\pi}, n=odd\end{cases}\qquad b_n=0$$

Therefore, according to Equation (3.1), the FS of this square waveform is shown as below:

$$f(t)=2+\frac{8}{\pi}(\cos\pi t-\frac{1}{3}\cos 3\pi t+\frac{1}{5}\cos 5\pi t-...) \tag{3.25}$$

Example 2:

A periodic signal can be analysed to realise the cosine and sine waves, and their sum can produce the original signal:

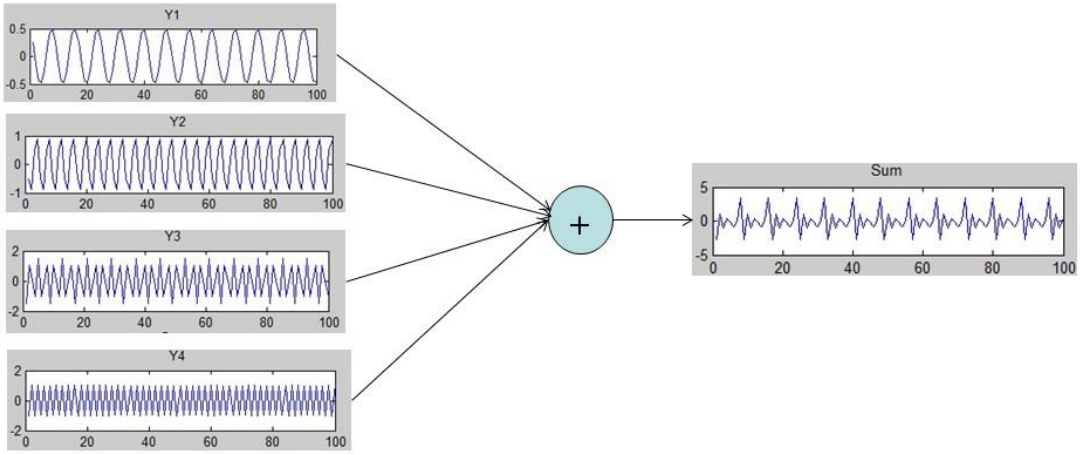

Figure 3-4 Diagram of Example 2

The equations for each signal are shown as below:

$$Y_1 = 0.5\cos(50\pi t + \frac{1}{3}\pi) \quad \textbf{(3.26)}$$

$$Y_2 = \cos(100\pi t + \frac{2}{3}\pi) \quad \textbf{(3.27)}$$

$$Y_3 = 1.5\cos(150\pi t + \pi) \quad \textbf{(3.28)}$$

$$Y_4 = 2\cos(200\pi t + \frac{4}{3}\pi) \quad \textbf{(3.29)}$$

The original signal $S = Y_1 + Y_2 + Y_3 + Y_4$

3.2.2 Fourier Transform

The FS is only applied to periodic signals. In the real word, most of signals are aperiodic. Any signals that have transient or random components are aperiodic. Hence a mathematical tool similar to the FS is desirable for aperiodic signals analysis which is referred to as the FT [22].

The period *T* is difficult to determine as aperiodic signal which does not in fact repeat. However, in order to obtain the answer to some extent, it is assumed to repeat after the

entire signal duration. The result of choosing a large period can lead to closely spaced harmonics.

When applied to a continuous, periodic signal in the time domain, FT yields a series of discrete frequency components in the frequency domain. Allowing the integration period T extend to infinity, the spacing between the harmonic frequencies is intended to zero.

Recalling the Fourier coefficients c_n, of equation (3.21), allowing $T \to \infty$, and multiplying by T, resulting in the FT.

$$F(f) = \int_{-\infty}^{\infty} f(t) e^{-j2\pi ft} dt \qquad \textbf{(3.30)}$$

where, f as f_0 tends to zero and n tends to infinity rather than a discrete variable.

The expression for the time domain function $f(t)$, which is also continuous and has infinite duration in terms of $F(f)$ is then

$$f(t) = \int_{-\infty}^{\infty} F(f) e^{j2\pi ft} dt \qquad \textbf{(3.31)}$$

$F(f)$ is considered as the spectral density function of $f(t)$. Equation (3.30) is referred to as the forward FT, which equation (3.31) is referred to as the inverse FT.

3.2.3 Discrete Fourier Transform

In practice, data is often available in the form of a sampled time function, illustrated by a time series of amplitudes, separated by fixed time intervals of limited duration. In order to analyse the data mentioned above, the DFT is used [22].

The DFT is a version of the FT which yields the frequency spectrum of a sampled digital signal $f[n]$

$$F(f) = \sum_{n=-\infty}^{\infty} f[\mathrm{n}] e^{\frac{-j2\pi fn}{f_s}} \qquad \textbf{(3.32)}$$

where f_s is the sampling frequency and f_n is the signal frequency.

The equation (3.32) is for non-causal signal. Assuming the signal is causal, then the first sample is at *n=0*, and the last sample is at *n=N-1*. Therefore, for causal signal *f* [*n*]

$$F(f) = \sum_{n=0}^{N-1} f[\mathrm{n}] e^{\frac{-j2\pi fn}{f_s}} \tag{3.33}$$

Furthermore, the computation time will also be limited, and the DFT should be evaluated at a finite number of frequncies. In the case where the frequncy domain specturm is a sample function, as well as the time domain function, the frequncy band of original signal period is divided into *N* discrete points, or $1/NT_s$ seconds then a discrete vairable *k* is introduced for frequncy. The equation (3.33) can be rewritten with time index *n*, and the frequency index k as

$$F(f_k) = \sum_{n=0}^{N-1} f[\mathrm{t}_n] e^{\frac{-j2\pi kn}{N}} \tag{3.34}$$

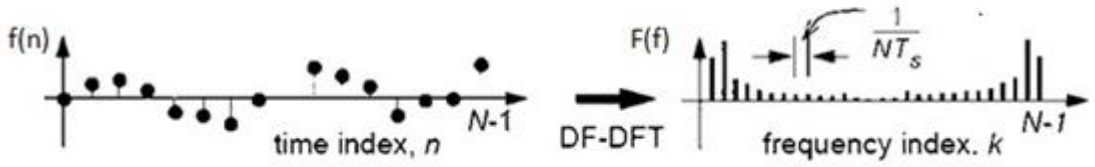

Figure 3-5 Diagram of DFT

The region around each of the *N* values is referred to as a frequency bin, and is of width $1/(NT_s)$ Hz. Assuming both the time domain function and the frequency domain spectrum are periodic as shown in Figure 3-6 [22], with a total of *N* samples per period, the discrete form of FT is most suited to numerical evaluation by digital computation.

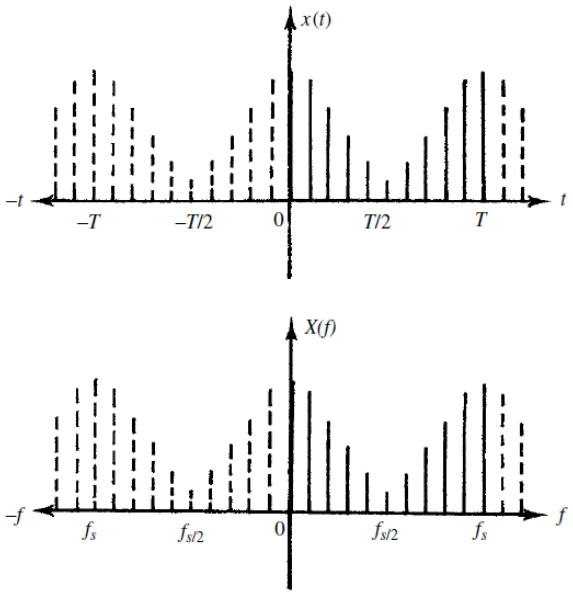

Figure 3-6 Diagram of DFT in terms of Time and Frequency Domains [22]

Consider equation (3.34) rewritten as follows,

$$F(f_k) = \sum_{n=0}^{N-1} f[t_n] W^{kn} \tag{3.35}$$

Here $W = e^{-j2\pi/N}$

Over all the frequency components, equation (3.30) becomes a matrix equation.

$$\begin{bmatrix} F(f_1) \\ F(f_2) \\ \vdots \\ F(f_k) \\ \vdots \\ F(f_{N-1}) \end{bmatrix} = \begin{bmatrix} 1 & 1 & \cdots & 1 & \cdots & 1 \\ 1 & W & \cdots & W^k & \cdots & W^{N-1} \\ \vdots & \vdots & \cdots & \vdots & \cdots & \vdots \\ 1 & W^k & \cdots & W^{k^2} & \cdots & W^{k(N-1)} \\ \vdots & \vdots & \cdots & \vdots & \cdots & \vdots \\ 1 & W^{N-1} & \cdots & W^{(N-1)k} & \cdots & W^{(N-1)^2} \end{bmatrix} \begin{bmatrix} f[t_0] \\ f[t_1] \\ \vdots \\ f[t_k] \\ \vdots \\ f[t_{N-1}] \end{bmatrix} \tag{3.36}$$

or in a condensed form

$$[F(f_k)] = [W^{kn}][f[t_n]] \tag{3.37}$$

In these equations, [F (f_k)] is a vector representing the *N* components of the function in the frequency domain, while [*f* [t_n]] is a vector representing the *N* samples of the function in the time domain.

Calculation of the N frequency components from the N time samples, requires a total of N^2 complex multiplications to implement in the above form. Each element in the matrix $[W^{kn}]$ denotes a unit vector with a clockwise rotation of $2n\pi / N$ ($n = 0,1,2,\ldots,(N-1)$) introduced between successive components. Depending on the value of N, a number of these elements are the same.

3.2.4 Fast Fourier Transform

For large values of N, the computational time and cost of executing the N^2 complex multiplications of the DFT can become prohibitive. The FFT was first popularised in the 1960's with the Cooley-Tukey, and Good/Thomas publication [70]. It takes advantage of the similarity of many of the elements in the matrix $[W^{kn}]$, and it produces the same frequency components using only $(N/2)\log_2 N$ multiplications to execute the solution of equation (3.37) Therefore, for example, let $N=1024=2^{10}$, there is a saving in computation time by a factor of over 200 [22].

This is realized by factorising the matrix $[W^{kn}]$ of equation (3.37) into $\log_2 N$ individual or factor matrices such that there are only two non-zero elements in each row of these matrices, one of which is always unity. Therefore, when multiplying by any factor matrix only N operations are required. The reduction in the number of multiplication required, to $(N/2)\log_2 N$, is obtained by recognising that

$$W^{N/2} = -W^0 \qquad \textbf{(3.38)}$$

$$W^{(N+2)/2} = -W^1 \qquad \textbf{(3.39)}$$

and etc.

In order to obtain the factor matrices, it is first necessary to re-order the rows of the full matrix. If rows are indicated by a binary representation, then the re-ordering is by bit reversal.

An example of harmonic analysis using FFT is illustrated below:

The input signal is the same as the one in FS example 2

$$S = 0.5\cos(50\pi t + \frac{1}{3}\pi) + \cos(100\pi t + \frac{2}{3}\pi) + 1.5\cos(150\pi t + \pi) + 2\cos(200\pi t + \frac{4}{3}\pi) \quad \textbf{(3.40)}$$

The FFT outputs of signal are magnitude spectrum and phase spectrum which are presented in Figure 3-7

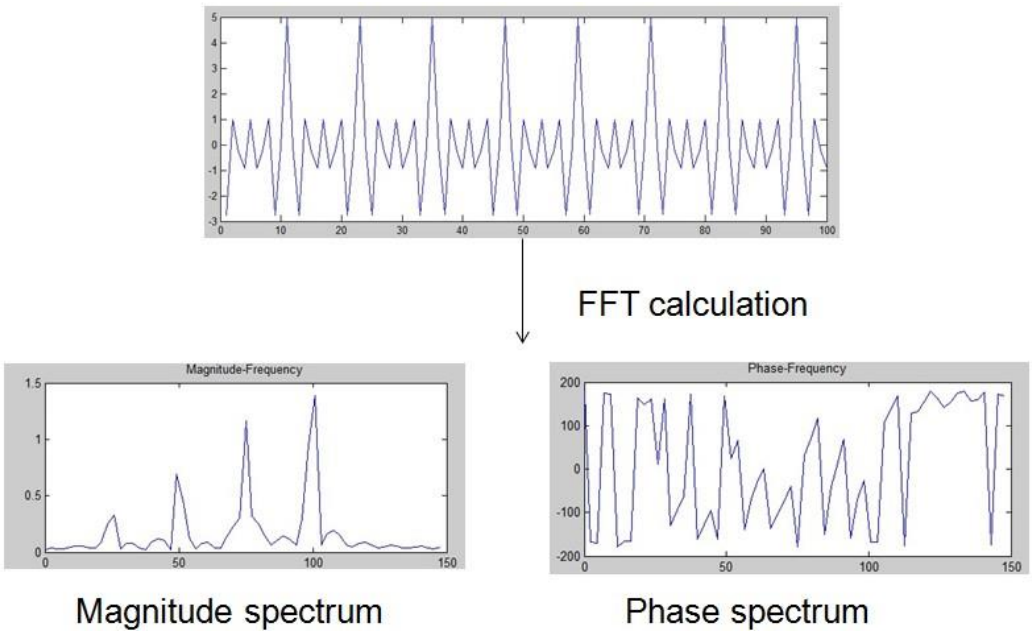

Figure 3-7 Input Signal with Its Magnitude Spectrum and Phase Spectrum

The techniques based on the Fourier analysis are the most widely utilised signal processing tools in power system harmonic analysis. However, these methods have some limitations which will be discussed in more detail in **Chapter 5**. To overcome these limitations of the Fourier analysis, the theoretical background and analysis method of WT is presented in the next section.

3.3 Wavelet Transform

The WT is originally developed to process seismic signal, and provides a fast and effective way of analysing non-stationary voltage and current waveforms. Compared to FT method, WT can decompose the signal analysed into frequency components. In addition, it can also tailor the frequency resolution, which are valuable characteristics in the process of finding the source of transient signals.

The ability of wavelets is to focus on short time intervals for high-frequency components and long intervals for low-frequency components, which improves the analysis of signals with localised impulses and oscillations, in particular for the fundamental and low-order harmonic signals.

3.3.1 Development of Wavelets

The conception of wavelet was firstly introduced in 1980 by J. Morlet, an engineer whose job was to process signal in the analysis of petroleum. However, his idea could not be recognised by famous mathematicians at that time. Fortunately with the development of mathematics and the pursuit of more precise analysis in signal processing, people had a renascent interest in wavelet [71].

In 1985, Y.Meyer invented a real wavelet occasionally which was the first non-trivial wavelet, but did not have the ability of compact support. He made a great effort to boost the advancement of wavelet. At the same time, beyond the scientist contributing to the wavelet, Ingrid Daubechies who is the author of [72], invented a set of orthonormal wavelet basis and played the most important role to popularise the conception and application of wavelet. As a result, the wavelet has received more and more attention [73].

In 1986, S. Mallat who was a graduate student specialised in computer vision and image analysis through Meyer' work, and conceived a layered structure used in image analysis for wavelet expansions. Then they jointly worked out the mathematical formulation of

'Multi-resolution Analysis' (MRA) which can be used to decompose the original signal into sub-bands with different scales [74].

3.3.2 Definition of Wavelet

A wavelet is a brief oscillating waveform that lasts for at most a few cycles. The fundamental idea behind wavelets is to analyse signal according to the scale and resulting in creating mathematical structures that can vary in terms of scale.

The first definition of the wavelet which was proposed by Grossmann and Morlet, is quite broad. Regarding their definition, "A wavelet is a function ψ (t) in $L^2(R)$ whose Fourier transform Ψ (ω) satisfies the condition $\int_0^\infty |\Psi(t\omega)|^2 \frac{dt}{t} = 1$ almost everywhere" [75].

The second definition of the wavelet related to the Littlewood-Paley-Stein theory. According to the theory, "A wavelet is a function ψ (t) in $L^2(R^n)$ whose Fourier transform Ψ (ω) satisfies the condition $\sum_{-\infty}^{\infty} \left|\Psi(2^{-j}\omega)\right|^2 = 1$ almost everywhere" [75]. If $\psi(t)$ is a wavelet in this sense, then $\sqrt{\log 2}\psi$ satisfies the Grossmann-Morlet condition.

The third definition of the wavelet was proposed by Haar and Stromberg. "A wavelet is a function $\psi(t)$ in $L^2(R)$ such that $2^{j/2}\psi(2^j x - k)$, $j, k \in Z$, is an orthonormal basis for $L^2(R)$" [75]. Such a wavelet $\psi(t)$ necessarily satisfies the second definition.

3.3.3 Wavelet Basic

In this section, a brief outline of the WT is presented, while the full WT theory and its applications can be found in [72] [76] [77] [78] [43].

3.3.3.1 Wavelet Transform

Let $\psi(t)$ be a complex-valued function, it should satisfy the following conditions:

$$\int_{-\infty}^{+\infty} |\psi(t)|^2 d(t) < \infty \quad \textbf{(3.41)}$$

$$C_\psi = 2\pi \int_{-\infty}^{+\infty} \frac{|\Psi(\omega)|^2}{|\omega|} d\omega < \infty \quad \textbf{(3.42)}$$

Where ψ (t) is the mother wavelet, Ψ (ω) denotes the FT of ψ (t). The first condition implies finite energy of the function ψ (t), and the second condition, namely admissibility condition, implies that if Ψ (ω) is smooth then Ψ (0) = 0.

3.3.3.2 Continuous Wavelet Transform

The definition of the CWT for a real signal is

$$CWT(a,b) = \frac{1}{\sqrt{|a|}} \int_{-\infty}^{+\infty} \psi'\left(\frac{t-b}{a}\right) f(t) dt \quad \textbf{(3.43)}$$

Where f (t) denotes the real signal to be transformed. ψ' (t) is the complex conjugate of the ψ (t) which is defined on the open (b,a) half plane ($b \in$ R,$a > 0$). The parameter a corresponds to the scale of the analysing wavelet and the parameter b corresponds to the time shift of ψ (t). If the $\psi_{a,b}(t)$ is a dilated and translated version of the ψ (t), then

$$\psi_{a,b}(t) = a^{-1/2} \psi\left(\frac{t-b}{a}\right) \quad \textbf{(3.44)}$$

The equation (3.43) can be written as a scalar or inner product of the real signal f (t) with the function $\psi_{a,b}(t)$

$$CWT(a,b) = \int_{-\infty}^{+\infty} \psi'_{a,b}(t) f(t) dt \quad \textbf{(3.45)}$$

The original signal f (t) can be obtained from the WT coefficients $CWT(a,b)$ by the inverse CWT shown as followed

$$f(t) = \frac{1}{C_\psi} \int_{-\infty}^{+\infty} \int_{-\infty}^{+\infty} CWT(b,a) \psi_{a,b}(t) \frac{dadb}{a^2} \quad \textbf{(3.46)}$$

Where C_ψ is the constant value for normalisation.

The CWT maps a one-dimensional time signal to a two-dimensional time-scale joint representation. The time bandwidth produced by the CWT is the square of the signal.

3.3.3.3 Discrete Wavelet Transform

However, the goal of analysis method with signal processing is to represent the signals efficiently with few parameters in many applications. The use of the DWT can reduce the time bandwidth produced by the WT.

Instead of continuous dilation and translation, the $\psi(t)$ maybe dilated and translated discretely by choosing $a = a_0^m$ and $b = nb_0a_0^m$, where both a_0 and b_0 are fixed constants with $a_0 > 1$, $b_0 > 0$, $m,n \in Z$ and Z is the set of positive integers. Then, the discretised mother wavelet is shown as follow,

$$\psi_{m,n}(t) = a_0^{-m/2}\psi(\frac{t - nb_0a_0^m}{a_0^m}) \quad \textbf{(3.47)}$$

And the DWT formula is given by

$$DWT(m,n) = \int_{-\infty}^{+\infty} \psi'_{m,n}(t) f(t)dt \quad \textbf{(3.48)}$$

The most common choice of a_0 and b_0 are $a_0 = 2$ and $b_0 = 1$, resulting in a binary dilation of 2^{-m} and dyadic translation of $2^m n$. The inverse DWT becomes

$$s(t) = \frac{1}{C_\psi}(\sum_m \sum_n DWT(m,n)\psi_{m,n}(t)) \quad \textbf{(3.49)}$$

The function $\psi_{m,n}(t)$ provides sampling points on the scale-time plane: linear sampling in the time direction but logarithmic in the scale direction. The DWT can be implemented by using MRA which can decompose a signal into scales with different time and frequency resolution.

3.3.3.4 Discrete Wavelet Packet Transform

The wavelet packets are defined by the following equations:

$$\psi_{2k}(t) = 2\sum_{l=0}^{2N-1} g(l)\psi_k(2t-l) \quad \textbf{(3.50)}$$

$$\psi_{2k+1}(t) = 2\sum_{l=0}^{2N-1} h(l)\psi_k(2t-l) \quad \textbf{(3.51)}$$

With the initial condition $\psi_1(t) = \psi(t)$

Where g (l) and h (l) are high-pass (HP) and low-pass (LP) filters respectively with the length of 2N. The wavelet packets are obtained from a linear combination of the scaled and translated version of the mother wavelet ψ (t).

3.3.4 Examples of Wavelet Function

Some popular wavelets are introduced below [71], [77] and [78]:

Haar Wavelet: is the simplest wavelet function and it is the one of the CWT with discrete coefficients.

Assume that ϕ (t) is a box function satisfying the following:

$$\phi(\mathrm{t}) = \begin{cases} 1 & if\ 0 \le t \le 1 \\ 0 & otherwise \end{cases} \quad \textbf{(3.52)}$$

Let the function ψ (t) is equal to ϕ (2t) - ϕ (2t-1), the following function can be obtained:

$$\psi(\mathrm{t}) = \begin{cases} 1 & if\ 0 < t \le 1/2 \\ -1 & if\ 1/2 < t \le 1 \\ 0 & otherwise \end{cases} \quad \textbf{(3.53)}$$

The function ϕ (t) is the Haar scaling function, and ψ (t) is the Haar wavelet. This function is orthogonal to its own translations and dilations,

$$\psi_{m,n}(t) = 2^{-m/2}\psi(2^{-m}t - n), \quad m,n \in Z \quad \textbf{(3.54)}$$

where Z is the real integer, constitutes an orthonormal basis for $L^2(R)$. Generally the Haar function was the original wavelet. This wavelet is not continuous, while its FT $\Psi(\omega)$ decays only like $|\omega|^{-1}$, corresponding to bad frequency localisation.

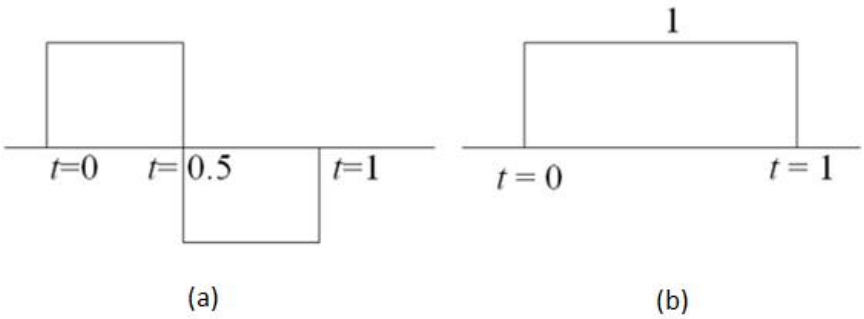

Figure 3-8 (a) Haar Wavelet; (b) Scaling Function [71]

Morlet Wavelet: is the most popular complex wavelet used in practice, which was often used by R. Kronland-Martiner and J.Morlet. Its FT is a shifted Gaussian, adjusted slightly so that Ψ (0) =0:

$$\Psi(\omega) = e^{-(\omega-\omega_0)^2/2} - e^{-\omega^2/2}e^{-\omega_0^2/2} \quad \textbf{(3.55)}$$

$$\psi(t) = (e^{-i\omega_0 t} - e^{-\omega^2/2})e^{-t^2/2} \quad \textbf{(3.56)}$$

where ω_0 is the central frequency of the mother wavelet. In practice one often takes ω_0=5. For this value of ω_0, the second term in equation (3.55) is very small that is can be neglected in practice. Thus in some references the mother wavelet definition of the Morlet wavelet can be written as:

$$\psi(t) = e^{-i\omega_0 t}e^{-t^2/2} \quad \textbf{(3.57)}$$

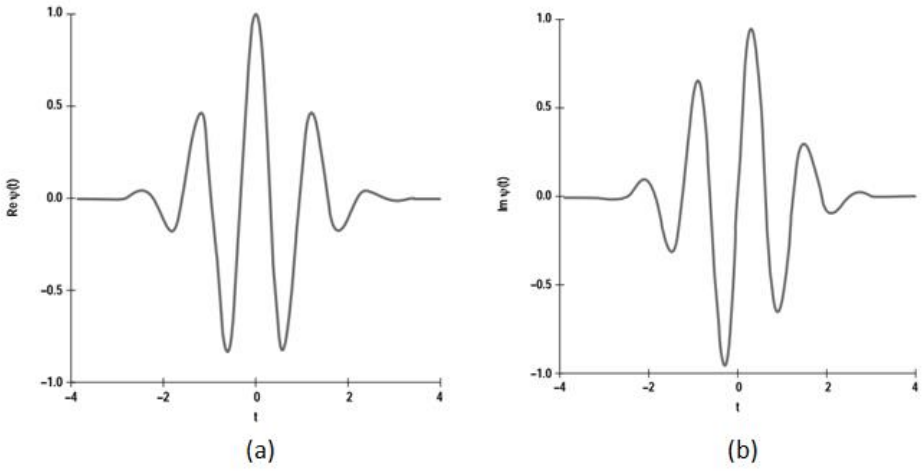

Figure 3-9 Morlet Wavelet for ω_0=5 (a) Real part (b) Imaginary part [71]

Meyer Wavelet: Yves Meyer constructed a smooth orthonormal wavelet basis as below. Suppose the FT form $\Phi(\omega)$ of a scaling function $\phi(t)$ as:

$$\Phi(\omega) = \begin{cases} 1 & if\ |\omega| \le \frac{2}{3}\pi \\ \cos[\frac{\pi}{2} v(\frac{3}{4\pi}|\omega| - 1)] & if\ \frac{2}{3}\pi \le |\omega| \le \frac{4}{3} \\ 0 & otherwise \end{cases} \quad \textbf{(3.58)}$$

where v is a smooth function satisfying the following conditions

$$v(t) = \begin{cases} 0 & if t \le 0 \\ 1 & if t \ge 1 \end{cases} \quad \textbf{(3.59)}$$

with the additional property $v(t) + v(1-t)=1$. This function $\Phi(\omega)$ is graph in Figure 3-10 (a).

The wavelet function $\psi(t)$ can be easily obtained from $\Phi(\omega)$ by the FT of $\psi(t)$. The function $\Psi(\omega)$ is plotted in Figure 3-10 (b), which is calculated as:

$$\Psi(\omega) = e^{i\omega/2}[\Phi(\omega + 2\pi) + \Phi(\omega - 2\pi)]\Phi(\omega/2) \quad \textbf{(3.60)}$$

$\psi(t)$ can be obtained by taking the inverse FT and shows a plot of Meyer wavelet in Figure 3.10 (c).

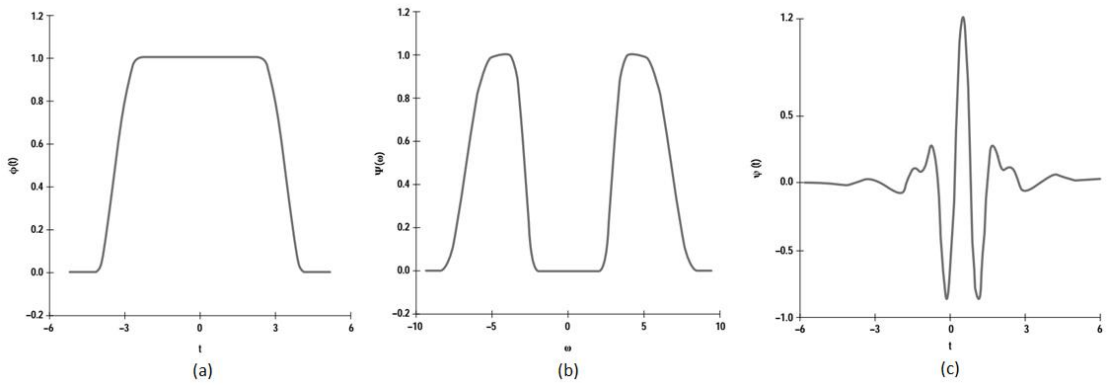

Figure 3-10 (a) Fourier Transform of the Scaling Function for the Meyer Basis; (b) Fourier Transform of the Meyer Wavelet; (c) The Meyer Wavelet [71]

Mexican Hat Wavelet: is the second derivative of the Gaussian function,

$$\psi(t) = n(1-t^2)e^{-t^2/2} \quad \textbf{(3.61)}$$

where n is a normalisation factor. A complex version of the Mexican hat wavelet can easily be constructed by setting the analytic version signal of the real-valued mother wavelet. However, the Morlet wavelet is used when a complex wavelet function is required in practice.

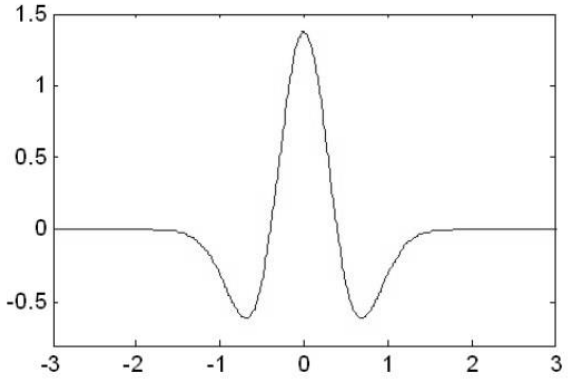

Figure 3-11 Maxican Hat Wavelet [71]

Daubechies (Db) Wavelet: is perhaps the most commonly used wavelet which is constructed by Ingrid Daubechies which is a kind of the DWT. All examples of orthonormal wavelet bases consist of infinitely supported functions, except for the Haarbasis. The Db wavelet is an orthonormal wavelet in which ψ (t) is compactly supported. The way to certify compact support for the wavelet ψ (t) is to choose a Db N-coefficient scaling function ϕ (t) with compact support. In general, ϕ (t) is a solution to the dilation equation:

$$\phi(t) = \sum_{k=-\infty}^{\infty} a_k \phi(St-k) \quad \textbf{(3.62)}$$

The dilation factor S = 2 is selected as a convenient choice. The constant coefficients a_k are known as filter coefficients and are obtained by imposing some conditions on the scaling function.

In order for the wavelet to have compact support and some type of smoothness, three conditions must be imposed on the ϕ (t).

- First, the scaling function has a non-vanishing integral

$$\int_{-\infty}^{\infty} \phi(t)dt = 1 \quad \textbf{(3.63)}$$

This leads to $$\sum_{k=-\infty}^{\infty} a_k = 2 \quad \textbf{(3.64)}$$

- Second, the scaling function is orthogonal to its translation, as in

$$\int_{-\infty}^{\infty} \phi(t)\phi(t+m)dt = \delta_{0,m} \quad \textbf{(3.65)}$$

This orthogonality condition implies that

$$\sum_{k=-\infty}^{\infty} a_k a_{k+2m} = 2\delta_{0,m} \quad \textbf{(3.66)}$$

- Third, the mother wavelet ψ (t) must have vanishing moments (must satisfy the moment conditions)

$$\int_{-\infty}^{\infty} \psi(t)t^p = 0 \quad p = 0,1 \quad \textbf{(3.67)}$$

This implies that $$\sum_{k=-\infty}^{\infty} a_k k^p = 0, \quad p = 0,1 \quad \textbf{(3.68)}$$

The corresponding wavelet function ψ (t) is obtained from the scaling function ϕ (t) can be written as:

$$\psi(t) = \sum_{k=-\infty}^{\infty} (-1)^k a_{N-1-k}\phi(2t-k) \quad \textbf{(3.69)}$$

where N is the coefficient number of scaling function. Assuming that N is equal to 4, the scaling function and wavelet for Db 4 are shown in Figure 3-12.

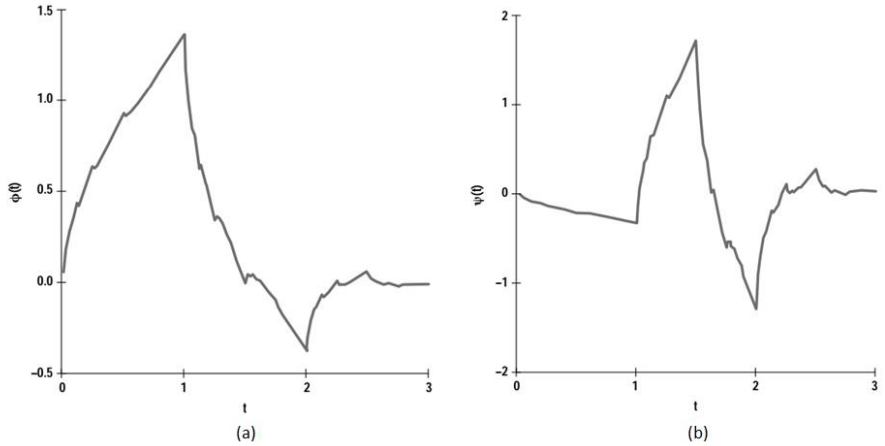

Figure 3-12 (a) The Daubechies Scaling Function for N=4; (b) The Daubechies Wavelet for N=4 [71]

3.4 Wavelet Transform Filter Bank

The WT provides a Multi-resolution Analysis (MRA). Based on the MRA, the WT can be implemented by using the filter bank which can decompose and reconstruct a signal into different time and frequency resolution. In frequency domain, the FFT is the fast and efficient implementation of the FT. Similarly the WT filter bank is the fast and efficient implementation of the WT. Figure 3.13 shows the coverage of the time-scale space for the WT, and as a comparison, that for the short-time Fourier transform (STFT). Filter bank will be introduced in this section.

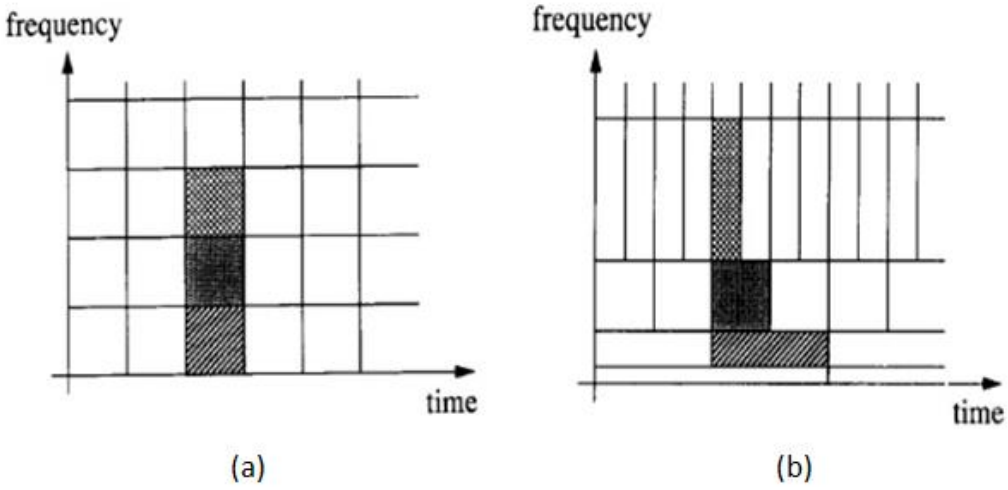

Figure 3-13 (a) Coverage of Time-frequency Plane in STFT Analysis; (b) Coverage of Time-frequency Plane in WT Analysis [74]

3.4.1 Filter Bank Design Criteria

3.4.1.1 Multi-resolution Analysis

S.Mallat invented MRA which can decompose the original signal into several other signals with different scales. The full theory can be found in [74]. This technique can decompose any given signals into high frequency and low frequency components. The high frequency component is referred to as the detail version which contains sharp edges, transition, and jumps; while the low frequency component is referred to as the smoothed version. Therefore, the decomposed signal at scale j are $a_j(n)$ and $d_j(n)$, where

$a_j(n)$ is the approximation coefficients which represent the smoothed part of signal $f(n)$, and $d_j(n)$ is the detail coefficients. The definitions are shown as:

$$a_j(n) = \sum_k h(k-2n)\, f_{j-1}(k) \quad \textbf{(3.70)}$$

$$d_j(n) = \sum_k g(k-2n)\, f_{j-1}(k) \quad \textbf{(3.71)}$$

where, $h(n)$ and $g(n)$ are the associated filter coefficients that decomposed $f(n)$ into $a_j(n)$ and $d_j(n)$. The Figure 3-14 shows that a signal $f(n)$ is decomposed into two layers by MRA

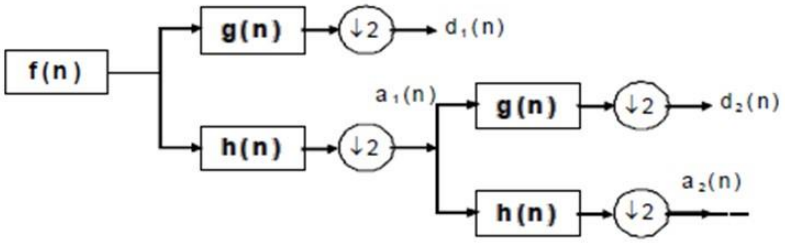

Figure 3-14 Two Level Wavelet Decomposition of a Signal *f*(*n*) based on MRA

3.4.1.2 Down-sampling and Up-sampling

The development of the MRA can be explained from the knowledge of the sub-band filtering. In sub-band filtering, the signal is passed through a set of LP and HP filters and the frequency spectrum is split. Since the wavelet function in the WT is a band-pass filter, the WT coefficients is the result of passing the signal through an appropriated band pass filter. The implementation of the WT using filter bank is shown in Figure 3-15

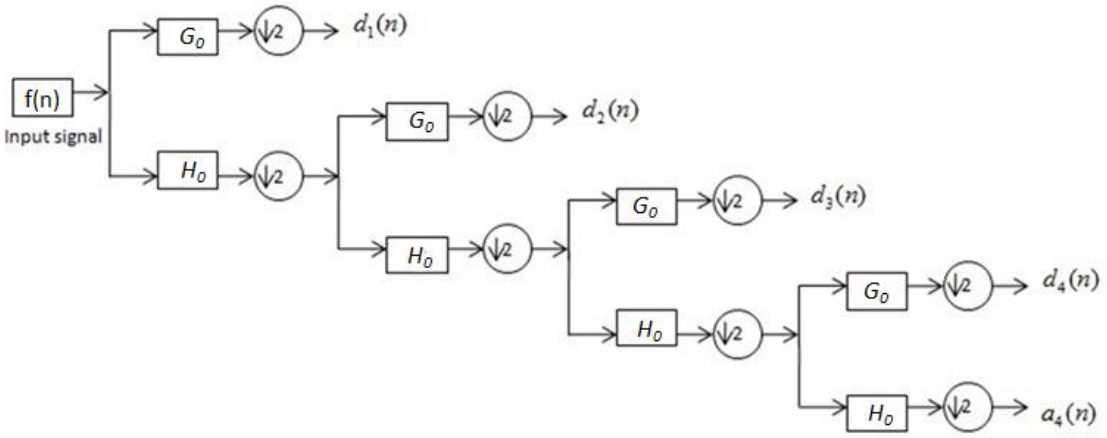

Figure 3-15 Decomposition of a Signal into Four-level Based on WT Filter Bank

In this filter bank, G_0 and H_0 are HP and LP filters, respectively. G_0 associate with the wavelet function ψ (t), which is also called mother wavelet, While H_0 associates with the scaling function ϕ (t) which serves time scale of the input sequence. The down-sampling denoted by $\downarrow 2$ is the process of removing every second point in the signal sequence. The filter bank decomposes the original signal f (n) into finer scale components d_1, d_2, d_3 and d_4 are the WT coefficients of f (n).

In order to remove the aliasing ,the reconstruction should be done [77]. The coefficients of the WT can be used to generate the reconstructed time domain signal. Figure 3-16 is the four-level WT resonstruction.

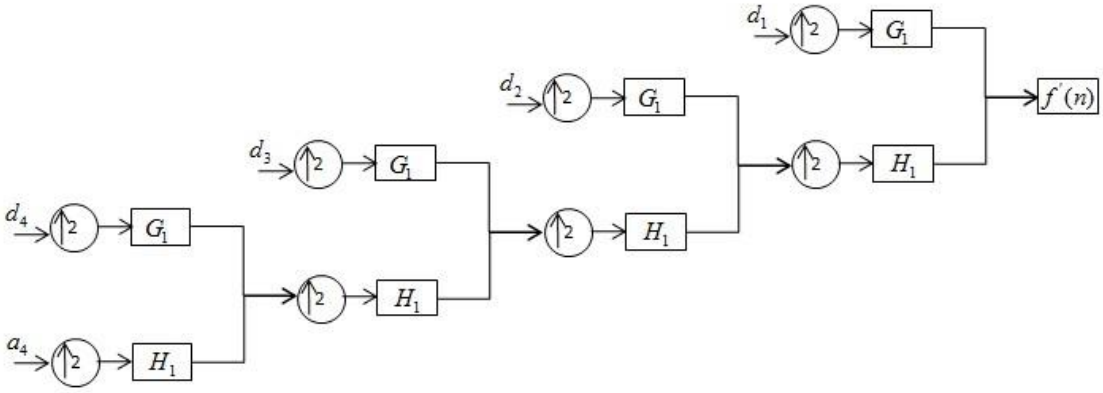

Figure 3-16 Reconstruction of a Signal into Four-level based on WP Filter Bank

In the filter bank of Figure 3-16, the G_1 and H_1 are the synthesis filters. The outputs form G_1 and H_1 are combined to produce the output $f'(n)$. The up-sampling operation denoted by $\uparrow 2$ is the process of inserting zeros at every second point in the signal sequence.

3.4.1.3 Perfect Reconstruction

A filter bank is a set of filters, linked by sampling operators and sometimes by delays. Figure 3-17 is a one-level WT filter bank, the analysis filters are normally LP and HP filters. The down-sampling operators are decimators, while the up-sampling operators are expanders. In practice, the filters cannot be realised ideal with the transition band exists. Besides aliasing, this leads to an amplitude and phase distortion in each of the scales of the filter band. In order to obtain a perfect reconstruction, G_1 and H_1 must satisfy certain relationsip with G_0 and H_0. Futhermore, some design criteria for both the analysis and synthesis filters should be met to prevent aliasing and distortion in order to gurantee a perfect reconstruction [76].

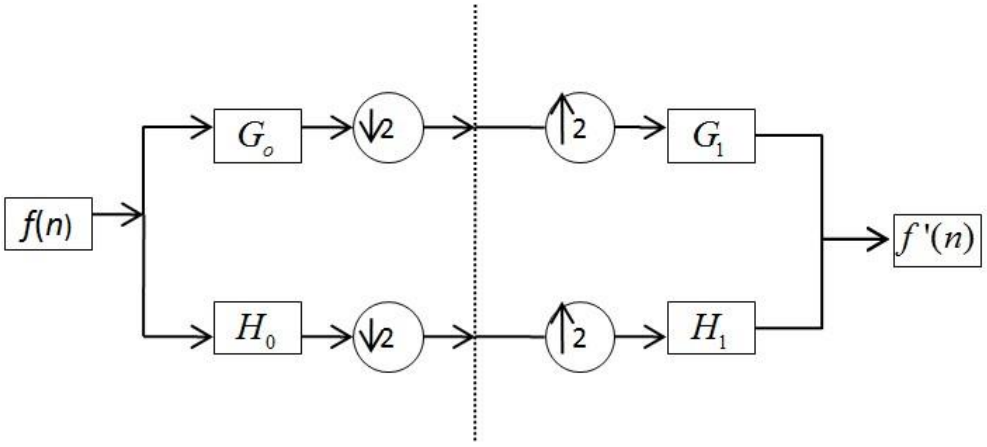

Figure 3-17 One-level Wavelet Transform Filter Bank

In the z-domain, the output from H_0 in the lower path is $H_0(z)F(z)$, after down-sampling, it becomes

$$0.5[H_0(z^{1/2})F(z^{1/2}) + H_0(-z^{1/2})F(-z^{1/2})] \quad \textbf{(3.72)}$$

After up-sampling, the component in equation 3.72 becomes

$$0.5[H_0(z)F(z) + H_0(-z)F(-z)] \quad \textbf{(3.73)}$$

The component $H_0(-z)F(-z)$ is the image of $H_0(z)F(z)$. The corresponding output from the LP filter can be written as

$$0.5H_1(z)[H_0(z)F(z)+H_0(-z)F(-z)] \quad \textbf{(3.74)}$$

In the same way, the output of the HP filter is obtained by

$$0.5G_1(z)[G_0(z)F(z)+G_0(-z)F(-z)] \quad \textbf{(3.75)}$$

The outputs are combined to reconstruct the original signal

$$F^{'}(z)=0.5[H_0(z)H_1(z)+G_0(z)G_1(z)]F(z)+0.5[H_0(-z)H_1(z)+G_0(-z)G_1(z)]F(-z) \quad \textbf{(3.76)}$$

For perfect reconstruction with time delay l, $F^{'}(z)$ must be $z^{-l}F(z)$. Thus the 'distortion term' must be z^{-l} and the 'aliasing term' must be zero.

A one-level filter banke provides perfect reconstrction when

$$H_0(z)H_1(z)+G_0(z)G_1(z)=2z^{-l} \quad \textbf{(3.77)}$$

$$H_0(-z)H_1(z)+G_0(-z)G_1(z)=0 \quad \textbf{(3.78)}$$

In order to remove the aliasing, choose:

$$H_1(z)=G_0(-z) \quad \textbf{(3.79)}$$

$$G_1(z)=-H_0(-z) \quad \textbf{(3.80)}$$

To eliminate distortion, rewirte equation 3.77 with product filter which is defined by $P_0(z)=H_1(z)\mathrm{H}_0(z)$. While the HP filter is $P_1(z)=G_1(z)G_0(z)$.

$$P_0(z)-P_1(-z)=2z^{-l} \quad \textbf{(3.81)}$$

Overall, the perfect reconstruction filter bank can be designed in following steps:

- Design a low-pass filter P_0 satisfying the equation 3.81
- Factor P_0 into $H_1(z)$ $H_0(z)$. Then use the equation 3.79 and 3.80 to calculate the high-pass filter $G_1(z)$ and $G_0(z)$.

3.4.2 DWT Filter Bank

In the DWT filter bank, the input signal is decomposed and reconstracted by HP filter and LP filter into its high frequency band and low frequency band, respectively. The input spectrum at each stage is always decomposed into two bands at a time, the lower frequency band is split further while the higher frequency band becomes one of the outputs. Figure 3-18 shows a two-level decomposition DWT filter bank. The frequency range of the outputs can be obtained by the signal sampling frequncy f_s and the number of levels of decomposition N. The upper and lower frequnceis of the sub-band d_j are calculated by

$$f_{hd_j} = \frac{f_s}{2^j} \tag{3.82}$$

$$f_{ld_j} = \frac{f_{hd_j}}{2} \tag{3.83}$$

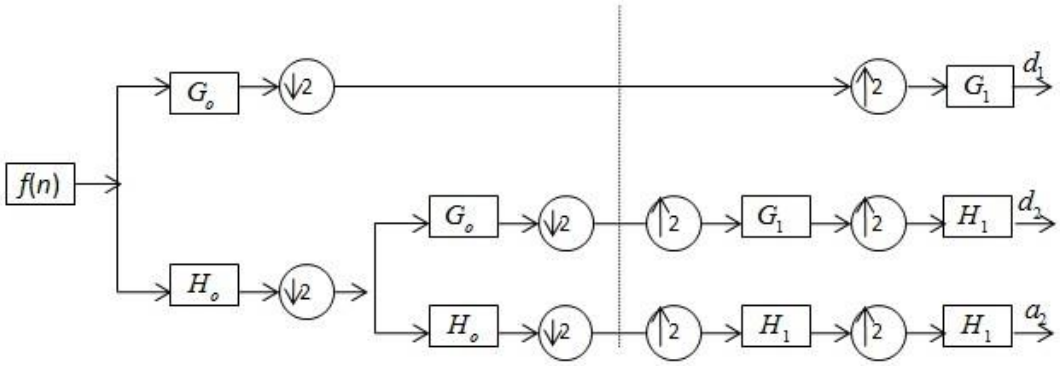

Figure 3-18 Two-level DWT Filter Bank

This DWT filter bank can be used to separate the high frequency transients from the low frequency steady state components and decomposes the signal into non-uniform sub-bands. The sub-band spectrum is proportional to its average frequency. As a result, the higher average frequency has wider spectra, while the lower average frequency has narrower spectra. It can be seen in Figure 3-19 which shows the sub-band spectrum of the four-level decomposition in Figure 3.18. The sample frequency of the input signal is 800 Hz.

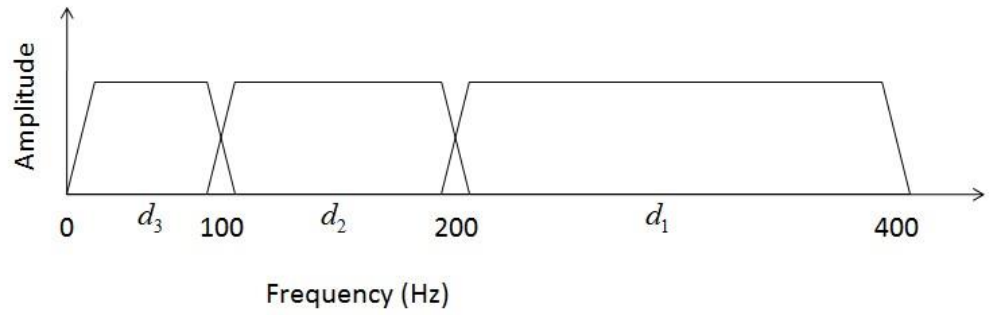

Figure 3-19 Sub-band Spectrum of the Four-level Decomposition

However, the non-uniform sub-band is not good at analysing some kind of signals, for exmaple, the signal with high-order harmonic. Further splitting for the high band may be required. To overcome the limitation of the DWT filter bank, the DWPT filter bank is applied to decompose the signal, in order to obtain the uniform sub-bands.

3.4.3 DWPT Filter Bank

In the DWPT filter bank, both the lower frequency band and higher frequency band are split further. The decomposed sub-bands have uniform bandwidths. It is a decomposition method with a better time-frequency characteristic. The frequency bandwidth of each output sub-band is f_s / 2N, where f_s is the signal sampling frequency and N is the total number of output sub-band. The range of the frequency of each sun-band is determined by the frequency of corresponding wavelet packet's oscillation which is given in eqaution 3.50 and 3.51. In Figure 3-20, the frequency of the input siganl f (n) with a frequency bandwidth of 800Hz is decomposed into eight uniform sub-bands of 100Hz interval.

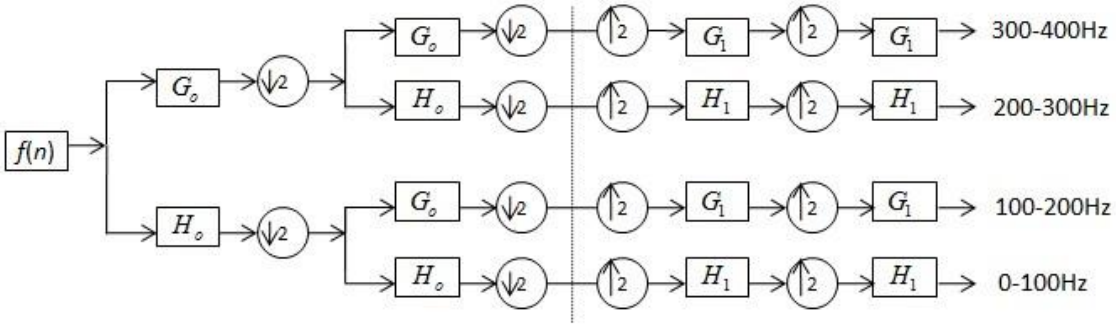

Figure 3-20 Two-level DWPT Filter Bank

Compared with the DWT filter bank, the DWPT filter bank can decompose the input signal into smaller frequency range time domain components of smaller frequency bands.

3.5 Conclusion

This chapter has introduced two methods of waveform transformations: Fourier analysis and wavelet analysis. The concepts, principles and features of Fourier analysis and wavelet analysis has been explained in detail respectively. Fourier analysis has been viewed as the conventional signal processing method to analyse power waveform distortion. However, Fourier analysis provides limited information of the signals from the aspect of time domain, the Fourier analysis cannot obtain accurate values of amplitude and phases from harmonics with frequencies different from that of the window function frequency. These characteristics are considered as most important limitations.

In order to overcome the limitations of Fourier analysis and obtain better results, wavelet analysis has been proposed. It is able to analyses signals in both time and frequency domains, and able to be adjusted for various frequencies by using various window sizes. Wavelet analysis is viewed as MRA, and thus provided more accuracy analysis results than Fourier analysis. In practice, DWT or DWPT filter banks are used and designed to perform wavelet analysis, and thus filter bank design concepts and criteria for DWT and DWPT are presented in detail in **Section 3.4.**

PQ has been considered as an important concept from electricity supply to customers. Moreover, it can have negative impacts on both industrial process and users if it cannot meet the quality requirements. Therefore, it is necessary to employ a more accuracy method to classify PQ disturbance, in order to improve the quality of power. On the other hand, harmonic studies also require a more accuracy method as harmonic content sometimes has non-integer harmonic that cannot be analysed by conventional Fourier analysis. Consequently, it is necessary to employ the proposed wavelet analysis in PQ classification and harmonic analysis to obtain a more accuracy results, compared to conventional Fourier method. Concepts, principles and examples of PQ classification and harmonic analysis in detail with wavelet analysis method will be presented in **Chapter 4** and **Chapter 5** respectively.

Chapter 4 Wavelet Transform Based Fuzzy Logic for Power Quality Classification

4.1 Introduction

In recent years, PQ study has become an important subject. In order to avoid the high cost of equipment failures, all customers want to enjoy an electricity supply with high PQ. Poor PQ is normally caused by power-line disturbances, such as voltage sag/swell, harmonic, flicker, momentary interruption, and impulses, and it has a large detrimental effect on both the industrial process and commercial users. In order to improve the quality of power, the sources and causes of such disturbances must be known. When the disturbance type has been classified accurately, the PQ engineer can define the major effects at the load and analyse the disturbance waveforms. Thus it is desirable to develop methods for detecting, identifying and analysing all kinds of disturbances.

In this chapter, a fuzzy-expert system based on wavelet is presented for PQ disturbance waveform classification. The WT decomposition based on DWT filter bank and Parseval's theorem are first introduced. To extract features in PQ disturbance, the energy distribution of wavelet at each decomposition level is calculated. Then, a fuzzy-expert system is employed to classify disturbance according to the wavelet decomposition level and the numerical values of the energy distribution. Based on the energy distribution patterns, the membership functions of input and rule base are generated. Finally, the fuzzy set of the output variable is converted to a crisp number, in terms of which the disturbances are classified. The types of disturbances concerned are related to voltage sag/swell, interruption, harmonic, and flickers.

This chapter is organized as follows. Firstly, the existing methods for PQ classification are listed in **Section 4.2**. Secondly, the WT decomposition and the energy calculation

method of a signal at each wavelet decomposition level is introduced in **Section 4.3**. Thirdly, the feature extraction is presented in **Section 4.4**. Fourthly, the fuzzy-expert system for PQ disturbances classification is proposed in **Section 4.5**. Fifthly, in **Section 4.6**, the application and result are given. Finally, conclusions are presented in **Section 4.7**.

4.2 Existing Methods for Power Quality Classification

Since the traditional methods to analyse and identify power disturbances are mainly based on visual inspection of the disturbance waveforms, the PQ engineers' knowledge plays a serious position, and the PQ engineers cannot always handle huge amount of data to inspect. Therefore, many new and powerful automatic tools for the analysis and classification of PQ disturbance have been developed in the last few years. However, the correct classification rate for the actual event is not high enough; there is still space for improving accuracy [1]. In the following section, a brief review of these methods is presented.

In [7], a novel classifier using a rule-based method and a wavelet packet-based Hidden Markov Model (HMM) is proposed. The rule-based method is used to classify the time-characterized-feature disturbances, while the wavelet packet-based HMM is used for the frequency-characterized-feature power disturbances. In [8], a wavelet-based neural-network classifier for recognizing PQ disturbances is constructed and tested under many kinds of PQ disturbances. The DWT technique is integrated with the probabilistic neural-network model to build the classifier. In [9] [10], the proposed recognition scheme is carried out in the wavelet domain using a set of multiple neural networks, and the outcomes of the networks are then integrated using decision making schemes. Thus the classifier is capable of providing a degree of belief for the identified disturbance waveform. In [11], minimum Euclidean distance, k-nearest neighbor, and neural network classifiers are used to automatically classify PQ disturbance. In [12], the classifier is based on neural-fuzzy technology for the recognition of PQ disturbances. The classifier implements neural networks in the architecture of frequency sensitive competitive leaning and leaning vector quantization. In [13], a wavelet-based extended fuzzy reasoning is presented to identify PQ disturbances. Based on the features obtained from wavelet decomposition level, rule bases are generated for extended fuzzy reasoning. The PQ disturbance features are finally recorded as a real number through extended fuzzy reasoning, in terms of which various PQ disturbances are classified. In [14], wavelet decomposition is used to extract the features from different disturbances,

and then decision tree is used for classifying the disturbances. In [15], a hybrid scheme using a Fourier linear combiner and a fuzzy expert system is proposed. The signal is processed through a Fourier linear combiner block to generate normalized peak amplitude and phase, and then the fuzzy expert diagnostic module is used to identify the class to which the disturbance belongs. In [16] [17], the time-frequency ambiguity plane with kernel techniques is employed to extract the disturbance features, and then classify the disturbance by using the Heaviside-function linear classifier and neural networks with feed forward structures.

4.3 Wavelet Transform Decomposition and Parseval's Theorem

4.3.1 Wavelet Transform Decomposition by DWT Filter

The WT is a mathematical tool which has its energy concentrated in time and analyses transient，non-stationary or time varying phenomena [74]. Compared with FT, the most important advantage of the WT is that it has the ability to analyse signal in both time and frequency domains. Furthermore, the WT also has the ability to be adjusted automatically for low or high frequencies because it uses short windows at high frequencies and long windows at low frequencies, thus leading to an optimal time-frequency resolution in all the frequency ranges [67]. As a result, the WT is applied to analyse the power disturbance signals.

The main characteristic in the WT is the DWT filter bank which can decompose the original signal into several other signals with different scales. A detailed introduction of the DWT filter bank is given in **Section 3.4**. Figure 4-1 is the wavelet decomposition of a signal distorted with voltage sag by using two-level DWT filter bank. The distorted signal is decomposed to two detailed versions and one smooth version. The features in the decomposed waveform have the ability to extract important information from the distorted signal.

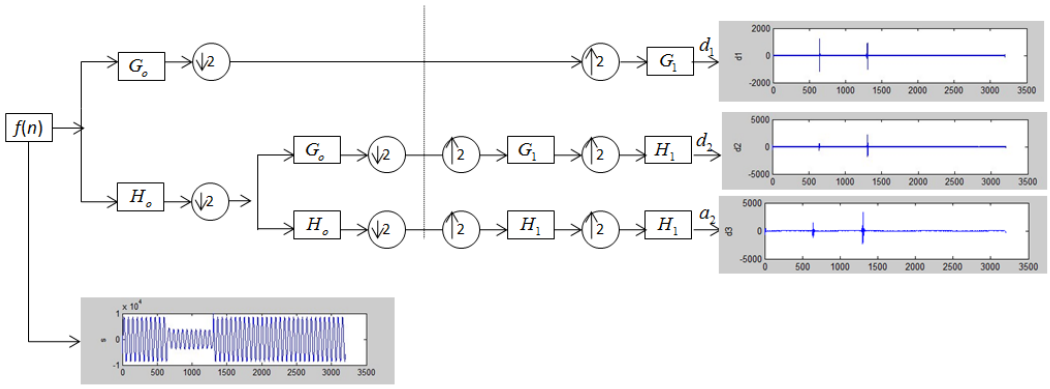

Figure 4-1 Wavelet Decomposition of a Signal *f* (*n*) Based on two-level DWT Filter Bank

The choice of analysing wavelet plays a significant role in detecting and extracting PQ disturbance features. In this proposal, the Db wavelet is chosen to analyse different PQ disturbances, because of its sensitivity to irregular and non-stationary signal. As presented in [43], among Db wavelets, the Db4 and Db6 wavelets are experts for short and fast transient disturbances, while the Db8 and Db10 wavelets are good for slow transient disturbances. The Db 4 wavelet has the smallest number of coefficients, and it is the shortest one among the Db wavelet family, thus it is the only wavelet that can detect the small fluctuation of signals. As a result, Db4 could be the optimal choice because it is the most localised in time.

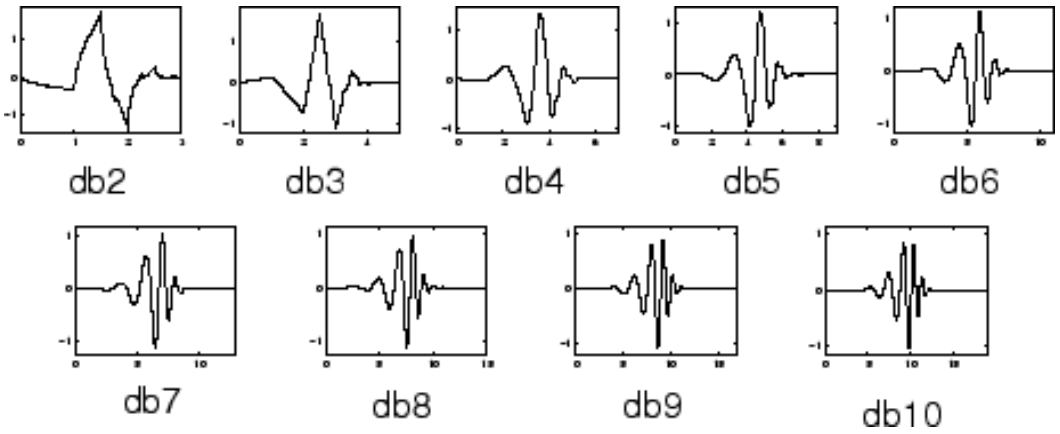

Figure 4-2 Db Wavelet with Different Coefficients [43]

4.3.2 Parseval's Theorem in DWT Application

According to the Parseval's theorem, the energy of the distorted signal is related to the energy in each of the expansion components and their wavelet coefficients. It means that the energy of the signal can be separated according to the following expansion [78]:

$$\int |f(t)|^2 d(t) = \sum_k |a(k)|^2 + \sum_{j=0}^{j-1} \sum_k |d_j|^2 \quad \textbf{(4.1)}$$

Therefore, the energy of distorted signal E_{signal} can be defined by wavelet coefficient as formula

$$E_{signal} = E_{ao} + \sum_{j=0}^{j-1} E_{dj} \quad \textbf{(4.2)}$$

$$E_{ao} = \sum_k |a(k)|^2 \quad \textbf{(4.3)}$$

$$E_{dj} = \sum_{k} \left| d_j(k) \right|^2 \quad \textbf{(4.4)}$$

where E_{ao} is the energy of the approximated version of the decomposed signal and E_{dj} is the disturbance energy at the detail version. The energy distribution features of the detailed version from distorted signal will be utilised to extract the features of power disturbances. Therefore, the detailed energy will be calculated at each decomposition level to extract the feature curve.

4.4 Feature Extraction

4.4.1 Wavelet Decomposition Levels of Feature Extraction Curve

In this case, in order to ensure all disturbance features in both high and low frequency are extracted, a12-level DWT filter bank is used. The outputs are twelve detailed decomposed scales and one smooth decomposed scale. The first scale signal has frequency range of $f/2$-$f/4$, where f is the sample frequency of the time domain disturbance signal. The second, third, fourth … k^{th} scale signals have frequency ranges of, $f/4$-$f/8$, $f/8$-$f/16$, $f/16$-$f/32$… $f/2^k$-$f/2^{k+1}$, respectively, and a_k contains the frequencies lower than $f/2^{k+1}$.

In general, it is possible to categorise three properties of energy distribution of the distorted signal based on wavelet decomposition levels. These properties become the features for classifying the disturbance.

- When a sag or swell or interruption occurs, the great variations of energy will show in normal frequency sag and swell zone.
- When the voltage suffers a disturbance of the high frequency elements, the obvious variations of energy will show in high frequency disturbance zone.
- When the voltage suffers a disturbance of the low frequency elements, the obvious variations of energy will show in low frequency disturbance zone.

The Figure 4-3 is a PQ feature extraction curve for pure sine wave. The x-axis of this figure is wavelet decomposition level, while the y-axis is numerical value of the energy distributions at each wavelet level.

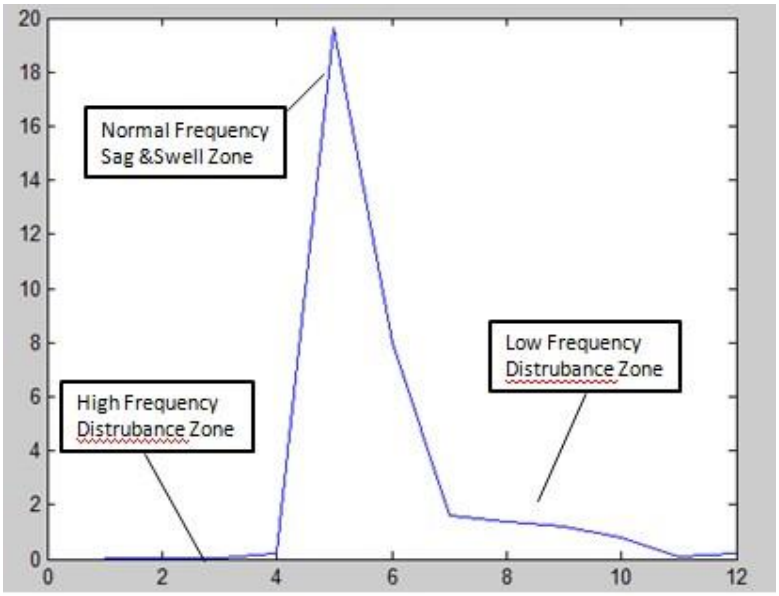

Figure 4-3 Generalized Power Quality Feature Extraction Curve (Pure Sine Wave)

4.4.2 Energy in Feature Extraction Curve

The amplitude of the feature extraction curve is the numerical value of the energy distributions at each wavelet level. The peak value of feature extraction curve generated by pure sine wave could be viewed as the fundamental. The fundamental is used to compare with other peak values of feature extraction curve generated by the other kinds of distorted signals. They can become the features for classifying the disturbances.

4.5 The Proposed Fuzzy-expert System for Power Quality Disturbance Classification

Many of PQ disturbance classifications use the neural network. This method shows relatively good results; however, the performance of the neural network depends on the training process, and once the neural network is trained, making changes need retrain the network. In order to overcome the limitations of the neural network, fuzzy-expert systems are applied to PQ disturbance classification. The advantages of the fuzzy-expert system are listed as follows [80][81]. Firstly, fuzzy rules are more comprehensible than the neural network. Secondly, the fuzzy-expert system reduces the need for training. Although the rule set need to be generated by typical cases, they are not mandatory. The reason is the rule set can be improved or generated by the experts with the required knowledge. Thirdly, the fuzzy-expert system is quite flexible. It means that the input, output, the number of the fuzzy rules in rule set and the rules can be changed conveniently if needed. In this section, the fuzzy logic is introduced briefly and then a usefulness fuzzy-expert system is proposed.

4.5.1 Introduction to Fuzzy-expert System

Fuzzy logic refers to a logic system which represents knowledge and reasons in an imprecise of fuzzy manner for reasoning under uncertainty. Unlike the classical logical systems, it is motivated by observing that human reasoning can employ concepts and knowledge that do not have exactly or sharp boundaries [80]. The fundamental element of a fuzzy logic system is the membership function. The degree of membership in a set is expressed by a number between 0 and 1 in which a membership value 0 indicates that it is entirely not in the set, a value of 1 means that the variable is completely satisfactory for the fuzzy set. Therefore, a fuzzy set can be defined as a function called the membership function that maps objects into the domain of concern to their membership values in the set. The most widely used membership functions are the triangular and trapezoidal functions.

A fuzzy-expert system is an expert system that utilises a collection of fuzzy sets and rules for reasoning about data. The rule in a fuzzy- expert system can take the following form:

If *a* is low and *b* is high, then *c* is medium

where *a* and *b* are input and *c* is the output, and low high medium are membership functions defined for *a, b* and *c*. The set of rules in a fuzzy-expert system is known as the knowledge base or rule base. In general, the computation of the output variable usually takes several steps which can be mathematically stated as follows [80].

Let that the following rules describe a mapping from $U_1 \times U_2 \times \cdots \times U_r$ including U_i to *W*, where *W* is the universe of discourse of the according variables

R_i : if x_1 is $\boldsymbol{A}_{i1,}$ x_2 is A_{i2} ….and x_r is A_{ir}, then y is B_i

where x_j (j=1,2, … , r) are the input and y is the output. A_{ij} and B_i are fuzzy sets for x_j and y. The input

x_1 is $A_1^{'}$, x_2 is $A_2^{'}$, … , and x_r is $A_r^{'}$

where $A_1^{'}$, $A_2^{'}$, … , and $A_r^{'}$ are the fuzzy subsets of U_1, U_2, … , U_r.

The contribution of rule R_i to the output is a fuzzy set, whose membership function is calculated as follow

$$\mu_{B_i^{'}} = (\alpha_{i1} \wedge \alpha_{i2} \wedge ... \wedge \alpha_{in}) \wedge (\mu_{B_i}(y)) \quad \textbf{(4.5)}$$

where α_{ij} is the matching degree between x_j and R_i's condition about x_j is computed by

$$\alpha_{ij} = \sup_{x_j}(\mu_{A_j^{'}}(x_j) \wedge \mu_{A_{ij}}(x_j)) \quad \textbf{(4.6)}$$

where '$\wedge$' means the fuzzy conjunction operator and 'sup' means the continuous maximum operator.

Therefore, the fuzzy set output can be obtained by using the maximum defuzzification method, shown as

$$\mu_B(y) = \max\{\mu_{B_1^{'}}(y), \mu_{B_2^{'}}(y), ..., \mu_{B_i^{'}}(y)\} \quad \textbf{(4.7)}$$

Finally, the crisp value of y_B can be obtained by

$$\mu_B(y_B) = \sup_y \mu_B(y) \quad \textbf{(4.8)}$$

4.5.2 The Proposed Fuzzy-expert System

In this proposal, a 12-level DWT filter bank is used to obtain the detail coefficients d_1-d_{12} for each distorted signal. Using equation 4.4, one can obtain energy distribution. The wavelet decomposition levels of feature extraction curve and energy in feature extraction curve will be applied to the fuzzy-expert system for classifying the distorted signals. The proposed fuzzy-expert system is shown in Figure 4-4

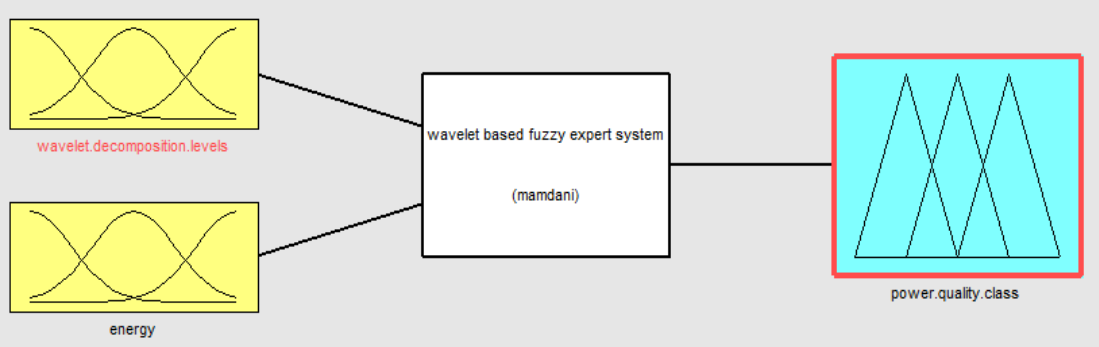

Figure 4-4 Proposed Fuzzy-expert System Based on Mamdani Type Fuzzy Implication

The mamdani-type fuzzy inference system with two inputs and one output has been considered in the proposed fuzzy-expert system. The two inputs include wavelet decomposed levels and energy, while the output is PQ class.

4.6 Application and Result

4.6.1 Recognition of Extracted Features

In order to illustrate the usefulness of the proposed fuzzy-expert system, simulations have been made by using the MATLAB/Simulink. In this paper, the SimPowerSystems Blockset Toolbox in MATLAB /Simulink is employed to generate pure sine wave signal and five sample distorted signals. These distorted signals involve voltage sag/swell, momentary interruption, harmonic distortion, and flicker. The frequency is 50Hz; amplitude is 1p.u. Parameters of electrical components are changed in order to generate different disturbance waveforms. The energy distribution patterns after performing the WT are used to set the parameters of input membership. The fuzzy-expert system is provided by Fuzzy Logic Toolbox (FIS) in MATLAB.

Figure 4-5 is the original signal and its decomposition waveforms of pure sine wave. The x-axis of this figure is sample points, while the y-axis is voltage value. The energy distribution pattern of pure sine wave is presented in Figure 4-6. The x-axis of this figure is wavelet decomposition level, while the y-axis is numerical value of the energy distributions at each wavelet level. The following figures from Figure 4-7 to Figure 4-16 are refer to other disturbances.

Case 1 Pure Sine Wave

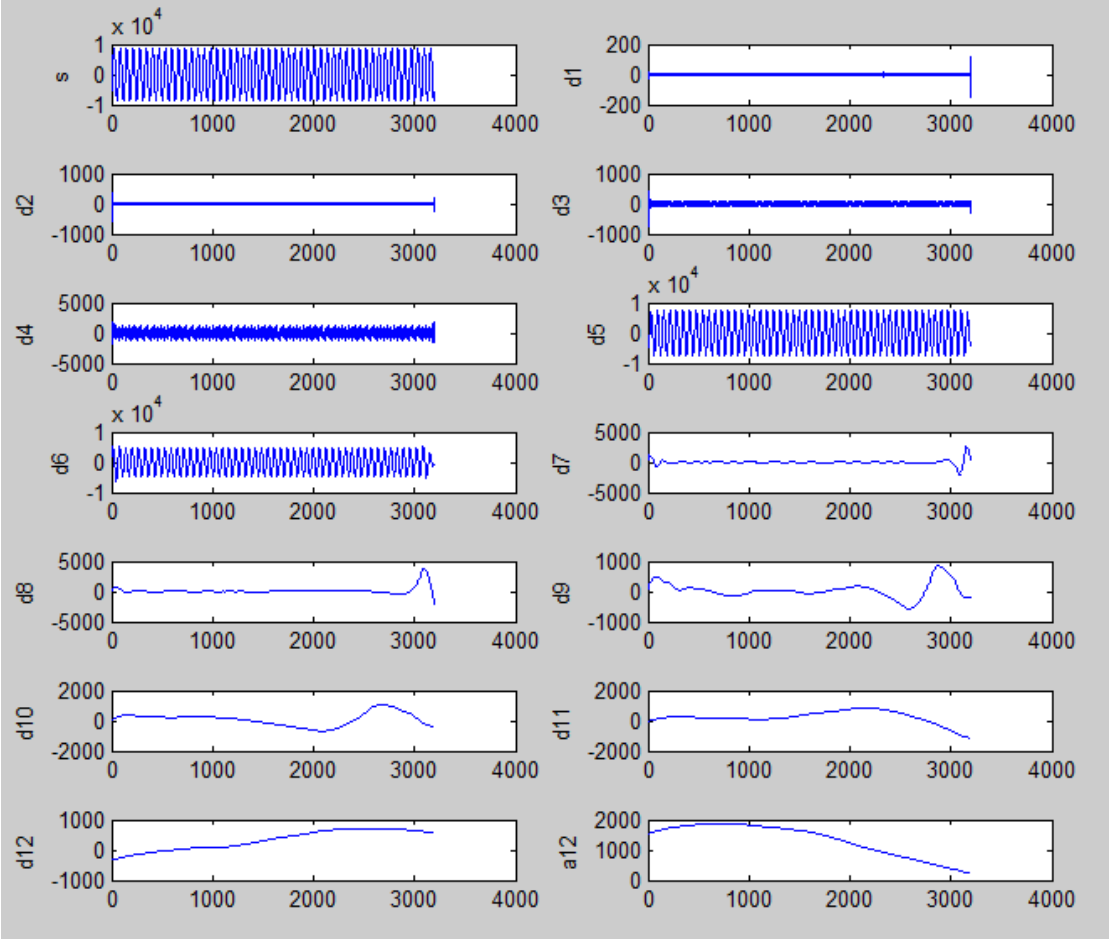

Figure 4-5 DWT Filter Bank Based Decomposition of Pure Sine Wave

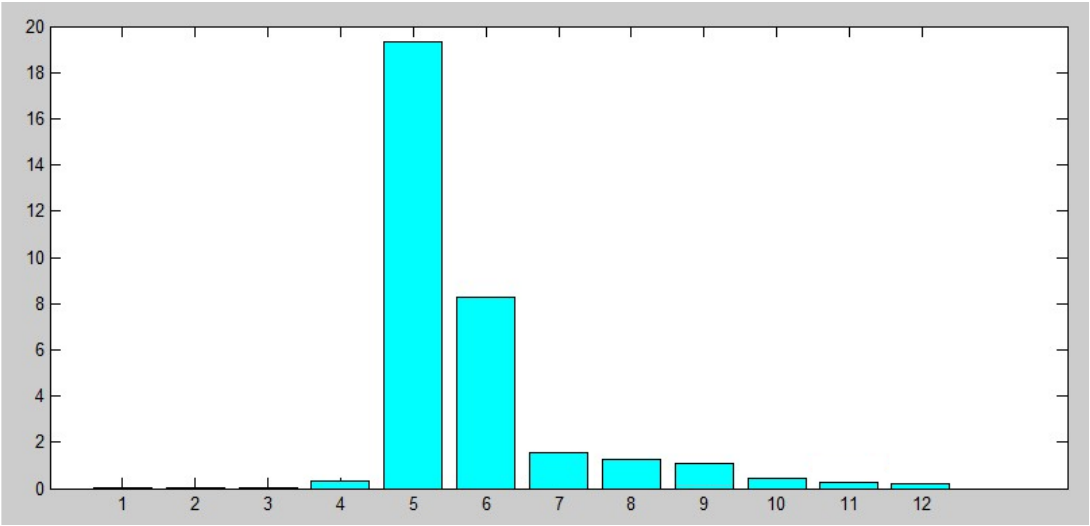

Figure 4-6 Energy Distribution Pattern of Pure Sine Wave

Case 2 Voltage Sag

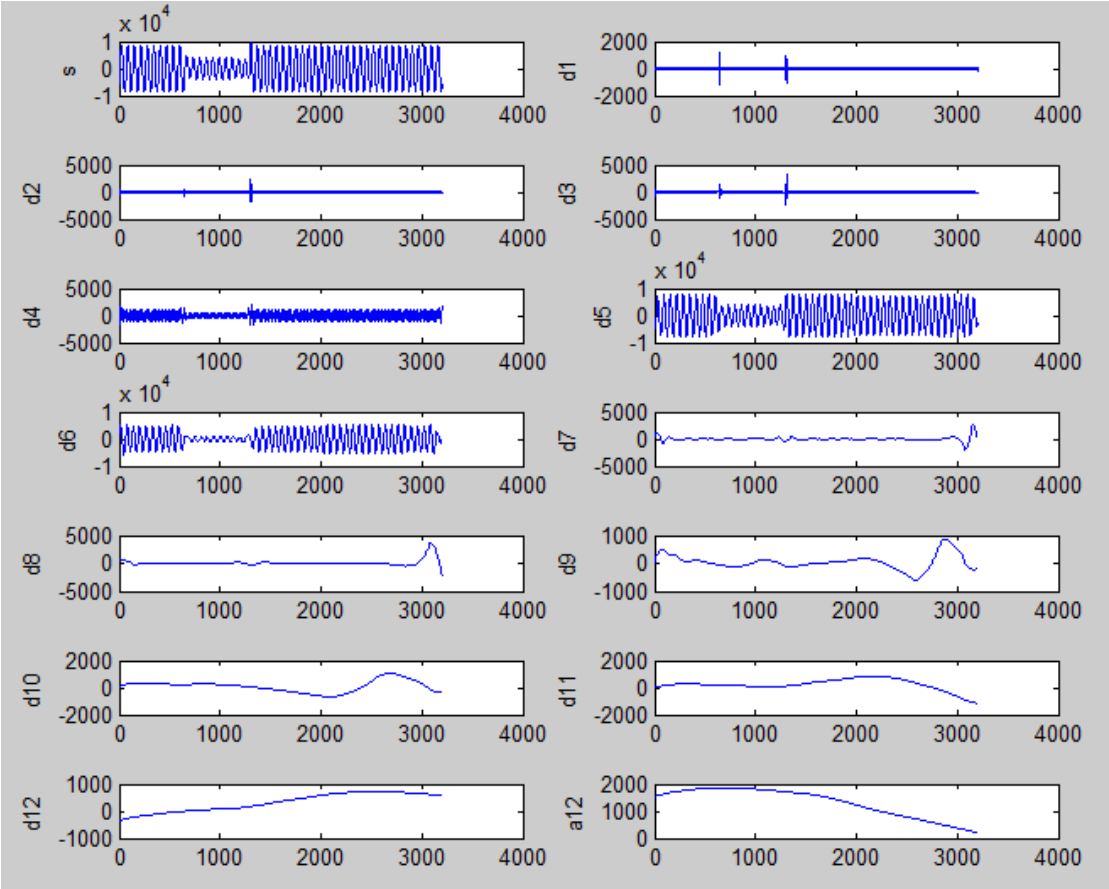

Figure 4-7 DWT Filter Bank Based Decomposition of Voltage Sag

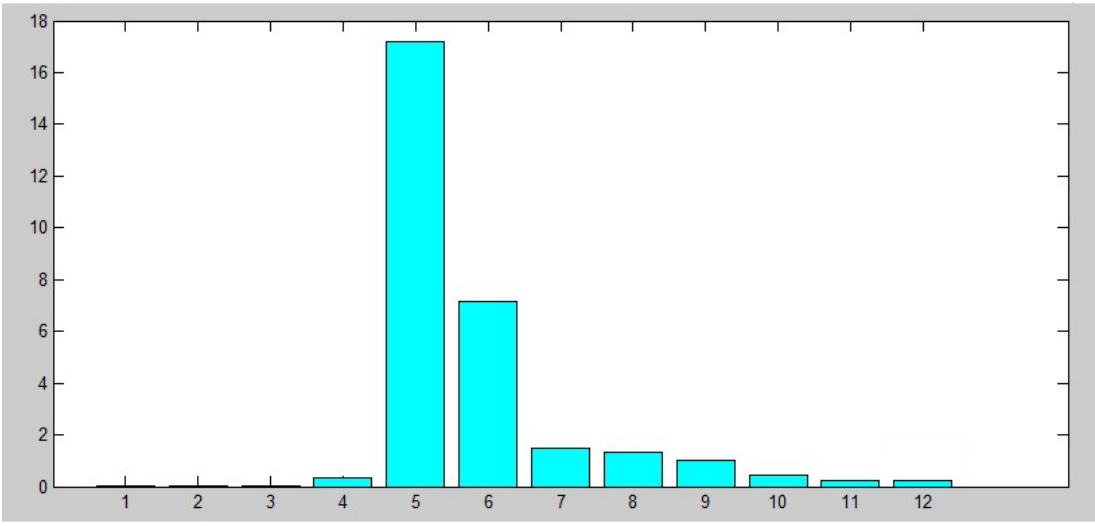

Figure 4-8 Energy Distribution Pattern of Voltage Sag

Case 3 Voltage Swell

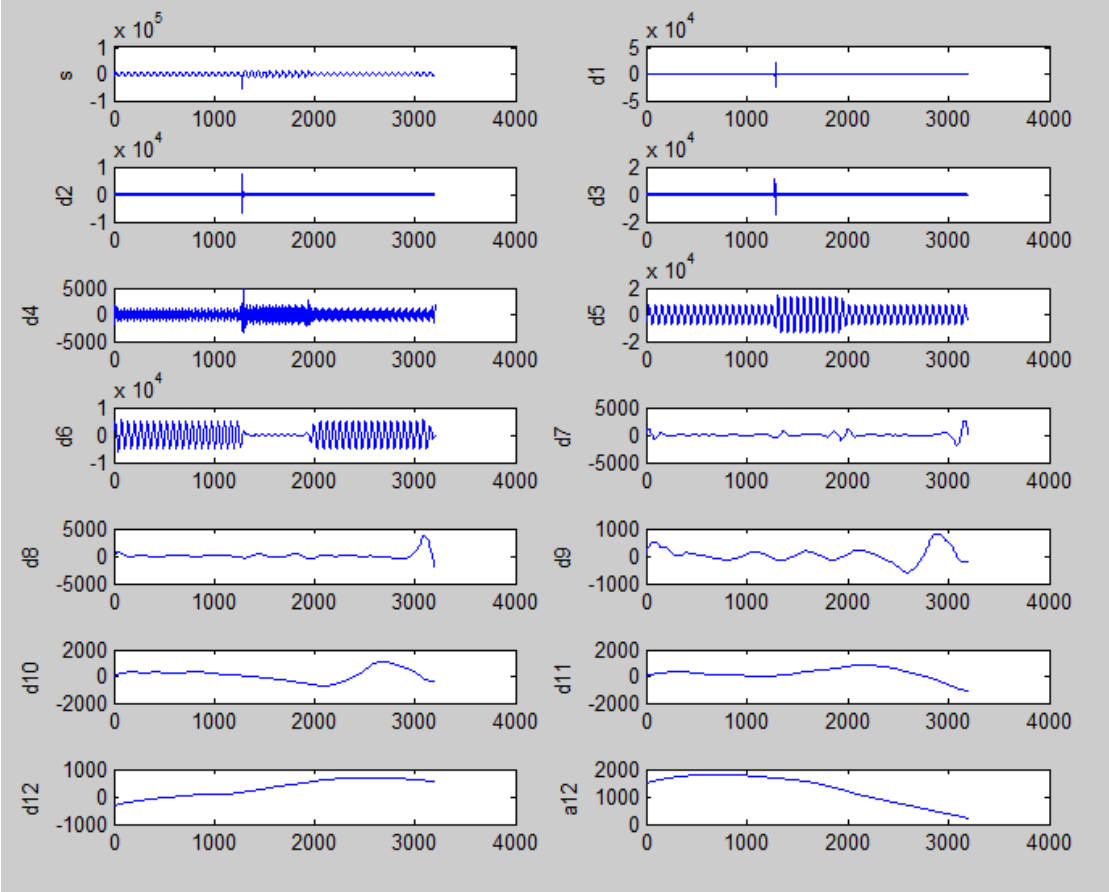

Figure 4-9 DWT Filter Bank Based Decomposition of Voltage Swell

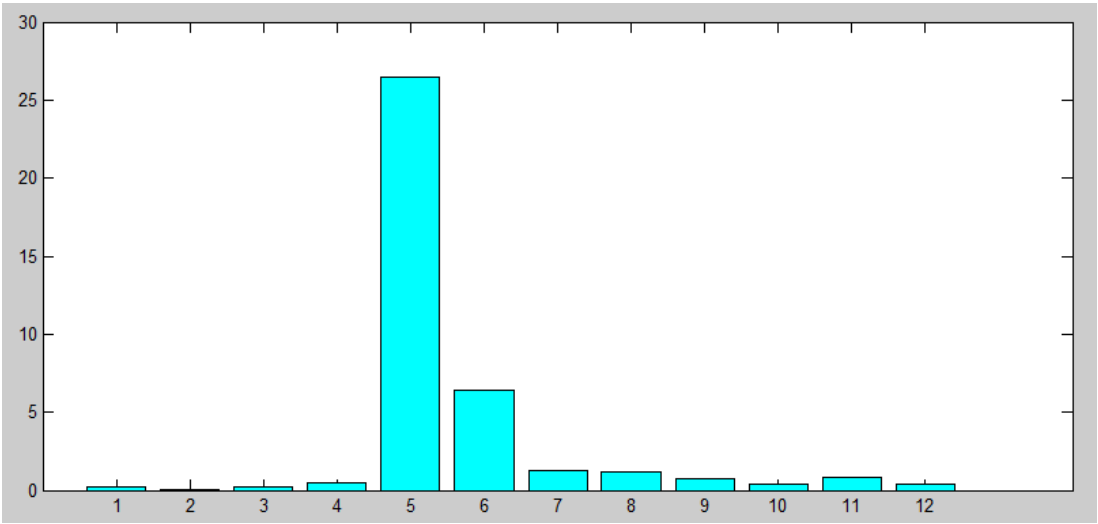

Figure 4-10 Energy Distribution Pattern of Voltage Swell

Case 4 Momentary Interruption

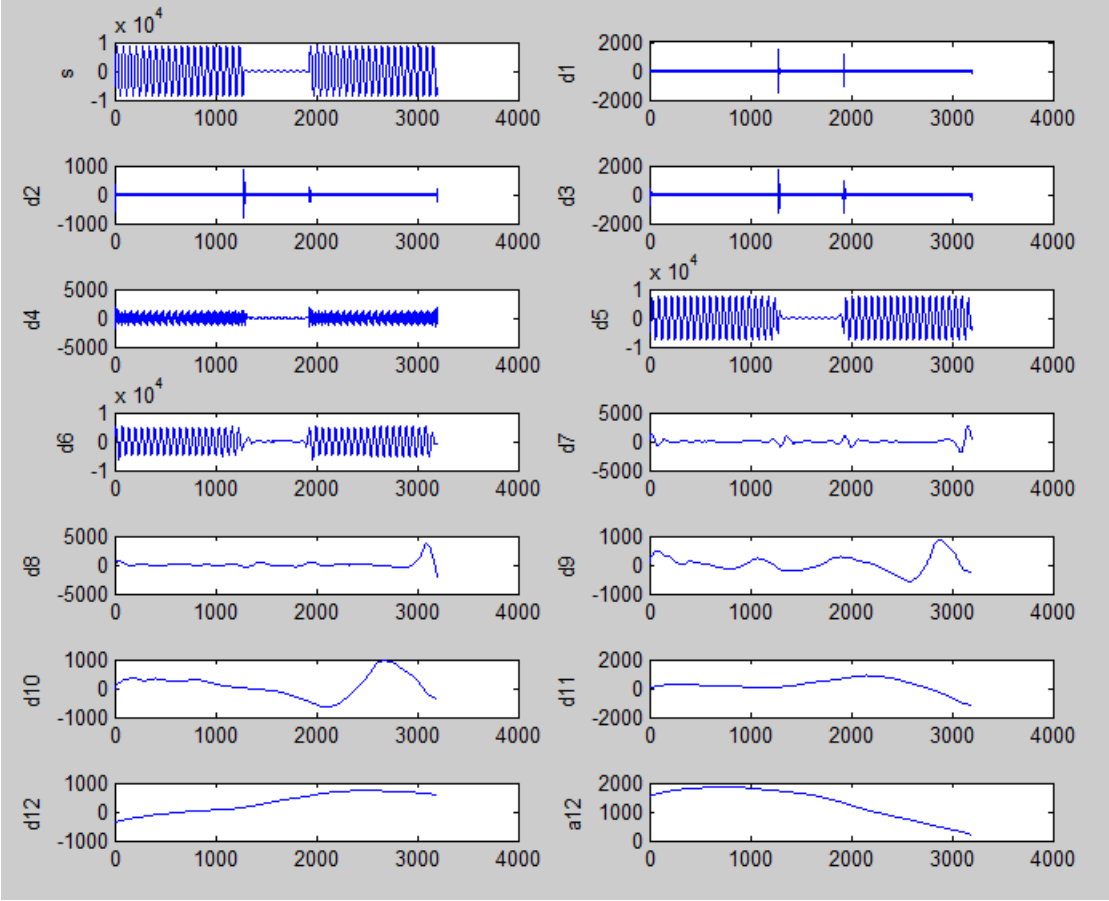

Figure 4-11 DWT Filter Bank Based Decomposition of Momentary Interruption

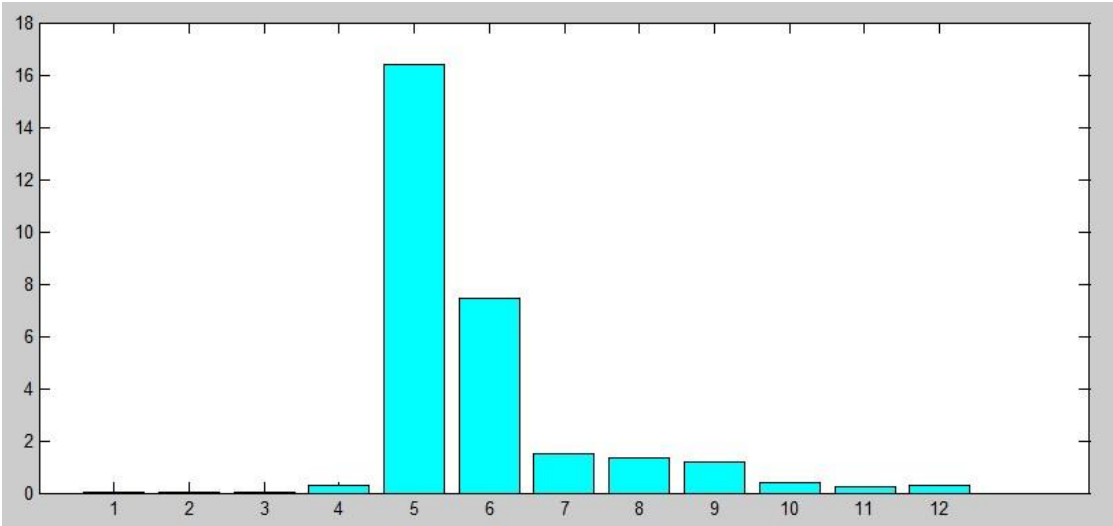

Figure 4-12 Energy Distribution Pattern of Momentary Interruption

Case 5 Harmonic Distortion

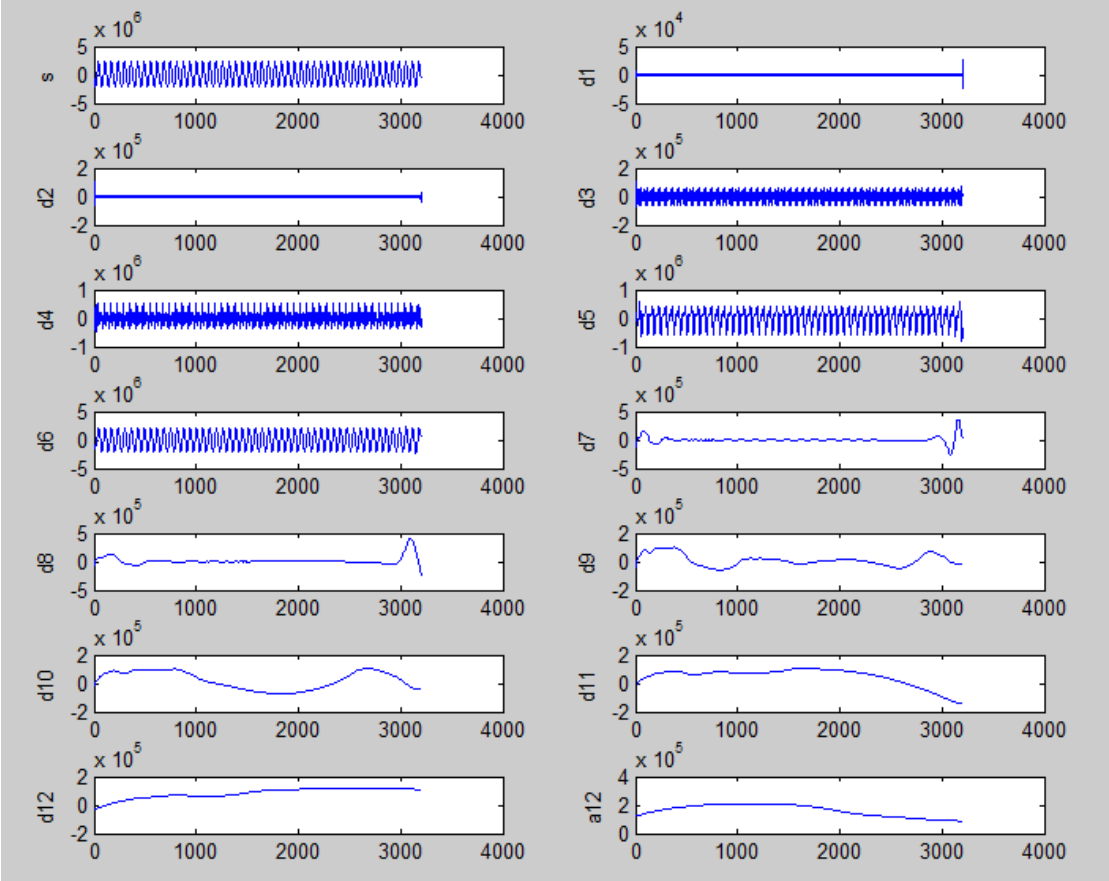

Figure 4-13 DWT Filter Bank Based Decomposition of Harmonic Distortion

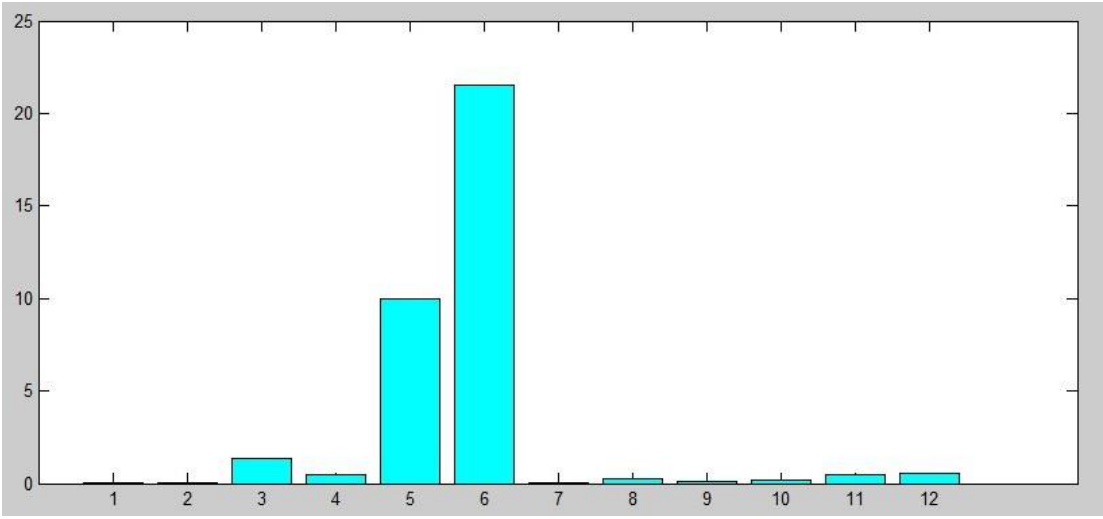

Figure 4-14 Energy Distribution Pattern of Harmonic Distortion

Case 6 Flicker

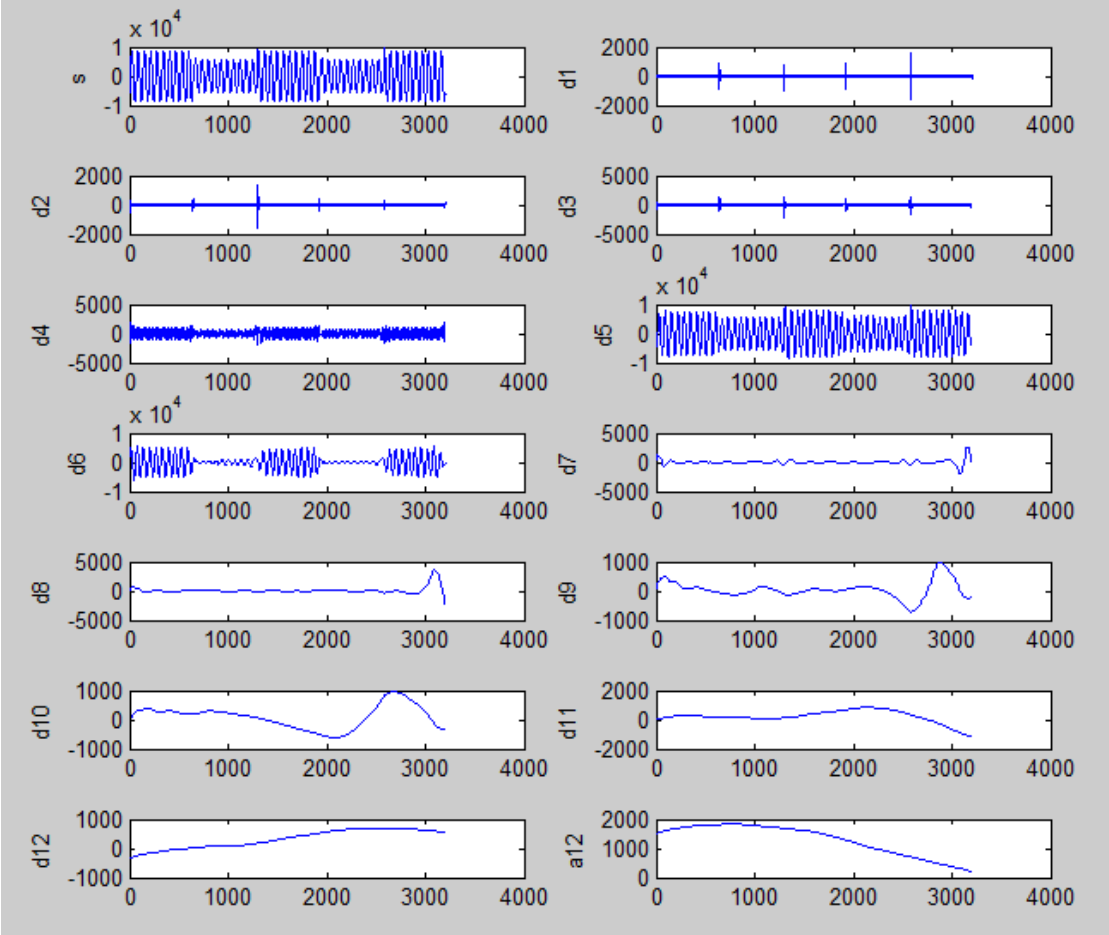

Figure 4-15 DWT Filter Bank Based Decomposition of Flicker

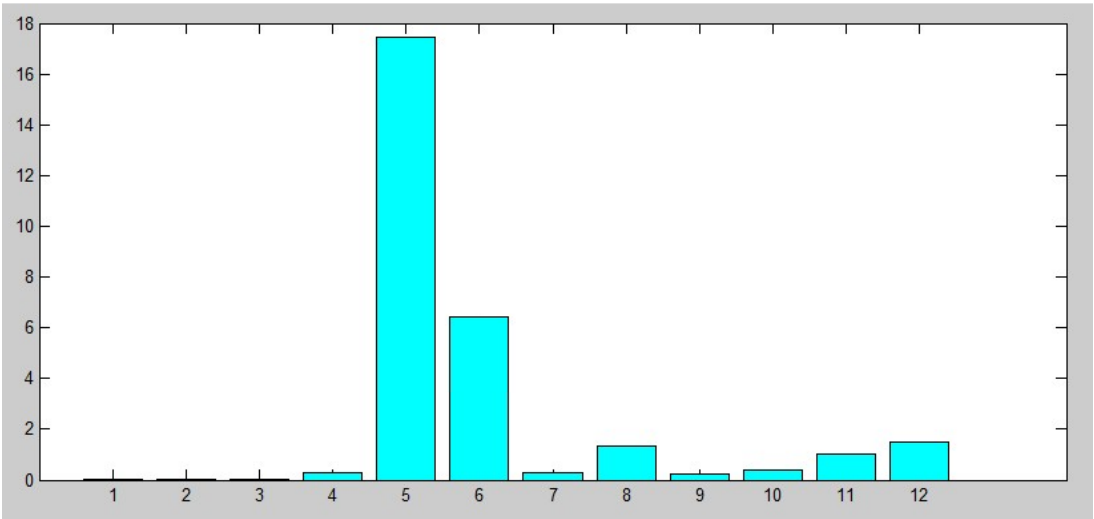

Figure 4-16 Energy Distribution Pattern of Flicker

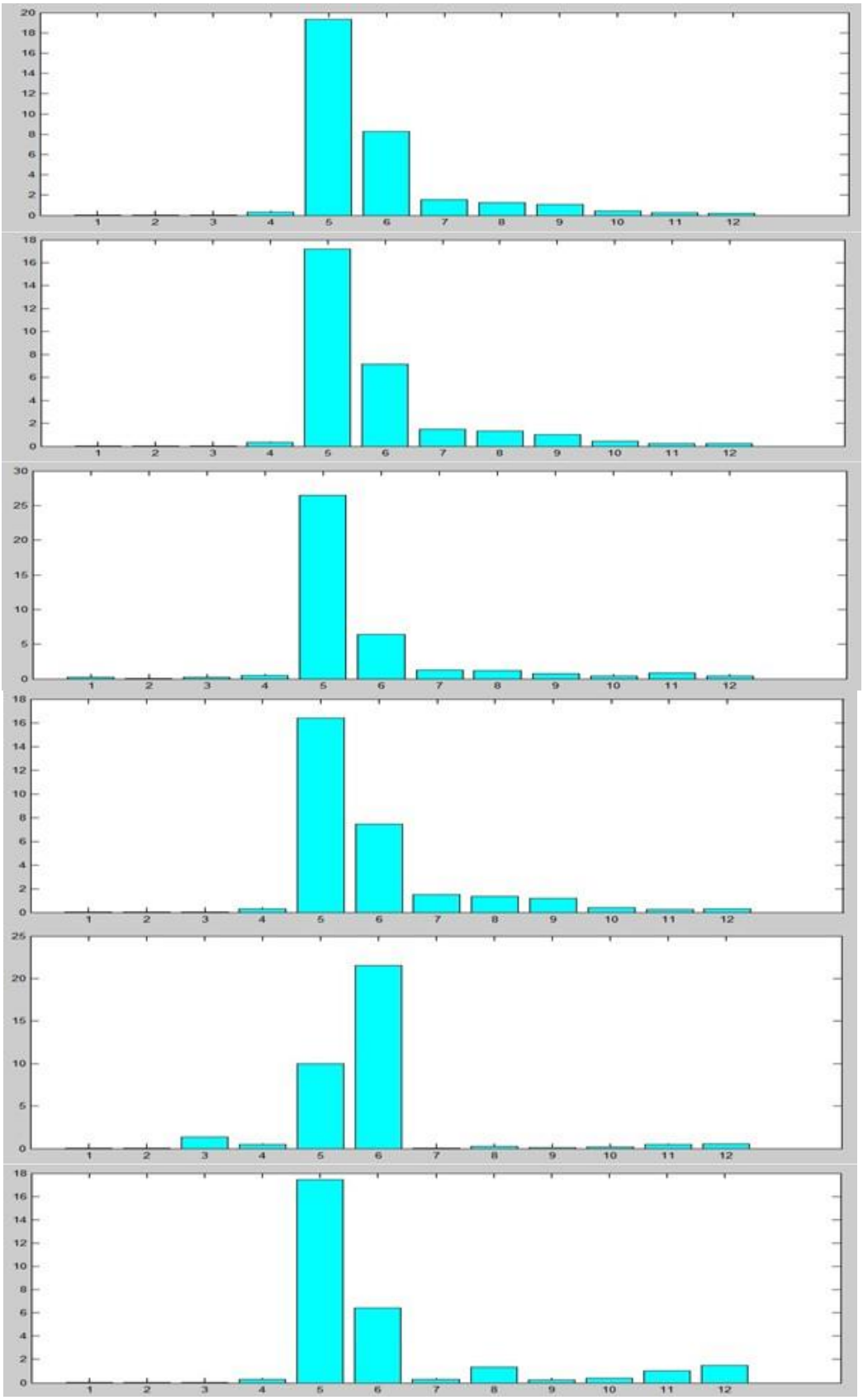

Figure 4-17 Energy Distribution Pattern Corresponding to level 1~12 using Db4 Wavelet: (a) Pure Sine Wave, (b) Voltage Sag, (c) Voltage Swell, (d) Momentary Interruption, (e) Harmonic Distortion, (f) Flicker.

Figure 4-17 shows the energy distribution patterns of six typical disturbance waveforms for a 12-level decomposition by using the Db4 wavelets. The X-axis is the decomposition level and the Y-axis is the energy.

Figure 4-18 shows six feature curves extracted from the energy distribution pattern on the same three-dimensional (3-D) coordinate axis.

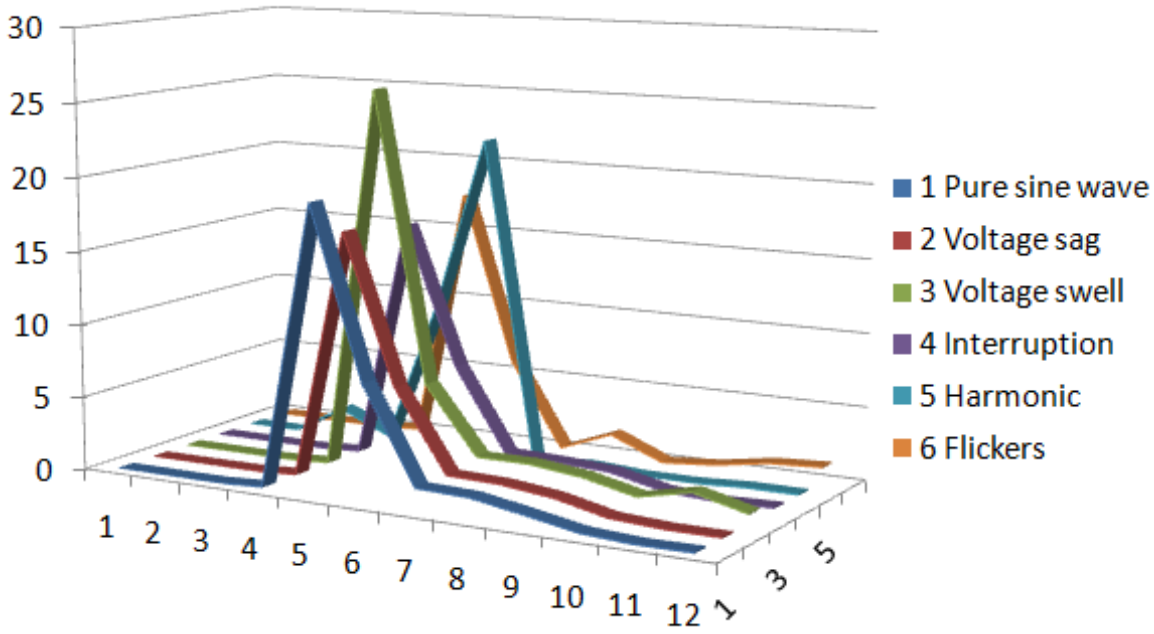

Figure 4-18 Differences in feature extraction curve of all signals

Figure 4-18 shows the difference of feature extraction curve between different signals.

- In voltage sag or swell or momentary interruption, the energy in 5^{th} and 6^{th} wavelet decomposed levels will show obvious variation.
- For harmonic distorted voltage, the energy in 2^{nd}, 3^{rd}, and 4^{th} wavelet decomposed levels shows obvious variation.
- For voltage flicker, the energy in 7^{th}, 8^{th}, and 9^{th} wavelet decomposed levels will show obvious variation.

4.6.2 Membership Functions

The membership functions for the two inputs variables are according to the Figure 4-17 energy distribution patterns. The wavelet decomposition levels designed as low frequency disturbance zone (*lf*), fundamental frequency zone (*fn*), high frequency disturbance zone (*hf*). The membership function for the first input is shown in Figure 4-19

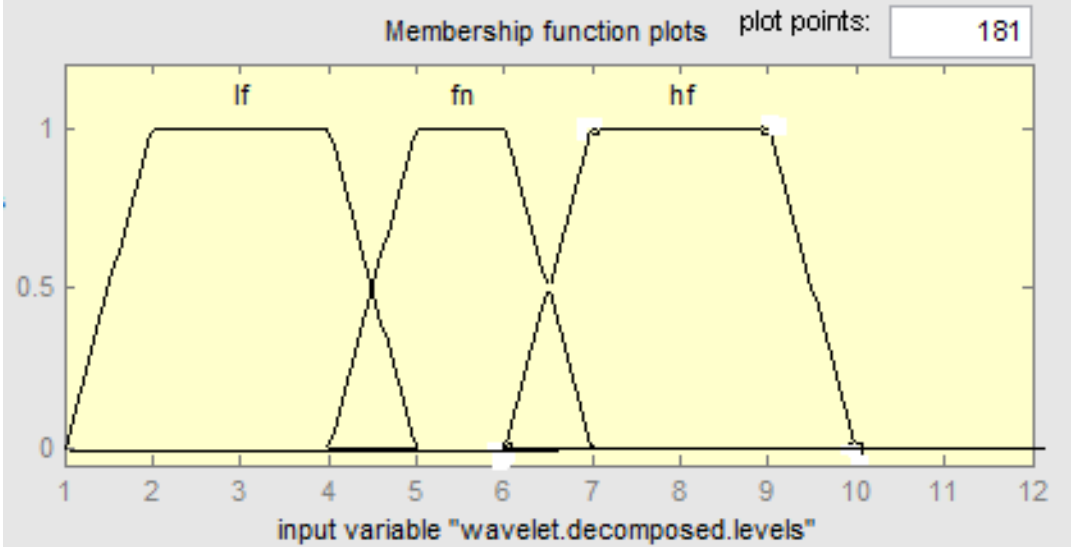

Figure 4-19 Membership Function for Wavelet Decomposition Levels of Feature Extraction Curve

The second input membership function is determined by the numerical values of energy distribution patterns. The variables are distinguished by four labels: much lower amplitude peak (*ml*), lower amplitude peak (*lv*), amplitude peak corresponding to fundamental (*nm*) and higher amplitude peak (*hv*). The membership function is shown as follows

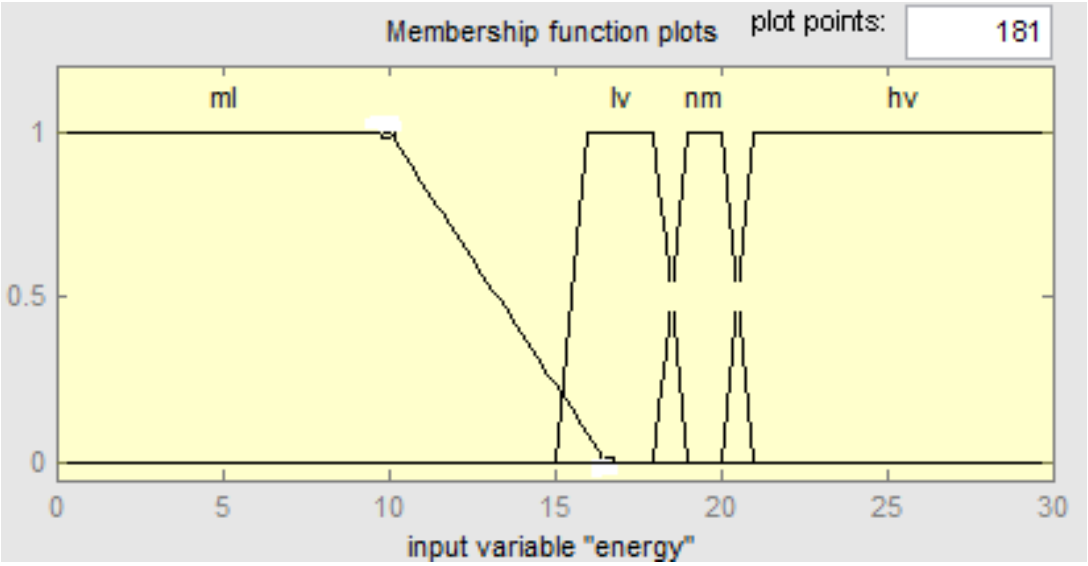

Figure 4-20 Membership Function for Energy in Feature Extraction Curve

4.6.3 Generation of Rules

Base on the fuzzy set of two input variables and the output variables. Six If-Then rules have been generated for classifying PQ disturbances. The rule base for the fuzzy-expert system is given as follows:

If (wavelet decomposition level is *fn*) and (energy is *nm*), then (output is pure sine wave).
If (wavelet decomposing level is *fn*) and (energy is *lv)*, then (output is voltage sag).
If (wavelet decomposition level is *fn*) and (energy is *hv*), then (output is voltage swell).
If (wavelet decomposition level is *fn*) and (energy is *ml*), then (output is interruption).
If (wavelet decomposition level is *lf*) and (energy is *hv*), then (output is harmonic distortion)
If (wavelet decomposition level is *hf*) and (energy is *lv*), then (output is flicker)

According to equation 4.5-4.8, the fuzzy set of the output variable can be converted to a crisp number. The numerical result of output is shown as Table 4-1.

Table 4-1 Numerical Result of Output

Type of disturbance	Output
Pure sine wave	2.64
Voltage sag	7.08
Voltage swell	12.3
Interruption	17.7
Harmonic	22.5
Flickers	26.7

The surface view of the fuzzy-expert system is described as Figure 4-21. The surface viewer is a GUI tool which can examine the output surface of the fuzzy-expert system, for any one or two inputs. The X-axis is the energy numerical value and the Y-axis is the wavelet decomposition level, as well the output variable is represented on the Z-axis. It can be seen that each category of waveform can be classified by using the fuzzy-expert system.

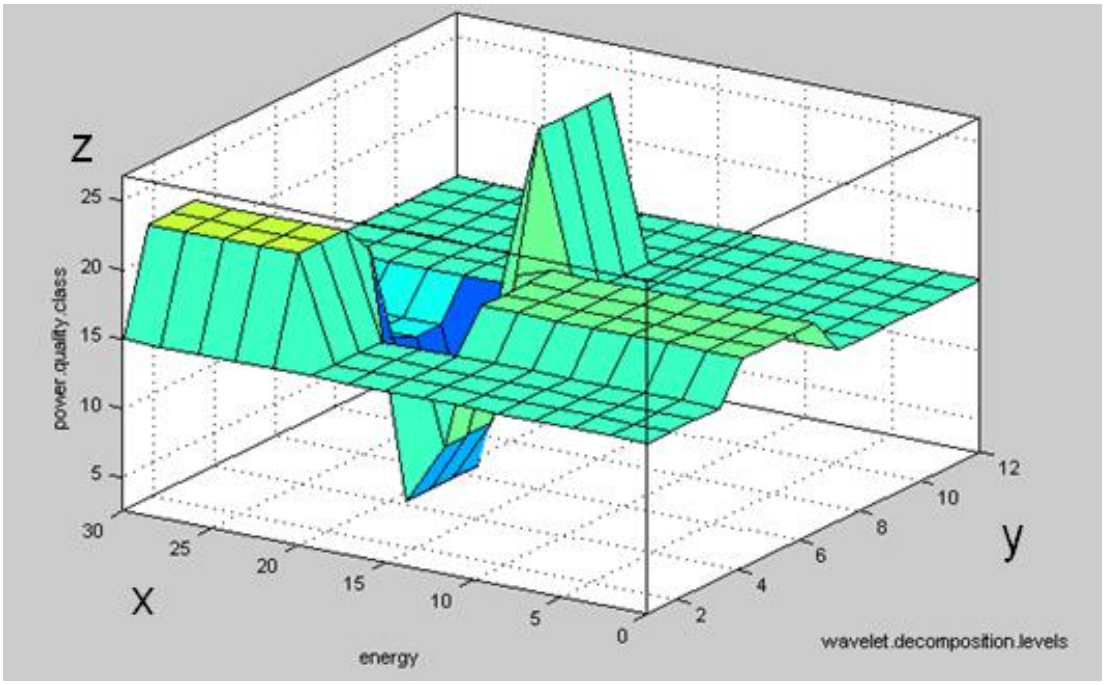

Figure 4-21 Surface view of the proposed fuzzy-expert system

4.6.4 Test with Unseen Cases

Once the fuzzy-expert system is designed, the classification of different disturbances can then be made. To test the accuracy of the proposed fuzzy-expert system, ten new distorted voltage waveforms are randomly generated and which has a different time of occurrence, duration, and amplitude. After calculating the energy on each wavelet decomposition level, the feature extraction curve is obtained, and then the classification of each waveform into different category by using the fuzzy-expert system is performed. The flowchart of using proposed fuzzy-expert system for PQ disturbance classification is shown as follows:

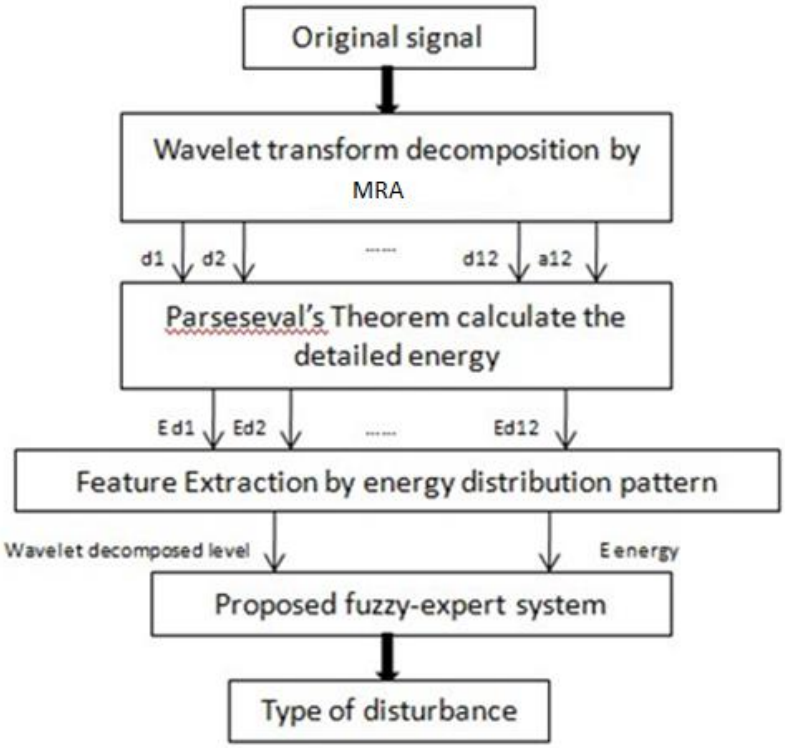

Figure 4-22 Flowchart of Proposed Fuzzy-expert System for Disturbance Classification

The classification results of the generated disturbances using the proposed system are shown in Table 4-2.

Table 4-2 Classification Results by using the Proposed Fuzzy-expert System

Type of disturbance	Number of disturbance	Number of case correctly classified	Classification accuracy
Pure sine wave	10	10	100%
Voltage sag	10	9	90%
Voltage swell	10	10	100%
Interruption	10	10	100%
Harmonic	10	10	100%
Flickers	10	10	100%
Sum	60	59	98.3

It can be seen that the proposed fuzzy-expert system has classified correctly 59 disturbances of the total number of 60 tested disturbances, thus having a classification accuracy of 98.3%. The only one mistake occurs when the magnitude of the voltage sag is too small. The fuzzy-expert system misclassified that voltage sag into interruption. These tests show that the proposed methods for feature extraction and designed fuzzy-expert system are efficient for PQ disturbance classification. Although six types of waveform are classified, it is possible to classify more than six types. To classify new type of PQ disturbance new rule base will need to be developed based on the feature extraction curve of the new disturbances.

4.7 Conclusion

This chapter has given an overview of conventional methods for PQ classification firstly. Then, a fuzzy-expert system has been developed for classifying PQ disturbances. The energy distribution patterns in the wavelet domain are used to extract features. Based on the feature extraction curve, the membership functions of inputs and rule base are generated. Finally, the fuzzy set of the output variable is mapped into a crisp number, in terms of which the disturbances are classified according to the numerical value. The proposed fuzzy-expert system uses 12-level DWT filter bank, and has been tested with ten unseen new distorted voltage waveforms to verify its classification accuracy. The results show that the proposed fuzzy-expert system has correctly classified 98.3% of the tested waveform. . In practice, in order to improve the quality of power, the type of such disturbances must be know accurately. Therefore, a powerful PQ disturbances classification tool is necessary. The proposed fuzzy-expert system can be considered to be sufficiently accurate in classifying PQ disturbances

Chapter 5 Wavelet Transform Based Approach to Harmonic Analysis

5.1 Introduction

The use of renewable sources for electricity generation is actively developing all over the world. One major renewable source is the use of wind power for electricity generation. The output of wind power unlike conventional generation is intermittent and depends very much on wind speed. In the case of wind power generation, the designs of the systems involve some power electronic devices to act as reactive power compensators, variable-speed controllers or power convertors. All of these would introduce harmonics into the distribution networks and as a consequence would affect power quality at the customer ends. The harmonic studies have become an important subject recently. Nowadays, power electronic devices can produce not only integer but also sub and non-integer harmonics in power system waveforms. It is necessary to determine the harmonic content and to reduce them to yield high power quality [13] [82].

The conventional signal processing tool in power system harmonic analysis is FT. However, FT provides signals which are only localised in the frequency domain and it does not give any information of the signals in the time domain. Furthermore, with a fixed window length and frequency in the FT, it cannot obtain accurate values of amplitude and phases from harmonics with frequencies different from that of the window function frequency [23] [24] [25].

In this chapter, to overcome the limitations of FT, WT is applied for harmonic analysis. The main advantages of wavelets are that they have the ability to analyse signal in both time and frequency domains, and they also have ability to be adjusted automatically for low or high frequencies because it uses short windows at high frequencies and long windows at low frequencies, thus leading to an optimal time-frequency resolution in all

the frequency ranges [67]. Analogously to the Fourier analysis, the DWT is digital representation of the CWT. The DWT can be implemented by using the DWT filter bank which can decompose a signal into different time and frequency resolution [83]. In DWT filter bank, a signal is decomposed into non-uniform frequency sub-bands to extract detailed information. However, for harmonic analysis, it is better to evaluate the uniform frequency sub-bands. This can be achieved by using DWPT filter bank [84].

In this chapter, the WT approach which is the combination of the DWPT filter bank and CWT is proposed. Base on the decomposition by using DWPT filter bank, the CWT is employed to identify the harmonic contents of power system waveform. This chapter is organized as follows. Firstly, brief summaries of existing methods for harmonic analysis are introduced in **Section 5.2**. Secondly, in **Section 5.3**, the DWPT filter bank is used to decompose and reconstruct the signal for the uniform frequency sub-band, and then the CWT is presented to calculate the harmonic components which contain frequencies, amplitudes and phases. Thirdly, the tests of proposed method with the synthesised signal including time-invariant waveforms and non-stationary waveforms, and blindtest waveform have been done in **Section 5.4**. All of these results are compared with the results of the FFT and the results of the combination of the DWT filter bank and CWT, respectively. Finally, a brief conclusion is given in **Section 5.5**.

5.2 Existing Methods for Harmonic Analysis

Harmonic analysis is a process of calculating the magnitudes and phases of the fundamental and higher-order harmonics. The resulting series can be obtained by the FS which represents the special case of the FT applied to a periodic signal. However, the outputs of the FS often contain spurious components and spectral leakage. The DFT uses window functions to mitigate the spectral leakage effect. In order to reduce the huge computational demand of the DFT, the FFT can be applied to implement the DFT. However, with a fixed window length and frequency in the DFT, it cannot obtain accurate values of amplitude and phases from harmonics with frequencies different from that of the window function frequency.

The main drawbacks most often encountered in using the FT appear to be spectral leakage, picket fence effect and aliasing [23] [24] [25] [85].

Spectral leakage: when the FT is applied to analyse the frequency content of a signal, it is inherently assumed that the data from the signal is a single period of a periodically repeating waveform as shown in Figure 5-1. The first period *T* is the sample, and the waveform corresponding to this period is then repeated in time to produce the periodic waveform.

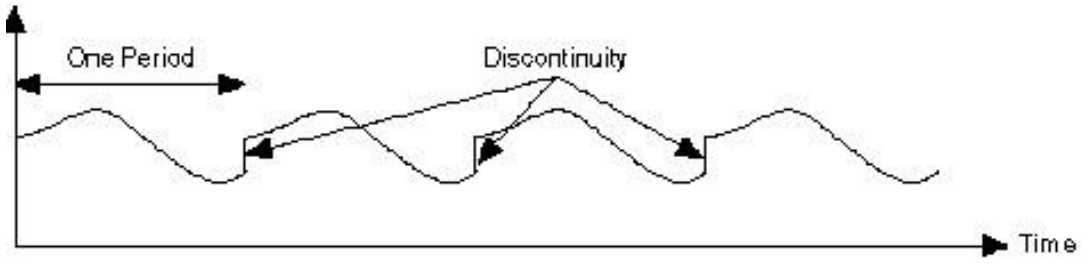

Figure 5-1 Periodic Extension [23]

With the assumption of periodicity of the waveform, discontinuities between successive periods will occur. This happens when the sample number of cycles are non-integer, such as 5.5. These artificial discontinuities turn up as very high frequencies in the

spectrum of the signal, frequencies that were not present in the original signal. These frequencies could be much higher than the Nyquist frequency [87], and will be aliased somewhere between 0 and $f_s/2$. Therefore, the spectrum obtained by using the FFT will be a smeared version, instead of the actual spectrum of the original signal. It appears as if the energy at one frequency has leaked out into all the other frequencies. This phenomenon is referred to as spectral leakage..

Picket fence effect: FFT can only produce spectral analysis results at discrete frequencies: 0, $\Delta f \times 1$, $\Delta f \times 2$ …, $\Delta f \times N/2$, where N is the FFT size and $\Delta f = f_s/N$. In practice, the real spectrum of the signal can be continuous or discrete but different from those discrete frequencies calculated by FFT. Observation of the spectrum with FFT is analogous to looking at it through a sort of "picket-fence". If a frequency peak of the signal falls exactly to a FFT spectral line, then it will be observed with correct magnitude, otherwise, its energy will be shared by the its adjacent FFT spectral lines, which in effect smears the peak or even causes it to be undetectable.

Aliasing: occurs when a signal is sampled at less than twice of the highest frequency present in the signal. It causes frequency components that are higher than half of the sampling frequency to "fold over" and overlap with the lower frequency components. For example, an aliased frequency f in the range of $f_s/2 \sim f_s$ becomes $f' = f_s - f$. That is, if a 7 kHz sinusoidal signal is sampled at 8 kHz, then it will be shown as 1 kHz in the spectrum due to aliasing.

It can be seen from Figure 5-2, the red waveform is a 7 kHz sinusoidal signal, while the blue waveform is a 1 kHz sinusoidal signal. These two signals share exactly the same set of sampled data points if sampled at 8 kHz, thus they cannot be distinguished with each other after being sampled.

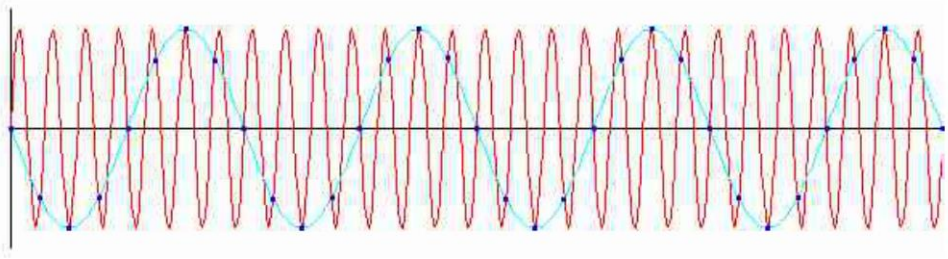

Figure 5-2 Example of Aliasing [23]

Then more methods based on FT have been developed to overcome the limitations. In reference [88], the parametric analysis method is proposed to obtain more accurate value of harmonic amplitude and phase from DFT. Although the accuracy of the result by using this method is satisfactory, the computational requirement is very high and not suitable for analysing non-stationary signals.

5.3 Harmonic Analysing by Using Wavelet Transform

5.3.1 Signal Decomposition by Using WT Filter Bank

The development of signal decomposition by using the WT filter bank is a very important part of harmonic analysis. Signals can be decomposed into sub-bands of smaller frequency spectrum. The decomposition of the signal can separate the high frequency transient harmonics from the fundamental components and low frequency harmonics. The features of harmonics can be extracted from the sub-bands for further studies.

5.3.1.1 Signal Decomposition by Using DWT Filter Bank

The DWT filter bank can decompose the original signal into sub-bands with different scales. The detailed introduction can be obtained in **Section 3.4.2**. In this case, the input signal is decomposed by using the four level DWT filter bank into four high frequency bands and one low frequency band. The high frequency band represents the detail version of the high-frequency components of the signal, while the low frequency band represents the smoothed version of the low-frequency components. $d_j(n)$ and $a_j(n)$ are the detail coefficient and the approximation coefficients, respectively. The detail coefficients of the DWT can be used to calculate the energy of the signal, the full application can be found in **Chapter 4**.

The DWP filter bank decomposes the signal into non-uniform sub-bands. The sub-band spectrum is proportional to its average frequency. Because of that, the higher average frequency has wider spectra, while the lower average frequency has narrower spectra. It can be seen in Figure 5-3 which shows the sub-band spectrum by using four-level DWT filter bank. The sample frequency of the input signal is 800 Hz.

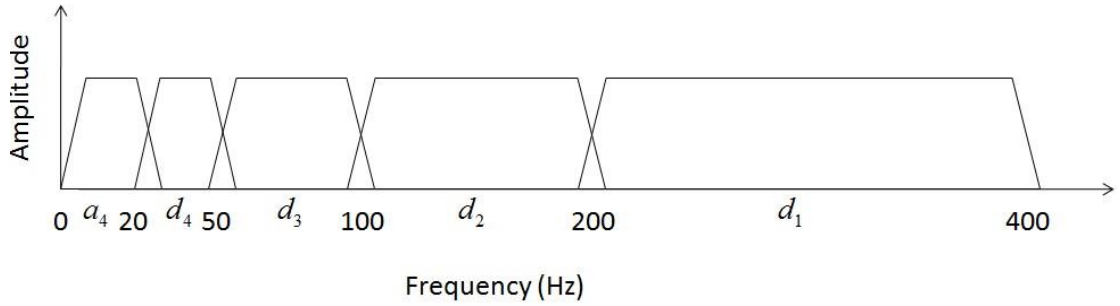

Figure 5-3 Sub-band Spectrum by Using the Four-level DWT Filter Bank

However, the non-uniform sub-band is not good at analysing the high-order harmonic of the signal. It is also possible to do the further splitting for the higher band. To overcome the limitation of the DWT filter bank, the DWPT filter bank is applied to decompose the signal, in order to obtain the uniform sub-bands.

5.3.1.2 Signal Decomposition by Using DWPT Filter Bank

The DWPT filter bank is a decomposition method with a better time-frequency characteristic, due to the uniform bandwidths of output sub-bands. The detailed introduction of DWPT filter bank is listed in **Section 3.4.3**. A four-level DWPT filter bank is employed to decompose the input signal instead of DWT filter bank which is shown in Figure 5-4. The sample frequency of the input signal is also 800Hz. The input signal is decomposed into sixteen uniform sub-bands of 25Hz interval by using the DWPT filter bank. Compared with the DWT filter bank, the DWPT filter bank can decompose the input signal into smaller frequency range time domain components of smaller frequency bands. As a result, harmonics of high frequencies can be split from the fundamental and fast transient events can be obtained.

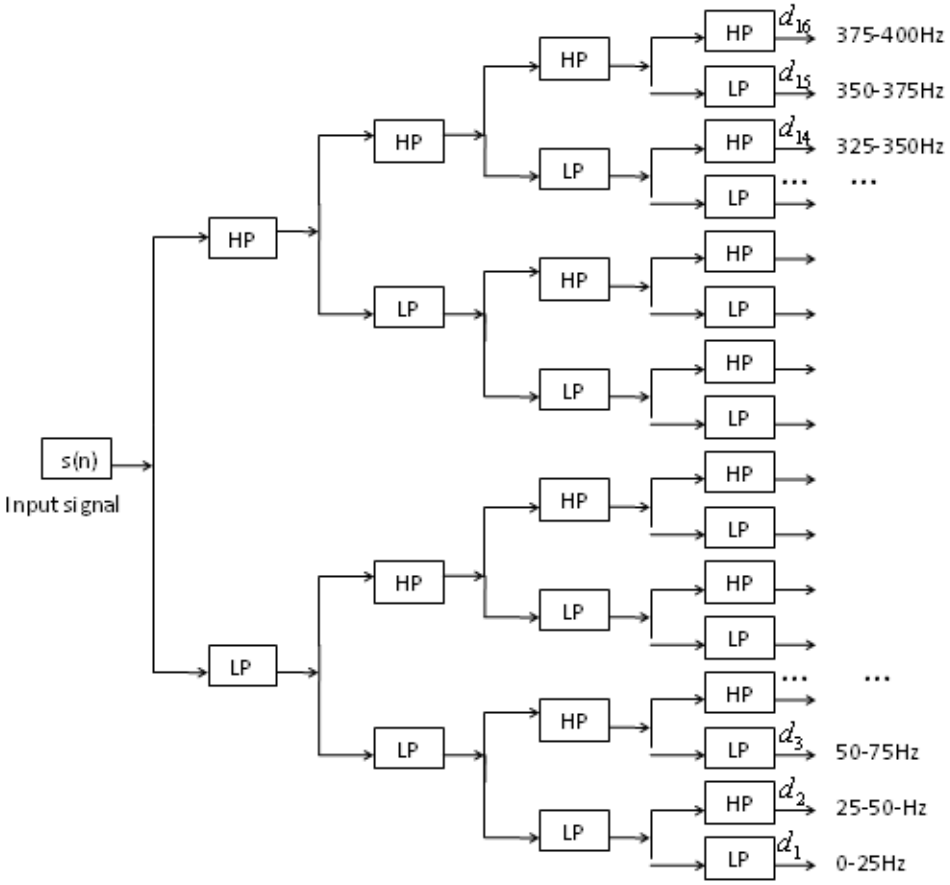

Figure 5-4 Four-level DWPT Filter Bank

Depending on application, it is important to choose the appropriate wavelet packet. The rule is to choose the wavelet packet with similar characteristics as the signal to be analysed. For harmonic analysis, the high order Db wavelet packets (Db20 to Db45) which are the smooth orthogonal ones are suitable, because the harmonic is smooth and sinusoidal. In this proposal, the Db 45 wavelet is chosen to analyse the harmonic.

5.3.2 Harmonic Identification by Using CWT

After decomposing the signal by using the DWPT filter bank, the CWT can be used to analysis the nonzero time-domain components by using equation 3.45. For the analysed section, if the starting time is t_1 and ending time is t_2, the equation 3.45 can be rewritten as

$$CWT(a,b) = \int_{t_1}^{t_2} \psi'_{a,b}(n)\, f(n) dt \qquad \textbf{(5.1)}$$

where $f(n)$ and $\psi_{a,b}(n)$ are sampled version of the input signal $f(t)$ and continuous wavelet $\psi_{a,b}(t)$. The Morlet mother wavelet is chosen as mother wavelet of CWT for harmonic analysis because it is a smooth and oscillating waveform similar as the harmonic. The Morlet wavelet has the ability to extract the amplitude and phase from the harmonic effectively [73]. A brief introduction of the Morlet wavelet is given in **Section 3.3.4**.

According to references [72][76][77], as the scaling parameter a varies, the frequency of the $\psi(t)$ varies as well. More close frequencies between the frequency of the $\psi_{a,b}(t)$ and the frequency of the harmonic in $f(t)$ can lead to large coefficient of the CWT, otherwise it is small. Thus, harmonic identification method is followed:

Let the frequency of the mother wavelet $f_0 \in [f_{0\min}, f_{o\max}]$, where $f_{0\min}=f_1 a$, $f_{0\max}=f_h a$, f_1 and f_h are the lowest and highest frequencies respectively of the analysed output frequency sub-band. The increment value of the frequency is 0.01Hz which gives the frequency resolution of the algorithm. For a fixed f_0, change the variable parameters a and b to obtain the maximum coefficients of CWT. The position of the maximum coefficient value is the corresponding harmonic. And then the frequency, amplitude and phase of the harmonic corresponding to the CWT coefficients is

$$f_{CWT(a,b)} = f_0 / a \tag{5.2}$$

$$A = \frac{C_\psi \sqrt{a}\,|CWT(a,b)|}{T} \tag{5.3}$$

$$\theta = arc\tan\frac{\mathrm{Im}(CWT(a,b))}{\mathrm{Re}(CWT(a,b))} - \theta_0(b) \tag{5.4}$$

Where f_0 is the frequency of the mother wavelet, C_ψ is a constant -and $\theta_0(b)$ is the phase shift caused by the shifting parameter b. T is the duration of the analysed signal. The detailed procedure for calculating can be found in [89].

5.4 Application and Result

5.4.1 Synthesised Waveform Analysis: Time-invariant Signal

5.4.1.1 Time-invariant Signal for Simulation

In order to illustrate the usefulness of the proposed method, simulations have been done by using the MATLAB. A synthesised signal is employed to generate harmonics. The equation of the synthesised distorted waveform is given as followed

$$\begin{aligned} f(t) = {} & 0.3\cos(2\pi f_1 t + 70^\circ) + 0.2\cos(2\pi f_2 t + 60^\circ) + 1.0\cos(2\pi f_3 t) \\ & + 0.4\cos(2\pi f_4 t + 80^\circ) + 0.5\cos(2\pi f_5 t + 50^\circ) + 0.6\cos(2\pi f_6 t + 30^\circ) \\ & + 0.35\cos(2\pi f_7 t + 20^\circ) + 0.55\cos(2\pi f_8 t + 45^\circ) + 0.6\cos(2\pi f_9 t + 75^\circ) \\ & + 0.5\cos(2\pi f_{10} t + 40^\circ) \end{aligned} \quad \textbf{(5.5)}$$

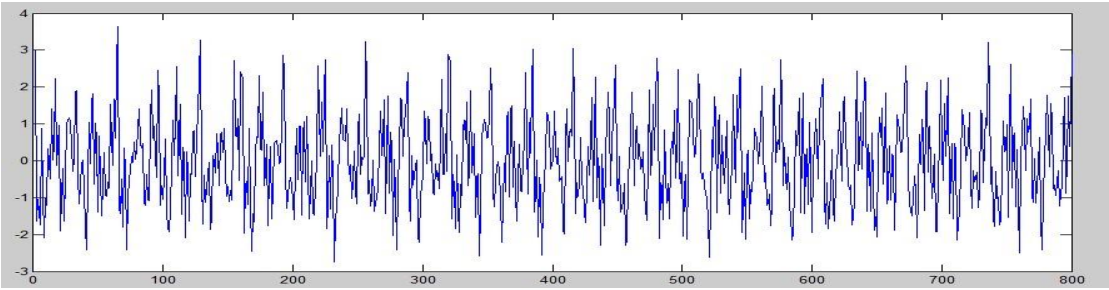

Figure 5-5 Synthesised Time-invariant Waveform

where f_1, f_2, f_3, f_4, f_5, f_6, f_7, f_8, f_9 and f_{10} are 25Hz, 35.85Hz, 50Hz, 86.6Hz, 125Hz, 150Hz, 175.5Hz, 250Hz, 285Hz, 300Hz, respectively. The frequency of fundamental component is 50Hz. The 150Hz, 250Hz and 300Hz components are third, fifth, sixth high-order harmonics, 35.85Hz, 86.6Hz and 175.5Hz components are the non-integer harmonics and 25Hz component is a low-order integer sub-harmonic.

5.4.1.2 Test Plan

The frequency bandwidth of $f(t)$ is from 25Hz to 300Hz. In order to ensure all features in both high and low frequency are extracted, a four-level DWPT filter bank is used to decompose the synthesised signal into sixteen uniform sub-bands. The sample

frequency f_s is 800Hz. The simulation time is 10 seconds. According to the Niquist Theorem which is an important principle in digital signal processing [87], the signal can be perfectly reconstructed if the sampling frequency is greater than twice the highest frequency in the original signal. As a result, the highest frequency contained in the signal f_h is the half of the f_s, thus f_h is 400Hz. The f_1 is determined as 24 Hz because of the lowest frequency of harmonic is 25Hz.

For comparison, $f(t)$ is analysed by three methods. Case one is analysing the input signal by using FFT. Case two is decomposed the input signal by DWT filter bank and then calculated by CWT. And the last case 3 is using the CWT to calculate the coefficients which are decomposed form the input signal by DWPT filter bank.

5.4.1.3 Result and Discussion

The results generated by these three cases are shown in Table 5-1. The Figure 5-5 – Figure 5-7 provide the numerical result of the frequencies and amplitude of harmonics components by these three methods.

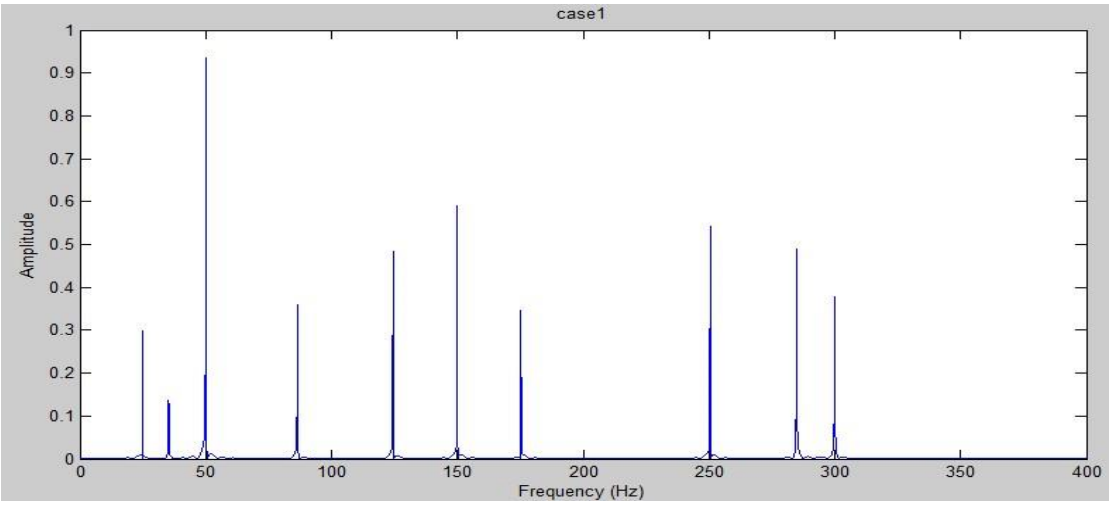

Figure 5-6 Harmonic Identification by Using FFT

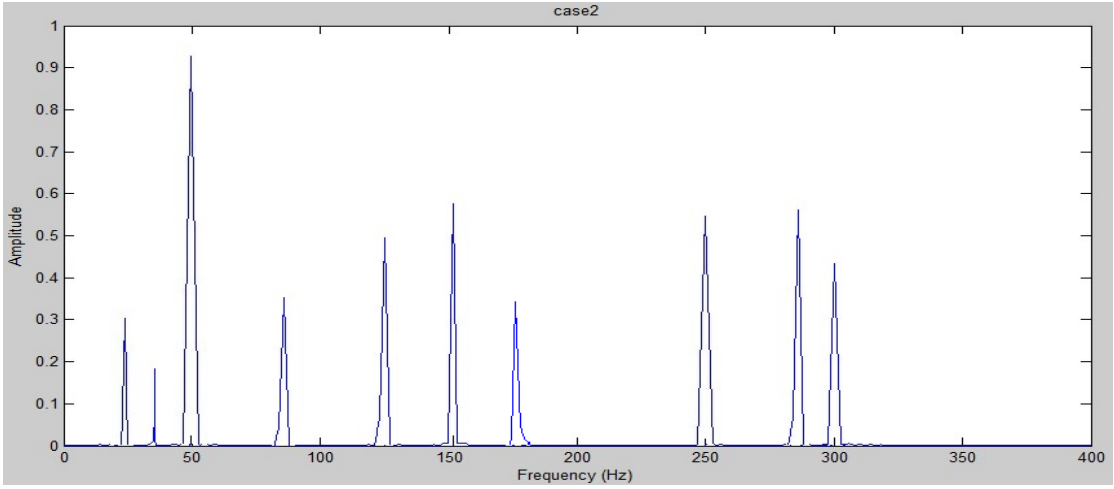

Figure 5-7 Harmonic Identification by Using DWT Filter Bank and CWT

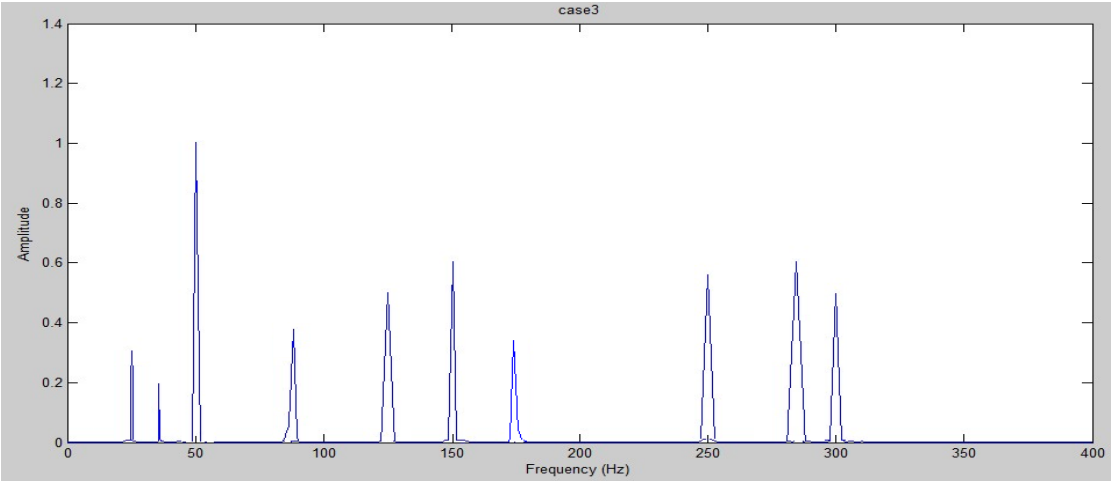

Figure 5-8 Harmonic Identification by Using DWPT Filter Bank and CWT

Table 5-1 Time-invariant Harmonic Identification by Using Three Methods

Frequency (Hz)							**Amplitude (A)**							**Phase (Degree)**						
Actual	*Method 1*	*Error %*	*Method 2*	*Error %*	*Method 3*	*Error %*	*Actual*	*Method 1*	*Error %*	*Method 2*	*Error %*	*Method 3*	*Error %*	*Actual*	*Method 1*	*Error %*	*Method 2*	*Error %*	*Method 3*	*Error %*
25	24.98	0.08	25.00	0.00	25.00	0.00	0.3	0.29	3.33	0.30	0.00	0.30	0.00	70	66.12	5.54	69.72	0.40	69.98	0.03
35.85	35.80	0.14	35.82	0.08	35.86	0.03	0.2	0.14	30.00	0.18	10.00	0.19	5.00	60	53.59	10.68	59.02	1.63	59.95	0.08
50	49.98	0.04	50.00	0.00	50.00	0.00	1.0	0.94	6.00	0.96	4.00	1.00	0.00	0	10.07		0.10		0.02	
86.6	86.82	0,25	86.65	0.06	86.62	0.02	0.4	0.36	10.00	0.35	12.50	0.38	5.00	80	26.62	66.73	82.30	2.88	80.12	0.15
125	124.89	0.11	125.11	0.09	125.10	0.08	0.5	0.48	4.00	0.50	0.00	0.50	0.00	50	140.73	181.5	50.14	0.28	49.98	0.16
150	149.96	0.03	150.18	0.12	150.00	0.00	0.6	0.58	3.33	0.59	1.67	0.60	0.00	30	48.52	61.73	32.73	9.10	30.10	0.33
175	175.50	0.29	175.33	0.19	175.12	0.07	0.35	0.34	2.86	0.34	2.86	0.34	2.86	20	58.67	193.3	24.03	20.15	20.15	0.75
250	250.02	0.01	250.04	0.02	250.00	0.00	0.55	0.54	1.81	0.54	1.82	0.55	0.00	45	134.88	199.7	43.76	2.76	45.03	0.07
285	285.50	0.18	285.08	0.03	285.02	0.01	0.6	0.48	20.00	0.56	6.67	0.58	3.33	75	136.41	81.88	73.69	1.75	75.10	0.13
300	299.96	0.01	300.08	0.03	300.00	0.00	0.5	0.38	24.00	0.44	12.00	0.50	0.00	40	51.50	28.75	42.09	5.23	40.06	0.15

It can be seen from Table 5-1 that all three methods can obtain accurate frequencies of harmonic components. However, the third one has the highest correct rate among these methods. For the results of the amplitude, two methods using WT provides much better results than FFT method, and between two WT methods, the result of the one which uses the DWPT filter bank is more close to the real value, especially in high frequency area. The results of the phase obtain by FFT method are erroneous, while the accurate of the third method is also better than the second one.

Both Table and Figurers show the difference of output result among these methods. Firstly, the FFT method and WT methods will be compared. The pulses generated by FFT have much border bases and narrower that the pulses generated by WT. This is the spectral leakage effect which is mentioned in **Section 5.2**. That means the FFT cannot accurately calculate the amplitudes and phases of the harmonics which are close to the fundamental components. The WT methods are good at overcoming this limitation because of the analysing wavelet has the ability to modulate the amplitude. Table 5-1 provides that the results by using FFT method are not satisfactory, excluding the values of frequencies. Secondly, the results are compared between two WT methods. Although both of them have ability to overcome the limitation of the FFT, the DWPT filter bank decomposition method is more professional than DWT filter bank one in high-order harmonic components evaluation because the DWPT filter bank can decompose the original signal into uniform sub-band in both high and low frequency areas. Therefore, the method which is decomposed the input signal by DWPT filter bank and then evaluation using CWT is the optimal one. To proof these, more simulations should be done.

5.4.2 Synthesised Waveform Analysis: Non-stationary Signal

5.4.2.1 Non-stationary Signal for Simulation

The non-stationary simulations have been done by using the MATLAB. A 72KV, 100MVA three-phase arc furnace model is employed to generate harmonics. The sampling frequency is 6000Hz, while the fundamental frequency of the waveform is 60 Hz. Figure 5-9 shows the original non-stationary synthesised waveform with its first five decomposed sub-bands which are obtained by using the four-level DWPT filter bank.

.

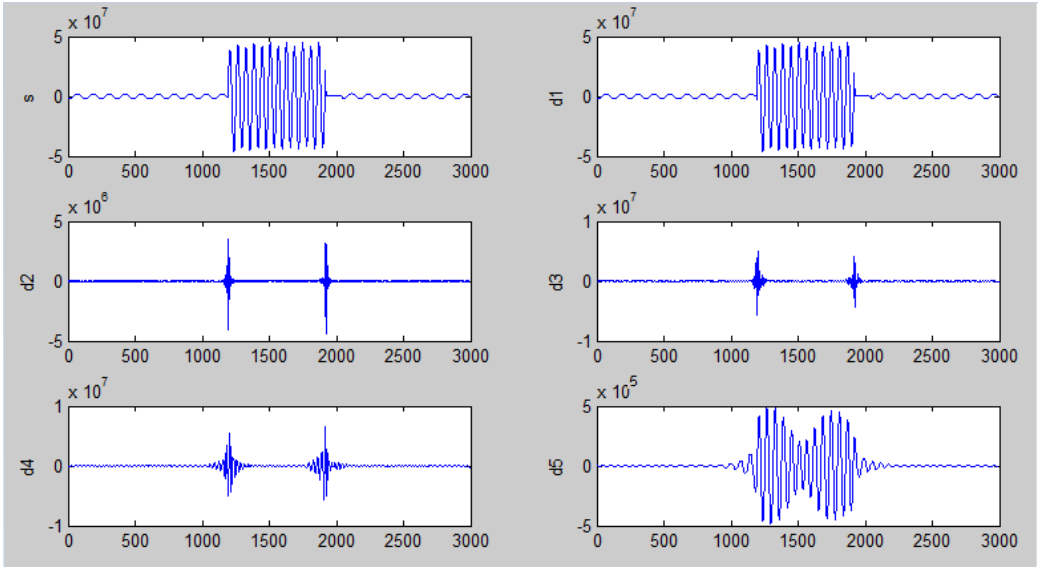

Figure 5-9 Synthesised Non-stationary Waveform with Its Decomposed Sub-bands d1-d5

5.4.2.2 Test Plan

The synthesised non-stationary signal is decomposed into sixteen uniform output components by a four-level DWPT filter bank; each has a bandwidth of 187.5 Hz. The simulation time is 0.5 seconds. Harmonics occurred from 0.2 to 0.32 sec.

Similarly, $f(t)$ is analysed by three methods as well. Case one is analysing the input signal by using FFT. The case two is decomposed the input signal by DWT filter bank and then calculated by CWT. And the last case is using the CWT to calculate the coefficients which are decomposed form the input signal by DWPT filter bank.

5.4.2.3 Result and Discussion

The results produced by these three cases are listed in Table 5-2. It is the same situation as in time-invariant case. For the results of the frequency, all three methods can obtain a high correct rate. Among these methods, the third one has the highest accuracy. The results of the amplitude obtain by the WT provides much better results that the FFT, and the method based on DWPT filter bank is still shown its outstanding analysis ability for high frequency harmonics.

Table 5-2 Non-stationary Harmonic Identification by Using Three Methods

Frequency (Hz)							**Amplitude (A)**						
Actual	Method 1	Error %	Method 2	Error %	Method 3	Error %	Actual	Method 1	Error %	Method 2	Error %	Method 3	Error %
60	65.52	9.20	60.92	1.53	60.21	0.35	327.50	301.37	7.98	325.46	0.62	327.12	0.12
120	117.37	2.19	118.70	2.19	120.77	0.64	25.22	22.56	10.55	26.69	5.83	24.97	0.99
180	183.82	2.12	181.02	1.08	180.83	0.46	18.99	18.64	1.84	19.10	0.58	19.07	0.42
240	235.69	1.80	241.31	0.55	239.73	0.11	8.19	7.33	10.50	8.13	0.73	8.15	0.49
312	313.72	0.55	313.03	0.33	311.42	0.19	13.76	13.32	3.20	13.83	0.51	13.80	0.29
420	416.76	0.77	421.17	0.28	420.57	0.14	10.15	12.97	27.78	10.78	6.21	10.39	2.36

5.4.3 Blind test Waveform Analysis: Cyclo-converters

5.4.3.1 Blind-test Signal for Simulation

To illustrate the practicability, the proposed method is employed to analyse field-test waveform. The site-test phase voltages and currents are recorded at a 33 kV,100kVA bus feeder of the power system. This time-invariant waveform contains sub-harmonics, inter-harmonics and integer harmonics which are generated by cyclo-converters. The waveform is sampled at 3030Hz.

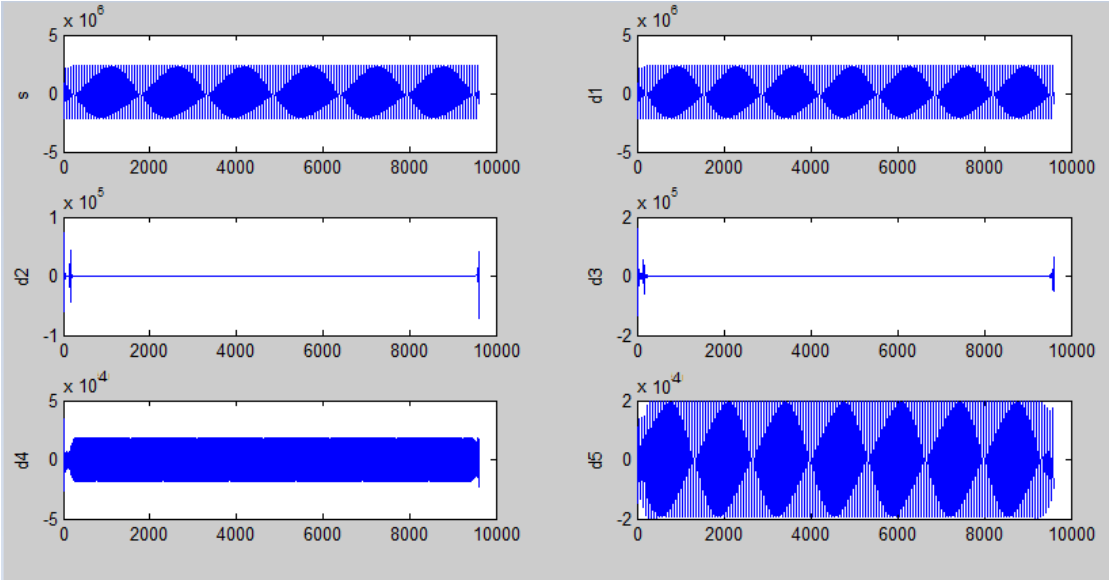

Figure 5-10 Field-test Waveform with Its Decomposed Sub-bands d1-d5

5.4.3.2 Test Plan

The filed-text signal is decomposed into sixteen uniform sub-bands by a four-level DWPT filter bank. The frequency bandwidth of each sun-band is 94.69 Hz. The simulation time is 3 seconds. For comparison purpose, $f(t)$ is analysed by three methods as well. Case one analyses the input signal by using FFT. The case two is to decompose the input signal by DWT filter bank and then calculated by CWT. And the last case employs the CWT to calculate the coefficients which are decomposed form the input signal by DWPT filter bank.

5.4.3.3 Result and Discussion

Table 5-3 Harmonic Identification of Cyclo-conerters by Using Three Methods

Frequency (HZ)			Amplitude (A)		
Method 1	Method 2	Method 3	Method 1	Method 2	Method 3
15.52	15.73	15.70	2.75	27.76	28.97
18.33	18.97	19.01	3.37	10.25	10.53
27.54	27.50	26.63	7.46	10.74	10.02
44.87	45.96	45.08	4.07	102.35	101.54
50.78	50.08	50.00	401.09	442.53	445.13
85.79	86.02	85.55	3.09	3.07	3.05
94.98	95.77	95.49	2.58	1.73	1.53
129.98	125.79	125.89	3.47	5.78	5.78
151.35	150.97	150.09	2.78	2.33	2.73
177.57	178.78	178.41	4.12	7.01	7.33
249.98	250.69	250.06	2.63	3.34	3.27
275.76	280.52	281.34	4.11	6.65	6.62
294.89	295.44	296.02	1.05	1.63	1.59
340.79	338.76	340.02	5.08	2.03	4.49
353.21	350.46	350.04	1.81	2.44	2.02
397.13	396.29	396.79	4.95	1.18	1.06
430.76	431.93	430.93	3.46	3.24	3.38
467.83	475.44	475.42	2.07	4.11	4.67
552.33	553.89	554.02	3.33	4.05	4.27

Analysis results produced by these three cases are listed in Table 5-3. Among integer harmonics of the 3rd, 5th, 6th, 7th, 8th, and 11th order, sub-harmonics and inter-harmonics are exist in the signal. As shown in the Table, the results of frequency obtained by the three methods differ only slightly. However, the large amplitude errors generated from FFT. It can be seen obviously that the difference in amplitude obtained from the FFT method and two WT methods is more substantial for sub-harmonics, inter-harmonics then integer harmonics. The large inaccuracy of amplitude obtained from FFT of these sub-harmonics is due to the spectral leakage effect which is mentioned in **Section 5.2**.

5.4.4 Blind test Waveform Analysis: Wind Turbine Generators

5.4.4.1 Blind test Signal for Simulation

The wind farm system operates with a voltage of 34.5 kV and connects to the grid through a 34.5/69 kV step-up transformer. The transmission line is 21 km. Then, a substation elevates the voltage to 230 kV in order to connect wind farm with the primary transmission system.

In this case, the DFIG is employed as WTG, which introduced in **Section 2.4.5**. It has a wide range of dynamic speed control, depending on the frequency converter. The stator winding is connected directly to the 50 Hz grid while the rotor is fed at variable frequency through the converter.

5.4.4.2 Test Plan

The filed-text signal is decomposed into sixteen uniform sub-bands by a four-level DWPT filter bank and then calculated by CWT to identify the harmonics and obtain their magnitudes. The simulation time is 6 seconds.

5.4.4.3 Result and Discussion

WTG produce only integer harmonic. According to the results from last several sections, all three methods can obtain a high correct rate for integer harmonic analysis. There is no need to do the comparison. Therefore, only the method based on DWPT filter bank and CWT is employed to evaluate the harmonic content which is listed in Table 5-4.

Table 5-4 Harmonic Identification of Wind Turbine Generators by Using DWPT Filter Bank and CWT

Harmonic order	Amplitude (A)	Harmonic order	Amplitude (A)
1	1382.513	16	5.119
2	8.152	17	6.254
3	4.843	18	1.927
4	4.702	19	5.812
5	9.645	20	3.183
6	3.76	21	3.231
7	9.832	22	2.815
8	6.602	23	3.474
9	4.289	24	1.812
10	7.748	25	3.230
11	19.259	26	2.906
12	3.529	27	2.490
13	25.695	28	2.076
14	5.811	29	3.697
15	1.799	30	1.633

5.5 Conclusion

This chapter starts by introducing the conventional methods for harmonic analysis. Then, a novel WT-based approach to analyse harmonic contents of power system waveforms has been proposed by using DWPT filter bank decomposition and CWT identification. The proposed method has been tested with a large number of applications. These application designs contain a variety of signals, such as time-invariant, non-stationary and field-test signals, which include integer, sub and non-integer harmonic contents. In addition, other conventional harmonic analysis methods, i.e. FFT method and the combination method of DWT filter bank and CWT calculation have been tested for comparison. The results obtained demonstrate that the proposed WT-based method can achieve the best results in terms of quantifying harmonic frequencies, amplitudes and phases, compared to the other two methods. The effect of the harmonic is huge in power system, in order to eliminate the harmonic, it is important to evaluate the harmonic content, Therefore, the proposed method is very advantageous in terms of analysing harmonics in power system waveform and has the potential in practice for a more accuracy analysis.

Chapter 6 Harmonic Penetration Evaluation in Power System

6.1 Introduction

With increasing of wind power generators in power networks, it introduces PQ problems caused by harmonic injection. The harmonics have great influence on the power system equipment as well as on its operation. They can lead to operation failure of electrical and electronic components failure of power factor correction capacitors, loss in power generation and transmission, and interference with protection, control and communication networks as well as customer loads. High levels of harmonic distortion can also increase generator, transformer, capacitor or motor heating. Some published standards such as IEEE 519, IEC 61000 and Engineering Recommendation G5/4 are used as a guide to limit the harmonics in power system. Snice the content of harmonics have calculated accurately in Chapter 5, an efficient, reliable and accurate algorithm that is used to evaluate the steady state network voltage and current at harmonic frequencies is necessary. This process is defined as harmonic power flow evaluation [26]. According to reference **Error! Reference source not found.**, if the harmonics generated by the nonlinear components are independent, the above process is called harmonic penetration evaluation. In this chapter, the process of evaluating the steady state network voltages at harmonic frequencies is defined as harmonic power flow evaluation as well as harmonic penetration evaluation. The purpose of this chapter is essential to calculate the harmonic penetration and investigate the effects to power networks.

In this chapter, a 100MV，33KV，118 bus power system is employed to do the simulation. A method named Fast Hybrid Method (FHM) from reference [90][91][92][93] is used to calculate the harmonic power flow. This is a simply and reliable method which combines the secant approach, the Newton-Downhill-based approach and the decoupled methods together to calculate steady state harmonic power

flow in power system with discrete frequencies. The WTGs, arc-furnaces and convertors will be connecter to the power system as harmonic sources.

In order to investigate the effects on the harmonic penetration with increasing of renewable power generations in power networks, two tests are designed and proposed. For the Test 1, the location and number of WTGs are fixed, but replace with larger capacity WTGs and hence the total power capacities are increased. For the Test 2， with increasing of the number and location of WTGs, the total power capacities are increased. In both of these two test, the number and power capacity of converters and arc furnaces are fixed, and the total renewable power generations raise from 20 % (874.98MW) to 30% (1312.47MW), and then increase from 30% to 40 % (1749.96MW).

The results and discussions of these two tests are presented through these two aspects:

- The effect of the result waveforms of Root Mean Square (RMS) values of bus current and voltage magnitudes are investigated.
- The number of buses that Total Harmonic Voltage Distortion (THDv) values exceed the level of limit 3% is investigated.

This chapter is organized as follows. In **Section 6.2** the test power system, evaluation method and the harmonic sources are introduced. Then, the brief summaries of two tests are presented in **Section 6.3**. Thirdly, in **Section 6.4,** the effect of increasing renewable power generations to the harmonic power flow is investigated through two aspects. Then, result and analysis is presented in **Section 6.5**. Finally, a brief conclusion is given in **Section 6.6**

6.2 Harmonic Penetration Evaluation Method

A large number of different harmonic penetration evaluation methods have been developed until now. In this chapter, a method named FHM is used for harmonic penetration evaluation. This is a simple and reliable method which combines the secant approach, the Newton-Downhill based approach and the decoupled methods together to calculate steady state harmonic power flow in power system with discrete frequencies [90]. It can complement the other methods' limitations, such as long computing time, not high enough accuracy and considerable memory storage.

At first, the secant method is employed to establish the initial value in order to overcome the convergence problem. And then the Newton-Downhill and decoupled methods are applied to make the iterative processes monotonic decrease. It can reduce the calculation procedure of Jacobian matrix in order to increase the calculation speed and converge successfully.

Secant Method: is an iterative approach of solving non-linear equations. It uses a succession of roots of secant lines to better approximate a root of non-linear function *f* [91].

Newton-Downhill Method: is an algorithm often used in optimasation problem. It is well known that in order to make the Newton-Raphson method converge, the initial iterative value must be close to the expected value. However sometimes it is very difficult to choose the initial value to meet the requirements of convergence conditions. To overcome this limitation, the Newton-Downhill algorithm is applied to solve this problem with a large scale convergence [92].

Decoupled Method: is an approach for calculating the harmonic power flow by ignoring the harmonic couplings between harmonic orders. Thus the calculation procedure is carried out separately for each harmonic order. Because of this, it can reduce the computing time and improve the convergence problem. This approach

provides an advantage of balancing the computational complexity and the result accuracy [93].

The flowchart of this proposed approach is shown in Figure 6-1. It can be seen from this block diagram that inputs of guess values are firstly entered into the secant method to generate the initial values for the calculation at fundamental frequency. Secondly, the approach which is the combination of the Newton-Downhill and the decoupled method is used to calculate the power flow at fundamental frequency in order to reduce the calculation process and converge successfully. Then if the result converges, it moves to the next step. Eventually, n admittance-matrix base equation is employed to calculate the harmonic penetration directly, and the initial values at higher harmonic frequencies are put into the calculation directly. The fully theory of this approach can be found in [91].

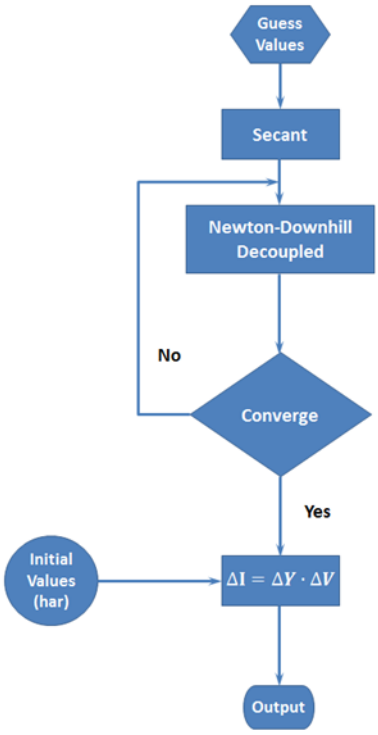

Figure 6-1 Flow Chart of the Proposed Approach

6.3 Harmonic Sources

Non-linear equipment or components integrated in the power system causes harmonic distortion of voltage and current. In this chapter, the wind turbine generator, cyclo-converter, and arc furnace are regarded as harmonic sources. The wind turbine generator represents the renewable energy generator. Cyclo-converters and arc furnaces are the major sources of harmonics in power system, especially the converter which contains sub-harmonic and inter-harmonic frequencies. It expands the range of harmonic frequency, which is not only on integer-harmonic, and makes the simulation more practical.

All of these harmonic injection currents of each harmonic level including fundamental frequency are obtained from **Chapter 5.** The value of harmonic injection current are listed in Table 6-1, Table 6-2 and Table 6-3 respectively and shown as per unit.

Wind Turbine Generator:

Table 6-1 Harmonic Injection Currents Generated by Wind Turbine Generators

Harmonic order 'h'	Amplitude (p.u.)	Harmonic order 'h'	Amplitude (p.u.)
1	476.97 e^{-3}	16	1.7661 e^{-3}
2	2.8124 e^{-3}	17	2.1576 e^{-3}
3	1.6708 e^{-3}	18	0.6648 e^{-3}
4	1.6222 e^{-3}	19	2.0051 e^{-3}
5	3.3275 e^{-3}	20	1.0981 e^{-3}
6	1.2972 e^{-3}	21	1.1147 e^{-3}
7	3.3920 e^{-3}	22	0.9712 e^{-3}
8	2.2777 e^{-3}	23	1.1985 e^{-3}
9	1.4797 e^{-3}	24	0.6251 e^{-3}
10	2.6731 e^{-3}	25	1.1144 e^{-3}

11	6.6444 e^{-3}	26	1.0026 e^{-3}
12	1.2175 e^{-3}	27	0.8590 e^{-3}
13	8.8648 e^{-3}	28	0.7162 e^{-3}
14	2.0048 e^{-3}	29	1.2755 e^{-3}
15	0.6207 e^{-3}	30	0.5634 e^{-3}
I_{base}=2898.55A			

Arc Furnace:

Table 6-2 Harmonic Injection Currents Generated by Arc Furnace

Harmonic order 'h'	Amplitude (p.u.)	Harmonic order 'h'	Amplitude (p.u.)
1	235.80 e^{-3}	4	5.897 e^{-3}
2	18.158 e^{-3}	5.2	9.907 e^{-3}
3	13.673 e^{-3}	6	7.3080 e^{-3}
I_{base}=1388.89A			

Cyclo-converter:

Table 6-3 Harmonic Injection Currents Generated by Cyclo-Converter

Harmonic order 'h'	Amplitude (p.u.)	Harmonic order 'h'	Amplitude (p.u.)
0.314	9.5601 e^{-3}	5.000	1.0791 e^{-3}
0.380	3.4749 e^{-3}	5.627	2.1846 e^{-3}
0.533	3.3066 e^{-3}	5.920	0.5247 e^{-3}
0.902	33.508 e^{-3}	6.800	1.4817 e^{-3}
1.000	146.89 e^{-3}	7.000	0.6667 e^{-3}
1.711	1.0065 e^{-3}	7.936	0.3498 e^{-3}
1.910	0.5049 e^{-3}	8.619	1.1154 e^{-3}
2.518	1.9074 e^{-3}	9.508	1.5411 e^{-3}
3.000	0.9009 e^{-3}	11.080	1.4091 e^{-3}
3.568	2.4189 e^{-3}		
I_{base}=3030.30A			

6.4 Test Procedure for Harmonic Penetration Analysis

6.4.1 Test system

In this chapter, a 100MV，33KV，118 bus power system is employed to do the simulation. The single line diagram of this test system is illustrated in Figure 6-2. This IEEE 118 bus system contains 54 generators, 177 lines, 9 transformers and 91 loads. Bus 69 is considered as the reference bus. [94].

6.4.2 Case study

In order to investigate the effects on the harmonic penetration with increasing of renewable power generations in power networks, two tests are designed and proposed. Regarding the Test 1, the location and number of WTGs are fixed, but replace with larger capacity WTGs and hence the total power capacities are increased. For the Test 2 with increasing of the number and location of WTGs, the total power capacities are increased. In both test, the number and power capacity of converters and arc furnaces are fixed .In each test, three cases are designed and listed in Table 6-4 and Table 6-5.

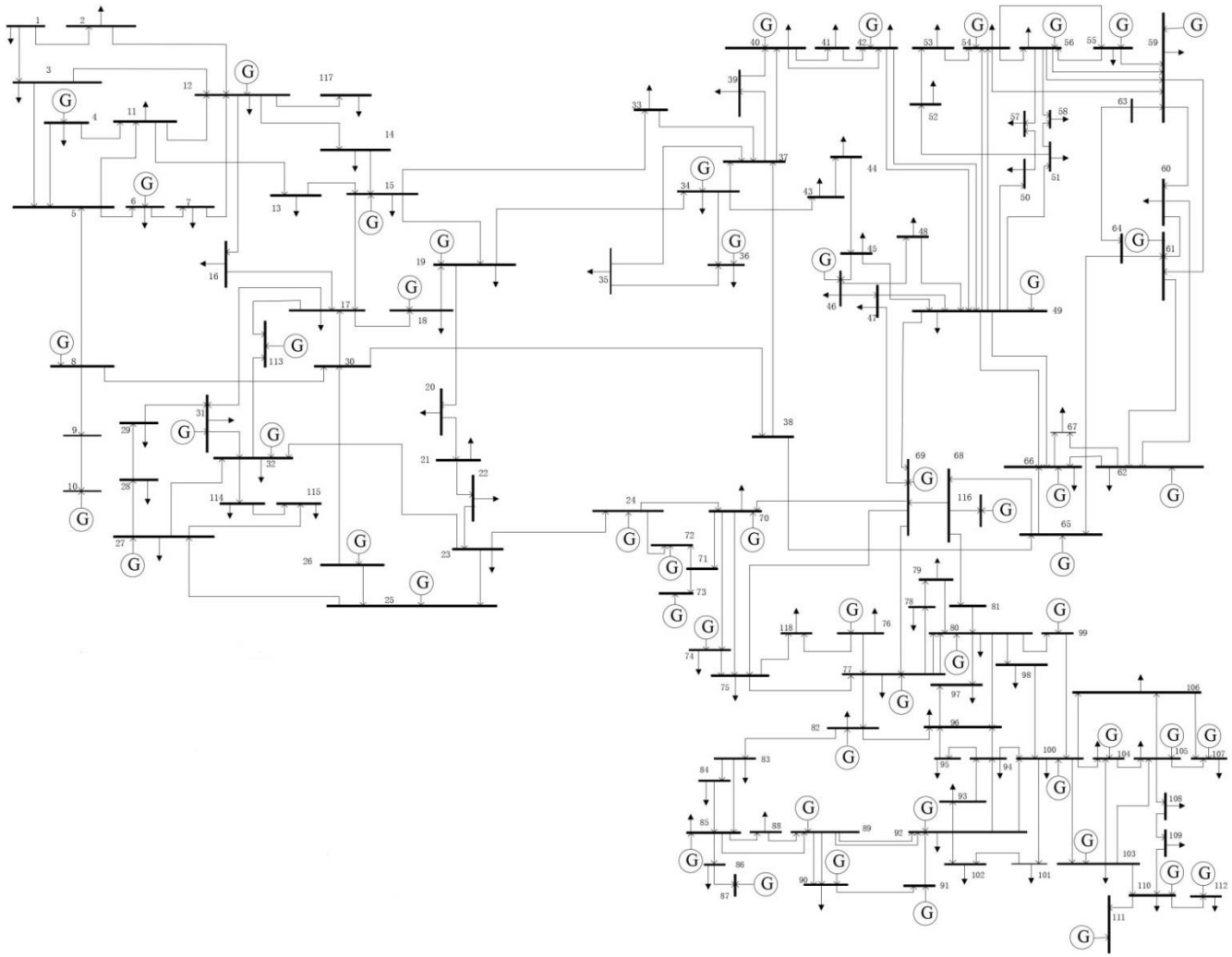

Figure 6-2 IEEE 118 Bus Test System Bus Single Line Diagram

Table 6-4 Test 1: Change Capacity of WTG

Case 1	Harmonic Source	No. of Units	Power Capacity
	Wind Turbine Generator	5	20%(874.98MW)
	Arc furnace	8	5% (212.1MW)
	Converter	7	5% (212.1MW)
Case 2	Harmonic Source	No. of Units	Power Capacity
	Wind Turbine Generator	5	30%(1312.47MW)
	Arc furnace	8	5% (212.1MW)
	Converter	7	5% (212.1MW)
Case 3	Harmonic Source	No. of Units	Power Capacity
	Wind Turbine Generator	5	40%(1749.96MW)
	Arc furnace	8	5% (212.1MW)
	Converter	7	5% (212.1MW)

Table 6-5 Test 2: Change Numbers of WTG

Case 1	Harmonic Source	No. of Units	Power Capacity
	Wind Turbine Generator	5	20%(874.98MW)
	Arc furnace	8	5% (212.1MW)
	Converter	7	5% (212.1MW)
Case 2	Harmonic Source	No. of Units	Power Capacity
	Wind Turbine Generator	6	30%(1312.47MW)
	Arc furnace	8	5% (212.1MW)
	Converter	7	5% (212.1MW)
Case 3	Harmonic Source	No. of Units	Power Capacity
	Wind Turbine Generator	7	40%(1749.96MW)
	Arc furnace	8	5% (212.1MW)
	Converter	7	5% (212.1MW)

Table 6-5 lists the plan of Test 2. With increasing number and locations of WTGs, the total power capacities are increased. For Case 1 and Case 2, the number of WTGs increases from 5 to 6. Compared to Case 2 and Case 3, the number of WTGs increases from 6 to 7. The increased locations are marked in Figure 6-3: the five initial WTGs are marked by red square; the increased WTG of Case 2 is marked by yellow square; while the increased WTG of Case 3 is marked by green square. All the WTGs replace the normal generators, but not added.

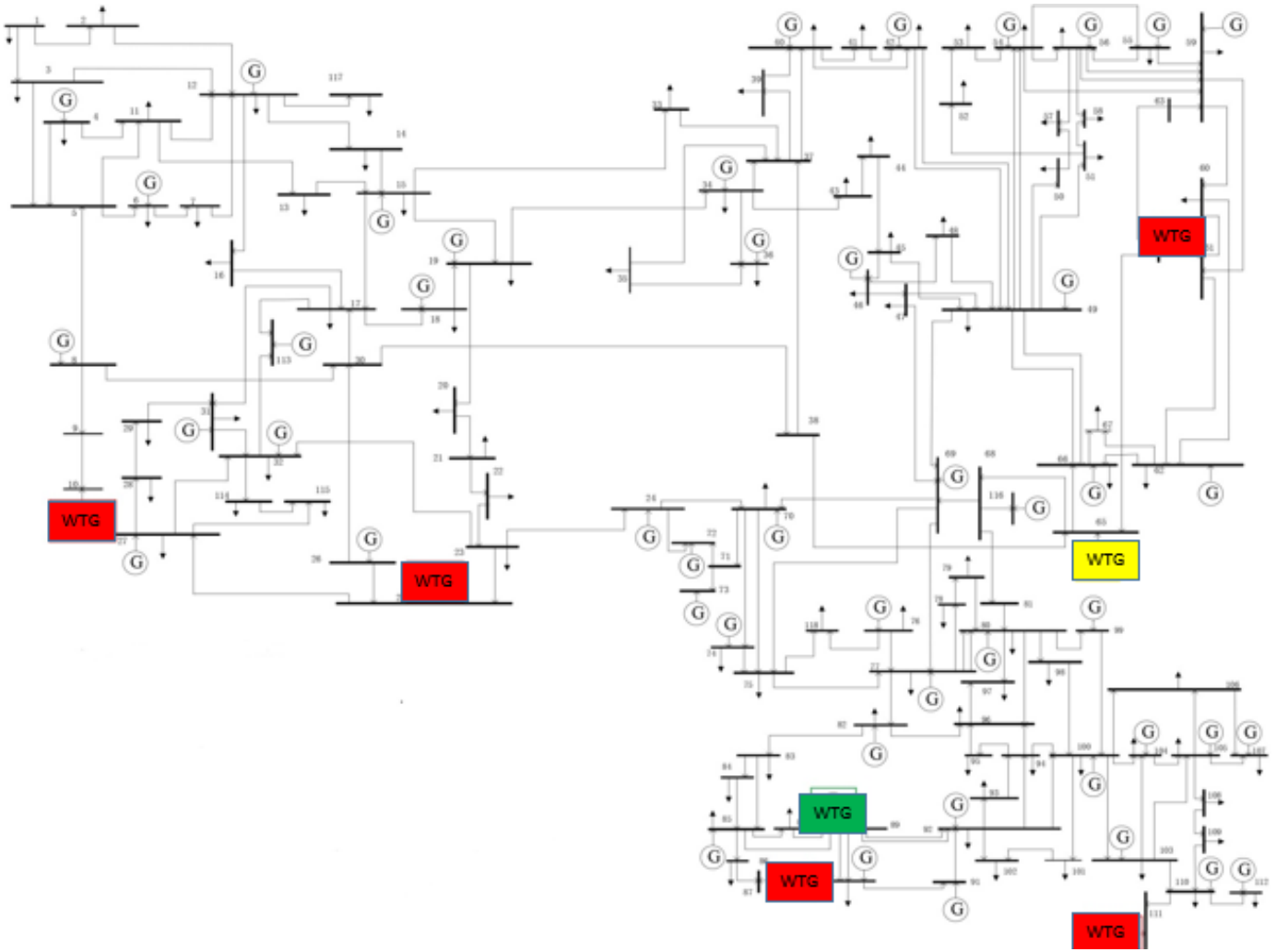

Figure 6-3 IEEE 118 Bus Test System Bus Single Line Diagram

6.5 Result and Discussion

In order to investigate the effects of changing renewable generators' harmonic capacities to the harmonic penetration, harmonic capacities increased by following two aspects:

- Increase capacity of WTGs: fixed the location and number of WTGs, only replace the initial WTGs with larger capacity's WTGs.
- Increase number and location of WTGs: fixed the power capacity of each WTG only increased the number and location of WTGs.

The results and discussions are presented through these two aspects in this section.

6.5.1 Increase Capacity of WTG

In this section, results achieved from three cases are listed and compared to investigate the effects of increasing power capacities of WTGs to the harmonic penetration. The number, location and power capacities of converters and arc-furnaces are fixed respectively. The number and location of WTGs are fixed. With replace larger capacity's WTGs, the total renewable power generations increase from 20 % (874.98MW) to 30% (1312.47MW), and then increase from 30% to 40 % (1749.96MW). Their fundamental and harmonic injection currents increase by 10 % accordingly.

6.5.1.1 Current Magnitude

There are three scenarios defined, e.g. Case 1, Case 2 and Case 3, for currents in terms of RMS with 118 nodes in total. For Case 1, the power capacity of WTGs is 20% (874.98MW) of total generation capacity. With Regard to Case 2, power capacity of WTGs is 30% (1312.47MW) of total generation capacity. With Respect to Case 3, power capacity of WTGs is 40% (1749.96MW) of total generation capacity. The results of three cases are illustrated in Figure 6-4, Figure 6-5 and Figure 6-6 respectively. For

these three figures, the unit for X-axis is per unit, while Y-axis represents 118 bus of power system.

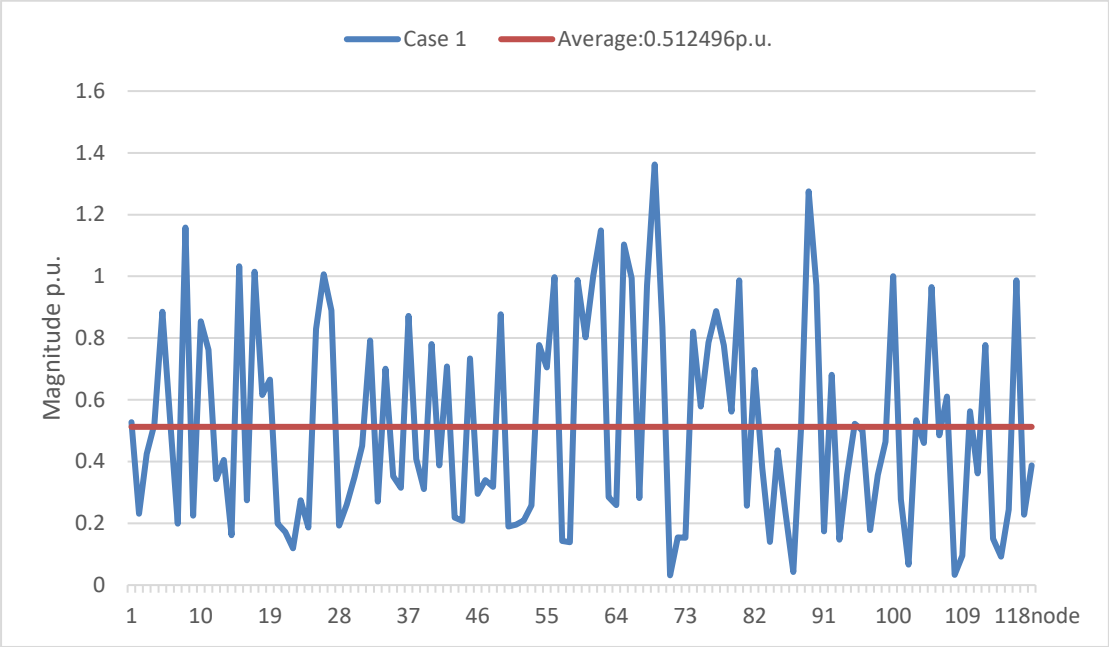

Figure 6-4 Current Magnitude Result for Case 1

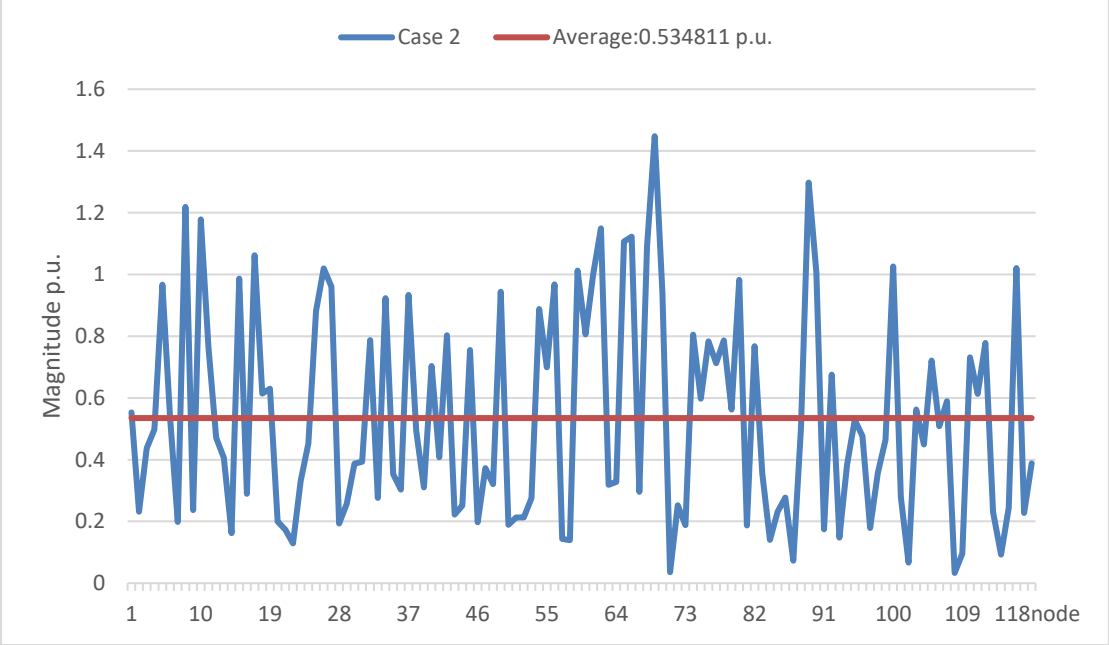

Figure 6-5 Current Magnitude Result for Case 2

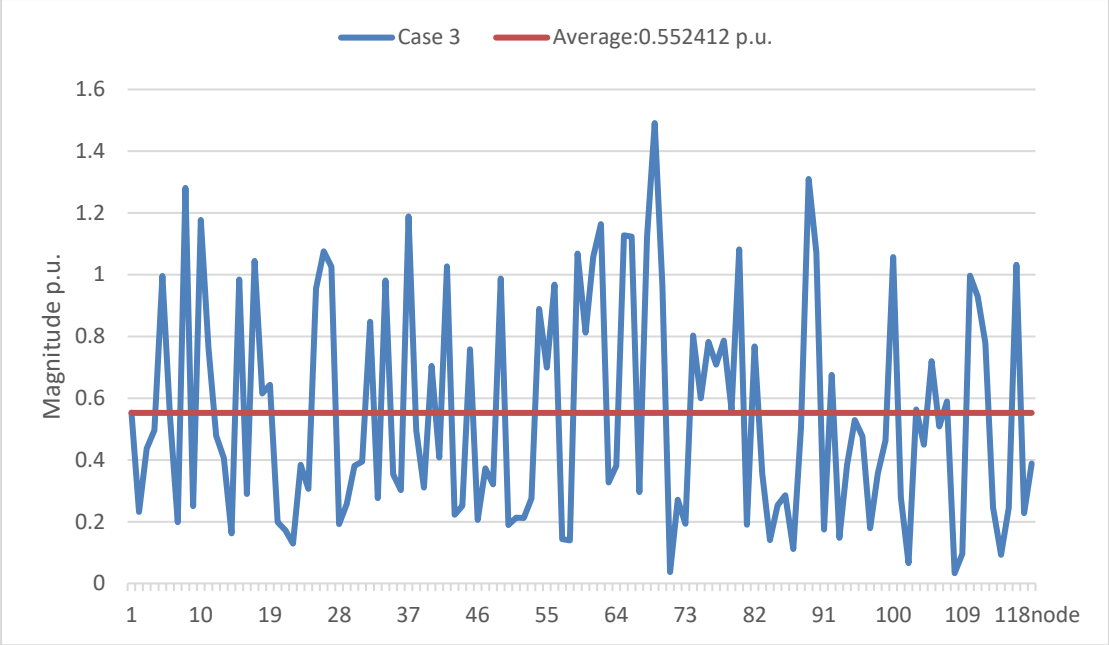

Figure 6-6 Current Magnitude Result for Case 3

Taking the result of Case 1 into account, the average of I_{rms} is equal to 0.512496*p.u*.The peak sample is at 69th node, reaching the value of 1.362301 *p.u*, and the second largest value is 1.275623 *p.u* at 89th node. The minimum value of I_{rms} is 0.031628 *p.u* at 71th node. According to Figure 6-5, the largest value for Case 2 is equivalent to 1.447611*p.u* and is also located at 69th node while the positions of the second largest and the minimum values are changed to 89th and 108th nodes, achieving the values of 1.29753 *p.u* and 0.033202 *p.u* respectively. Compared to Case 1, the average of Case 2 has increase to 0.534811 *p.u*. Like Case 2, the maximum and minimum values for Case 3 in Figure 6-6 are 1.491129 *p.u* and 0.033245 *p.u* at 69th and 108th nodes respective, and the average for Case 3 reaches 0.552412 *p.u*. The comparison result of the three scenarios is listed in Table 6-6.

Table 6-6 Statistics Analysis for Three Scenarios of Current Magnitude

	Case 1	Case 2	Case 3
Average (*p.u*)	0.512496	0.534811	0.552412
Maximum (*p.u*)	1.362301	1.447611	1.491129
Minimum (*p.u*)	0.031628	0.033202	0.033245

Though the average values of three cases are different, the difference is only around 0.1 *p.u.*, which can be viewed as the slight difference and thus it might imply that there is little influence on the RMS values of current magnitudes with increasing of power capacities of WTGs. In order to further analyse the results, the differences between Cases 1-2, and Cases 2-3 are compared respectively. The difference between Case 2 and Case 1 is shown in Figure 6-7. In this figure, the unit for X-axis is per unit, while the Y-axis represents the 118 bus of power system. Here, the difference is defined by the subtracting the magnitude of Case 1 from that of Case 2. If the difference is positive, it is seen that the result of Case 2 is larger than that of Case 1. However the situation is opposite if the difference is negative. In this thesis, a threshold for the difference between two cases is defined. If the absolute value of the results is within the defined threshold, it indicates the magnitudes of the same nodes for the two cases are viewed as identical. It is important to note that this definition of threshold is used throughout the entire **Chapter 6** and a threshold of 0.1 is defined. Taking this strategy into account, there are 12 nodes changed in total when the power capacities of WGTs have increased: values of 9 nodes are positive while 3 nodes' values are negative. Of the positive values, the 10th node reaches a peak value of 0.324696, because of the capacity of WTG at 10th node increased. For the negatives, the most negative values is located at 46th node, with the value of minus 0.097311.

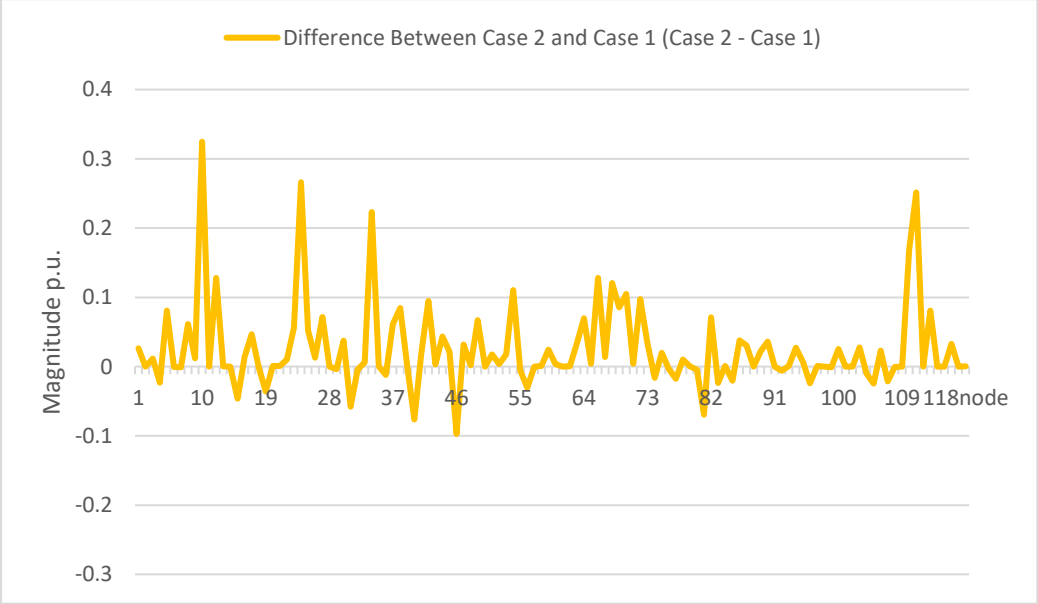

Figure 6-7 Result of Current Magnitude Comparison between Case 2 and Case 1

In addition, the difference of Case 3 and Case 2 is also analysed and the result is shown in Figure 6-8. For Figure 6-8, the unit for X-axis is per unit, while the Y-axis represents the 118 bus of power system

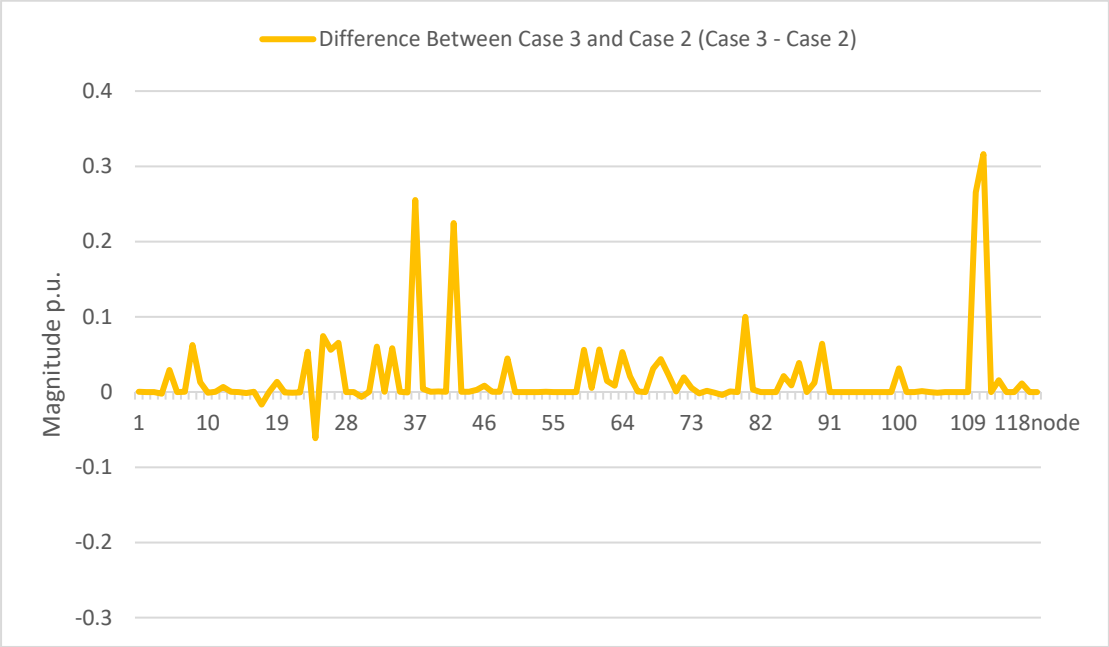

Figure 6-8 Result of Current Magnitude Comparison between Case 3 and Case 2

Following the rules and strategy defined, a total of 5 nodes changed in value: 4 nodes are positive and only 1 node is negative, with the threshold value of 0.1. According to Figure 6-8, the largest difference occurs at the 111th node, achieving the value of 0.316229 because of the capacity of WTG at 111th node increased. The negative value is equivalent to minus 0.067311 at the 24th node. Based on the results obtained, a number of values of RMS current has changed and the majority of values have increased, as the proportion of capacity in wind power.

6.5.1.2 Voltage Magnitude

Similarly, there are also three scenarios for the voltage in terms of RMS with 118 nodes. Following the scenarios defined in **Section 6.5.1.2**, the power capacity of WTGs for Case 1, Case 2 and Case 3 is 20%, 30% and 40% respectively. The results of three cases are illustrated in Figure 6-9, Figure 6-10 and Figure 6-11 respectively. For these three figures, the unit for X-axis is per unit, while Y-axis represents 118 bus of power system.

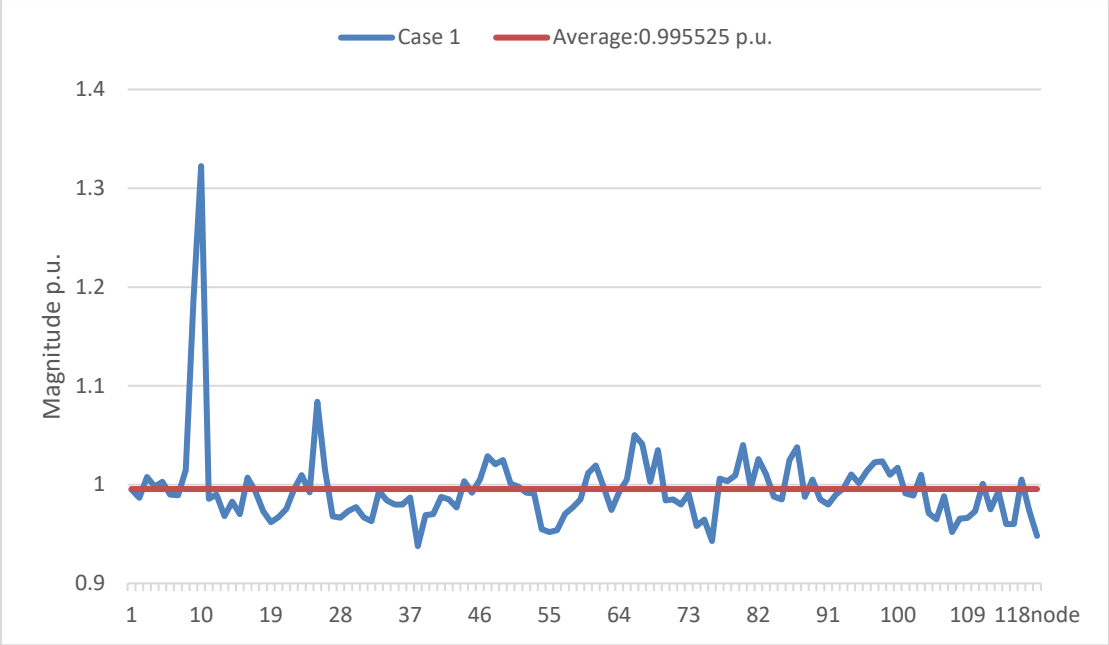

Figure 6-9 Voltage Magnitude Result for Case 1

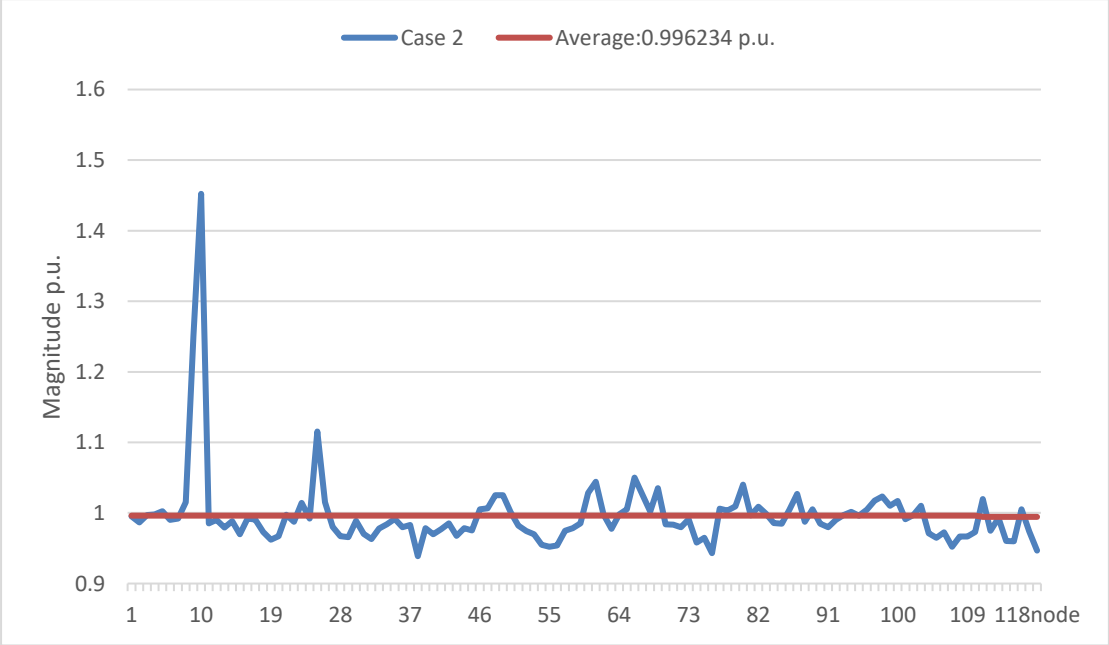

Figure 6-10 Voltage Magnitude Result for Case 2

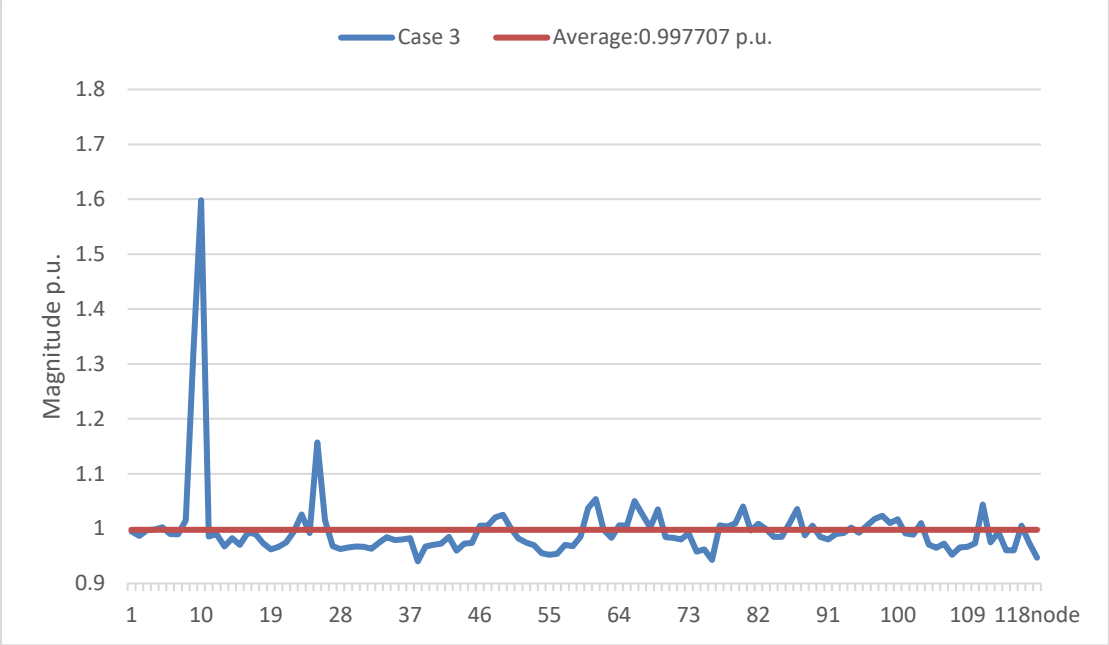

Figure 6-11 Voltage Magnitude Result for Case 3

Taking Case 1 shown in Figure 6-9 into account, the average of V_{rms} is equal to 0.995525 *p.u*. The peak sample is at 10^{th} node, reaching the value of 1.322385 *p.u*, and the minimum value of V_{rms} is 0.937752 *p.u* at 38^{th} node. The maximum and minimum results of Case 2 have the same location as Case 1, i.e. 10^{th} and 38^{th} nodes, with the values of 1.452210 *p.u* and 0.938752 *p.u* respectively. According to Figure 6-10, the average of Case 2 is equal to 0.996234 *p.u.* Similarlly, it can be found clearly that the maximum and minimum values for Case 3 in Figure 6-11 are 1.598122 *p.u* and 0.940155 *p.u* at 10^{th} and 38^{th} nodes respective, and the average for Case 3 reaches 0.997707 *p.u*. The comparison result of three scenarios is listed in Table 6-7.

Table 6-7 Statistics Analysis for Three Scenarios of Voltage Magnitude

	Case 1	Case 2	Case 3
Average (*p.u*)	0.995525	0.996234	0.997707
Maximum (*p.u*)	1.322385	1.452210	1.598122
Minimum (*p.u*)	0.937752	0.938752	0.940155

Like analysis of current magnitude, a further analysis of Case 1, Case 2 and Case 3 are performed. The definition of positive and negative result details previously and remains the same. Furthermore, a new value of threshold is defined for the voltage magnitude

analysis. The threshold of 0.01 *p.u.* is defined for this case, which implies the result is viewed as identical if the absolute value of the difference is within the threshold defined.

The difference between Case 2 and Case 1 is shown in Figure 6-12, and the unit for X-axis is per unit, while the Y-axis represents the 118 bus of power system. There are 27 nodes changed in total when the power capacities of WTGs have increased: values of 11 nodes are positive while 16 nodes' values are negative. Of the positive values, 10th node reached the peak value of 0.129825. For the negatives, the most negative value is located at 44th node, with the value of minus 0.025077.

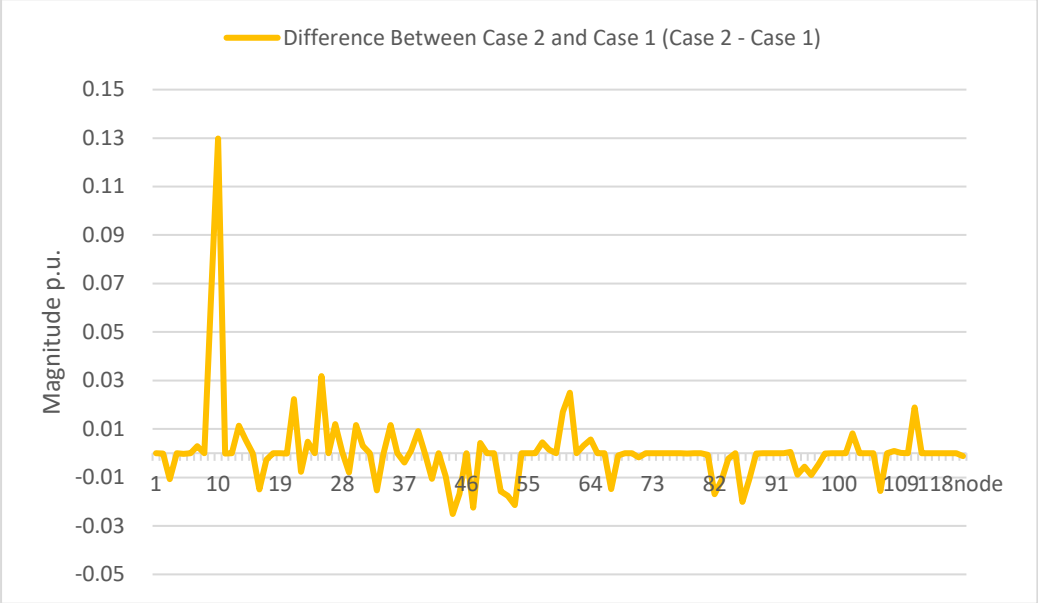

Figure 6-12 Result of Voltage Magnitude Comparison between Case 2 and Case 1

In addition, the difference of Case 3 and Case 2 is also analysed in this thesis, and the result is shown in Figure 6-13. In this figure, the unit for X-axis is per unit, while the Y-axis represents the 118 bus of power system.

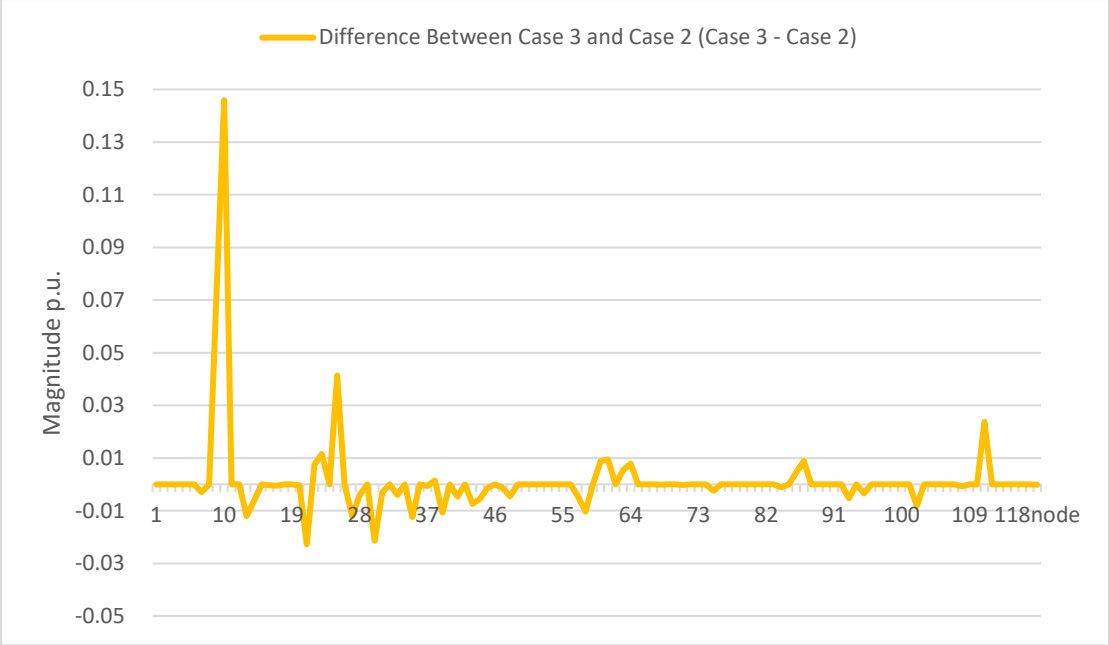

Figure 6-13 Result of Voltage Magnitude Comparison between Case 3 and Case 2

Following the rules and strategy defined, there are 12 nodes changed totally: 5 nodes are positive and only 7 nodes are negative, with the threshold value of 0.01 *p.u*. The rest of nodes are viewed as identical. According to Figure 6-13, the largest difference occurs also at the 10^{th} node, achieving the value of 0.145912. The negative value is equivalent to minus 0.022793 at 21^{st} node.

6.5.1.3 Total Voltage Harmonic Distortion (THDv)

According to **Section 2.5.3.1**, in harmonic current distortion limits, the THDi levels are not specified and here the THDv is an important factor to investigate and estimate the effects of changing power capacity of WTGS to the harmonic penetration. Following the scenarios of three cases defined before, the result can be analysed in terms of THDv and are shown in Figure 6-14, Figure 6-15 and Figure 6-16 respectively. In these three figures, the unit for X-axis is percentage, while the Y-axis represents the 118 bus of power system.

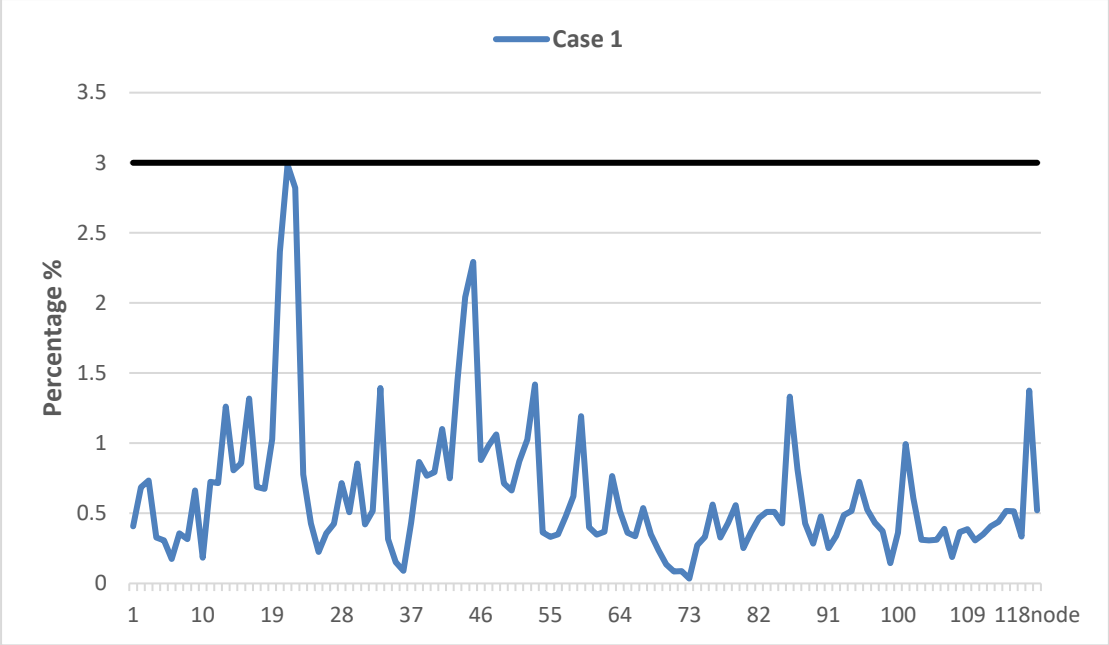

Figure 6-14 THDv Result for Case 1

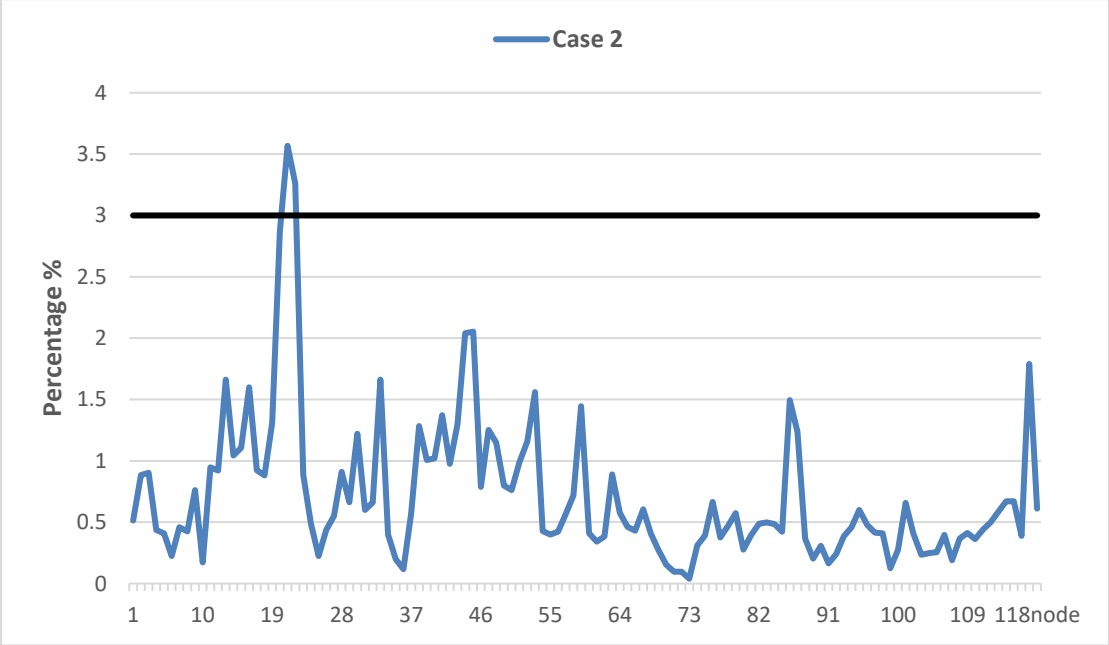

Figure 6-15 THDv Result for Case 2

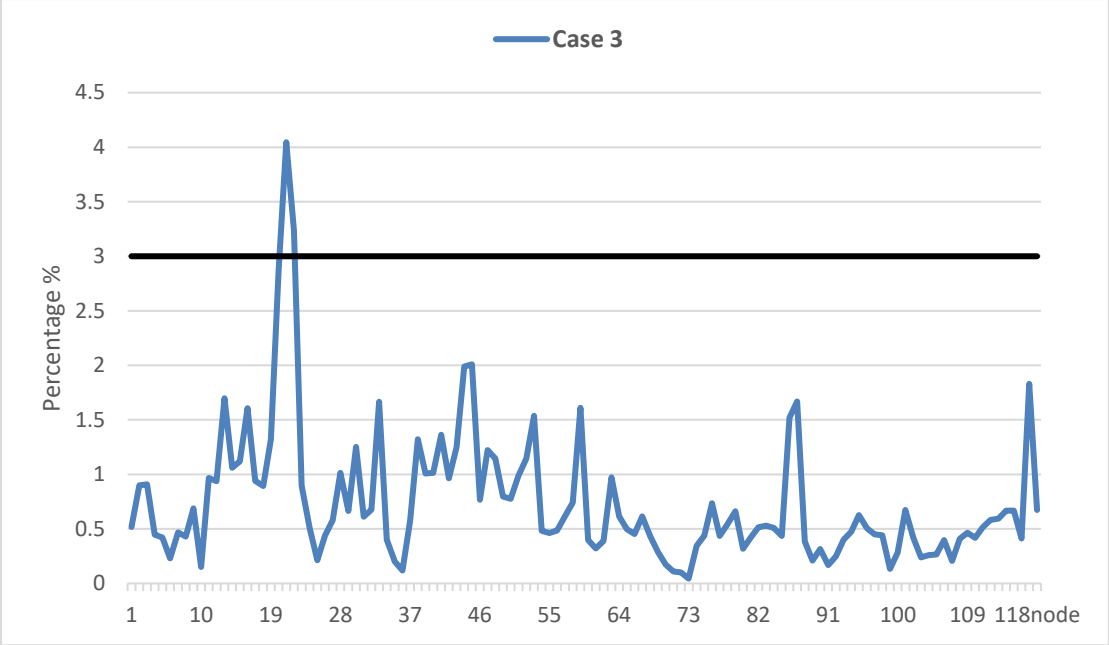

Figure 6-16 THDv Result for Case 3

The results of three cases have similar waveforms, and in order to investigate the results, all of data can be grouped into three parts by limit levels according to the Engineering Recommendation G5/4 in **Section 2.5.4.2**. For these figures, the limit level is defined as 3% and is described by black straight line in the figures. There are three penetration ranges for these cases: 0-1.5%, 1.5%-3% and over 3%, respectively.

The statistics of sample distributions and the analysis in terms of maximum and average values for Cases 1-3 are achieve in Table 6-8 and Table 6-9.

Table 6-8 Sampe Distribution for Different Cases with Various Range of THDv

Range of THDv(%)	Case 1	Case 2	Case 3
0-1.5%	113	108	105
1.5%-3%	5	8	11
>3%	0	2	2

Table 6-9 Maximum and Average Analysis of THDv for Different Cases

Scenarios	Case 1	Case 2	Case 3
Maximum (%)	2.985703	3.567816	4.045135
Average (%)	0.633508	0.722014	0.747201

According to Table 6-8 and Table 6-9, most of results are located within the range of under 1.5%, and the number is 113 for Case 1. The number within the range between 1.5% and 3% is 5 and no result is larger than 3%. The maximum and average values for Case 1 are 2.985703% at 21st node and 0.633508% respectively. For Case 2, the number for range of under 1.5% reduces while the numbers for the other two types of ranges increase, achieving 8 and 2 respectively. As a result, both maximum and averages arise from 2.985703% to 3.567816% and from 0.633508 to 0.722014 respectively, compared to Case 1. With respect to Case 3, the number of nodes whose value are under 1.5% further decreases while the number of those located between 1.5%-3% continue to increase, compared to Case 2. The maximum value for Case 3 increases from 3.567816% to 4.045135%. However, the average value continues to increase from 0.722014% to 0.747201%.

In summary, as the capacity of wind power increases, e.g. from 20%-30%, and 30%-40%, both maximum and average values of THDv raise gradually. In addition, the number over the limit level also increases.

6.5.2 Increase Number and Location of WTG

In this section, results achieved from three cases are listed and compared to investigate the effects by increasing the number and location of WTGs to the harmonic penetration. The number, position and power capacities of converters and arc-furnaces are fixed respectively. The capacity of each WTG is fixed. With the number and location of WTGs increase, the total renewable power generations raise from 20 % to 30%, and then increase from 30% to 40 %. Their fundamental and harmonic injection currents increase by 10 % accordingly.

6.5.2.1 Current Magnitude

Following the analysis method used in **Section 6.5.1**, another set of data for current magnitude is used to analyse the power system quality. Similarly, there are three scenarios defined, Case 1, Case 2 and Case 3 for analysing the currents in terms of RMS considering 118 nodes in total, and the three cases are divided according to the proportion of power capacity of WTGs in entire power generators' capacity: 20%, 30% and 40% are for Case 1, Case 2 and Case 3 respectively. The results of three cases are illustrated in Figure 6-17, Figure 6-18 and Figure 6-19 respectively. For these three figures, the unit for X-axis is per unit, while Y-axis represents 118 bus of power system.

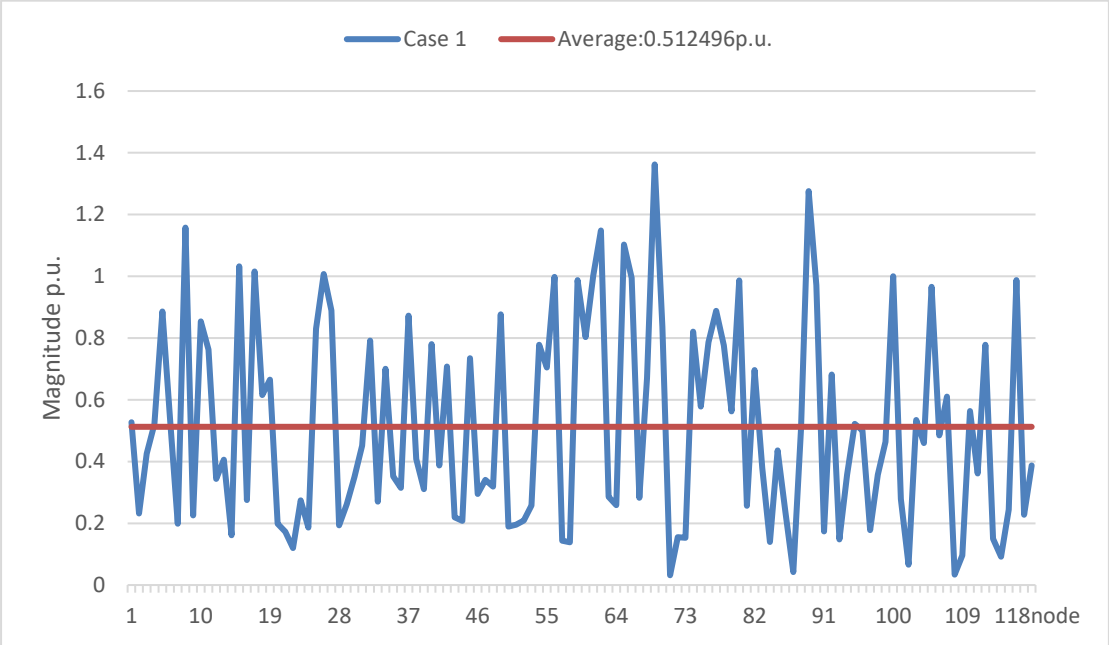

Figure 6-17 Current Magnitude Result for Case 1

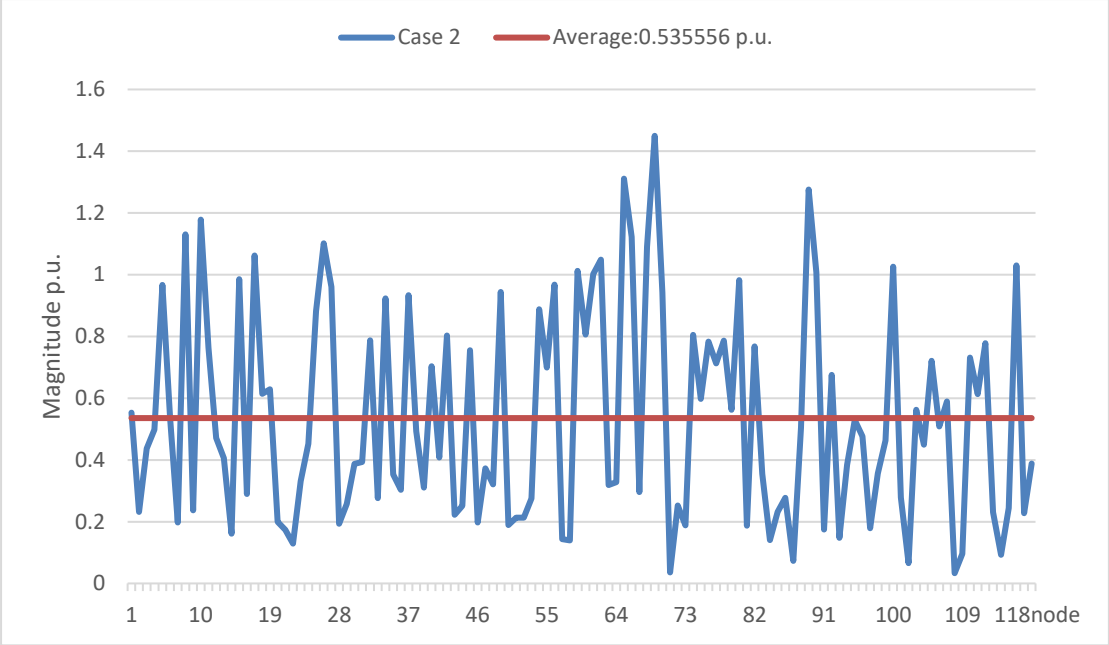

Figure 6-18 Current Magnitude Result for Case 2

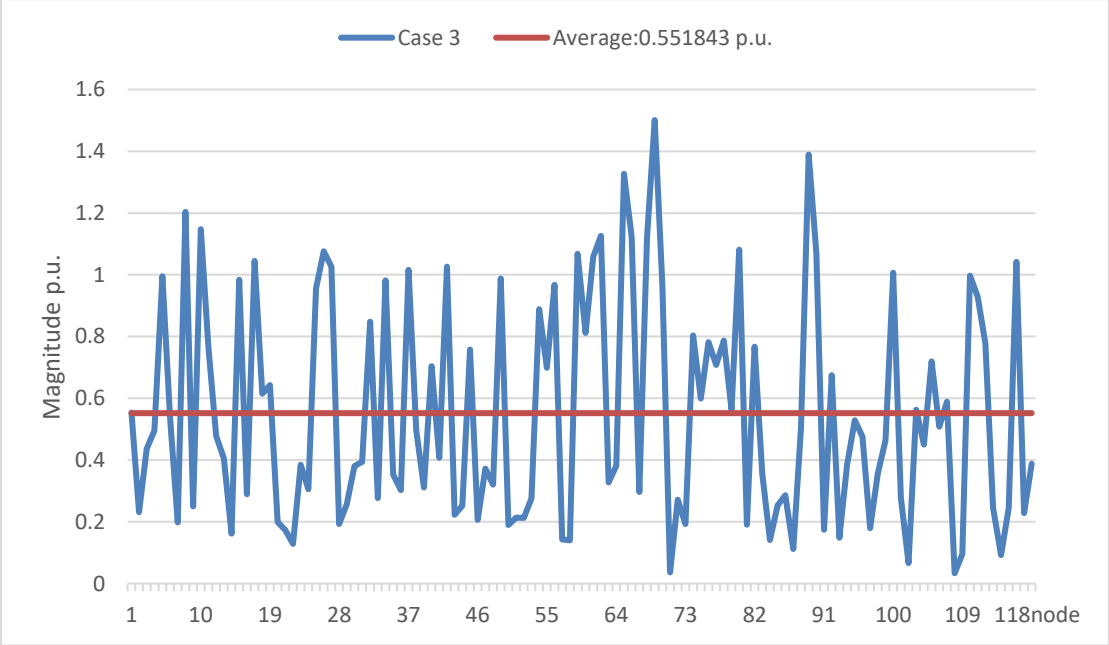

Figure 6-19 Current Magnitude Result for Case 3

According the Figure 6-17, the peak sample of Case 1 is at 69th node, reaching the value of 1.362301 *p.u*, and the minimum value of I_{rms} is 0.031628 *p.u* at 71th node. In addition, the average of I_{rms} is equal to 0.512496 *p.u* for Case 1. Compared to Case 1, the peak, minimum and the average values have all increased in Case 2. It can be seen from Figure 6-18, the peak value increases to 1.449776 *p.u* and is still located at 69th node.

The minimum value reaches 0.033202 *p.u* and occurs at 108th node. The average of current is equal to 0.535338 *p.u*. With respect to Case 3, the data which can be found in Figure 6-19, has further increased: maximum, minimum and average values raise to 1.501129*p.u*, 0.033245 *p.u* and 0.552412 *p.u* respectively. The comparison of three cases is summarised in Table 6-10, as illustrated below.

Table 6-10 Statistics Analysis for Three Scenarios of Current Magnitude

	Case 1	Case 2	Case 3
Average (*p.u*)	0.512496	0.535556	0.551843
Maximum (*p.u*)	1.362301	1.449776	1.501129
Minimum (*p.u*)	0.031628	0.033202	0.033245

Based on the rules defined in **Section 6.5.1**, the difference between Case 2 and Case 1 is shown in Figure 6-20, with the threshold of 0.1. In this figure, the unit for X-axis is per unit, while the Y-axis represents the 118 bus of power system. There are 13 nodes changed in total when the number and location of WTGs have increased: values of 10 nodes are positive while 3 nodes' values are negative. Of the positive values, 65th node reach the peak value of 0.348048, For the negatives, the most negative value is located at 62th node, with the value of minus 0.099474.

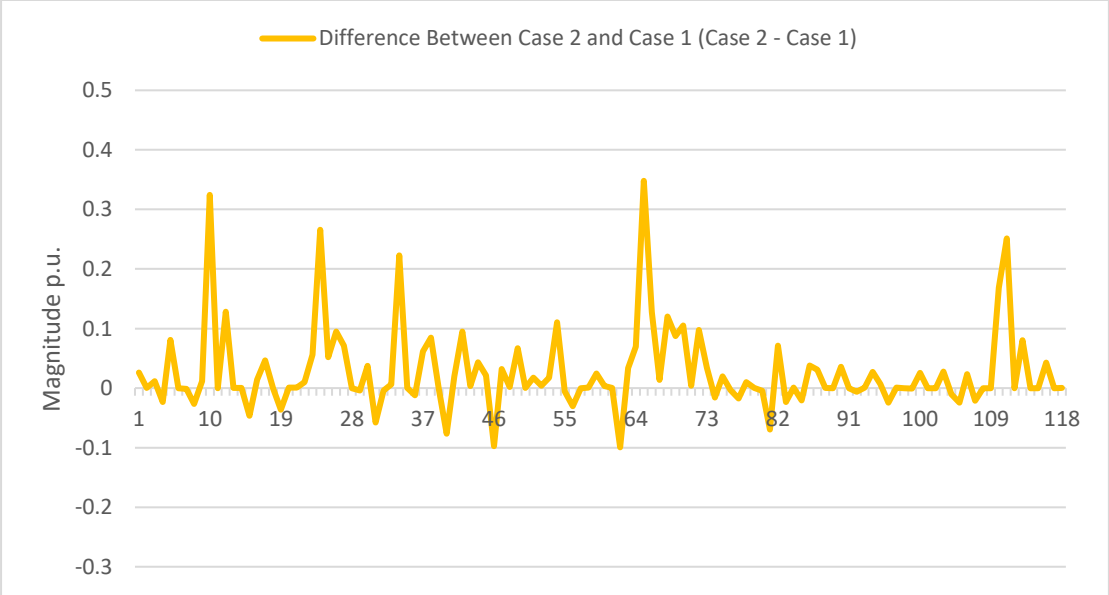

Figure 6-20 Result of Current Magnitude Comparison between Case 2 and Case 1

In addition, the difference of Case 3 and Case 2 is also analysed in this thesis, and the result is shown in Figure 6-21. Following the rules and strategy defined, there are 5 nodes changed in total: 4 nodes are positive and only 1 node is negative, with the threshold value of 0.1. According to Figure 6-21, the largest difference occurs at the 89th node, achieving the value of 0.414436, and the next largest one is located at 110th node. The negative value is equivalent to minus 0.062628 at 24th node. According to the comparisons of Cases 1-2 and Cases 2-3, it is seen that a number of values of RMS current have changed and the majority of values have increased, as the number and location of WTGs increased.

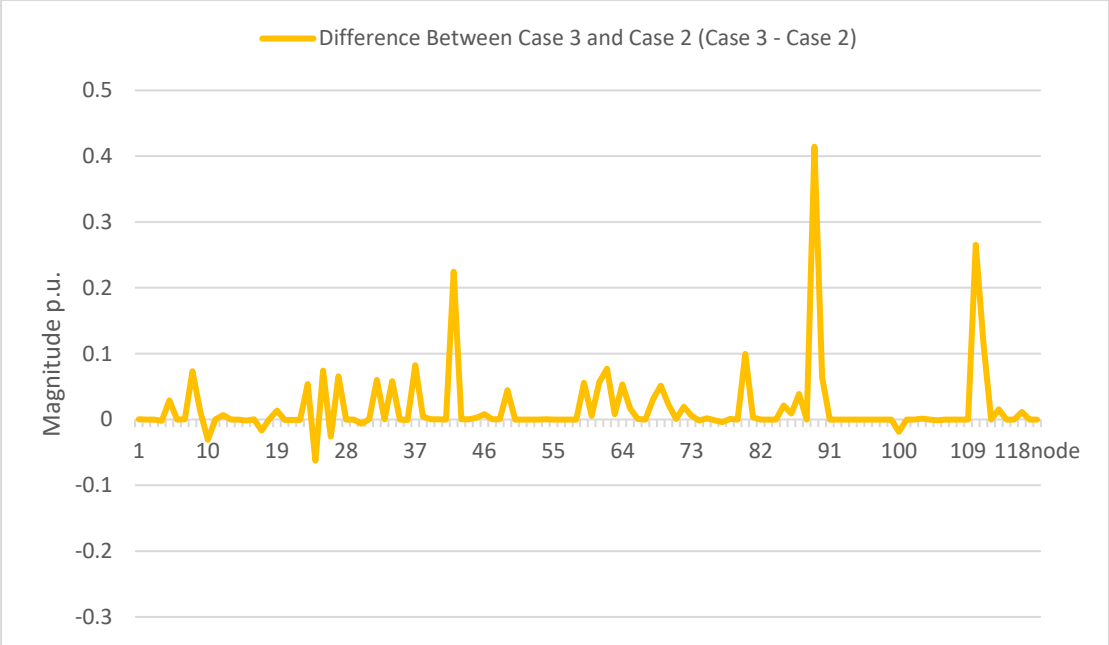

Figure 6-21 Result of Current Magnitude Comparison between Case 3 and Case 2

6.5.2.2 Voltage Magnitude

Based on the analysis previously, there are also three scenarios defined for analysing the voltage in terms of RMS for 118 nodes in total. Following the analysis method used, the proportion of WTGs' power capacity in entire power generations' capacity is 20% for Case 1. Case 2 and Case 3 occupy 30% and 40% respectively. The results of three cases are illustrated in Figure 6-22, Figure 6-23 and Figure 6-24 respectively. For these

three figures, the unit for X-axis is per unit, while Y-axis represents 118 bus of power system.

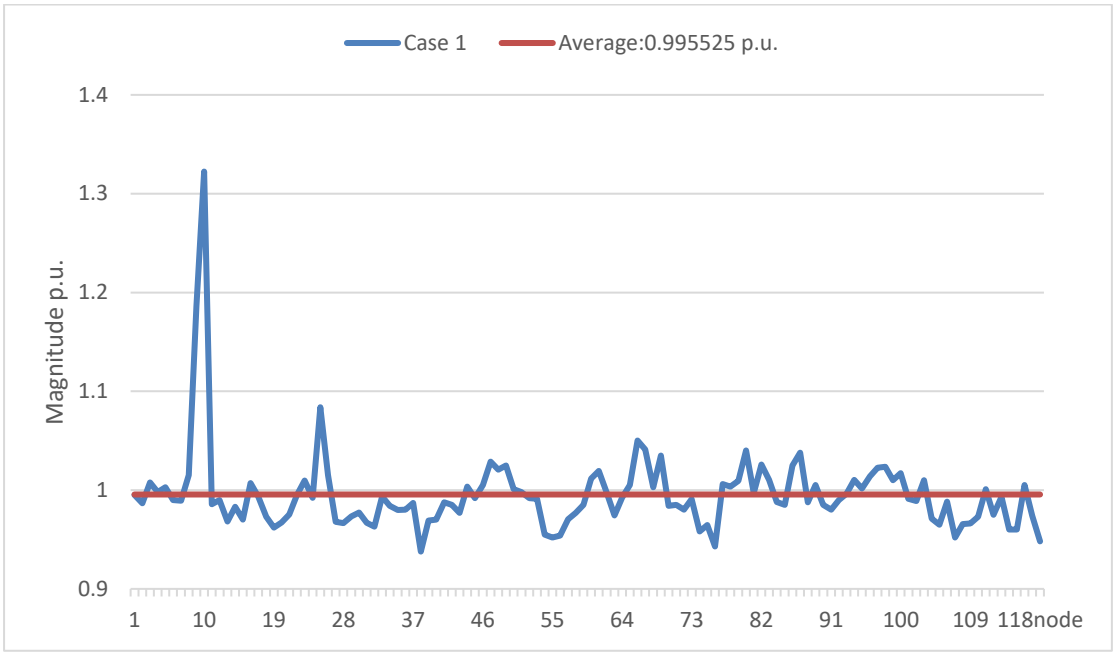

Figure 6-22 Voltage Magnitude Result for Case 1

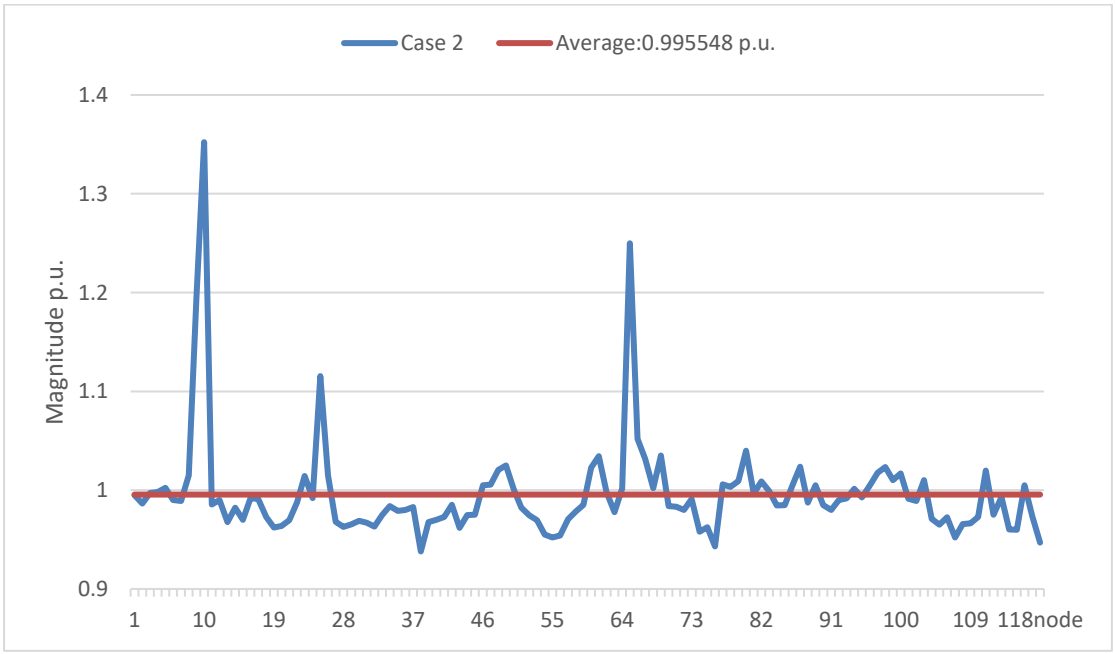

Figure 6-23 Voltage Magnitude Result for Case 2

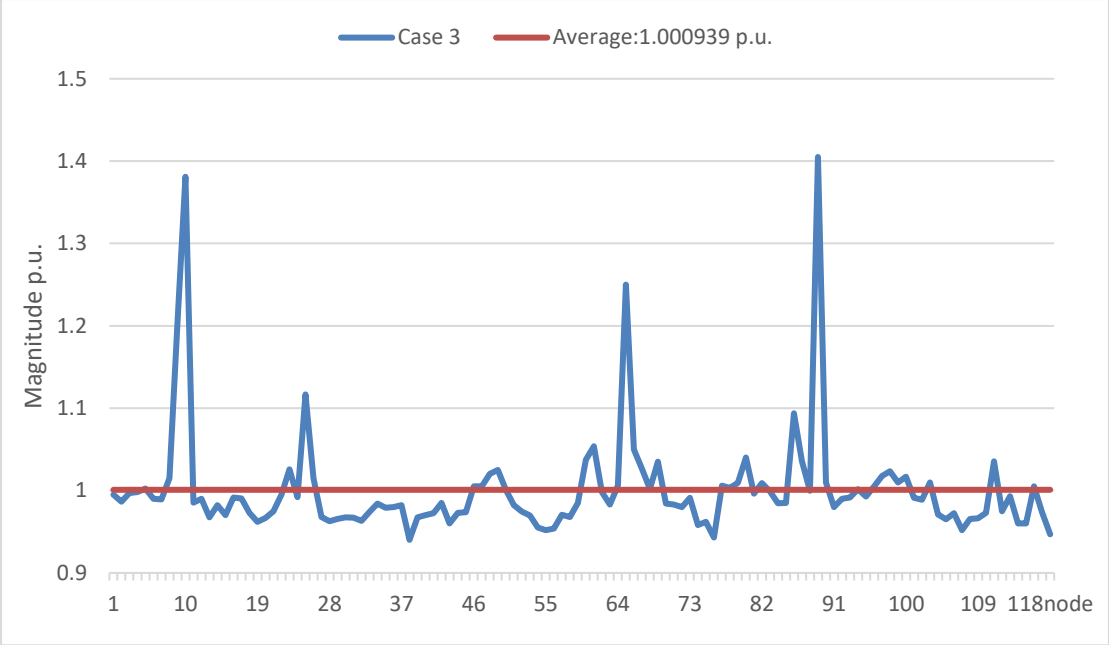

Figure 6-24 Voltage Magnitude Result for Case 3

According to Figure 6-22, the peak sample of Case 1 is at 10th node, reaching the value of 1.322385 *p.u*, and the minimum value is 0.937752 *p.u* at 38th node. In addition, the average is equal to 0.995525 *p.u*.. Compared to Case 1, the peak, minimum and the average values of Case 2 have all increased slightly. It can be seen in Figure 6-23 that the peak value of Case 2 increases to 1.352210 *p.u* and is still located at 10th node. The minimum value reaches 0.937975 *p.u* and occurs at 38th node. The average of current is equal to 0.995548 *p.u*. With respect to Case 2, these data obtained from Case 3 has further increased. According to Figure 6-24, the maximum, minimum and average values of Case 3 raise to 1.405001 *p.u*, 0.940156 *p.u* and 1.000939 *p.u* respectively. The location of the peak value changes to 89th node while the location of the minimum value remains the same. The comparison of three cases is summarised in Table 6-11, as illustrated below.

Table 6-11 Statistics Analysis for Three Scenarios of Voltage Magitude

	Case 1	Case 2	Case 3
Average (*p.u*)	0.995525	0.995548	1.000939
Maximum (*p.u*)	1.322385	1.352210	1.405001
Minimum (*p.u*)	0.937752	0.937975	0.940156

Based on the analysis defined before, the differences between Case 2 and Case 1 and Case 3 and Case 2 are further analysed and shown in Figure 6-25 and Figure 6-26 respectively. The unit for X-axis is per unit, while the Y-axis represents the 118 bus of power system. In this case, the threshold is defined as 0.01 *p.u.*

For the difference between Case 2 and Case 1 in Figure 6-25, there are 22 nodes changed in total when the power capacities of WTs have increased: values of 6 nodes are positive while 16 nodes' values are negative. Of the positive values, 65th node reaches the peak value of 0.245025. It might be relative to its fundamental and harmonic bus current magnitudes. For the negatives, the most negative value is located at 44th node, with the value of minus 0.028523.

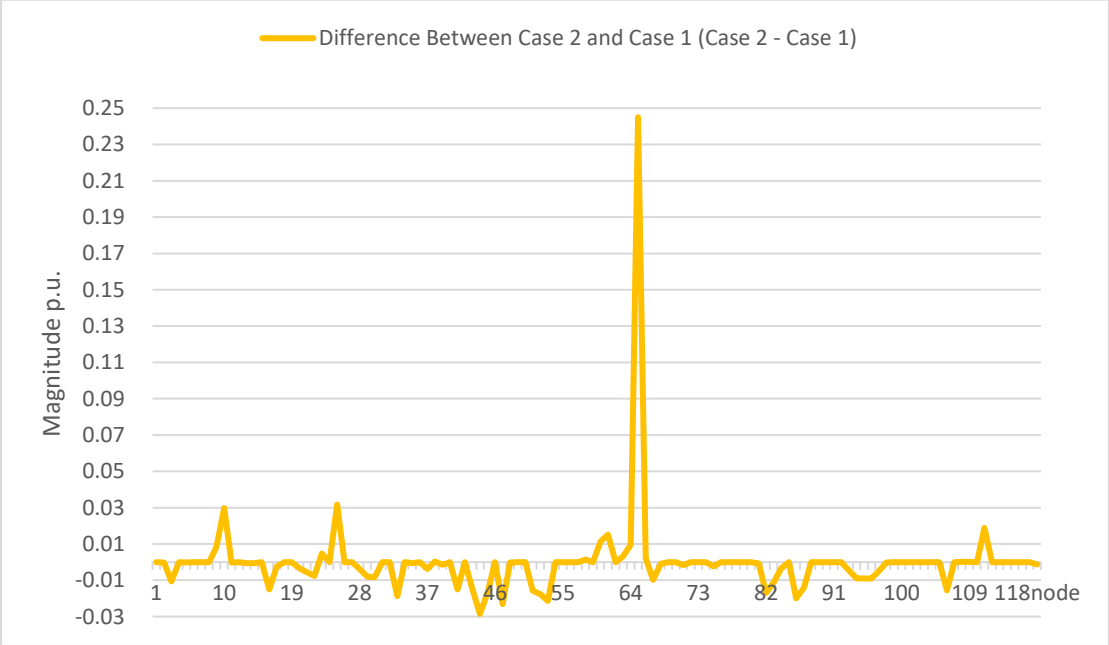

Figure 6-25 Result of Voltage Magnitude Comparison between Case 2 and Case 1

In addition, the difference of Case 3 and Case 2 is also analysed and the result is shown in Figure 6-26. Following the rules and strategy defined, there are 11 nodes changed in total: 10 nodes are positive and only 1 node is negative, with the threshold value of 0.01 *p.u.* According to Figure 6-26, the largest difference occurs at the 89th node, achieving the value of 0.400000. The negative value is equivalent to minus 0.010382 at 58th node.

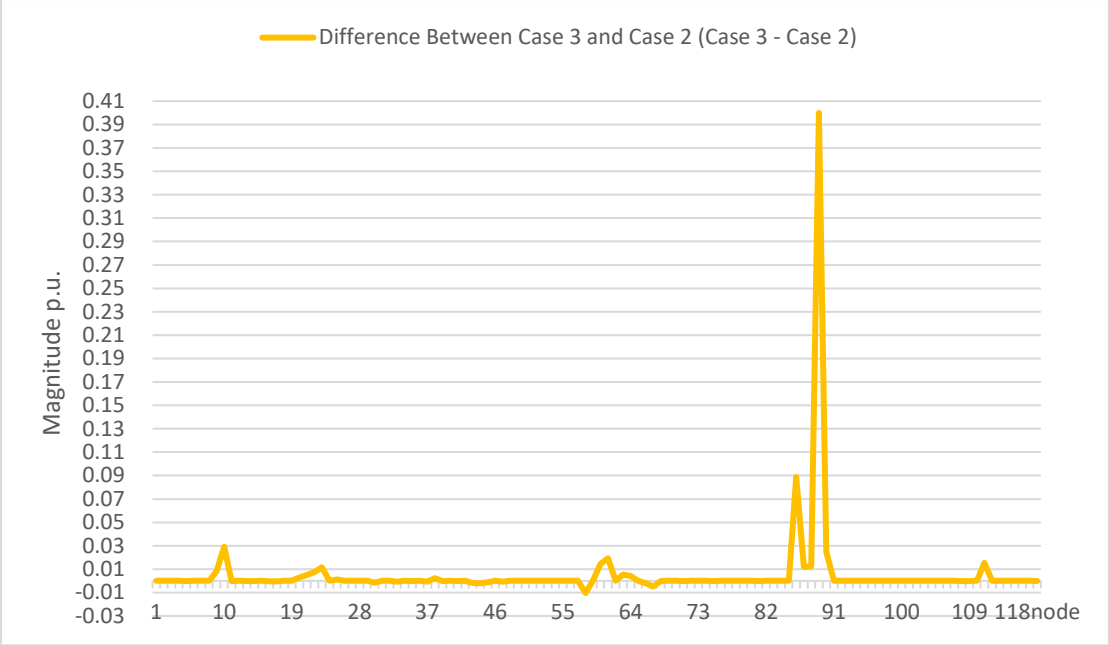

Figure 6-26 Result of Voltage Magnitude Comparison between Case 3 and Case 2

6.5.2.3 Total Voltage Harmonic Distortion (THDv)

Similarly, another set of data are used to analyse the impact on the power capacity in terms of THDv. Like all of scenarios defined, there are three cases, i.e. Case 1, Case 2 and Case 3, and the result of each case is shown in Figure 6-27, Figure 6-28 and Figure 6-29 respectively. For these three figures, the unit for X-axis is percentage, while the Y-axis represents the 118 bus of power system

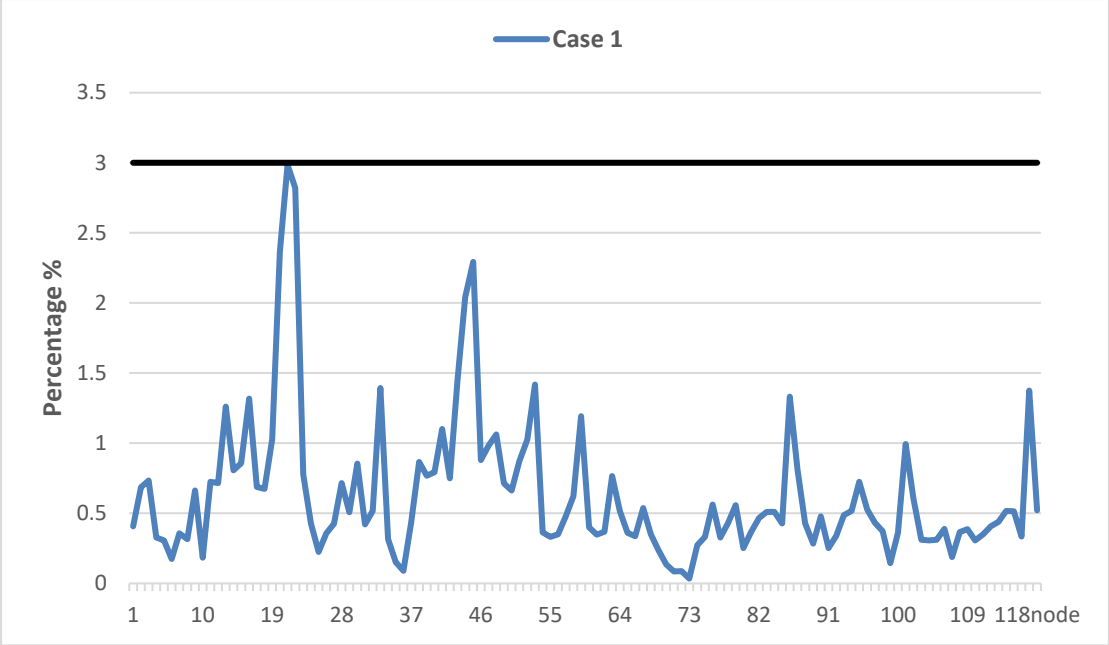

Figure 6-27 THDv Result for Case 1

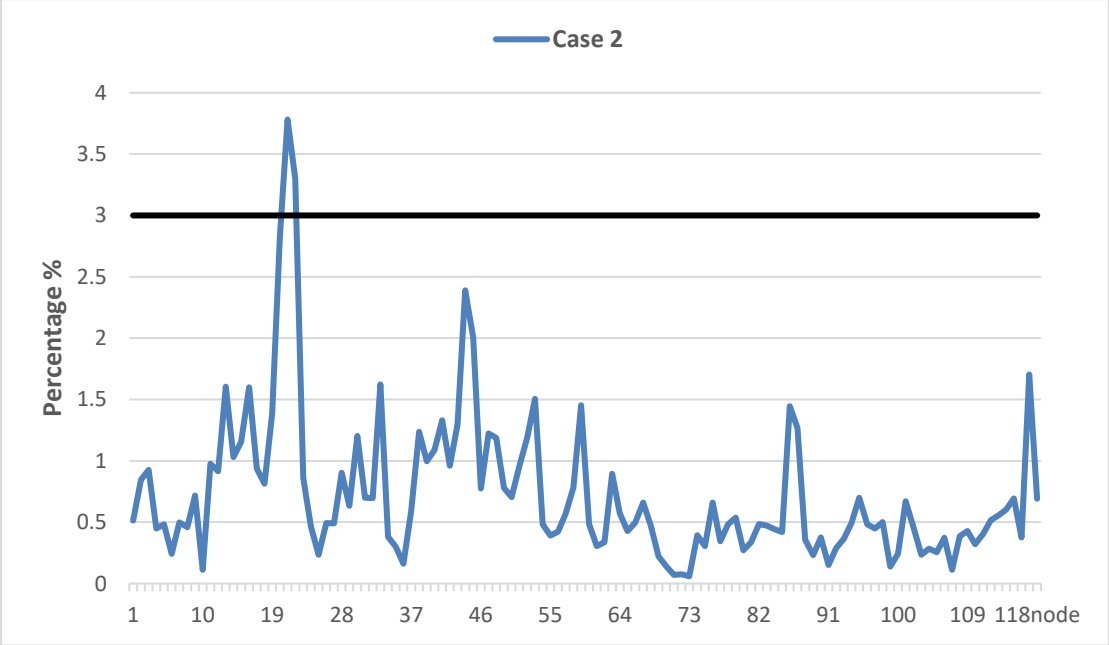

Figure 6-28 THDv Result for Case 2

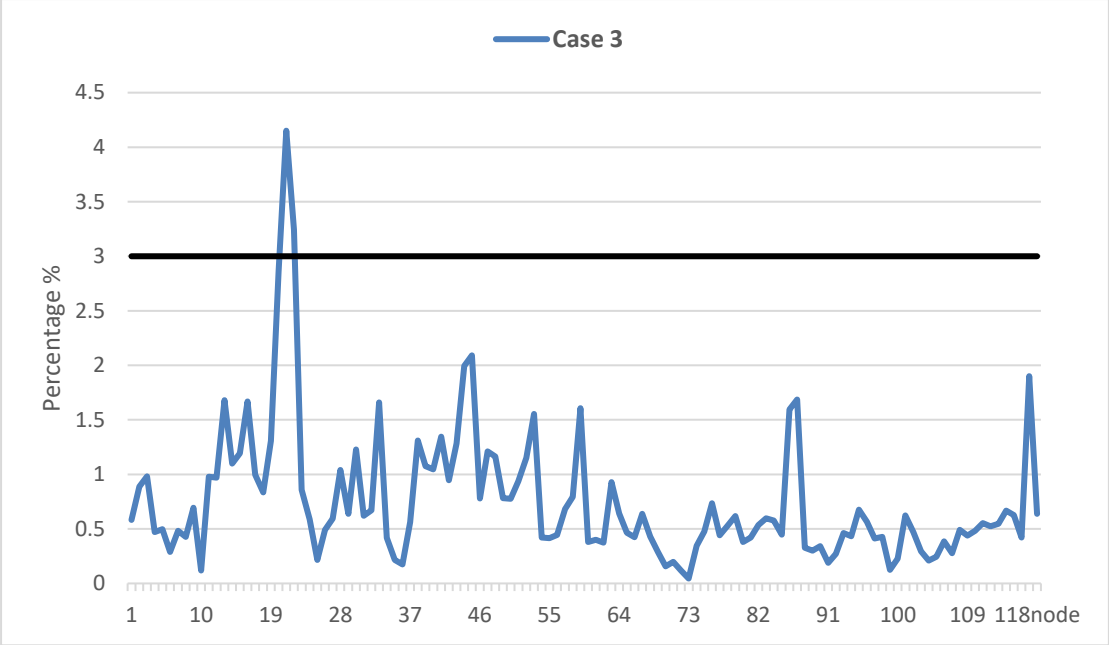

Figure 6-29 THDv Result for Case 3

Similarly, all the data can be divided into three groups according to the definition in **Section 6.5.2** to investigate the results, and thus the statistics of sample distribution and the results of Cases 1-3 are summariesd in Table 6-12 and Table 6-13 respectively.

Table 6-12 Sample Distribution for Different Cases with Various Ranges of THDv

Range of THDv(%)	Case 1	Case 2	Case 3
0-1.5%	113	108	105
1.5%-3%	5	8	11
>3%	0	2	2

Table 6-13 Maximum and Average Analysis of THDv for Different Cases

Scenarios	Case 1	Case 2	Case 3
Maximum (%)	2.985702	3.781557	4.151350
Average (%)	0.633508	0.728340	0.759595

According to Table 6-12, the majority of results are under the range of 0-1.5% with the number of 113 for Case 1. In addition, the number within the range between 1.5% and 3% is 25 and no sample is larger than 3%. The number of Case 2 within the range of 0-

1.5% drops to 108 while the numbers for the other two ranges increase. The figure within the range of 1.5%-3% is 8 and there are 2 samples over 3%. Furthermore, the number of Case 3 samples located within 1.5%-3% continues increasing to 11 from 8 for Case 2. The number of under 1.5% continues to decrease to 105 while the number for over 3% remains the same.

Based on the results of Table 6-13, the maximum and average values for Case 1 are 2.985702 at 21st node and 0.633508 respectively. For Case 2, both values continue to raise, and reach 3.781557 and 0.728340 respectively. The location of peak sample is still at 21st. The maximum value of Case 3 rises to 4.151350 at the same location, while the average continues to increase to the value of 0.759595. Considering the comparisons of three cases, both maximum and average values of THDv increase gradually and the number of values larger than the limit level defined also increase as the number of wind power generator raises.

6.5.3 Result and Analysis

In this chapter, the proposed method was applied to a 118-bus power system connecting with multiple types of harmonic sources to analyse the harmonic penetration. The WTGs is regarded as renewable generator. Two tests are designed to investigate the effects on the harmonic penetration with increasing of renewable power generations in power networks. One is used to increase the capacity of WTGs; the other is to increase the number and loacation of WTGs. For each test, the result is analysed in terms of RMS current magnitude, RMS voltage magnitude, and THDv, and the results of both tests are further compared and analysed in sections below

6.5.3.1 Current Magnitude

As described before, two methods are used to analyse the results: Test 1 is aimed at increasing the power capacity of WTGs while Test 2 is to use more numbers of WTGs. In both two tests, three scenarios are defined according to the percentage on power capacity of WTGs to the total power generation capacity: ratios of 20%, 30% and 40%

are defined for Case1, Case 2 and Case 3 respectively. The waveforms of RMS value for the current magnitude are almost the same, as described in Figure 6-4, Figure 6-5, Figure 6-6, Figure 6-17, Figure 6-18 and Figure 6-19, according to two scenarios for each test case. It is difficult to find out the difference only from the result diagrams. In order to catch the difference between these two tests, the further numerical comparisons are required.

In both two tests, the differences between Cases 1-2, and Cases 2-3 are compared respectively. A threshold for the difference between two cases is defined as 0.1. If any absolute values of the result are within the defined threshold, it indicates the magnitudes of the same nodes for two cases are viewed as equal. The differences are summarised in Table 6-14. In Table 6-14 the total changed number of nodes, including number of increased and number of decreased, max different location and its value are listed.

Table 6-14 Summary of Current Magnitude in terms of RMS between Cases

	Combination	Total No. Changed	No. of Increased	No. of Decreased	Max. Diff. Loc.	Max. Diff.
Test 1	Cases 1-2	12	9	3	10	0.324696
	Cases 2-3	5	4	1	111	0.316229
Test 2	Cases 1-2	13	10	3	65	0.348048
	Cases 2-3	5	4	1	89	0.414436

As is evident in Table 6-14, for two tests, the result of the values of total, increasing and decreasing numbers are almost the same. For Cases 1-2 with two different methods, the values of total, increasing and decreasing numbers are identical. With respect to Cases 2-3, there are slight changes on values of total number and increasing number for Test 1 and Test 2 while the value of decreasing number remains the same. However, the max different locations of two tests are not the same. For Cases 1-2, in Test 1, the max different location is at 10^{th} node with value of 0.324696, while in Test 2,, the max different location is at 65^{th} node with value of 0.348048. The reason for the different is the capacity of WTG increased at 10^{th} node in Test 1, while a new WTG added in Test 2's Case 2, and the location is at 65^{th} node. The same situation for Cases 2-3, two Tests'

different location is not the same, because of a new WTG added at 89th node in Test 2's Case 3

.

Table 6-15 Summary of Current Magnitude in terms of RMS for Each Case

		Ave. (*p.u*)	Max. (*p.u*)	Max. Loc.	Min. (*p.u*)	Min. Loc.
Test 1	Case 1	0.512496	1.362301	69	0.031628	71
	Case 2	0.534811	1.447611	69	0.033202	108
	Case 3	0.552412	1.491129	69	0.033245	108
Test 2	Case 1	0.512496	1.362301	69	0.031628	71
	Case 2	0.535556	1.449776	69	0.033202	108
	Case 3	0.551843	1.501129	69	0.033245	108

Table 6-15 list the maximum, minimum and average values for each case with two different methods. There are no changes on minimum values, slight changes on average values and be specific of changes on maximum values. Therefore, it can be seen from Table 6-14 and Table 6-15 that the two methods of increasing renewable power generation have the slight different effects on power system.

6.5.3.2 Voltage Magnitude

Similar to current magnitude, the waveforms of RMS value for the voltage magnitude are almost the same, as described in Figure 6-9, Figure 6-10, Figure 6-11, Figure 6-22, Figure 6-23 and Figure 6-24, according to two scenarios for each test case. In order to catch the difference between these two tests, the further numerical comparisons are required.

In both two tests, the differences between Cases 1-2, and Cases 2-3 are compared respectively. A threshold for the difference between two cases is defined as 0.1. If any absolute values of the result are within the defined threshold, it indicates the magnitudes of the same nodes for two cases are being viewed as equal. The differences are summarised in Table 6-16.

Table 6-16 Summary of Voltage Magnitude in terms of RMS between Cases

	Combination	Total No. Changed	No. of Increased	No. of Decreased	Max. Diff. Loc.	Max. Diff.
Test 1	Cases 1-2	27	11	16	10	0.129825
	Cases 2-3	12	5	7	10	0.145912
Test 2	Cases 1-2	22	6	16	65	0.245025
	Cases 2-3	11	10	1	89	0.400000

As is evident in Table 6-16, for two tests, the result of the values of total, increasing and decreasing numbers have some different. The max different locations of two tests are not the same. For Cases 1-2, in Test 1, the max different location is at 10^{h} node with value of 0.129825, while in Test 2, the max different location is at 65^{th} node with value of 0.245025. The reason for the different is a new WTG added in Test 2's Case 2, and the location is at 65^{th} node. The same situation for Cases 2-3, two Tests' different location is not the same, because of a new WTG added at 89^{th} node in Test 2's Case 3.

Table 6-17 Summary of Voltage Magnitude in terms of RMS for Each Case

		Ave. (*p.u*)	Max. (*p.u*)	Max. Loc.	Min. (*p.u*)	Min. Loc.
Test 1	Case 1	0.995525	1.322385	10	0.937752	38
	Case 2	0.996234	1.452210	10	0.938752	38
	Case 3	0.997707	1.598122	10	0.940155	38
Test 2	Case 1	0.995525	1.322385	10	0.937752	38
	Case 2	0.995548	1.352210	10	0.937975	38
	Case 3	1.000939	1.405001	89	0.940156	38

list the maximum, minimum and average values for each case with two different methods. There are slight changes on minimum values and average values and a little bit of changes on maximum values. Therefore, it can be seen from Table 6-16 and Table 6-17 that the two methods of increasing renewable power generation have the slight different effects on power system.

6.5.3.3 THDv

Similarly, the numerical comparisons of THDv are also used to investigate the difference between two tests. The THDv values in each different case were categorized into three penetration levels. They were ranges of 0-1.5%, 1.5%-3%, and over 3%.Therefore, the total numbers of THDv values in each penetration level in two tests is summarized in Table 6-18 below.

Table 6-18 Summary of Numbers of THDv Values

	Scenarios	0-1.5%	1.5%-3%	>3%
Test 1	Case1	113	5	0
	Case2	108	8	2
	Case3	105	11	2
Test 2	Case1	113	5	0
	Case2	108	8	2
	Case3	105	11	2

It is clear seen from Table 6-18 that the numbers of bus distribution for three ranges defined with two different methods of Test 1 and Test 2 are identical. Therefore, according to the results, it is safe to say that two methods proposed have almost the same effects on power system.

6.6 Conclusion

In this chapter, a 100MV，33KV，118 bus power system is employed to do the simulation. A method named FHM is proposed to calculate the harmonic power flow. The WTGs, arc-furnaces and convertors will be connecter to the power system as harmonic sources. In order to investigate the effects to the harmonic penetration with increasing of renewable power generations in power networks, two tests are designed: Test 1 is designed to replace larger capacity's WTGs with fixed location and number of WTGs; Test 2 is employed to increase of the number and location of WTGs with fixed power capacity of each WTG. In both of these two tests, the total renewable power generations raise from 20% to 40% respectively. A large number of results and discussions for these two tests are presented through these two aspects: RMS value and value of THD. It is demonstrated that, for Test 1, a part of values of RMS current and voltage have changed and the maximum and average values have increase. In addition, both maximum and average values of THDv raise, and the number over limit level defined also increases, considering the increase of capacity from 20%-30% and 30%-40%. With regard to Test 2, as total renewable power generations raises form 20%-40%, it is clearly seen that both maximum and average values increase gradually, and the number over the defined limit also increases. Taking all of these factors into consider, the changes of analysed RMS and THD values with the proposed two methods remain slight different. Therefore, according to the results, it is safe to say that the two methods proposed have almost the same effects on power system.

Chapter 7 Conclusion and Further Work

7.1 Conclusion

Global warning concern and continuous rising cost of raw industrial materials for electricity generation are becoming more and more obvious with the development of current society. Electricity generation with renewable source is a wise idea to solve such concerns, and thus has been widely and actively researched and developed all over the world in recent years. Nowadays, a larger number of renewable energy generator, more highly sensitive electronic equipment and more electronics or microprocessor controllers have already been used in power system. These have to bring in new challenges to current supply quality. In order to study and analyse the impact of these renewable device in the overall power system, concept of PQ has become increasingly important. Harmonic analysis plays an important role in PQ study because harmonic have great influence on the power system equipment as well as on their operation. Harmonics can lead to operation failure of electrical and electronic components, overheating of neutral wires and transformer, failure of power factor correction capacitors, loss in power generation and transmission, and interference with protection, control and communication networks as well as customer loads. Therefore, developing an advanced PQ disturbances classification system and a more accurate harmonic analysis method is the key of this thesis.

Determining the source and cause PQ disturbances plays one of the most important roles to solve PQ related problems. PQ engineers can define the major effects at the load and analyse the source of such disturbances based on accuracy classification of disturbance type. Many approach based on FT and neural network for the classification of PQ disturbance have been developed in the last few years The key factor of these methods is that the correct rate for the actual event is not high enough and thus there is still space to improve accuracy. Compared with FT, the most important advantage of

the WT is that it has the ability to analyse signal in both time and frequency domains. In addition, the WT also has the ability to be adjusted automatically for low or high frequencies because it uses short windows at high frequencies and long windows at low frequencies, thus leading to an optimal time-frequency resolution in all the frequency ranges. As a result, the WT can be applied to analyse the power disturbance signals. Compared to neural network, fuzzy-expert system has some obvious advantages: fuzzy rules are more comprehensible than neural network. Besides, fuzzy-expert system requires less time for training than neural network. Thirdly, fuzzy-expert system is quite flexible, which implies that input, output and fuzzy rules in rule set can be changed conveniently if necessary. Taking into account all of these considerations, a fuzzy-expert system with WT decomposition has been proposed to classify PQ disturbances. In order to ensure all disturbance features in both high and low frequency are extracted, a12-level DWT filter bank is used in this thesis. In order to illustrate the usefulness of the proposed fuzzy-expert system, a number of simulations have been made by using the MATLAB/Simulink to generate pure sine wave signal and five sample distorted signals. These distorted signals involve voltage sag/swell, momentary interruption, harmonic distortion, and flicker. The frequency is 50Hz; amplitude is 1p.u. The energy distribution patterns after performing the WT are used to set the parameters of input membership. Six If-Then rules have been generated for classifying PQ disturbances. Once the fuzzy-expert system is designed, ten new distorted voltage waveforms are randomly generated with different time of occurrence, duration and amplitude to test the accuracy of PQ classification with the proposed fuzzy-expert system. The result demonstrates that the proposed fuzzy-expert system with WT decomposition method has classified correctly 58 disturbances of the total number of 60 tested disturbances, thus having a classification accuracy of 98.3%. These tests show that the proposed methods for feature extraction and designed fuzzy-expert system are efficient for PQ disturbance classification. Therefore, the proposed fuzzy-expert system can be considered to be sufficiently accurate in classifying PQ disturbances.

Developing a new approach for the evaluation of harmonic contents of power system waveforms is the second objective of thesis. The conventional harmonic analysis method is Fourier analysis. However, Fourier analysis provides signals which are mainly localised in the frequency domain and it gives limited information of the signals

in the time domain. Furthermore, the FT cannot obtain accurate values of amplitude and phases from harmonics with frequencies different from that of the window function frequency. . In order to overcome the limitations of Fourier analysis and obtain better results, wavelet analysis has been proposed. A novel harmonic analysis method using DWPT filter bank decomposition and CWT identification has been proposed. In order to evaluate the performance and result of the proposed analysis method, another two conventional methods, i.e. FFT and the combination method of DWT filter bank and CWT calculation, are compared through a large number of identical applications. These application designs contain a variety of signals, such as time-invariant, non-stationary and field-test signals, and harmonics, such as integer, sub and non-integer harmonic contents. Based on the results obtained, it is seen that the proposed analysis can achieve the highest correct rate in terms of quantifying harmonic frequencies, amplitudes and phases, compared to other methods. For the results of the amplitude, the methods using WT provides much better results than FFT method, and between two WT methods, the result of the method using DWPT filter bank is more close to the real value, especially in high frequency area. Therefore, the proposed approach is very advantageous in terms of analysing harmonics in power system waveform and has the potential in practice for a more accuracy analysis.

Based on the harmonic analysis, the harmonic penetration is also considered and its effects to power networks are investigated. Due to usage of renewable power generations and modern electric devices, the power system contains several types of harmonic sources with a large frequency range, such as integer-harmonics, inter-harmonics and sub-harmonics. Therefore, the steady state harmonic power flow in power system with discrete frequencies is calculated to investigate the effects to the harmonic penetration with multiple types of harmonic sources in power networks. A 100MV，33KV，118 bus power system is employed to do the simulation. A method named FHM is proposed to calculate the harmonic power flow. The WTG, arc-furnace and convertors will be connected to the power system as harmonic sources. In order to investigate the effects to the harmonic penetration with increasing of renewable power generations in power networks, two tests are designed: Test 1 is designed to replace larger capacity's WTGs with fixed location and number of WTGs; Test 2 is employed to increase of the number and location of WTGs with fixed power capacity of each

WTG. In both of these two tests, the total renewable power generations raise from 20% to 40% respectively. A large number of results and discussions for these two tests are presented through these two aspects: RMS value and value of THD. It is demonstrated that, for Test 1, a part of values of RMS current and voltage have changed and the maximum and average values have increase. In addition, both maximum and average values of THDv raise, and the number over limit level defined also increases, considering the increase of capacity from 20%-30% and 30%-40%. With regard to Test 2, as total renewable power generations raises form 20%-40%, it is clearly seen that both maximum and average values increase gradually, and the number over the defined limit also increases. Taking all of these factors into consider, the changes of analysed RMS and THD values with the proposed two methods remain slight different. Therefore, it might be safe to say that the two methods proposed have almost the same effects on power system.

.

7.2 Further work

This thesis contributes to develop a fuzzy-expert system based on wavelet transforms to classify power supply waveforms into different groups or categories for power quality classification; develop a wavelet transform approach for the evaluation of harmonic contents of power system waveforms and evaluate the harmonic penetration to investigate the effects to power networks with increasing of renewable power generations. Though these proposed methods are analysed in detail and proofed by a variety of simulation, it still has several possible developments in the future. They are presented in the following aspects:

- In Chapter 4, the proposed fuzzy-expert system has classified correctly 58 disturbances of the total number of 60 tested disturbances, thus having a classification accuracy of 96.7%. These tests show that the proposed methods for feature extraction and deigned fuzzy-expert system are efficient for PQ disturbance classification. However, only six types of waveform are classified. In order to classify new type of PQ disturbance, new rule base will need to be developed based on the feature extraction curve of the new disturbances.

- Because the harmonic distortion limit in Engineering Recommendation G5/4 is generally based on the harmonic voltage, the results of the total harmonic voltage distortion THDv are mainly concerned in the study. However, it usually uses equipment to measure the harmonic current at each bus to analyse the harmonic penetration in industry. The total harmonic current distortion (THD_i) will be evaluated and analysed in the future.

- Harmonic penetration evaluation in power networks plays an important role in electricity market. The industries try to reduce the electricity price achieved by renewable generations in order to motivate more people to use green energy. However, the more renewable energy is generated, the more harmonics it produces. Hence, the result of harmonic penetration evaluation is very important for investigating the effects of increasing use of renewable energy to electricity pricing. More simulations should be done in this area.

Reference

[1] Ewald F. Fuchs and Mohammad A.S Masoum, "*Power Quality in Power Systems and Electrical machines*", Academic Press, pp 1-29, London, 2006.

[2] H. Siahkali, "*Power quality indexes for continue and discrete disturbances in a distribution area*," in Power and Energy Conference, 2008. PECon 20 08. IEEE 2nd International, 2008, pp. 678–683. 1

[3] IEEE Standard 1159-2009, *IEEE Recommended Practice for Monitoring Electric Power Quality*, June, 2009

[4] Roger C. Dugan, Mark F. McGranaghan, Surya Santoso, H. Waune Beaty; " *Electrical Power System Quality*", Second edition, November 2002.

[5] John Stones and Alan Collinson, "*Power Quality*", IEEE Power Engineering Journal, Vol. 15, pp. 58-64, 2001- helitavia.com

[6] IEC Std 61000, 1990. Electromagnetic compatibility (EMC).

[7] Jaehak Chung, Edward J. Powers, W. Mack Grady and Siddharth C. Bhatt, "*Power disturbance classifier using a rule-based method and wavelet packet-based hidden Markov model*," IEEE Transaction on Power Delivery, Vol. 17, No. 1, Jan 2002, pp. 233-241.

[8] Zwe-lee Gaing, "*Wavelet-based neural network for power disturbance recognition and classification*," IEEE Transaction on Power Delivery, Vol.19, No.4, Oct.2004, pp. 1560-1568.

[9] Surya Santoso, Edward J. Power, W. Mack Grady, and Antony C. Parsons, "*Power quality disturbance waveform recognition using wavelet –based neural classifier – Part 1: theoretical foundation*," IEEE Transaction on Power Delivery, Vol. 15, No. 1, Jan 2000, pp.222-228.

[10] Surya Santoso, Edward J. Power, W. Mack Grady, and Antony C. Parsons, "*Power quality disturbance waveform recognition using wavelet –based neural classifier – Part 2: application*," IEEE Transaction on Power Delivery, Vol. 15, No. 1, Jan 2000, pp. 229-235.

[11] A.M. Gaouda, S.H. Kanoun, M.M.A. Salama, and A.Y. Chikhani, "*Pattern recognition application for power system disturbance classification*," IEEE Transaction on Power Delivery, Vol. 17, No.3, July 2002, pp. 677-683.

[12] Jiansheng Huang, Michael Negnevitsky, and D. Thong Nguyen, "*A neural-fuzzy classifier for recognition of power quality disturbances*," IEEE Transaction on Power Delivery, Vol. 17, No. 2, April 2002, pp. 609-616.

[13] T.X.Zhu, S.K.Tso and K.L.Lo, "*Wavelet-based fuzzy reasoning approach to power-quality disturbance recognition*," IEEE Transaction on Power Delivery, Vol. 19, No. 4, Oct 2004, pp. 1928-1935.

[14] Ying-hui kong, Jin-sha yuan, Jing an, Lin-lin che, "*Online power quality disturbances detection and classification using one-pass wavelet decomposition and decision tree*," In Proceedings of International Conference on Machine Learning and Cybernetics, Hong Kong, China, Aug 2007, Vol. 5, pp. 2990-2995.

[15] P.K. Dash, S.Mishra, M.M.A Salama, and A.C. Liew, "*Classification of power system disturbances using a fuzzy expert system and a Fourier linear combiner*," IEEE Transaction on Power Delivery, Vol. 15, No.2, April 2000, pp. 472-477.

[16] Min Wang, Mamishev.A.V, "*Classification of power quality events using optimal time-frequency representations-Part 1: Theory*," IEEE Transaction On Power Delivery, Vol. 19, No. 3, July 2004, pp. 1488-1495.

[17] Min Wang, Rowe.G.I, Mamishev.A.V, "*Classification of power quality events using optimal time-frequency representations-Part 2: Application*," IEEE Transaction On Power Delivery, Vol. 19, No. 3, July 2004, pp. 1496-1503.

[18] European Wind Energy Association, "*Wind in power, 2016 European Statist ics*," [Online]，European Wind Energy Association，February 2017，Availab le at:https://windeurope.org/wp-content/uploads/files/about-wind/statistics/WindEurope-Annual-Statistics-2016.pdf

[19] European Wind Energy Technology Platform, "*Strategic research agenda/ m arket deployment strategy (sra/mds)*," [Online], European Wind Energy Ass ociation, March 2014. Available at:https://www.nachhaltigwirtschaften.at/resources/iea_pdf/reports/iea_wind_strategic_research_agenda_2014.pdf

[20] European Wind Energy Association, *2030: the next steps for EU climate a nd energy policy*, [Online], European Wind Energy Association, September

2013. Available at:http://www.ewea.org/fileadmin/files/library/publications/reports/2030.pdf

[21] Fourier, J.B.J., *Theorie analytique de la chaleur*, Paris 1822.

[22] Arrillage J, Brandley D.A, Bodgoer P.S, *Power System Harmonics Second Edition*, John Woley & Sons 2003.

[23] G.D. Bergland, *A guided tour of the fast Fourier transform*, in Digital Signal Processing, L.R. Rabiner and C.M. Raader, Eds. New York: IEEE Press, 1972, pp. 228-239.

[24] Sheng Z F, Xing G Z, Wei Y, "*The algorithm of interpolation windowed FFT for harmonic analysis of electric power system*," IEEE Transactions on Power Delivery, Vo1.16, Issue 2, April 2001, pp.160-164.

[25] Andria C, Savino M, "*Windows and interpolation algorithms to improve electrical measurement accuracy*", IEEE Transactions on Instrumentation and Measurement, Vol. 38, Issue 4, August 1989, pp.856-863.

[26] D. Xia and G. T. Heydt, "*Harmonic power flow studies part i-formulatio n and solution*," Power Apparatus and Systems, IEEE Transactions on, no. 6, pp. 1257-1265, 1982. 6.

[27] Math H. Bollen, "*Understanding Power Quality Problems: Voltage Sags and Interruptions*", Wiley-IEEE Press; 1 edition (September 24, 1999) pp 6-19.

[28] C.H.Hilger, 1972. "*What is the quality of electric power?* " Elektroteknikeren, 68 (19), 418-22.

[29] P.Meynaud, 1983. "*The quality of the voltage in the supply of electrical energy*".2nd National Colloquium and Exposition on Electromagnetic Compatibility, 1-3 June 1983, Tregastel, France, CNET.

[30] Heydt. G.T, Arizona State University, AZ; "*Electric power quality: a tutorial introduction*", P.D, pp 15-19, Jan 1998

[31] Angelo Baggini , "*Handbook of Power Quality*", Wiley. Blackwell, April 2008. pp 9-30.

[32] F.Martzloff, "*Power quality work at the International Electrotechnical Commission*," PQA97 Europe, June 1997, Stockholm, Sweden, Elforsk: Stockholm, Sweden

[33] IEEE Std 100-1992, *IEEE Standard Dictionary of Electrical and Electronic Terms*.

[34] EN 50160, *Voltage characteristics of electricity supplied by public distribution systems,* 1999

[35] IEEE Std 1250, 1995. *Guide for service to equipment sensitive to momentary voltage disturbances*.

[36] ANSI C84.1-2006, Revision of ANSI C84.1-1995 (R2001, R2005), American National Standard For Electric Power Systems and Equipment—Voltage Ratings (60 Hertz)

[37] Arrillaga, J., Watson, N. R. and Chen, S., "*Power System Quality Assessment*", John Wiley&Sons, 2000.

[38] UIE-DWG-3-92-G, UIE *Guide to Quality of Electrical Supply for Industrial Installations—Part 1: General Introduction to Electromagnetic Compatibility (EMC),* Types of Disturbances and Relevant Standards, 1994.

[39] A.J. Skorcz, "*Performance evaluation of an active filter non-regenerative AC drive*", a master thesis submitted to the Office of Graduate Studies of Texas A&M University, Dec. 2007

[40] J.Duncan Glover and Mulukutla S.Sarma, "*Power System Analysis and Design*", Thomson Learning, Third edition, Dec. 2001, pp 356-362.

[41] G. K. Singh, "*Power system harmonics research: a survey,*" European Transactionson Electrical Power, vol. 19, pp. 151–172, 2009. vi, 15, 16, 21, 28, 40

[42] W. M. Grady and S. Santoso, "*Understanding power system harmonics*," IEEE Power Engineering Review, vol. 21, no. 11, pp. 8–11, 2001. 15

[43] Surya Santoso, Edward J. Powers and W. Mack Grady, "*Power Quality Assessment via Wavelet Transform Analysis*", IEEE Transactions on Power Delivery, Vol.11, No.2, pp 924-930, April 1996.

[44] J. Li, N. Samaan, and S. Williams, "*Modeling of large wind farm systems for dynamic and harmonics analysis*," in Transmission and Distribution Conference and Exposition, 2008. T&D. IEEE/PES. IEEE, 2008, pp. 1–7. 28, 29, 30

[45] Z. Chen, J. M. Guerrero, and F. Blaabjerg, "*A review of the state of the art of power electronics for wind turbines*," Power Electronics, IEEE Transactions on, vol. 24, no. 8, pp. 1859–1875, 2009. 29

[46] E. Muljadi and A. Ellis, "*Final project report wecc wind generator development*," 2010, last date of access 20.05.2013. [Online]. Available: http://uc-ciee.org/downloads/WGM Final Report Appendix6.pdf 29

[47] H. Abniki, S. Nateghi, R. Ghandehari, and M. N. Razavi, "*Harmonic analyzing of wind farm based on harmonic modeling of power system components*," in Environment and Electrical Engineering (EEEIC), 2012 11th International Conference on. IEEE, 2012, pp. 667–672. 29

[48] R. King and J. Ekanayake, "*Harmonic modelling of offshore wind farms*," in Power and Energy Society General Meeting, 2010 IEEE, 2010, pp. 1–6. 29

[49] L. H. Kocewiak, J. Hjerrild, and C. L. Bak, "*The impact of harmonics calculation methods on power quality assessment in wind farms*," in Harmonics and Quality of Power (ICHQP), 2010 14th International Conference on. IEEE, 2010, pp. 1–9. 29, 30

[50] J. Plotkin, R. Hanitsch, and U. Schaefer, "*Power conditioning of a 132 mw wind farm*," in Power Electronics and Applications, 2007 European Conference on. IEEE, 2007, pp. 1–9. 30

[51] *Pacific power Utah power engineering handbook - Harmonic Distortion.* Engineering Standards and Technical Support Department. 9 Jun 1998

[52] Michael Z. Lowenstein, Harmonics Ltd. "*Harmonic Current and Voltage Distortion - Electrical Construction and Maintenance Understanding the causes, similarities, and differences between current and voltage distortion will help you pinpoint most power quality problems.*" Electrical Construction and Maintenance. Nov. 1, 2002

[53] Associated Power Technologies, "*Total Harmonic Distortion and Effects in Electrical Power Systems*"

[54] IEEE Std 519, 1992. *Recommended practices and requirements for harmonic control in electrical power systems. (ANSI)*. IEEE, New York.

[55] Ross N.W, "*Harmonic and ripple control carrier series resonances with P.F. correction caapcitor*", Trans. Electr. Supply Authority, 1982.

[56] Carol Gowan, Chad Loomis, PE, " *Power Quality and Harmonics: Causes, Effects and Remediation Techniques*", Cornell University PDC Electrical Design Section, 13 December 2006.

[57] Van Long Pham, "*Development of Wavelet Transform Based harmonic Analysis and Estimation Algorithms*", this thesis is presented for the degree of Doctor of Philosophy of The University of Western Australia, September 2000.

[58] IEC Std. 61000-2-1 (1990) *Electromagnetic Compatibility (EMC)—Part 2: Environment—Section 1: Description of the Environment–Electromagnetic Environment for Low-Frequency Conducted Disturbances and Signalling in Public Power Supply Systems*. IEC, Geneva.

[59] IEC Std. 61000-3-2 (2009). *Electromagnetic Compatibility (EMC) — Part 3: Limits. Section 2: Limits for harmonic current emissions(equipment input current< 16A per phase*. IEC, Geneva.

[60] IEC 61000-3-4 (1998). *Electromagnetic Compatibility (EMC) — Part 3: Limits. Section 4: Limitation of emission of harmonic currents in low-voltage power supply systems for equipment with rated current greater than 16A*. IEC, Geneva.

[61] IEC 61000-3-6 (2008) *Electromagnetic Compatibility (EMC) — Part 3: Limits. Section 6: Assessment of emission limits for the connection of distorting installations to MV, HV and EHV power system*. IEC, Geneva.

[62] ER G5/4 (2001) *Planning levels for harmonic voltage distortion and the connection of non-linear equipment to transmission systems and distribution networks in the UK*, Electricity Association, February 20f01

[63] IEC 61000-4-7 (2009) *Electromagnetic Compatibility (EMC) — Part 4: Testing and measurement techniques. Section 7: General guide on harmonics and interharmonics measurements and instrumentation, for power supply system and equipment connected thereto*. IEC, Geneva.

[64] IEC 61000-3-2 *Harmonics Standards Overview By Muhamad Nazarudin Zainal Abidin*, Schaffner EMC Inc., Edsion, NJ, USA

[65] IEC 61000-2-2: E*lectromagnetic compatibility (EMC) – Part 2: Environment – Section 2: Compatibility levels for low-frequency conducted disturbances and signaling in public low-voltage power supply systems.*

[66] IEC 61000-2-12: *Electromagnetic compatibility (EMC) – Part 2-12: Compatibility levels for low-frequency conducted disturbances* Harmonic Penetration Evaluation in Power Syste

[67] A.W. Galli, G.T. Heydt, P.F. Ribeiro, "*Exploring the power of wavelet Analysis*", IEEE Computer Applications in Power, Vol.9 Issue 4, October 1996, pp. 37-41.

[68] Francisco C. De La Rosa , "*Harmonics and Power System*," Taylor & Francis Group, 2006.

[69] Arrillage J, Watson Neville R, Wood Alan R, Smith B C, "*Power System Harmonic Analysis*," John Woley & Sons 1997.

[70] Brigham, E.O. , "*The Fast Fourier Transform*," Prentice Hall 1974.

[71] Sadiku, M.N.O. Akujuobi, C.M. Garcia, R.C, "*An introduction to wavelets in electromagnetics*". IEEE Microwave Magazine, Vol. 6, Issue 2, June 2005, pp. 63-72.

[72] Ingrid Daubechies, "*Ten Lectures on Wavelets*," SIAM, ISBN 0898712742, pp.vii-4, 1992.

[73] Amara Graps, "*An introduction to wavelets*", IEEE Computational Science & Engineering, Vol. 2, Issue 2, Summer 1995, pp. 50-61.

[74] S.Mallat, "*A wavelet tour of signal processing Second Edition*," Academic Press 1999, pp.15-64.

[75] S. Jaffard, Y. Meyer, and R.D. Ryan, "*Wavelets: Tools for Science and Technology*," Philadelphia, PA: SIAM, 2001, pp. 29-30,

[76] G.Strang and T.Nguyen, "*Wavelet and filter banks*," Wellesley, Cambridge Press 1996, pp.87-113.

[77] Y.T.Chan, "*Wavelet Basics*," Royal Military College of Canada, Kluwer acedemic publishers 1994, pp. 111-123.

[78] T.L.Daniel Lee and A.Yamamoto, "*Wavelet analysis: theory and applications*", Hewlett- Packard Journal, December 1994, pp. 44-54.

[79] S.Chen and H.Y.Zhu, "*Wavelet transform for processing power quality disturbances*", EURASIP Journal on Applied Signal Processing, Vol. 2007, No. 1, Jan 2007, pp. 176- 196.

[80] Yen.J, Langari.R, "*Fuzzy logic: intelligence, control, and information*," Englewood Cliffs, NJ: Prentice Hall, 1999.

[81] Hassoun MH, "*Fundamental of artificial neural networks*," Cambridge, MA: MIT Press, 1995.

[82] A A M Zin, H H Goh, K L Lo, "*Power Quality Disturbance Magnitude Characterization Using Wavelet Transformation Analysis Part1 – Theory,* and *Part 2 – Application*," Paper (203-3981) and (203-3981) i, International Journal of Power and Energy System, ACTA Press, Canada, 2007.

[83] P. Arboleya, G. Diaz, J.G. Aleixandre, "*A solution to the dilemma inrush/fault in transformer relaying using MRA and wavelets*", Electric Power Components and System. Vol. 34, Issue 3, February 2007, pp. 285–301.

[84] Julio Barros, Senior Member, IEEE, and Ramón I. Diego, "*Analysis of Harmonics in Power Systems Using the Wavelet-Packet Transform*", IEEE Transactions on Instrumentation and Measurement, Vol. 57, No.1, Jan. 2008.

[85] A. Girgis and F. Ham, "*A qualitative study of pitfalls in FFT*", IEEE Transactions on Aerospace and Electronic Systems, Vol. 16, No.4, July 1980, pp. 434–439.

[86] Wang Hongwei , "*FFT Basics and Case Study using Multi-Instrument*", Virtins Technology, 2009.

[87] Brigham,E.O., "*The Fast Fourier Transform*", Prentice-Hall.

[88] T T Nguyen, "*Parameteric harmonic analysis*", *IEEE Proceedings of Generation, Transmission, Distribution*, Vol. 144, No 1, January 1997, pp.21-25. .

[89] V L Pham and K P Wong, "*Wavelet transform-based algorithm for harmonic analysis of power quality waveforms*", IEE Proceedings of Generation Transmission and Distribution, Vol 146, No 3, May 1999, pp.249-254.

[90] J. Arrillaga and N. R. Watson, "*Power system harmonics*," Wiley. com, 2004. 6

[91] Jiangfeng Lu, "*A New Method for Harmonic Penetration Study in Power Networks with Renewable Generation*," presented for the degree of Doctor of Philosophy at the University of Strathclyde, 2014.

[92] H. Yang, F.Wen, L.Wang, and S. Singh, "*Newton-downhill algorithm for distribution power flow analysis*," in Proceedings of 2nd IEEE International Conference on Power and Energy (PECon), Johor Bahru, Malaysia, December 2008, pp. 1628–1632.

[93] A. Ulinuha, M. Masoum, and S. Islam, "*Harmonic power flow calculations for a large power system with multiple nonlinear loads using decoupled approach*," in Proceedings of Australasian Universities Power Engineering Conference (AUPEC), Perth, Australia, December 2007, pp. 1–6.

[94] http:// www.ee.washington.edu/research/pstca